

Proceedings of the
Electroporation-based Technologies and Treatments
International SCIENTIFIC WORKSHOP and POSTGRADUATE COURSE

Ljubljana, Slovenia
November 13-19, 2016

3	Welcome note
5	Lecturers' Abstract
7	Tadej Kotnik: <i>Resting and Induced Transmembrane Voltage</i>
13	Justin Teissié: <i>In vitro Cell Electroporation</i>
19	Damijan Miklavčič, Nataša Pavšelj: <i>Electric Properties of Tissues and their Changes during Electroporation</i>
27	Marie-Pierre Rols: <i>Nucleic acids electrotransfer in vitro: what imaging can tell us about the mechanisms of uptake</i>
35	Maja Čemažar: <i>Gene electrotransfer in vivo</i>
43	Véronique Preat: <i>Drug and gene delivery in the skin by electroporation</i>
47	Mounir Tarek: <i>Molecular Dynamics Simulations of Lipid Membranes Electroporation</i>
65	P. Thomas Vernier: <i>Nanoscale and Multiscale Electropulsation</i>
73	Gregor Serša: <i>Electrochemotherapy from bench to bedside: principles, mechanisms and applications</i>
79	Julie Gehl: <i>Electrochemotherapy in clinical practice: Lessons from development and implementation - and future perspectives</i>
83	Damijan Miklavčič, Matej Reberšek: <i>Development of devices and electrodes</i>
93	Lluis M. Mir: <i>Electroporation and electroporation - pieces of puzzle put together</i>
95	Invited lecturers
97	Aude Silve: <i>Detecting changes of membrane properties with electrical and optical diagnostics</i>
103	Rumiana Dimova: <i>Giant vesicles in electric fields: What can we learn about membrane properties and electroporation</i>
111	Wolfgang Frey: <i>PEF-Processing in Microalgae Valorization</i>
125	Eung Je Woo: <i>Conductivity Tensor Imaging using MRI</i>
121	Students' Abstract
141	Faculty members

ISBN 978-961-243-315-4



9 789612 433154

Proceedings of the Workshop is also available in PDF format at 2016.ebtt.org/proceedings



November 13-19, 2016
Ljubljana, Slovenia



Proceedings of the
**Electroporation-based
Technologies and Treatments**
International SCIENTIFIC WORKSHOP and POSTGRADUATE COURSE

Edited by:

Peter Kramar
Damijan Miklavčič
Lluis M. Mir

Organised by:

University of Ljubljana
Faculty of Electrical Engineering
Institute of Oncology, Ljubljana

Supported by:

Bioelectrochemical Society
Le Centre national de la recherche scientifique
International Union for Pure and Applied Biophysics IUPAB
Laboratory for Telecommunications LTFE

C3M
Gorenje
IGEA
Iskra Medical
Kemomed
Leroy Biotech
Omega

Course conducted in the scope of EBAM European Associated Laboratory (LEA)

www.ebtt.org

Electroporation based Technologies and Treatments - 2016





2nd World Congress on Electroporation and Pulsed Electric Fields In Biology, Medicine, Food & Environmental Technologies



Norfolk, Virginia USA

September 24-28, 2017

Tentative topics of the World Congress 2017

- Basics, biology of electroporation
- Basics, modeling of electroporation including MD studies
 - Technology for PEF and large treatment capacities
- Technology for electric pulses for research and medical applications
 - Medical applications (ECT, IRE, GET)
 - Food industry applications
 - Environmental applications
- Micro and Nanotechnologies (single cell electroporation, microfluidics ...)



wc2017.electroporation.net



November 13-19, 2016
Ljubljana, Slovenia

Proceedings of the

Electroporation-Based Technologies and Treatments

International SCIENTIFIC WORKSHOP and POSTGRADUATE COURSE

Edited by:

Peter Kramar
Damijan Miklavčič
Lluis M. Mir

Organised by:

University of Ljubljana
Faculty of Electrical Engineering

Institute of Oncology, Ljubljana

Organising committee:

Chair:

Peter Kramar

Members:

Matej Kranjc, Lea Vukanović,
Tadeja Forjanič, Duša Hodžič

Supported by:

Bioelectrochemical Society
Le Centre national de la recherche scientifique
International Union for Pure and Applied
Biophysics - IUPAB
Laboratory for Telecommunications LTFE

C3M
Gorenje
IGEA
Iskra Medical
Leroy Biotech
Kemomed
Omega

Course conducted in the scope of EBAM European Associated Laboratory (LEA).

www.ebtt.org

CIP - Kataložni zapis o publikaciji
Narodna in univerzitetna knjižnica, Ljubljana

602.621(082)
577.352.4(082)

PROCEEDINGS of the electroporation-based technologies and treatments : international scientific workshop and postgraduate course, November 13-19, 2016, Ljubljana, Slovenia / organised by University of Ljubljana, Faculty of Electrical Engineering [and] Institute of Oncology, Ljubljana ; edited by Peter Kramar, Damijan Miklavčič, Lluís M. Mir. - 1. izd. - Ljubljana : Založba FE, 2016

ISBN 978-961-243-315-4

1. Kramar, Peter, 1977- 2. Fakulteta za elektrotehniko (Ljubljana) 3. Onkološki inštitut (Ljubljana)
287066112

Copyright © 2016 Založba FE. All rights reserved.
Razmnoževanje (tudi fotokopiranje) dela v celoti ali po delih
brez predhodnega dovoljenja Založbe FE prepovedano.

Založnik: Založba FE, Ljubljana
Izdajatelj: UL Fakulteta za elektrotehniko, Ljubljana
Urednik: prof. dr. Sašo Tomažič

Natisnil: Tiskarna Bori
Naklada: 90 izvodov
1. izdaja

Welcome note

Dear Colleagues,

Dear Students,

The idea of organizing the Workshop and Postgraduate Course on Electroporation Based Technologies and Treatments at the University of Ljubljana had been developing for several years. After preliminary discussions, the Workshop and Course was organised for the first time in 2003. In 2016 the Course is organised for the 10th time! In these thirteen years the Course has been attended by 576 participants coming from 35 different countries. And this year again we can say with great pleasure: “with participation of many of the world leading experts in the field”.

The aim of the lectures at this Workshop and Course is to provide the participants with sufficient theoretical background and practical knowledge to allow them to use electroporation effectively in their working environments.

It also needs to be emphasized that all written contributions collected in this proceeding have been peer-reviewed and then thoroughly edited by Peter Kramar. We thank all authors, reviewers and editors. Finally, we would like to express our sincere thanks to colleagues working in our and collaborating laboratories for their lectures and for the preparation of the practical trainings delivered during the course, to the agencies that have been sponsoring our research work for years, and to Slovenian Research Agency and Centre National de la Recherche Scientifique (CNRS), to the Bioelectrochemical Society and International Union for Pure and Applied Biophysics (IUPAB) for supporting the Workshop and Course. We also would like to thank C3M (Slovenia), Gorenje (Slovenia), Igea (Italy), Iskra Medical (Slovenia), Kemomed (Slovenia), Leroy Biotech (France), and Omega (Slovenia) whose financial support allowed us to assist many students participating in this Workshop and Course. The course is conducted in the scope of the LEA EBAM (European Associated Laboratory on the Pulsed Electric Fields Applications in Biology and Medicine).

Thank you for participating in our Workshop and Course. We sincerely hope that you will benefit from being with us both socially and professionally.

Sincerely Yours,

Damijan Miklavčič and Lluis M. Mir

LECTURERS' ABSTRACTS

Resting and Induced Transmembrane Voltage

Tadej Kotnik

University of Ljubljana, Faculty of Electrical Engineering, Ljubljana, Slovenia

Abstract: Under physiological conditions, a resting voltage in the range of tens of millivolts is continually present on the cell plasma membrane. An exposure of the cell to an external electric field induces an additional component of transmembrane voltage, proportional to the strength of the external field and superimposing onto the resting component for the duration of the exposure. Unlike the resting voltage, the induced voltage varies with position, and also depends on the shape of the cell and its orientation with respect to the electric field. In cell suspensions, it also depends on the volume fraction occupied by the cells. There is a delay between the external field and the voltage induced by it, typically somewhat below a microsecond, but larger when cells are suspended in a low-conductivity medium. As a consequence of this delay, for exposures to electric fields with frequencies above 1 MHz, or to electric pulses with durations below 1 μ s, the amplitude of the induced voltage starts to decrease with further increase of the field frequency or further decrease of the pulse duration. With field frequencies approaching the gigahertz range, or with pulse durations in the nanosecond range, this attenuation becomes so pronounced that the voltages induced on organelle membranes in the cell interior become comparable, and can even exceed the voltage induced on the plasma membrane.

THE CELL AND ITS PLASMA MEMBRANE

A biological cell can be considered from various aspects. We will skip the most usual description, that of a biologist, and focus on two more technical ones, electrical and geometrical.

From the electrical point of view, a cell can roughly be described as an electrolyte (the cytoplasm) surrounded by an electrically insulating shell (the plasma membrane). Physiologically, the exterior of the cell also resemble an electrolyte. If a cell is exposed to an external electric field under such conditions, in its very vicinity the field concentrates within the membrane. This results in an electric potential difference across the membrane, termed the *induced transmembrane voltage*, which superimposes onto the *resting transmembrane voltage* typically present under physiological conditions. Transmembrane voltage can affect the functioning of voltage-gated membrane channels, initiate the action potentials, stimulate cardiac cells, and when sufficiently large, it also leads to cell membrane electroporation, with the porated membrane regions closely correlated with the regions of the highest induced transmembrane voltage [1].

With rapidly time-varying electric fields, such as waves with frequencies in the megahertz range or higher, or electric pulses with durations in the submicrosecond range, both the membrane and its surroundings have to be treated as materials with both a non-zero electric conductivity and a non-zero dielectric permittivity.

From the geometrical point of view, the cell can be characterized as a geometric body (the cytoplasm) surrounded by a shell of uniform thickness (the membrane). For suspended cells, the simplest model of the cell is a sphere surrounded by a spherical shell. For augmented generality, the sphere can be replaced by a spheroid (or an ellipsoid), but in this case, the requirement of uniform thickness complicates the description of the shell substantially. If its inner surface is a spheroid or an ellipsoid, its outer surface lacks a simple geometrical characterization, and vice versa.¹ Fortunately, this complication does not affect the steady-state voltage induced on the plasma membrane of such cells, which can still be determined analytically.

Spheres, spheroids, and ellipsoids may be reasonable models for suspended cells, but not for cells in tissues. No simple geometrical body can model a typical cell in a tissue, and furthermore every cell generally differs in its shape from the rest. With irregular geometries and/or with cells close to each other, the induced voltage cannot be determined analytically, and thus cannot be formulated as an explicit function. This deprives us of some of the insight available from explicit expressions, but using modern computers and numerical methods, the voltage induced on each particular irregular cell can still be determined quite accurately.

¹ This can be visualized in two dimensions by drawing an ellipse, and then trying to draw a closed curve everywhere equidistant to the ellipse. This curve is not an ellipse, and if one is content with an

approximation, the task is actually easier to accomplish by hand than with basic drawing programs on a computer.

RESTING TRANSMEMBRANE VOLTAGE

Under physiological conditions, a voltage in the range of -90 mV up to -40 mV is always present on the cell membrane [2,3]. This voltage is caused by a minute deficit of positive ions in the cytoplasm relative to the negative ones, which is a consequence of the transport of specific ions across the membrane. The most important actors in this transport are: (i) the Na-K pumps, which export Na^+ ions out of the cell and simultaneously import K^+ ions into the cell; and (ii) the K leak channels, through which K^+ ions can flow across the membrane in both directions. The resting transmembrane voltage reflects the electrochemical equilibrium of the action of these two mechanisms, and perhaps the easiest way to explain the occurrence of this voltage is to describe how the equilibrium is reached.

The Na-K pump works in cycles. In a single cycle, it exports three Na^+ ions out of the cell and imports two K^+ ions into it. This generates a small deficit of positive ions in the cytoplasm and a gradient of electric potential, which draws positive ions into the cell, and negative ions out of the cell. But at the same time, the pump also generates concentration gradients of Na^+ and K^+ , which draw the Na^+ ions into the cell, and the K^+ ions out of the cell. The K^+ ions are the only ones that possess a significant mechanism of passive transport through the membrane, namely the K leak channels, and through these the K^+ ions are driven towards the equilibration of the electrical and the concentration gradient. When this equilibrium is reached, the electrical gradient across the membrane determines the resting transmembrane voltage, which is continually present on the membrane.

The unbalanced ions responsible for the resting transmembrane voltage represent a very small fraction of all the ions in the cytoplasm, so that the osmotic pressure difference generated by this imbalance is negligible. Also, the membrane acts as a charged capacitor, with the unbalanced ions accumulating close to its surface, so that the cytoplasm can in general be viewed as electrically neutral.

INDUCED TRANSMEMBRANE VOLTAGE

When a biological cell is placed into an electric field, this leads to a local distortion of the field in the cell and its vicinity. As outlined in the introductory section of this paper, due to the low membrane conductivity, in the vicinity of the cell the field is concentrated in the cell membrane, where it is several orders of magnitude larger than in the cytoplasm and outside the cell. This results in a so-called induced transmembrane voltage, which superimposes to the resting component. In the following subsections, we

describe in more detail the transmembrane voltage induced on cells of various shapes and under various conditions. In each considered case, the principles of superposition allow to obtain the complete transmembrane voltage by adding the resting component to the induced one.

Spherical cells

For an exposure to a DC homogeneous electric field, the voltage induced on the cell membrane is determined by solving Laplace's equation. Although biological cells are not perfect spheres, in theoretical treatments they are usually considered as such. For the first approximation, the plasma membrane can also be treated as nonconductive. Under these assumptions, the induced transmembrane voltage $\Delta\Phi_m$ is given by a formula often referred to as the (steady-state) Schwan's equation [4],

$$\Delta\Phi_m = \frac{3}{2}ER\cos\theta, \quad (1)$$

where E is the electric field in the region where the cell is situated, R is the cell radius, and θ is the angle measured from the center of the cell with respect to the direction of the field. voltage is proportional to the applied electric field and to the cell radius. Furthermore, it has extremal values at the points where the field is perpendicular to the membrane, i.e. at $\theta = 0^\circ$ and $\theta = 180^\circ$ (the "poles" of the cell), and in-between these poles it varies proportionally to the cosine of θ (see Fig. 1, dashed).

The value of $\Delta\Phi_m$ given by Eq. (1) is typically established several μs after the onset of the electric field. With exposures to a DC field lasting hundreds of microseconds or more, this formula can safely be applied to yield the maximal, steady-state value of the induced transmembrane voltage. To describe the transient behavior during the initial microseconds, one uses the first-order Schwan's equation [5],

$$\Delta\Phi_m = \frac{3}{2}ER\cos\theta(1 - \exp(-t/\tau_m)), \quad (2)$$

where τ_m is the time constant of membrane charging,

$$\tau_m = \frac{R\epsilon_m}{2d\frac{\sigma_i\sigma_e}{\sigma_i + 2\sigma_e} + R\sigma_m} \quad (3)$$

with σ_i , σ_m and σ_e the conductivities of the cytoplasm, cell membrane, and extracellular medium, respectively, ϵ_m the dielectric permittivity of the membrane, d the membrane thickness, and R again the cell radius.

In certain experiments *in vitro*, where artificial extracellular media with conductivities substantially lower than physiological are used, the factor $3/2$ in Eqns. (1) and (2) decreases in value, as described in

detail in [6]. But generally, Eqns. (2) and (3) are applicable to exposures to sine (AC) electric fields with frequencies below 1 MHz, and to rectangular electric pulses longer than 1 μ s.

To determine the voltage induced by even higher field frequencies or even shorter pulses, the dielectric permittivities of the electrolytes on both sides of the membrane also have to be accounted for. This leads to a further generalization of Eqns. (2) and (3) to a second-order model [7-9], and the results it yields will be outlined in the last section of this paper.

Spheroidal and ellipsoidal cells

Another direction of generalization is to assume a cell shape more general than that of a sphere. The most straightforward generalization is to a spheroid (a geometrical body obtained by rotating an ellipse around one of its radii, so that one of its orthogonal projections is a sphere, and the other two are the same ellipse) and further to an ellipsoid (a geometrical body in which each of its three orthogonal projections is a different ellipse). To obtain the analogues of Schwan's equation for such cells, one solves Laplace's equation in spheroidal and ellipsoidal coordinates, respectively [10-12]. Besides the fact that this solution is by itself somewhat more intricate than the one in spherical coordinates, the generalization of the shape invokes two additional complications outlined in the next two paragraphs.

A description of a cell is geometrically realistic if the thickness of its membrane is uniform. This is the case if the membrane represents the space between two concentric spheres, but not with two confocal spheroids or ellipsoids. As a result, the thickness of the membrane modeled in spheroidal or ellipsoidal coordinates is necessarily nonuniform. By solving Laplace's equation in these coordinates, we thus obtain the spatial distribution of the electric potential in a nonrealistic setting. However, under the assumption that the membrane conductivity is zero, the induced transmembrane voltage obtained in this manner is still realistic. Namely, the shielding of the cytoplasm is then complete, and hence the electric potential everywhere inside the cytoplasm is constant. Therefore, the geometry of the inner surface of the membrane does not affect the potential distribution outside the cell, which is the same as if the cell would be a homogeneous nonconductive body of the same shape.² A more rigorous discussion of the validity of this approach can be found in [10]. Fig. 1 compares the transmembrane voltage induced on two spheroids with the axis of rotational

symmetry aligned with the direction of the field, and that induced on a sphere.

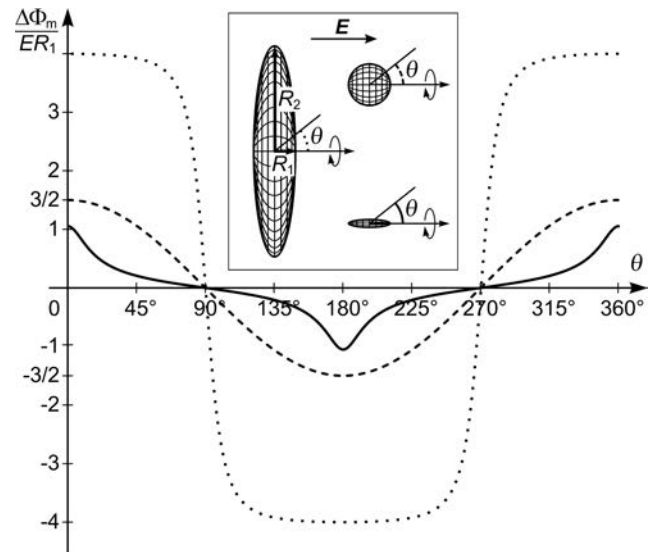


Figure 1: Normalized steady-state $\Delta\Phi_m$ as a function of the polar angle θ for spheroidal cells with the axis of rotational symmetry aligned with the direction of the field. Solid: a prolate spheroidal cell with $R_2 = 0.2 \times R_1$. Dashed: a spherical cell, $R_2 = R_1 = R$. Dotted: an oblate spheroidal cell with $R_2 = 5 \times R_1$.

For nonspherical cells, it is generally more revealing to express $\Delta\Phi_m$ as a function of the arc length than as a function of the angle θ (for a sphere, the two quantities are directly proportional). For uniformity, the normalized version of the arc length is used, denoted by p and increasing from 0 to 1 equidistantly along the arc of the membrane. This is illustrated in Fig. 2 for the cells for which $\Delta\Phi_m(\theta)$ is shown in Fig. 1, and all the plots of $\Delta\Phi_m$ on nonspherical cells will henceforth be presented in this manner.

² As a rough analogy, when a stone is placed into a water stream, the streamlines outside the stone are the same regardless of the stone's interior composition. Due to the fact that stone is impermeable to water, only its outer shape matters in this respect.

Similarly, when the membrane is nonconductive, or "impermeable to electric current", only the outer shape of the cell affects the current density and the potential distribution outside the cell.

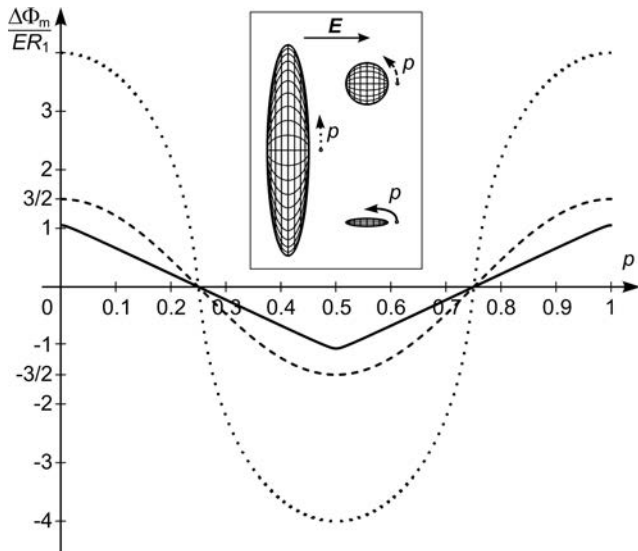


Figure 2: Normalized steady-state $\Delta\Phi_m$ as a function of the normalized arc length p for spheroidal cells with the axis of rotational symmetry aligned with the direction of the field. Solid: a prolate spheroidal cell with $R_2 = 0.2 \times R_1$. Dashed: a spherical cell, $R_2 = R_1 = R$. Dotted: an oblate spheroidal cell with $R_2 = 5 \times R_1$.

The second complication of generalizing the cell shape from a sphere to a spheroid or an ellipsoid is that the induced voltage now also becomes dependent on the orientation of the cell with respect to the electric field. To deal with this, one decomposes the field vector into the components parallel to the axes of the spheroid or the ellipsoid, and writes the induced voltage as a corresponding linear combination of the voltages induced for each of the three coaxial orientations [11,12]. Figs. 3 and 4 show the effect of rotation of two different spheroids with respect to the direction of the field.

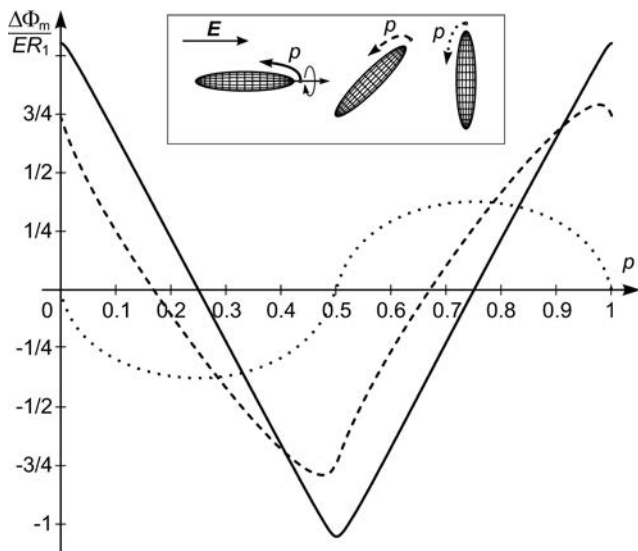


Figure 3: Normalized steady-state $\Delta\Phi_m(p)$ for a prolate spheroidal cell with $R_2 = 0.2 \times R_1$. Solid: axis of rotational symmetry (ARS) aligned with the field. Dashed: ARS at 45° with respect to the field. Dotted: ARS perpendicular to the field.

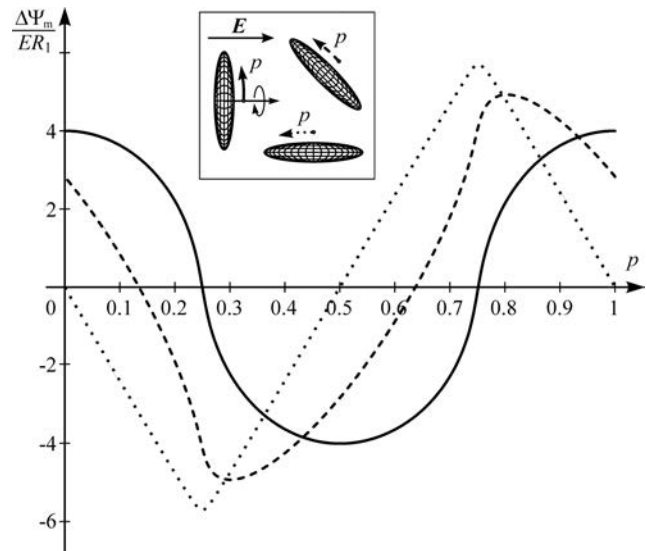


Figure 4: Normalized steady-state $\Delta\Phi_m(p)$ for an oblate spheroidal cell with $R_2 = 5 \times R_1$. Solid: axis of rotational symmetry (ARS) aligned with the field. Dashed: ARS at 45° with respect to the field. Dotted: ARS perpendicular to the field.

Irregularly shaped cells

For a cell having an irregular shape, the induced transmembrane voltage cannot be determined exactly, as for such a geometry Laplace's equation is not solvable analytically. Using modern computers and finite-elements tools such as COMSOL Multiphysics, the voltage induced on a given irregular cell can still be determined numerically, as described in detail in [13,14]. While the results obtained in this manner are quite accurate, they are only applicable to the particular cell shape for which they were computed. Fig. 5 shows examples of two cells growing in a Petri dish and the voltages induced on their membranes.

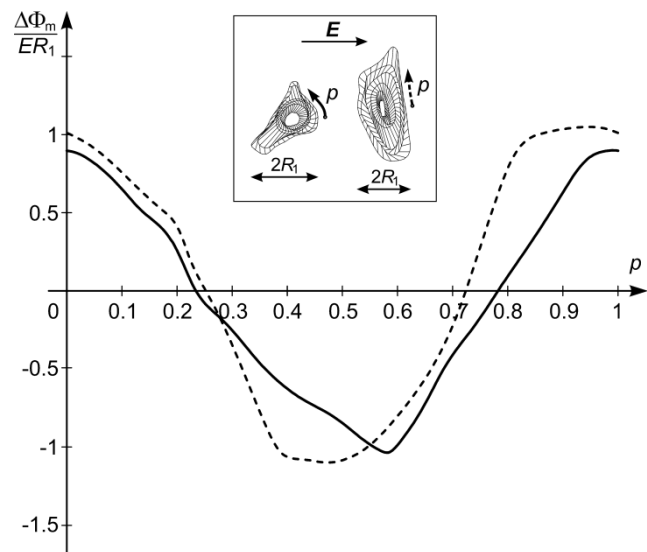


Figure 5: Normalized steady-state $\Delta\Phi_m(p)$ for two irregularly shaped cells growing on the flat surface of a Petri dish.

Cells in dense suspensions

In dilute cell suspensions, the distance between the cells is much larger than the cells themselves, and the local field outside each cell is practically unaffected by the presence of other cells. Thus, for cells representing less than 1 % of the suspension volume (for a spherical cell with a radius of 10 μm , this means up to 2 million cells/ml), the deviation of the actual induced transmembrane voltage from one predicted by Schwan's equation is negligible. However, as the volume fraction occupied by the cells gets larger, the distortion of the local field around each cell by the presence of other cells in the vicinity becomes more pronounced, and the prediction yielded by Schwan's equation less realistic (Fig. 6). For volume fractions over ten percent, as well as for clusters and lattices of cells, one has to use appropriate numerical or approximate analytical solutions for a reliable analysis of the induced transmembrane voltage [15,16]. Regardless of the volume fraction they occupy, as long as the cells are suspended, they are floating freely, and their arrangement is rather uniform. Asymptotically, this would correspond to a face-centered cubic lattice, and this lattice is also the most appropriate for the analysis of the transmembrane voltage induced on cells in suspension.

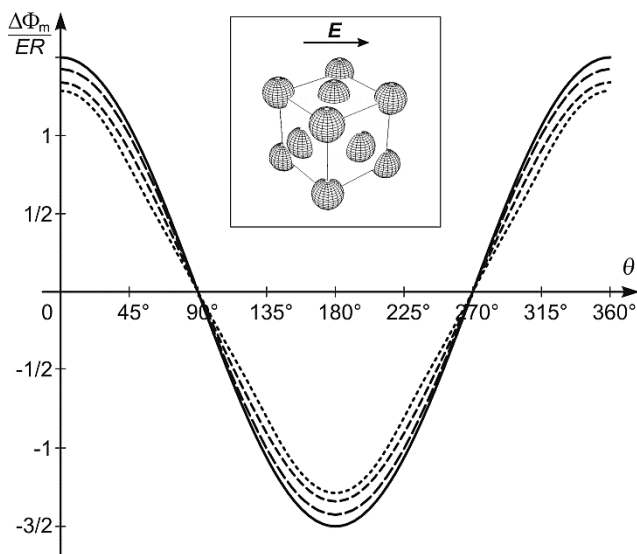


Figure 6: Normalized steady-state $\Delta\Phi_m(\theta)$ for spherical cells in suspensions of various densities (intercellular distances). Solid: The analytical result for a single cell as given by Eq. (1). Dashed: numerical results for cells arranged in a face-centered cubic lattice and occupying (with decreasing dash size) 10%, 30%, and 50% of the total suspension volume.

For even larger volume fractions of the cells, the electrical properties of the suspension start to resemble that of a tissue, but only to a certain extent. The arrangement of cells in tissues does not necessarily resemble a face-centered lattice, since cells can form

specific structures (e.g. layers). In addition, cells in tissues can be directly electrically coupled (e.g. through gap junctions). These and other specific features of the interactions between cells in tissues and electric fields will be considered in more detail in the paper that follows this one.

High field frequencies and very short pulses

The time constant of membrane charging (τ_m) given by Eq. (3) implies that there is a delay between the time courses of the external field and the voltage induced by this field. As mentioned above, τ_m (and thus the delay) is somewhat below a microsecond under physiological conditions, but can be larger when cells are suspended in a low-conductivity medium. For alternating (AC) fields with the oscillation period much longer than τ_m , as well as for rectangular pulses much longer than τ_m , the amplitude of the induced voltage remains unaffected. However, for AC fields with the period comparable or shorter than τ_m , as well as for pulses shorter than τ_m , the amplitude of the induced voltage starts to decrease.

To illustrate how the amplitude of the induced transmembrane voltage gets attenuated as the frequency of the AC field increases, we plot the normalized amplitude of the induced voltage as a function of the field frequency. For a spherical cell, the plot obtained is shown in Fig. 6. The low-frequency plateau and the downward slope that follows are both described by the first-order Schwan's equation, but the high-frequency plateau is only described by the second-order model [7-9], in which all electric conductivities and dielectric permittivities are accounted for.

With field frequencies approaching the GHz range, or with pulse durations in the nanosecond range, the attenuation of the voltage induced on the cell plasma membrane becomes so pronounced that this voltage becomes comparable to the voltage induced on organelle membranes in the cell interior. In certain circumstances, particularly if the organelle interior is electrically more conductive than the cytosol, or if the organelle membrane has a lower dielectric permittivity than the cell membrane, the voltage induced on the membrane of this organelle can temporarily even exceed the voltage induced on the plasma membrane [17]. In principle, this could provide a theoretical explanation for a number of recent reports that very short and intense electric pulses (tens of ns, millions or tens of millions of V/m) can also induce electroporation of organelle membranes [18-20].

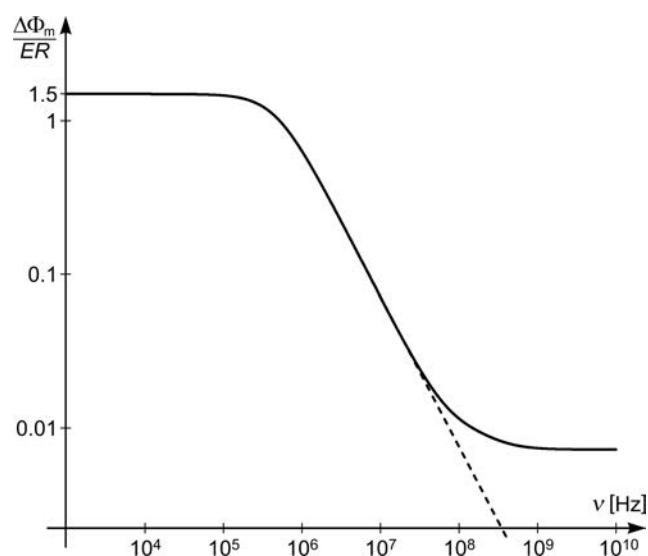


Figure 7: The amplitude of normalized steady-state $\Delta\Phi_m$ as a function of the frequency of the AC field. The dashed curve shows the first-order, and the solid curve the second-order Schwan's equation. Note that both axes are logarithmic.

REFERENCES

- [1] T. Kotnik, G. Pucihar, D. Miklavčič. Induced transmembrane voltage and its correlation with electroporation-mediated molecular transport. *J. Membrane Biol.* 236: 3-13, 2010.
- [2] K.S. Cole. *Membranes, Ions and Impulses*. University of California Press, Berkeley, USA, 1972.
- [3] H.L. Atwood, W.A. Mackay. *Essentials of Neurophysiology*. BC Decker, Toronto, Canada, 1989.
- [4] H.P. Schwan. Electrical properties of tissue and cell suspensions. *Adv. Biol. Med. Phys.* 5: 147-209, 1957.
- [5] H. Pauly, H.P. Schwan. Über die Impedanz einer Suspension von kugelförmigen Teilchen mit einer Schale. *Z. Naturforsch.* 14B: 125-131, 1959.
- [6] T. Kotnik, F. Bobanović, D. Miklavčič. Sensitivity of transmembrane voltage induced by applied electric fields — a theoretical analysis. *Bioelectrochem. Bioenerg.* 43: 285-291, 1997.
- [7] C. Grosse, H.P. Schwan. Cellular membrane potentials induced by alternating fields. *Biophys. J.* 63: 1632-1642, 1992.
- [8] T. Kotnik, D. Miklavčič, T. Slivnik. Time course of transmembrane voltage induced by time-varying electric fields — a method for theoretical analysis and its application. *Bioelectrochem. Bioenerg.* 45: 3-16, 1998.
- [9] T. Kotnik, D. Miklavčič. Second-order model of membrane electric field induced by alternating external electric fields. *IEEE Trans. Biomed. Eng.* 47: 1074-1081, 2000.
- [10] T. Kotnik, D. Miklavčič. Analytical description of transmembrane voltage induced by electric fields on spheroidal cells. *Biophys. J.* 79: 670-679, 2000.
- [11] J. Gimsa, D. Wachner. Analytical description of the transmembrane voltage induced on arbitrarily oriented ellipsoidal and cylindrical cells. *Biophys. J.* 81: 1888-1896, 2001.
- [12] B. Valič, M. Golzio, M. Pavlin, A. Schatz, C. Faurie, B. Gabriel, J. Teissié, M.P. Rols, D. Miklavčič. Effect of electric field induced transmembrane potential on spheroidal cells: theory and experiment. *Eur. Biophys. J.* 32: 519-528, 2003.
- [13] G. Pucihar, T. Kotnik, B. Valič, D. Miklavčič. Numerical determination of the transmembrane voltage induced on irregularly shaped cells. *Annals Biomed. Eng.* 34: 642-652, 2006.
- [14] G. Pucihar, D. Miklavčič, T. Kotnik. A time-dependent numerical model of transmembrane voltage inducement and electroporation of irregularly shaped cells. *IEEE T. Biomed. Eng.* 56: 1491-1501, 2009.
- [15] R. Susil, D. Šemrov, D. Miklavčič. Electric field induced transmembrane potential depends on cell density and organization. *Electro. Magnetobiol.* 17: 391-399, 1998.
- [16] M. Pavlin, N. Pavšelj, D. Miklavčič. Dependence of induced transmembrane potential on cell density, arrangement, and cell position inside a cell system. *IEEE Trans. Biomed. Eng.* 49: 605-612, 2002.
- [17] T. Kotnik, D. Miklavčič. Theoretical evaluation of voltage inducement on internal membranes of biological cells exposed to electric fields. *Biophys. J.* 90: 480-491, 2006.
- [18] K.H. Schoenbach, S.J. Beebe, E.S. Buescher. Intracellular effect of ultrashort electrical pulses. *Bioelectromagnetics* 22: 440-448, 2001.
- [19] S.J. Beebe, P.M. Fox, L.J. Rec, E.L. Willis, K.H. Schoenbach. Nanosecond, high-intensity pulsed electric fields induce apoptosis in human cells. *FASEB J.* 17: 1493-1495, 2003.
- [20] E. Tekle, H. Oubrahim, S.M. Dzekunov, J.F. Kolb, K.H. Schoenbach, P. B. Chock. Selective field effects on intracellular vacuoles and vesicle membranes with nanosecond electric pulses. *Biophys. J.* 89: 274-284, 2005.

ACKNOWLEDGEMENT

This work was supported by the Ministry of Higher Education, Science and Technology of the Republic of Slovenia.



Tadej Kotnik was born in Ljubljana, Slovenia, in 1972. He received a Ph.D. in Biophysics from University Paris XI and a Ph.D. in Electrical Engineering from the University of Ljubljana, both in 2000. He is currently a Full Professor and the Vice-dean for Research at the Faculty of Electrical Engineering of the University of Ljubljana. His research interests include membrane electrodynamics, as well as theoretical and experimental study of related biophysical phenomena, particularly membrane electroporation and gene electrotransfer.

Tadej Kotnik is the first author of 22 articles in SCI-ranked journals cited over 750 times excluding self-citations. His h-index is 23. In 2001 he received the Galvani Prize of the Bioelectrochemical Society, and for the year 2014 he was among the recipients of the annual award "Ten Most Prominent Research Achievements of the University of Ljubljana".

NOTES

In vitro Cell Electroporation

Justin Teissié

IPBS UMR 5089 CNRS and Université de Toulouse, Toulouse, France

Abstract: Electroporation (delivery of short lived electric pulses) is one of the most successful non-viral methods to introduce foreign molecules in living cells *in vitro*. This lecture describes the factors controlling electroporation to small molecules (< 4 kDa). Pulse durations are selected from submicroseconds to a few milliseconds. The description of *in vitro* events brings the attention of the reader on the processes occurring before, during and after electroporation of cells. The role of the different electrical parameters (Field strength, pulse duration, delay between pulses) is delineated. The kinetic of the processes affecting the cell surface is described outlining that most of the exchange across the membrane takes place after the pulse during the so called resealing. Cell contribution to this critical step is tentatively explained. The membrane events appear to be controlled by the cellular metabolism.

INTRODUCTION

The application of electric field pulses to cells leads to the transient permeabilization of the plasma membrane (electroporation). This phenomenon brings new properties to the cell membrane: it becomes permeabilized, fusogenic and exogenous membrane proteins can be inserted. It has been used to introduce a large variety of molecules into many different cells *in vitro* [1, 2].

The present lecture is reporting what is called “classical electroporation”. This means that it is relevant of the effect of field pulses lasting from μ s to several ms, with a rising time of a few hundreds of ns. In this time domain, dielectric spectroscopy of a cell shows that the membrane can be considered as a non conductive insulator (indeed some active leaks may be present). The physics of the process was part of Prof. Kotnik lecture.

One of the limiting problems remains that very few is known on the physicochemical mechanisms supporting the reorganisation of the cell membrane. Electroporation is not simply punching holes in a one lipid bilayer. The physiology of the cell is controlling many parameters. The associated destabilisation of the membrane impermeability is a stress for the cells and may affect the cell viability.

This lecture explains the factors controlling electroporation to small molecules (< 4 kDa). The events occurring before, during and after electroporation of cells are described.

Preamble: what is a biological membrane?

The main target of cell electroporation is the cell membrane, more precisely the plasma membrane. Organelles may be affected when they are shielded by the plasma membrane or by a back effect of the transport linked to the plasma membrane permeabilization (uptake of ions, leakage of secondary metabolites). In many approaches such as molecular dynamics simulations, the description of a biological

membrane is limited to a lipid bilayer. This is far from the biological complexity and should be used only for soft matter investigations. When the process is applied to a cell (and to a tissue), a more sophisticated description of the biological membrane organization is needed. It is a complex assembly between proteins and a mixture of lipids. It results from a network of weak forces resulting in a complex pattern of lateral pressure across the membrane. A lot of lateral and rotational movements of the membrane components on the sub-microsecond timescale is present. Spontaneous transverse movements are energy driven or result from membrane traffic related events (endocytosis, exocytosis). The distribution of lipids is not homogeneous as assumed in the fluid matrix model but localized specific accumulations are detected (rafts). This is due to the fact that a biological membrane is an active entity where a flow of components is continuously occurring (so called membrane traffic). Endocytosis and exocytosis are processes involved in the membrane organization. They are affected by stresses applied on the cell. The mechanical signals are transduced by the membrane. This costs a lot of energy provided by the cell metabolism. Another consequence is the ionic gradient across the membrane resulting from the balance between active pumping and spontaneous leaks. A final aspect is that damages to the membrane are repaired not only by an intramembraneous process (as for a viscoelastic material) but by a patching process mediated by cytosolic vesicles.

It is therefore very difficult to provide an accurate physical description of a biological membrane at the molecular level. Either oversimplifying approximations are used (using lipid vesicles, a soft matter approach) or a phenomenological description is provided with fitting to physical chemical equations (a life science approach). Both are valid as long as you keep aware of the limits in accuracy. The present lecture will be within the life science approach to give

the suitable informations for Clinical and well as biotechnological applications.

A- A biophysical description and a biological validation

A-1 The external field induces membrane potential difference modulation

An external electric field modulates the membrane potential difference as a cell can be considered as a spherical capacitor [3]. The transmembrane potential difference (TMP) induced by the electric field after a (capacitive) charging time, $\Delta\Psi_i$ is a complex function $g(\lambda)$ of the specific conductivities of the membrane (λ_m), the pulsing buffer (λ_o) and the cytoplasm (λ_i), the membrane thickness, the cell size (r) and packing. Thus,

$$\Delta\Psi_i = f \cdot g(\lambda) \cdot r \cdot E \cdot \cos\theta \quad (1)$$

in which θ designates the angle between the direction of the normal to the membrane at the considered point on the cell surface and the field direction, E the field intensity, r the radius of the cell and f , a shape factor (a cell being a spheroid). Therefore, $\Delta\Psi_i$ is not uniform on the cell surface. It is maximum at the positions of the cell facing the electrodes. These physical predictions were checked experimentally by videomicroscopy by using potential difference sensitive fluorescent probes [4-6]. More locally on the cell surface, it is affected by the local curvature and the associated defects in packing. This description is valid with dilute cell suspensions. In dense systems, self shielding in the cell population affects the local field distribution and reduces the local (effective) field distribution [7]. Stronger field intensities are needed to get the same induced potential. Another factor affecting the induced potential differences is the shape of the cells and their relative orientation to the field lines. When the resulting transmembrane potential difference $\Delta\Psi$ (i.e. the sum between the resting value of cell membrane $\Delta\Psi_o$ and the electroinduced value $\Delta\Psi_i$) reaches locally 250 mV, that part of the membrane becomes highly permeable for small charged molecules and transport is detected [3, 8].

One more parameter is that as the plasma membrane must be considered as a capacitor, there is a membrane charging time that may affect the magnitude of the TMP when the pulse duration is short (submicrosecond) or in poorly conducting pulsing buffers.

A-2 Parameters affecting electropermeabilization

A-2-1 Electric field parameters

Permeabilization is controlled by the field strength. Field intensity larger than a critical value ($E_{p,r}$) must be

applied to the cell suspension. From Eq. (1), permeabilization is first obtained for θ close to 0 or π . $E_{p,r}$ is such that:

$$\Delta\Psi_{i,perm} = f \cdot g(\lambda) \cdot r \cdot E_{p,r} \quad (2)$$

Permeabilization is therefore a local process on the cell surface. The extend of the permeabilized surface of a spherical cell, A_{perm} , is given by:

$$A_{perm} = A_{tot} \left(\frac{1 - \frac{E_{p,r}}{E}}{2} \right) \quad (3)$$

where A_{tot} is the cell surface and E is the applied field intensity. Increasing the field strength will increase the part of the cell surface, which is brought to the electropermeabilized state.

These theoretical predictions are experimentally directly supported on cell suspension by measuring the leakage of metabolites (ATP) [9] in a population or at the single cell level by digitised fluorescence microscopy [10, 11]. The permeabilized part of the cell surface is a linear function of the reciprocal of the field intensity. Permeabilization, due to structural alterations of the membrane, remained detected on a restricted cap at the cell surface. In other words, the cell obeys the physical predictions! The area affected by the electric field depends also on the shape (spheroid) and on the orientation of the cell with the electric field lines [12]. Changing the field orientation between the different pulses increases the fraction of the cell surface which is permeabilized.

Experimental results obtained either by monitoring conductance changes on cell suspension [13] or by fluorescence observation at the single cell level microscopy [10, 11] shows that the density of the local alterations is strongly controlled by the pulse duration. An increase of the number of pulses first leads to an increase of local permeabilization level.

The field strength controls the geometry of the part of the cell which is permeabilized. This is straightforward for spherical cells (and validated by fluorescence microscopy) but more complicated with other cell shapes. Within this cap, the density of defects is uniform and under the control of the pulse(s) duration.

A-2-2 Cell size

The induced potential is dependent on the size of the cell (Eq (1)). The percentage of electropermeabilized cells in a population, where size heterogeneity is present, increases with an increase in the field strength. The relative part of the cell surface which is permeabilized is larger on a larger cell at a given field strength [13]. Large cells are sensitive to lower field strengths than small one. Plated cells are permeabilized

with E_p value lower than when in suspension. Furthermore large cells in a population appear to be more fragile. An irreversible permeabilization of a subpopulation is observed when low field pulses (but larger than E_p) are applied. Another characteristic is that the 'loading' time is under the control of the cell size [14].

A-3 Forces acting on the membrane

The external electrical field pulse generates a net transient mechanical force which tends to stretch the spherical membrane [15]. This force appears due to Maxwell stresses existing in the spherical dielectric shell which cause deformation. The total radial force acts on the membrane during the transient process and tends to stretch the microorganism. It can even lead to rupture of the membrane resulting in the death of the microorganism [16]. But as the cellular elasticity is based upon the actin cytoskeleton, this stretching would affect the internal cell organization by signal transduction.

B- Structural Investigations

B-1 P31 NMR investigations of the polar head region of phospholipids

NMR of the phosphorus atom in the phosphatidylcholine headgroup was strongly affected when lipid multilayers were submitted to electric field pulses. It is concluded that the conformation of the headgroup was greatly affected while no influence on the structure and dynamics of the hydrocarbon chains could be detected [17]. On electropermeabilized CHO cells, a new anisotropic peak with respect to control cells was observed on 31 P NMR spectroscopic analysis of the phospholipid components [18]. A reorganization of the polar head group region leading to a weakening of the hydration layer may account for these observations. This was also thought to explain the electric field induced long lived fusogenicity of these cells..

B-2 Structural approaches with advanced technologies

Atomic Force Microscopy (AFM) has been extensively used to image live biological samples at the nanoscale cells in absence of any staining or cell preparation. [19]. AFM, in the imaging modes, can probe cells morphological modifications induced by EP. In the force spectroscopy mode, it is possible to follow the nanomechanical properties of a cell and to probe the mechanical modifications induced by EP. transient rippling of membrane surface were observed as consequences of electropermeabilization and a decrease in membrane elasticity by 40% was measured

on living CHO cells [20]. An inner effect affected the entire cell surface that may be related to cytoskeleton destabilization.

Due to the nonlinear and coherent nature of second harmonic generation (SHG) microscopy, 3D radiation patterns from stained neuronal membranes were sensitive to the spatial distribution of scatterers in the illuminated patch, and in particular to membrane defect formation. Higher scatterers (membrane alterations) densities, lasting < 5 milliseconds, were observed at membrane patches perpendicular to the field whereas lower density was observed at partly tangent locations [21, 22]. Higher pore densities were detected at the anodic pole compared to cathodic pole.

Unpublished results using CARS (coherent anti Stokes raman spectroscopy) are indicative of an alteration of the interfacial water molecules.

C-Practical aspects of electropermeabilization

C-1 Sieving of electropermeabilization

Electropermeabilization allows a post-pulse free-like diffusion of small molecules (up to 4 kDa) whatever their chemical nature. Polar compounds cross easily the membrane. But the most important feature is that this reversible membrane organisation is nevertheless long-lived in cells. Diffusion is observed during the seconds and minutes following the ms pulse. Most of the exchange took place after the pulse [10, 11]. Resealing of the membrane defects and of the induced permeabilization is a first order multistep process, which appears to be controlled by protein and organelles reorganisation. But as for other macroscopic damage to a plasma membrane, electropermeabilization has been shown to cause internal vesicles (lysosomes) to undergo exocytosis to repair membrane damage, a calcium mediated process called lysosomal exocytosis. Membrane resealing is thus a cellular process.

C-2 Associated transmembrane exchange

Molecular transfer of small molecules (< 4 kDa) across the permeabilized area is mostly driven by the concentration gradient across the membrane. Electrophoretic forces during the pulse may contribute [10]. Concentration driven diffusion of low weight polar molecules after the pulse can be described by using the Fick equation on its electropermeabilized part [9]. This gives the following expression for a given molecule S and a cell with a radius r:

$$\phi(S,t) = 2\pi r^2 \cdot P_S \cdot \Delta S \cdot X(N,T) \left(1 - \frac{E_{pr}}{E}\right) \exp(-k \cdot (N,T) \cdot t) \quad (4)$$

where $\Phi(S, t)$ is the flow at time t after the N pulses of duration T (the delay between the pulses being short compared to t), P_s is the permeability coefficient of S across the permeabilized membrane and ΔS is the concentration difference of S across the membrane. X is reporting the density of conducting defects in the field affected cap on the cell surface. E_p depends on r (size). The delay between pulses is clearly playing a role in the definition of X but this remains to be investigated in details. Characterization of electropermeabilization is clearly dependent on the transport of S through P_s and the sensibility of its detection. For a given cell, the resealing time (reciprocal of k) is a function of the pulse duration but not of the field intensity as checked by digitised videomicroscopy [9]. A strong control by the temperature is observed. The cytoskeletal integrity should be preserved [24]. Resealing of cell membranes is a complex process which is controlled by the ATP level. Starved cells are fragile. An open question is to know if it is a self-resealing or other components of the cell are involved. Organelle fusion may be involved as in the case of other membrane repair occurring with after laser induced damage.

C-3 Cellular responses

Reactive oxygen species (ROS) are generated at the permeabilized loci, depending on the electric field parameters [25]. These ROS can affect the viability. This is a major drawback for the transfer of sensitive species (nucleic acids). Adding antioxydants is a safe approach [26].

When a cell is permeabilized, an osmotic swelling may result, leading to an entrance of water into the cell. This increase of cell volume is under the control of the pulse duration and of course of the osmotic stress [27].

There is a loss of the bilayer membrane asymmetry of the phospholipids on erythrocytes [28] due to the induced osmotic swelling bringing hemolysis.

When cells are submitted to short lived electric field pulses, a leakage of metabolites from the cytoplasm is observed which may bring a loss in viability. This can occur just after the pulse (short term death) or on a much longer period when cells have resealed (long term death) [23].

CONCLUSION

All experimental observations on cell electropermeabilization are in conflict with a naive model where it is proposed to result from holes punched in a lipid bilayer (see [29] as a recent review). Biochemical modifications such as lipid oxidation may be present as suggested by membrane blebbings formed just after the pulse delivery [30, 31]. Structural changes in the membrane organization supporting

permeabilization remains poorly characterized. New informations appear provided by coarse grained computer-based simulations. Nevertheless it is possible by a careful cell dependent selection of the pulsing parameters to introduce any kind of polar molecules in a mammalian cell while preserving its viability. The processes supporting the transfer are very different for different molecules. Transfer is electrophoretically mediated during the pulse and is mostly present after the pulse driven by diffusion for small charged molecules (drugs) [32, 9]. SiRNA are only transferred by the electrophoretic drag present during the pulse [33]. DNA plasmids are accumulated in spots on the electropermeabilized cell surface during the pulse and slowly translocated in the cytoplasm along the microtubules by a metabolic process [34, 35]

ACKNOWLEDGEMENT

Supports from the CNRS and the region Midi Pyrénées must be acknowledged.

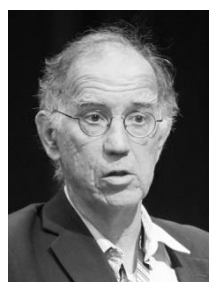
This state of the art in Electropermeabilization is mostly due to the collective work of scientists and students in my former group of "Cell Biophysics" in Toulouse. Discussions with many colleagues were appreciated.

Research conducted in the scope of the EBAM European Associated Laboratory (LEA) and in the framework of COST Action TD1104,

REFERENCES

- [1] Potter, H., *Application of electroporation in recombinant DNA technology*, in *Methods in Enzymology*, vol. 217, I. Academic Press, Editor. 1993.
- [2] Orłowski, S. and L.M. Mir, *Cell electropermeabilization: a new tool for biochemical and pharmacological studies*. *Biochim Biophys Acta*, 1993. 1154(1): 51-63.
- [3] Teissié, J. and M.P. Rols, *An experimental evaluation of the critical potential difference inducing cell membrane electropermeabilization*. *Biophys J*, 1993. 65(1): 409-13.
- [4] Gross, D., L.M. Loew, and W.W. Webb, *Optical imaging of cell membrane potential changes induced by applied electric fields*. *Biophys J*, 1986. 50: 339-48.
- [5] Lojewska, Z., et al., *Analysis of the effect of medium and membrane conductance on the amplitude and kinetics of membrane potentials induced by externally applied electric fields*. *Biophys J*, 1989. 56(1): 121-8.
- [6] Hibino, M., et al., *Membrane conductance of an electroporated cell analyzed by submicrosecond imaging of transmembrane potential*. *Biophys J*, 1991. 59(1): 209-20.
- [7] Pucihar, G., et al., *Electropermeabilization of dense cell suspensions*. *Biophys J*. 2007 36(3): 173-185
- [8] Teissié, J. and T.Y. Tsong, *Electric field induced transient pores in phospholipid bilayer vesicles*. *Biochemistry*, 1981. 20(6): 1548-54.
- [9] Rols, M.P. and J. Teissie, *Electropermeabilization of mammalian cells. Quantitative analysis of the phenomenon*. *Biophys J*, 1990. 58(5): 1089-98.
- [10] Gabriel, B. and J. Teissie, *Direct observation in the millisecond time range of fluorescent molecule asymmetrical*

- interaction with the electropermeabilized cell membrane. *Biophys J*, 1997. 73(5): 2630-7.
- [11] Gabriel, B. and J. Teissie, *Time courses of mammalian cell electropermeabilization observed by millisecond imaging of membrane property changes during the pulse*. *Biophys J*, 1999. 76(4): 2158-65.
- [12] Valič B, Golzio M, Pavlin M, Schatz A, Faurie C, Gabriel B, Teissie J, Rols MP, Miklavčič D. *Effect of electric field induced transmembrane potential on spheroidal cells: theory and experiment*. *Eur. Biophys. J.* **32**: 519-528, 2003
- [13] Kinoshita, K., Jr. and T.Y. Tsong, *Voltage-induced conductance in human erythrocyte membranes*. *Biochim Biophys Acta*, 1979. 554(2): 479-97.
- [14] Sixou, S. and J. Teissie, *Specific electropermeabilization of leucocytes in a blood sample and application to large volumes of cells*. *Biochim Biophys Acta*, 1990. 1028(2): 154-60.
- [15] Winterhalter M and Helfrich W *Deformation of spherical vesicles by electric fields* *J. Colloid Interface Sci.* 1988. 122 583-6
- [16] Harbich W. and Helfrich W *Alignment and opening of giant lecithin vesicles by electric fields* *Z Naturforsch* 1991 34a, , 133-1335.
- [17] Stulen G. *Electric field effects on lipid membrane structure*. *Biochim Biophys Acta.* 1981 ; 640(3):621-7
- [18] Lopez A, Rols MP, Teissie J. *³¹P NMR analysis of membrane phospholipid organization in viable, reversibly electropermeabilized Chinese hamster ovary cells*. *Biochemistry.* 1988 ;27(4):1222-8
- [19] Pillet F, Chopinet L, Formosa C, Dague E *Atomic Force Microscopy and pharmacology: From microbiology to cancerology* *Biochimica et Biophysica Acta* 1840 (2014) 1028-1050
- [20] Chopinet L, Roduit C, Rols MP, Dague E *Destabilization induced by electropermeabilization analyzed by atomic force microscopy* *Biochimica et Biophysica Acta* 2013 1828 2223-2229
- [21] Zalvidea D, Claverol-Tintur'e E *Second Harmonic Generation for time-resolved monitoring of membrane pore dynamics subserving electroporation of neurons* *Biomedical Optics Express* 2011 / Vol. 2, No. 2 / 305-314
- [22] Moen, EK, Iby, BL, Beier HT *Detecting Subtle Plasma Membrane Perturbation in Living Cells Using Second Harmonic Generation Imaging* *Biophysical Journal* 2014 106 L37-L40
- [23] Gabriel, B. and J. Teissie, *Control by electrical parameters of short- and long-term cell death resulting from electropermeabilization of Chinese hamster ovary cells*. *Biochim Biophys Acta*, 1995. 1266(2): 171-8.
- [24] Teissie, J. and M.P. Rols, *Manipulation of cell cytoskeleton affects the lifetime of cell membrane electropermeabilization*. *Ann N Y Acad Sci*, 1994. 720: 98-110.
- [25] Gabriel, B. and J. Teissie, *Generation of reactive-oxygen species induced by electropermeabilization of Chinese hamster ovary cells and their consequence on cell viability*. *Eur J Biochem*, 1994. 223(1): 25-33.
- [26] Markelc B, Tevz G, Cemazar M, Kranjc S, Lavrencak J, Zegura B, Teissie J, Sersa G. *Muscle gene electrotransfer is increased by the antioxidant tempol in mice*. *Gene Ther.* 2011. doi: 10.1038
- [27] Golzio, M., et al., *Control by osmotic pressure of voltage-induced permeabilization and gene transfer in mammalian cells*. *Biophys J*, 1998. 74(6): 3015-22.
- [28] Haest, C.W., D. Kamp, and B. Deuticke, *Transbilayer reorientation of phospholipid probes in the human erythrocyte membrane. Lessons from studies on electroporated and resealed cells*. *Biochim Biophys Acta*, 1997. 1325(1): 17-33.
- [29] Teissie J, Golzio M, Rols MP *Mechanisms of cell membrane electropermeabilization: a minireview of our present (lack of ?) knowledge*. *Biochim Biophys Acta*, 2005 .1724(3): 270-80
- [30] Gass GV, Chernomordik LV *Reversible large-scale deformations in the membranes of electrically-treated cells: electroinduced bleb formation*. *Biochim Biophys Acta.* 1990 1023(1):1-11
- [31] Escande-Géraud ML, Rols MP, Dupont MA, Gas N, Teissie J. *Reversible plasma membrane ultrastructural changes correlated with electropermeabilization in Chinese hamster ovary cells*. *Biochim Biophys Acta.* 1988 939(2):247-59
- [32] Pucihar G, Kotnik T, Miklavcic D, Teissie J. *Kinetics of transmembrane transport of small molecules into electropermeabilized cells* *Biophys J.* 2008; **95**(6) :2837-48
- [33] Paganin-Gioanni A, Bellard E, Escoffre JM, Rols MP, Teissie J, Golzio M. *Direct visualization at the single-cell level of siRNA electrotransfer into cancer cells*. *Proc Natl Acad Sci U S A.* 2011; **108**(26): 10443-7.
- [34] Wolf H, Rols MP, Boldt E, Neumann E, Teissie J. *Control by pulse parameters of electric field-mediated gene transfer in mammalian cells*. *Biophys J.* 1994; **66**(2):524-31.
- [35] Golzio M, Teissie J, Rols MP. *Direct visualization at the single-cell level of electrically mediated gene delivery*. *Proc Natl Acad Sci U S A.* 2002; **99**(3): 1292-7.



Teissie Justin was born 24 March 1947 in Poitiers, France. Got a degree in Physics at the Ecole supérieure de Physique et de Chimie Industrielles de Paris (ESPCI) in 1970. Got a PhD in Macromolecular Chemistry on a project on fluorescence detection of action potential under the supervision of Prof. Monnerie (ESPCI) and Changeux (Institut Pasteur) in 1973. Got a DSC in Biophysics on a project on fluorescence characterisation of Langmuir Blodgett films in Toulouse in 1979. Was a Post Doc at the Medical School of the John Hopkins University in Baltimore in 1979-81. Present position: Directeur de recherches au CNRS emeritus. Author of more than 250 papers.

NOTES

Electric Properties of Tissues and their Changes during Electroporation

Damijan Miklavčič, Nataša Pavšelj

University of Ljubljana, Faculty of Electrical Engineering, Ljubljana, Slovenia

Abstract: Passive electric properties of biological tissues such as permittivity and conductivity are important in applied problems of electroporation. The current densities and pathways resulting from an applied electrical pulse are dictated to a large extent by the relative permittivity and conductivity of biological tissues. We briefly present some theoretical basis for the current conduction in biologic materials and factors affecting the measurement of tissue dielectric properties that need to be taken into account when designing the measurement procedure. Large discrepancies between the data reported by different researchers are found in the literature. These are due to factors such as different measuring techniques used, the fact that macroscopic tissue properties show inhomogeneity, dispersions, anisotropy, nonlinearity, as well as temperature dependence and changes over time. Furthermore, when biological tissue is exposed to a high electric field, changes in their electric properties occur.

INTRODUCTION

The electrical properties of biological tissues and cell suspensions have been of interest for over a century. They determine the pathways of current flow through the body and are thus very important in the analysis of a wide range of biomedical applications. On a more fundamental level, knowledge of these electrical properties can lead to the understanding of the underlying, basic biological processes. To analyze the response of a tissue to electric stimulus, data on the conductivities and relative permittivities of the tissues or organs are needed. A microscopic description of the response is complicated by the variety of cell shapes and their distribution inside the tissue as well as the different properties of the extracellular media. Therefore, a macroscopic approach is most often used to characterize field distributions in biological systems. Moreover, even on a macroscopic level the electrical properties are complicated. They can depend on the tissue orientation relative to the applied field (directional anisotropy), the frequency of the applied field (the tissue is neither a perfect dielectric nor a perfect conductor) or they can be time and space dependent (e.g., changes in tissue conductivity during electroporation) [1]-[3].

BIOLOGICAL MATERIALS IN THE ELECTRIC FIELD

The electrical properties of any material, including biological tissue can be broadly separated into two categories: conducting and insulating. In a conductor the electric charges move freely in response to the application of an electric field whereas in an insulator (dielectric) the charges are fixed and not free to move – the current does not flow.

If a conductor is placed in an electric field, charges will move within the conductor until the resulting internal field is zero. In the case of an insulator, there are no free charges so net migration of charge does not

occur. In polar materials, the positive and negative charge centers in the molecules (e.g. water) do not coincide. An applied field, E_0 , tends to orient the dipoles and produces a field inside the dielectric, E_p , which opposes the applied field. This process is called polarization [4]. Most materials contain a combination of dipoles and free charges. Thus the electric field is reduced in any material relative to its free-space value. The resulting internal field inside the material, E , is then

$$E = E_0 - E_p$$

The resulting internal field is lowered by a significant amount relative to the applied field if the material is an insulator and is essentially zero for a good conductor. This reduction is characterized by a factor ϵ_r , which is called the relative permittivity or dielectric constant, according to

$$E = \frac{E_0}{\epsilon_r}$$

In practice, most materials, including biological tissue, actually display some characteristics of both, insulators and conductors, because they contain dipoles as well as charges which can move, but in a restricted manner.

On a macroscopic level we describe the material as having a permittivity, ϵ , and a conductivity, σ . The permittivity characterizes the material's ability to trap or store charge or to rotate molecular dipoles whereas the conductivity describes its ability to transport charge. The permittivity also helps to determine the speed of light in a material so that free space has a permittivity $\epsilon_0 = 8.85 \times 10^{-12}$ F/m. For other media:

$$\epsilon = \epsilon_r \epsilon_0$$

The energy stored per unit volume in a material, u , and the power dissipated per unit volume, p , are:

$$u = \frac{\epsilon E^2}{2} \quad p = \frac{\sigma E^2}{2}$$

Consider a sample of material which has a thickness, d , and cross-sectional area, A (Figure 1).

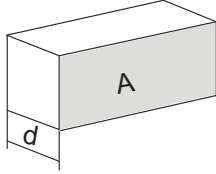


Figure 1: A considered theoretical small part of a material.

If the material is an insulator, then we treat the sample as a capacitor with capacitance (C); if it is a conductor, then we treat it as a conductor with conductance (G):

$$C = \epsilon \cdot A/d \quad G = \sigma \cdot A/d$$

A simple model for a real material, such as tissue, would be a parallel combination of the capacitor and conductor. If a constant (DC) voltage V is applied across this parallel combination, then a conduction current $I_C = GV$ will flow and an amount of charge $Q = CV$ will be stored. However, if an alternating (AC) voltage was applied to the combination:

$$V(t) = V_0 \cos(\omega t)$$

The charge on the capacitor plates is now changing with frequency f . We characterize this flow as a displacement current:

$$I_d = \frac{dQ}{dt} = -\omega CV_0 \sin(\omega t)$$

The total current flowing through the material is the sum of the conduction and displacement currents, which are 90° apart in phase. The total current is $I = I_C + I_d$, hence

$$I = GV + C \cdot dV/dt = (\sigma + i\omega\epsilon)A \cdot V/d$$

The actual material, then, can be characterized as having an admittance, Y^* , given by:

$$Y^* = G + i\omega C = (A/d)(\sigma + i\omega\epsilon)$$

where $*$ indicates a complex-valued quantity. In terms of material properties we define a corresponding, complex-valued conductivity

$$\sigma^* = (\sigma + i\omega\epsilon)$$

Describing a material in terms of its admittance emphasizes its ability to transport current. Alternatively, we could emphasize its ability to restrict the flow of current by considering its impedance $Z^* = 1/Y^*$, or for a pure conductance, its resistance, $R = 1/G$.

We can also denote total current as:

$$I = (\epsilon_r - \frac{i\sigma}{\omega\epsilon_0}) i\omega\epsilon_0 A/d = C \frac{dV}{dt}$$

We can define a complex-valued, relative permittivity:

$$\epsilon^* = \epsilon_r - \frac{i\sigma}{\omega\epsilon_0} = \epsilon_r' - i\epsilon_r''$$

with $\epsilon_r' = \epsilon_r$ and $\epsilon_r'' = \sigma/(\omega\epsilon_0)$. The complex conductivity and complex permittivity are related by:

$$\sigma^* = i\omega\epsilon^* = i\omega\epsilon_0\epsilon_r^*$$

We can consider the conductivity of a material as a measure of the ability of its charge to be transported throughout its volume in a response to the applied electric field. Similarly, its permittivity is a measure of the ability of its dipoles to rotate or its charge to be stored in response to the applied field. Note that if the permittivity and conductivity of the material are constant, the displacement current will increase with frequency whereas the conduction current does not change. At low frequencies the material will behave like a conductor, but capacitive effects will become more important at higher frequencies. For most materials, however, σ^* and ϵ^* are frequency-dependent. Such a variation is called dispersion and is due to the dielectric relaxation – the delay in molecular polarization following changing electric field in a material. Biological tissues exhibit several different dispersions over a wide range of frequencies [4].

Dispersions can be understood in terms of the orientation of the dipoles and the motion of the charge carriers. At relatively low frequencies it is relatively easy for the dipoles to orient in response to the change in applied field whereas the charge carriers travel larger distances over which there is a greater opportunity for trapping at a defect or interface like cell membrane [5]. The permittivity is relatively high and the conductivity is relatively low. As the frequency increases, the dipoles are less able to follow the changes in the applied field and the corresponding polarization disappears. In contrast, the charge carriers travel shorter distances during each half-cycle and are less likely to be trapped. As frequency increases, the permittivity decreases and, because trapping becomes less important, the conductivity increases. In a heterogeneous material, such as biological tissue, several dispersions are observed as illustrated in Figure 2. In short, alpha dispersion in the kilohertz range is due to cell membrane effects such as gated channels and ionic diffusion and is the first of the dispersions to disappear with tissue death. Beta dispersion can be observed around the megahertz range due to the capacitive charging of cell membranes. Above beta dispersion the impedance of cell membranes drops drastically, allowing the electric current to pass through not only extracellular, but also intracellular space. This dispersion is particularly interesting as it is also

apparent in the conductivity of the material. The last, gamma dispersion (above the gigahertz range) is due to dipolar mechanisms of water molecules in the material.

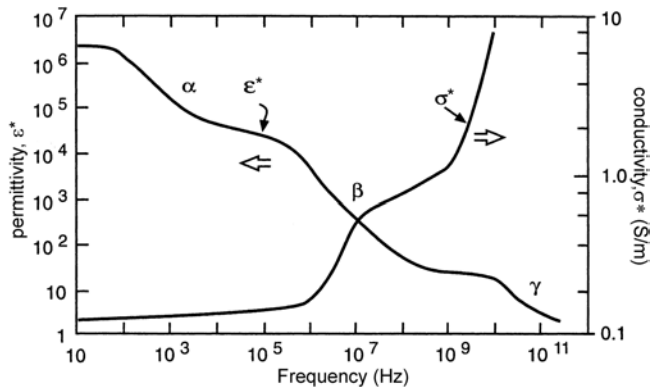


Figure 2: Typical frequency dependence of the complex permittivity and complex conductivity of a heterogeneous material such as biological tissue.

DIELECTRIC MEASUREMENTS OF TISSUES

There is a large discrepancy between various data on electrical properties of biological materials found in the literature. The measurement of tissue dielectric properties can be complicated due to several factors, such as tissue inhomogeneity, anisotropy, the physiological state of the tissue, seasonal, age and disease-linked changes and electrode polarization [1].

Inhomogeneity of tissues

Tissue is a highly inhomogeneous material. The cell itself is comprised of an insulating membrane enclosing a conductive cytosol. A suspension of cells can be regarded at low frequencies simply as nonconducting inclusions in a conducting fluid [6]. The insulation is provided by the cell membrane. At frequencies in the MHz range capacitive coupling across this membrane becomes more important, allowing the electric current to pass not only around the cell, but also through it. In tissue, the cells are surrounded by an extracellular matrix, which can be extensive, as in the case of bone, or minimal, as in the case of epithelial tissue. Tissue does not contain cells of a single size and function. The tissue is perfused with blood and linked to the central nervous system by neurons. It is thus difficult to extrapolate from the dielectric properties of a cell suspension to those of an intact tissue.

Anisotropy of tissues

Some biological materials, such as bone and skeletal muscle, are anisotropic. Therefore, when referring to measured conductivity and permittivity values, one needs to include data on the orientation of the electrodes relative to the major axis of the tissue; e.g., longitudinal, transversal or a combination of both. For example, muscles are composed of fibers, very

large individual cells aligned in the direction of muscle contraction. Electrical conduction along the length of the fiber is significantly easier than conduction in the direction perpendicular to the fibers. Therefore, muscle tissue manifests typical anisotropic electric properties. The longitudinal conductivity is significantly higher than the transverse conductivity (can be up to 8 times higher).

Moreover, tissue anisotropy is frequency dependent. Namely, if the frequency of the current is high enough, the anisotropic properties disappear. Specifically for muscle tissue, that happens in the MHz frequency range, i.e. at beta dispersion.

Physiological factors and changes of tissue

Any changes in tissue physiology should produce changes in the tissue electrical properties. This principle has been used to identify and/or monitor the presence of various illnesses or conditions [7].

Tumors generally have higher water content than normal cells because of cellular necrosis but also irregular and fenestrated vascularization. Higher conductivity of tumors in the MHz frequency range could lead to their selective targeting by radio-frequency hyperthermia treatment [8]. In addition, there may be differences in the membrane structure. Also, fat is a poorer conductor of electricity than water. Changes in the percentage of body fat or water are reflected in tissue impedance changes [7].

Further, tissue death or excision results in significant changes in electrical properties. Tissue metabolism decreases after the tissue has been excised and often the temperature falls. If the tissue is supported by temperature maintenance and perfusion systems, the tissue may be stabilized for a limited period of time in a living state in vitro (ex vivo). If the tissue is not supported, however, irreversible changes will occur, followed by cell and tissue death. For these reasons considerable caution must be taken in the interpretation of electrical measurements which were performed on excised tissues.

The electrical properties of tissue also depend on its temperature. The mobility of the ions which transport the current increases with the temperature as the viscosity of the extracellular fluid decreases. The rapid increase of conductivity with temperature was suggested to be used e.g. to monitor the progress of hyperthermia treatment. Also, possible other changes, such as cell swelling and edema, or blood flow occlusion, all affect tissue properties.

Electrode polarization

Electrode polarization is a manifestation of molecular charge organization which occurs at the tissue/sample-electrode interface in the presence of

water molecules and hydrated ions. The effect increases with increasing sample conductivity.

In a cell suspension a counterion layer can form at each electrode. The potential drop in this layer reduces the electric field available to drive charge transport in the bulk suspension, resulting in apparently lower suspension conductivity. As the frequency increases, the counterion layer is less able to follow the changes in the applied signal, the potential drop at the sample-electrode interface decreases, and the apparent conductivity of the suspension increases. Thus electrode polarization is more pronounced at lower frequencies.

The process is more complicated in tissue. Insertion of electrodes can first cause the release of electrolytes due to trauma from the surrounding tissue and later the development of a poorly-conductive wound region may occur. This region can shield part of the electrode from the ionic current and thus reduce the polarization effects compared to an ionic solution equivalent in conductivity to the intracellular fluid.

The material of the electrode plays an important part in determining its polarization impedance, the relative importance of which decreases with increasing frequency. It is considered a good practice to measure tissue impedance *in-vivo* after waiting a sufficient time for the electrode polarization processes to stabilize. A typical time might be on the order of thirty minutes.

Two different electrode set-ups are used to measure the electric properties of biological materials; the two-electrode and the four-electrode method.

Two-electrode method: Suitable for alternating current (AC) measurements. Cannot be used as such for direct current (DC) measurements because of the electrode polarization, which consequently gives incorrect results for the conductivity of the sample between the electrodes. For AC measurements the frequency range over which electrode polarization is important depends to some extent on the system being measured and the electrode material. For cell suspensions it is important up to nearly 100 kHz whereas for tissue measured *in vivo* it is significant only up to about 1 kHz. By varying the separation of the electrodes, the contribution of the electrode polarization can be determined and eliminated.

Four-electrode method: Can be used for both DC and AC measurements. Two pairs of electrodes are used: the outer, current electrodes and the inner, voltage electrodes. The current from the source passes through the sample. Voltage electrodes of known separation are placed in the sample between the current electrodes. By measuring the current as the voltage drop across a resistor in series with the sample and the voltage drop across the inner electrodes, one can determine the conductivity of the sample between the

inner electrodes. The advantage of this method is that the polarization on the current electrodes has no influence on the voltage difference between the voltage electrodes. Polarization at the voltage electrodes is negligible for both DC and AC due to the high input impedance of the measurement system.

ELECTRICAL RESPONSE OF TISSUE TO ELECTRIC FIELD

Changes in tissue conductivity have been observed *in vivo* if the tissue is subjected to a high enough electric field. Having said that, we can use the dielectric properties of liver and try to calculate the theoretical electrical response to a short rectangular voltage pulse having the duration of 100 μs and the rise time of 1 μs (typical pulse parameters used for electrochemotherapy). We used the parallel RC circuit to model the electrical response of the tissue (see Figure 3).

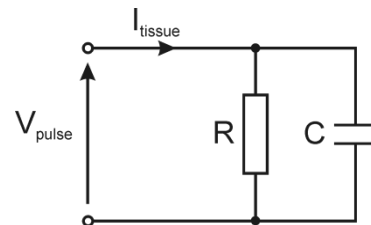


Figure 3: Parallel RC circuit: a theoretical representation of tissue response to electric pulses.

The complications arise from the facts that i) the pulse parameters (the pulse duration, the rise and the fall time) determine the span of its frequency spectrum and ii) the tissue conductivity and permittivity are frequency dependent. The obtained response for the first pulse is presented in Figure 4. At the onset of voltage pulse, capacitive transient displacement current is observed. As membranes charge, voltage across them rises and the measured current decreases. Soon steady state is reached and current stabilizes through the conductance of extracellular fluid. Since the model describing dielectric dispersions is linear, change of the applied voltage proportionally scales the amplitude of the current.

We can compare this calculated response with the measured response on rat liver *in vivo* for the same pulse as above and different pulse amplitudes spanning up to electroporative field strengths (Figure 5) [9]. For the lowest applied voltage we can see a good agreement with calculated response. As the field intensity is increased, the electrical response of tissue is no longer linear and increase of conductivity during the pulse is observed. Measuring the passive electrical properties

of electroporated tissues could provide real time feedback on the outcome of the treatment [9], [10].

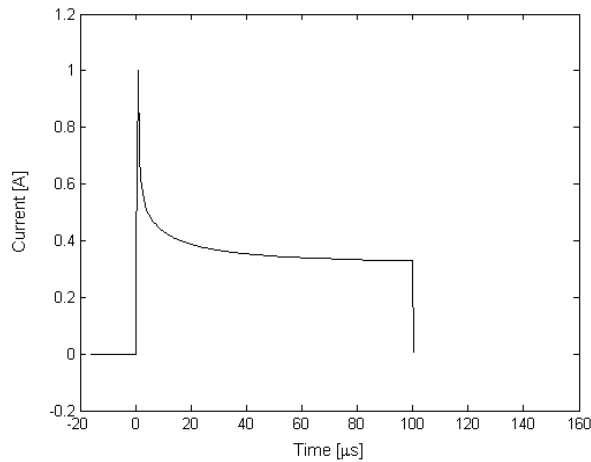


Figure 4: Calculated tissue response during delivery of rectangular voltage pulse with the duration of 100 μs having the rise time of 1 μs and the amplitude of 120 V. Plate electrodes with 4.4 mm interelectrode distance were assumed.

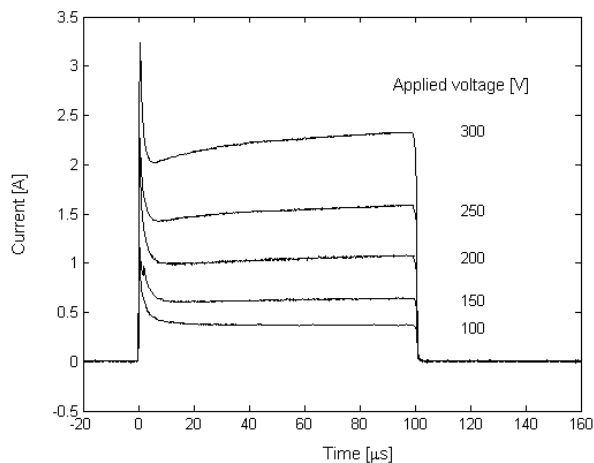


Figure 5: Measured tissue response during delivery of 100 μs rectangular pulses of different amplitudes to rat liver *in vivo*. Adapted from Cukjati *et al.* [9]. Pulses were generated using Jouan GHT1287B; plate electrodes with 4.4 mm interelectrode distance were used.

The measured response is consistent with the hypothesis that the bulk tissue conductivity should also increase measurably since on a cellular level electroporation causes the increase of membrane conductance [11]-[15]. In measuring *ex vivo* tissue and phantom tissue made of gel like material [16] using MREIT we were able to demonstrate that electric conductivity changes due to membrane electroporation are amplitude dependent and occur in tissue only but not in phantom tissue. It is not clear, however, to which value tissue conductivity increases as a consequence of

plasma membrane electroporation. It has been stipulated that this could be close to the value in beta dispersion range [17].

Further, in applications where electric pulses to skin or tissues underneath (such as subcutaneous tumor) are applied externally, through skin, one might expect high (too high) voltage amplitudes needed in order to breach the highly resistive skin tissue and permeabilize tissues underneath. Namely, tissues between the electrodes can be seen as serially connected resistors. Applying voltage on such a circuit (voltage divider) causes the voltage to be distributed between the resistors proportionally to their resistivities [18]. Upon applying electric pulses, almost the entire applied voltage thus rests across the most resistive (least conductive) tissue, in our case skin. That means a very high electric field in skin tissue, while the electric field in other tissues stays too low for a successful cell electroporation. If our goal is the electrochemotherapy of the underlying tumor, one might wonder how a successful electrochemotherapy of subcutaneous tumors is possible when external plate electrodes are used. The answer lies in the increase in bulk conductivities of tissues during electroporation, a phenomenon that was also observed *in vivo*. This conductivity increase leads to a changed electric field distribution, which exposes the tumor to an electric field high enough for a successful cell membrane permeabilization [19]. To further support this hypothesis, we described this process with a numerical model, taking into account the changes of tissue bulk electrical properties during the electroporation. In Figure 6 six steps of the electroporation process in the subcutaneous tumor model for the voltage of 1000 V between the electrodes are shown. The electric field distribution is shown in V/cm. Step 0 denotes the electric field distribution as it was just before the electroporation process started, thus when all the tissues still had their initial conductivities. When the voltage is applied to the electrodes, the electric field is distributed in the tissue according to conductivity ratios of the tissues in the model. The field strength is the highest in the tissues with the lowest conductivity, where the voltage drop is the largest, and the voltage gradient the highest. In our case, almost the entire voltage drop occurs in the skin layer which has a conductivity of about 10-100 times lower than the tissues lying underneath.

If we look at the last step of the sequential analysis, step 5, at 1000 V (Figure 6) the tumor is entirely permeabilized, in some areas the electric field is also above the irreversible threshold.

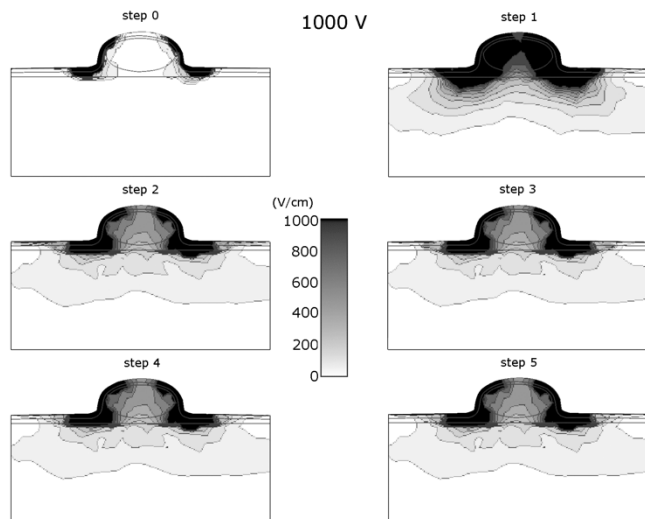


Figure 6: Six steps of the sequential analysis of the electroporation process in the subcutaneous tumor model at 1000 V between two plate electrodes with distance of 8 mm [19]. Time intervals between steps are in general not uniform. Different steps follow a chronological order but do not have an exact time value associated with them. The electric field distribution is shown in V/cm.

A similar situation can be encountered when applying electric pulses on a skin fold with external plate electrodes as a method to enhance *in vivo* gene transfection in skin [20]. Skin consists of three main layers: epidermis, dermis and subcutaneous tissue (Figure 7). Skin epidermis is made up of different layers, but the one that defines its electrical properties the most is the outermost layer, the stratum corneum. Although very thin (typically around 20 μm), it contributes a great deal to the electrical properties of skin. Its conductivity is three to four orders of magnitude lower than the conductivities of deeper skin layers. Again, when electric pulses are applied on skin fold through external plate electrodes, almost the entire applied voltage rests across the stratum corneum, which causes a very high electric field in that layer, while the electric field in deeper layers of skin – the layers targeted for gene transfection – stays too low. Similarly as in the case of subcutaneous tumors, the increase in bulk conductivities of skin layers during electroporation exposes the skin layers below stratum corneum to an electric field high enough for a successful permeabilization [21].

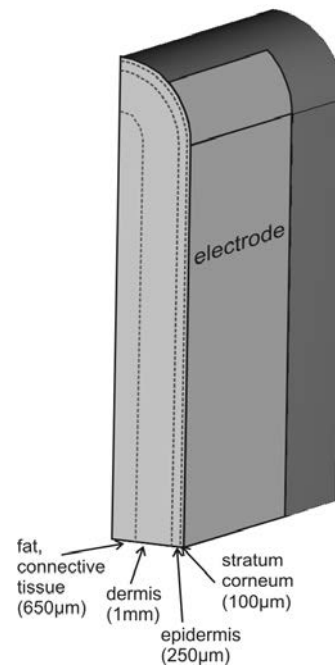


Figure 7: Schematics of a skinfold as described in a numerical model. Only one quarter of the skinfold is presented here.

Theoretical explanation of the process of electroporation offers useful insight into the understanding of the underlying biological processes and allows for predicting the outcome of the treatment [22]-[24]. Therefore, due effort needs to be invested into measurements of tissue electrical properties and their changes during electroporation [25].

Further, one of the concerns associated with electroporation could be the amount of resistive heating in the tissue. Excessive heating is unwanted not only to avoid skin burns and assure patient safety, but also to avoid damage to viable cells. Potential excess of the resistive heating during electroporation has been demonstrated [26], therefore thermal aspect in treatment planning and theoretical analysis of specific applications of electroporation-based treatments should be considered [27]. In order to stay within the safety limit while achieving successful treatment, heating needs to be estimated, by means of theoretical models, as a part of treatment planning [28]-[31].

REFERENCES

- [1] D. Miklavčič, N. Pavšelj, FX Hart. Electric Properties of Tissues. Wiley Encyclopedia of Biomedical Engineering, John Wiley & Sons, New York, 2006.
- [2] K.R. Foster and H.P. Schwan. Dielectric properties of tissues and biological materials: a critical review. *Critical Reviews in Biomedical Engineering* 17: 25-104, 1989.
- [3] C. Gabriel, A. Peyman and E.H. Grant. Electrical conductivity of tissue at frequencies below 1 MHz. *Phys. Med. Biol.* 54(16): 4863-4878, 2009.
- [4] Applied Bioelectricity, From Electrical Stimulation to Electropathology, J. Patrick Reilly, Springer-Verlag New York, 1998.
- [5] Kyle C. Smith and James C. Weaver. Electrodiffusion of Molecules in Aqueous Media: A Robust, Discretized Description for Electroporation and Other Transport Phenomena. *IEEE Trans. Biomed. Eng.* 59(6), 1514-1522, 2012.
- [6] S. Huclova, D. Erni and J. Frohlich. Modelling and validation of dielectric properties of human skin in the MHz region focusing on skin layer morphology and material composition. *J. Phys. D: Appl. Phys.* 45(2): 025301, 2012.
- [7] F.X. Hart. Bioimpedance in the clinic. *Zdravniški vestnik-Slovenian Medical Journal* 78(12): 782-790, 2009.
- [8] A. Peyman, B. Kos, M. Djokić, B. Trotošek, C. Limbaeck-Stokin, G. Serša, D. Miklavčič. Variation in dielectric properties due to pathological changes in human liver. *Bioelectromagnetics* 36: 603-612, 2015.
- [9] D. Cukjati, D. Batiuskaite, D. Miklavčič, L.M. Mir. Real time electroporation control for accurate and safe *in vivo* nonviral gene therapy. *Bioelectrochemistry* 70: 501-507, 2007.
- [10] A. Ivorra and B. Rubinsky. *In vivo* electrical impedance measurements during and after electroporation of rat liver. *Bioelectrochemistry* 70: 287-295, 2007.
- [11] M. Pavlin, D. Miklavčič. Effective conductivity of a suspension of permeabilized cells: A theoretical analysis. *Biophys. J.* 85: 719-729, 2003.
- [12] M. Pavlin, M. Kanduser, M. Rebersek, G. Pucihar, F.X. Hart, R. Magjarevic and D. Miklavcic. Effect of cell electroporation on the conductivity of a cell suspension. *Biophys. J.* 88: 4378-4390, 2005.
- [13] A. Ivorra, B. Al-Sakere B, B. Rubinsky and L.M. Mir. *In vivo* electrical conductivity measurements during and after tumor electroporation: conductivity changes reflect the treatment outcome. *Phys. Med. Biol.* 54(19):5949-5963, 2009.
- [14] Y. Granot, A. Ivorra, E. Maor and B. Rubinsky. *In vivo* imaging of irreversible electroporation by means of electrical impedance tomography. *Phys. Med. Biol.* 54(16): 4927-4943, 2009.
- [15] M. Essone Mezeme, G. Pucihar, M. Pavlin, C. Brosseau, D. Miklavčič. A numerical analysis of multicellular environment for modeling tissue electroporation. *Appl. Phys. Lett.* 100: 143701, 2012.
- [16] M. Kranjc, F. Bajd, I. Serša, D. Miklavčič. Magnetic resonance electrical impedance tomography for measuring electrical conductivity during electroporation. *Physiol. Meas.* 35: 985-996, 2014.
- [17] R.E. Neal, P.A. Garcia, J.L. Robertson, R.V. Davalos. Experimental Characterization and Numerical Modeling of Tissue Electrical Conductivity during Pulsed Electric Fields for Irreversible Electroporation Treatment Planning. *IEEE Trans. Biomed. Eng.* 59(4): 1076 – 1085, 2012.
- [18] N. Pavšelj, D. Miklavčič. Numerical modeling in electroporation-based biomedical applications. *Radiol. Oncol.* 42:159-168, 2008.
- [19] N. Pavšelj, Z. Bregar, D. Cukjati, D. Batiuskaite, L.M. Mir and D. Miklavčič. The course of tissue permeabilization studied on a mathematical model of a subcutaneous tumor in small animals. *IEEE Trans. Biomed. Eng.* 52(8):1373-1381, 2005.
- [20] N. Pavšelj and V. Prát. DNA electrotransfer into the skin using a combination of one high- and one low-voltage pulse. *Journal of Controlled Release* 106:407-415, 2005.
- [21] N. Pavšelj, V. Prát, D. Miklavčič. A numerical model of skin electroporeabilization based on *in vivo* experiments. *Annals Biomed. Eng.* 35:2138-2144, 2007.
- [22] D. Miklavčič, M. Snoj, A. Županič, B. Kos, M. Čemažar, M. Kropivnik, M. Bračko, T. Pečnik, E. Gadžijev, G. Serša. Towards treatment planning and treatment of deep-seated solid tumors by electrochemotherapy. *Biomed. Eng. Online* 9: 10, 2010.
- [23] Edhemović I, Gadžijev EM, Breclj E, Miklavčič D, Kos B, Županič A, Mali B, Jarm T, Pavliha D, Marčan M, Gašljevič G, Gorjup V, Mušič M, Pečnik Vavpotič T, Čemažar M, Snoj M, Serša G. Electrochemotherapy: A new technological approach in treatment of metastases in the liver. *Technol. Cancer Res. Treat.* 10: 475-485, 2011.
- [24] A. Županič, B. Kos, D. Miklavčič- Treatment planning of electroporation-based medical interventions: electrochemotherapy, gene electrotransfer and irreversible electroporation. *Phys. Med. Biol.* 57: 5425-5440, 2012.
- [25] J. Langus, M. Kranjc, B. Kos, M. Šuštar, D. Miklavčič. Dynamic finite-element model for efficient modelling of electric currents in electroporated tissue. *Sci. Rep.* 6: 26409, 2016.
- [26] I. Lacković, R. Magjarević, D. Miklavčič. Three-dimensional finite-element analysis of joule heating in electrochemotherapy and *in vivo* gene electrotransfer. *IEEE T. Diel. El. Insul.* 15: 1338-1347, 2009.
- [27] B. Kos, P. Voigt, D. Miklavčič, M. Moche. Careful treatment planning enables safe ablation of liver tumors adjacent to major blood vessels by percutaneous irreversible electroporation (IRE). *Radiol. Oncol.* 49: 234-241, 2015.
- [28] Pavšelj N, Miklavčič D. Resistive heating and electroporeabilization of skin tissue during *in vivo* electroporation: A coupled nonlinear finite element model. *Int. J. Heat Mass Transfer* 54: 2294-2302, 2011.
- [29] Županič A, Miklavčič D. Tissue heating during tumor ablation with irreversible electroporation. *Elektroteh. Vestn.* 78: 42-47, 2011.
- [30] Robert E. Neal II, Paulo A. Garcia, John L. Robertson, Rafael V. Davalos, Experimental Characterization and Numerical Modeling of Tissue Electrical Conductivity during Pulsed Electric Fields for Irreversible Electroporation Treatment Planning *IEEE Trans. Biomed. Eng.* 59(4), 1076-1085, 2012.
- [31] P.A. Garcia, R.V. Davalos, D. Miklavčič. A numerical investigation of the electric and thermal cell kill distributions in electroporation-based therapies in tissue. *PLOS One* 9(8): e103083, 2014.

ACKNOWLEDGEMENT

This work was supported by the Slovenian Research Agency and the European Commission and performed in the scope of LEA EBAM.



Damijan Miklavčič was born in Ljubljana, Slovenia, in 1963. He received a Masters and a Doctoral degree in Electrical Engineering from University of Ljubljana in 1991 and 1993, respectively. He is currently Professor and the Head of the Laboratory of Biocybernetics at the Faculty of Electrical Engineering, University of Ljubljana.

His research areas are biomedical engineering and study of the interaction of electromagnetic fields with biological systems. In the last years he has focused on the engineering aspects of electroporation as the basis of drug delivery into cells in tumor models *in vitro* and *in vivo*. His research includes biological experimentation, numerical modeling and hardware development for electrochemotherapy, irreversible electroporation and gene electrotransfer.



Nataša Pavšelj was born in Slovenia, in 1974. She received her B.Sc., M.Sc. and Ph.D. degrees from the University of Ljubljana in 1999, 2002 and 2006, respectively. Her main research interests lie in the field of electroporation, including finite element numerical modeling of electric field distribution in different biological

tissue setups (subcutaneous tumors, skin fold) and comparison of the theoretical results with the experimental work. In recent years Nataša Pavšelj is interested in transdermal drug delivery by means of electroporation and modeling of mass transport, heat transfer and electric phenomena.

NOTES

Nucleic acids electrotransfer in vitro: what imaging can tell us about the mechanisms of uptake

Marie-Pierre Rols

Institut de Pharmacologie et de Biologie Structurale, Toulouse, France

Abstract: Cell membranes can be transiently permeabilized under application of electric pulses. This process, called electroporation, allows hydrophilic molecules, such as anticancer drugs and DNA, to enter into cells and tissues. Electroporation is nowadays used in clinics to treat cancers. Vaccination and gene therapy are other fields of application of DNA electrotransfer. Open questions exist about the behavior of the membranes both while the field is on (μ s to ms time range) and after its application (from seconds to several minutes and hours). Also, there is a lack of understanding on how molecules are transported in complex environments, such as those found in tissues. As our objectives are to give a complete molecular description of the mechanisms, our strategy is to use different complementary systems with increasing complexities (model membranes, cells in 2D and 3D culture, spheroids and tissues in living mice) and different microscopy tools to analyze the processes. Single cell imaging experiments revealed that the uptake of molecules (nucleic acids, antitumor drugs) takes place in well-defined membrane regions and depends on their chemical and physical properties (size, charge). If small molecules freely cross the electroporated membrane and have a free access to the cytoplasm, heavier molecules, such as plasmid DNA, face physical barriers (plasma membrane, cytoplasm crowding, nuclear envelope) which reduce transfection efficiency and engender a complex mechanism of transfer. Gene electrotransfer requires that the DNA is present during the application of the electric field pulses and involves different steps, occurring over relatively large time scales. As will be presented, these steps include the initial interaction with the electroporated membrane, the crossing of the membrane, the transport within the cell and finally gene expression.

INTRODUCTION

The use of electroporation to deliver therapeutic molecules including drugs, proteins and nucleic acids in a wide range of cells and tissues has been developed over the last decade (1-5). This strategy is nowadays used in clinics to treat cancers. Vaccination and oncology gene therapy are also major fields of application of DNA electrotransfer (6, 7). Translation of preclinical studies into clinical trials in human and veterinary oncology has started (8-10). The first phase I dose escalation trial of plasmid interleukin electroporation has been carried out in patients with metastatic melanoma and has shown encouraging results (11). The method has also been successfully used for the treatment of dogs and horses (8, 12). But the safe and efficient use of this physical method for clinical purposes requires the knowledge of the mechanisms underlying the electroporation phenomena. Despite the fact that the pioneering work on plasmid DNA electrotransfer in cells was initiated 34 years ago (13), many of the mechanisms underlying DNA electrotransfer remain to be elucidated (14, 15). Even if *in vitro* electrotransfer is efficient in almost all cell lines, *in vivo* gene delivery and expression in tumors are usually not. It is still mandatory, for increasing gene transfer and expression, to increase our knowledge of the process. Our strategy consists on using different imaging tools, to directly visualize the processes, and different experimental models with increasing complexities.

MEMBRANE ELECTROPORATION

The use of video microscopy allows visualization of the permeabilization phenomenon at the single cell level. Propidium iodide uptake in the cytoplasm is a fast process that can be detected seconds after the application of electric pulses. Exchange across the permeabilized membrane is not homogeneous on the whole cell membrane. It occurs at the sides of the cells facing the electrodes in an asymmetrical way where it is more pronounced at the anode-facing side of the cells than at the cathode (Figure 1), i.e. in the hyperpolarized area than in the depolarized area, which is in agreement with theoretical considerations.

Electroporation can be described as a 3-step process in respect with electric field: (i) before electroporation, the plasma membrane acts as a physical barrier that prevents the free exchange of hydrophilic molecules between the cell cytoplasm and external medium; (ii) during electroporation, the transmembrane potential increases which induces the formation of transient permeable structures facing the electrodes and allows the exchange of molecules; (iii) after electroporation, membrane resealing occurs.

A direct transfer into the cell cytoplasm of the negatively charged small molecules such as siRNA is observed on the side facing the cathode. When added after electroporation, siRNA do not penetrate the cells. Therefore, electric field acts on both the permeabilization of the membrane and on the electrophoretic drag of the charged molecules from the

bulk into the cytoplasm. The mechanism involved is clearly specific for the physico-chemical properties of the electrotransferred molecule (16).

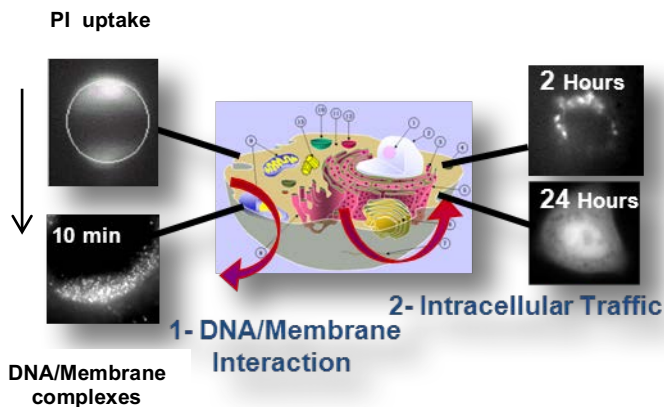


Figure 1: Molecule electrotransfer mechanisms. Left: During electric pulses application: Plasma membrane is electroporabilized facing the 2 electrodes (PI uptake). DNA aggregates are formed. This interaction takes place only on the membrane facing the cathode. Right: About 2 h after electric pulses application, DNA molecules are present around the nucleus. Finally, eGFP expression is detected for hours. The arrow indicates the direction of the electric field.

Progress in the knowledge of the involved mechanisms is still a biophysical challenge. One of our objectives was to detect and visualize at the single-cell level the incidence of phospholipid scrambling and changes in membrane order (17, 18). The pulses induced the formation of long-lived permeant structures and resulted in a rapid phospholipid flip/flop within less than 1s and were exclusively restricted to the regions of the permeabilized membrane. Our results could support the existence of direct interactions between the movement of membrane zwitterionic phospholipids and the electric field. We also performed experiments on lateral mobility of proteins and showed that electroporation affects the lateral mobility of Rae-1, a GPI anchored protein. Our results suggest that 10-20 % of the membrane surface is occupied by defects or pores and that these structures propagate rapidly over the cell surface.

We also took advantage of atomic force microscopy to directly visualize the consequences of electroporation and to locally measure the membrane elasticity. We visualized transient rippling of membrane surface and measured a decrease in membrane elasticity. Our results obtained both on fixed and living CHO cells give evidence of an inner effect affecting the entire cell surface that may be related to cytoskeleton destabilization. Thus, AFM appears as a useful tool to investigate basic process of electroporation on living cells in absence of any staining (19, 20).

MECHANISMS OF ELECTROTRANSFER OF DNA MOLECULES INTO CELLS

Single-cell microscopy and fluorescent plasmids can be used to monitor the different steps of electrotransfection (16, 21, 22). DNA molecules, which are negatively charged, migrate electrophoretically when submitted to the electric field. Under electric fields which are too small to permeabilize the membrane, the DNA simply flows around the membrane in the direction of the anode. Beyond a critical field value, above which cell permeabilization occurs, the DNA interacts with the plasma membrane.

1) DNA/Membrane interaction

This interaction only occurs at the pole of the cell opposite the cathode and this demonstrates the importance of electrophoretic forces in the initial phase of the DNA/membrane interaction. When the DNA-membrane interaction occurs, one observes the formation of “microdomains” whose dimensions lie between 0.1 and 0.5 μm (Figure 1). Also seen are clusters or aggregates of DNA which grow during the application of the field. However once the field is cut the growth of these clusters stops. DNA electrotransfer can be described as a multi-step-process: the negatively charged DNA migrates electrophoretically towards the plasma membrane on the cathode side where it accumulates.

This interaction, which is observed for several minutes, lasts much longer than the duration of the electric field pulse. Translocation of the plasmid from the plasma membrane to the cytoplasm and its subsequent passage towards the nuclear envelope take place with a kinetics ranging from minutes to hours (23). When plasmid has reached the nuclei, gene expression can take place and this can be detected up to several days in the case of dividing cells or weeks in some tissues such as muscles.

The dynamics of this process has been poorly understood because direct observations have been limited to time scales that exceed several seconds. We studied experimentally the transport of two types of molecules into cells (plasmid DNA and propidium iodide) which are relevant for gene therapy and chemotherapy with a temporal resolution of 2 ms allowing the visualization of the DNA/membrane interaction process during pulse application (24). DNA molecules interact with the membrane during the application of the pulse. At the beginning of the pulse application plasmid complexes or aggregates appear at sites on the cell membrane. The formation of plasmid complexes at fixed sites suggests that membrane domains may be responsible for DNA uptake and their lack of mobility could be due to their interaction with the actin cytoskeleton. Data reported evidences for the involvement of cytoskeleton (Figure 2). Actin indeed

polymerizes around the DNA/membrane complexes (25-28).

We also investigated the dependence of DNA/membrane interaction and gene expression on electric pulse polarity, repetition frequency and duration. Both are affected by reversing the polarity and by increasing the repetition frequency or the duration of pulses (29, 30). The results revealed the existence of 2 classes of DNA/membrane interaction: (i) a metastable DNA/membrane complex from which DNA can leave and return to external medium and (ii) a stable DNA/membrane complex, where DNA cannot be removed, even by applying electric pulses of reversed polarity. Only DNA belonging to the second class leads to effective gene expression (29).

2) Intracellular traffic of plasmid DNA.

Even if the first stage of gene electrotransfection, i.e. migration of plasmid DNA towards the electropermeabilised plasma membrane and its interaction with it, becomes understood we are not totally able to give guidelines to improve gene electrotransfer. Successful expression of the plasmid depends on its subsequent migration into the cell. Therefore, the intracellular diffusional properties of plasmid DNA, as well as its metabolic instability and nuclear translocation, represent other cell limiting factors that must be taken into account (31). The cytoplasm is composed of a network of microfilament and microtubule systems, along with a variety of subcellular organelles present in the cytosol. The mesh-like structure of the cytoskeleton, the presence of organelles and the high protein concentration means that there is substantial molecular crowding in the cytoplasm which hinders the diffusion of plasmid DNA. These apparently contradictory results might be reconciled by the possibility of a disassembly of the cytoskeleton network that may occur during electropermeabilisation, and is compatible with the idea that the cytoplasm constitutes an important diffusional barrier to gene transfer. In the conditions induced during electropermeabilisation, the time a plasmid DNA takes to reach the nuclei is significantly longer than the time needed for a small molecule. Therefore, plasmid DNA present in the cytosol after being electrotransferred can be lost before reaching the nucleus, for example because of cell division. Finally, after the cytoskeleton, the nuclear envelope represents the last, but by no means the least important, obstacle for the expression of the plasmid DNA. The relatively large size of plasmid DNA (2-10 MDa) makes it unlikely that the nuclear entry occurs by passive diffusion. We studied how electrotransferred DNA is transported in the cytoplasm towards the nucleus (26, 32). We have performed single particle tracking (SPT) experiments of individual DNA aggregates in living

cells (25). We analyzed the modes of DNA aggregates motion in CHO cells. We showed fast active transport of the DNA aggregates over long distances. Tracking experiments in cells treated with different drugs affecting both the actin and the tubulin networks demonstrate that this transport is related to the cellular microtubule network. In addition, we performed flow cytometry and SPT experiments using inhibitors of endocytosis and endosomal markers and showed that during active transport, DNA is routed through endosomal compartments. The electrotransferred DNA uses the classical endosomal trafficking pathways.

3) New developments.

As mentioned above, the dense latticework of the cytoskeleton impedes free diffusion of DNA in the intracellular medium. Electrotransferred plasmid DNA, containing specific sequences could then use the microtubule network and its associated motor proteins to move through the cytoplasm to nucleus (33). Clear limits of efficient gene expression using electric pulses are therefore due to the passage of DNA molecules through the plasma membrane and to the cytoplasmic crowding and transfer through the nuclear envelope. A key challenge for electro-mediated gene therapy is to pinpoint the rate limiting steps in this complex process and to find strategies to overcome these obstacles. One of the possible strategies to enhance DNA uptake into cells is to use short (10-300 ns) but high pulse (up to 300 kV/cm) induce effects that primarily affect intracellular structures and functions. As the pulse duration is decreased, below the plasma membrane charging time constant, plasma membrane effects decrease and intracellular effects predominate (34, 35). An idea, to improve transfection success, is thus to perform classical membrane permeabilisation allowing plasmid DNA electrotransfer to the cell cytoplasm, and then after, when DNA has reached the nuclear envelope, to specifically permeabilise the nuclei using these short strong nanopulses. Thus, when used in conjunction with classical electropermeabilisation, nanopulses gave hope to increase gene expression. However, data showed that nsEPs have no major contribution to gene electrotransfer in CHO cells and no effect on constitutive GFP expression in HCT-116 cells (36). Another idea was to combine electric pulses and ultrasound assisted with gas microbubbles. Cells were first electropermeabilised with plasmid DNA and then sonoporated. Twenty-four hours later, cells that received electrosonoporation demonstrated a four-fold increase in transfection level and a six-fold increase in transfection efficiency compared with cells having undergone electroporation alone (37).

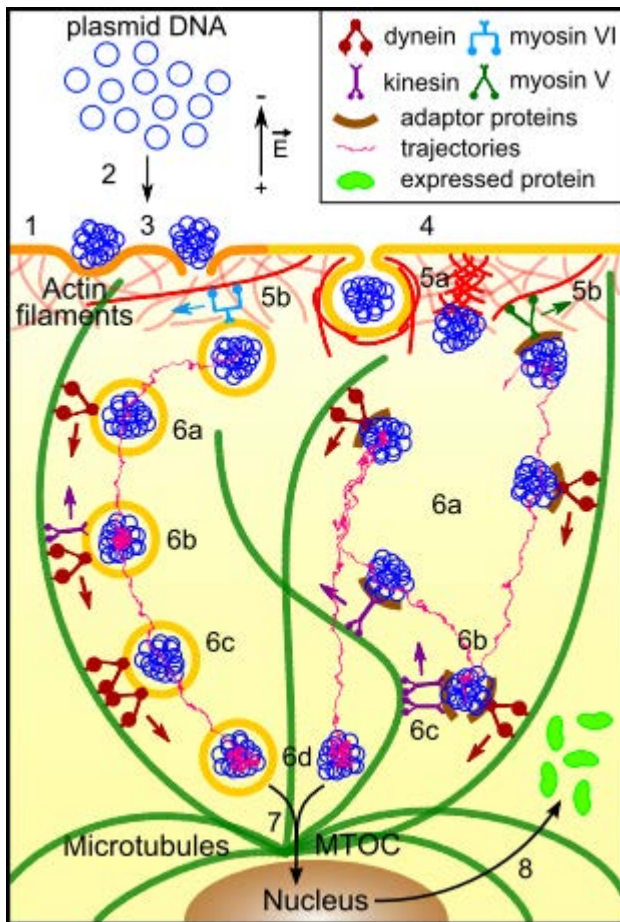


Figure 2: DNA electrotransfer as a multistep process. During the application of the electric field, (1) the plasma membrane is permeabilized (orange), (2) DNA is electrophoretically pushed onto the cell membrane side facing the cathode, which results in (3) DNA/membrane interactions. DNA aggregates are inserted into the membrane and remain there for about 10 minutes. After the application of the electric field and resealing of the membrane (yellow), (4) DNA is internalized with the following approximate contributions: 50% caveolin/raft-mediated endocytosis (caveolin/raft-ME), 25% macropinocytosis, and 25% clathrin-mediated endocytosis (clathrin-ME). (5) While being actively transported in the cytoplasm, DNA aggregates pass through the different endosomal compartments. For gene expression to occur, (6) DNA must escape from endosomal compartments. This most likely occurs from early or late endosomes (solid line arrow) but it may also be possible from recycling endosomes and lysosomes (dashed line arrow). Once in the perinuclear region, (7) DNA must cross the nuclear envelope to be finally expressed and (8) yield proteins released into the cytoplasm. From (26).

Although electroporation induced the formation of DNA aggregates into the cell membrane, sonoporation induced its direct propulsion into the cytoplasm. Sonoporation can therefore improve the transfer of electro-induced DNA aggregates by allowing its free and rapid entrance into the cells. These results demonstrated that *in vitro* gene transfer by electrosonoporation could provide a new potent method for gene transfer.

Other questions about cell organelle alterations remain unanswered. We recently reported evidence for a number of ultrastructural alterations in mammalian cells exposed to electric pulses (38). Specifically, CHO cells subjected to trains of 10 pulses lasting 5ms using an electric field of 800V/cm, i.e. under conditions leading both to membrane permeabilization, gene transfer and expression, were observed to undergo morphological alterations of the mitochondria and nucleus. These modifications, detected in the minutes following pulse delivery, were transient and may have direct consequences on molecule delivery and therefore may explain various aspects of the mechanisms of DNA electrotransfer.

LIPID VESICLES AND SPHEROIDS AS CONVENIENT (NEW) EXPERIMENTAL APPROACHES TO STUDY GENE ELECTROTRANSFER

Other experimental approaches are necessary to going deeper in the characterization of the membranes domains observed during electrotransfer. For that purpose, we used giant unilamellar vesicles to study the effect of permeabilizing electric fields in simple membrane models. GUVs (Giant Unilamellar Vesicles) represent a convenient way to study membrane properties such as lipid bilayer composition and membrane tension. They offer the possibility to study and visualize membrane processes due to their cell like size in absence of any constraint due to cell cytoskeleton. Experiments showed a decrease in vesicle radius which is interpreted as being due to lipid loss during the permeabilization process (Figure 3).

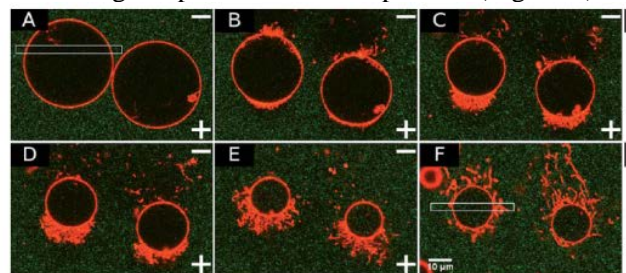


Figure 3: Microscopic observations of GUVs submitted to electric pulses in the presence of pDNA. From (39).

Three mechanisms responsible for lipid loss were directly observed and will be presented: pore formation, vesicle formation and tubule formation, which may be involved in molecules uptake (40). We also gave evidence that GUVs are a good model to study the mechanisms of electrofusion, with a direct interest to their use as vehicles to deliver molecules (41). However, a direct transfer of DNA into the GUVs took place during application of the electric pulses (39). That gives clear evidence that “lipid bubble” is not a cell and a tissue is not a simple assembly of single cells.

Therefore, in the last past few years, we decided to use an *ex vivo* model, namely tumor multicellular tumor spheroids, for the understanding of the DNA electrotransfer process in tissues.

Upon growth, spheroids display a gradient of proliferating cells. These proliferating cells are located in the outer cell-layers and the quiescent cells are located more centrally. This cell heterogeneity is similar to that found in avascular microregions of tumors. We used confocal microscopy to visualize the repartition of permeabilized cells in spheroids submitted to electric pulses. Electrotransfer of bleomycin and cisplatin confirmed the relevance of the model in the case of electrochemotherapy and doxorubicin showed its potential to screen new antitumor drug candidates for ECT. Confocal microscopy was used to visualize the topological distribution of permeabilized cells in 3D spheroids. Our results revealed that cells were efficiently permeabilized, whatever their localization in the spheroid, even those in the core. The combination of antitumor drugs and electric pulses led to changes in spheroid macroscopic morphology and cell cohesion, to tumor spheroid growth arrest and finally to its complete dislocation, mimicking previously observed *in vivo* situations.

Using this 3D spheroid cell culture model we also studied the effect of calcium electroporation and electrochemotherapy using bleomycin on human cancer cell lines and on primary normal human dermal fibroblasts. The results showed a clear reduction in spheroid size in all three cancer cell spheroids after treatment with respectively calcium electroporation or electrochemotherapy using bleomycin. Strikingly, the size of normal fibroblast spheroids was neither affected after calcium electroporation nor electrochemotherapy indicating that calcium electroporation, like electrochemotherapy, will have limited adverse effects on the surrounding normal tissue when treating with calcium electroporation (42). Taken together, all these results indicate that the spheroid model is relevant for the study and optimization of electromediated drug delivery protocols (43). Small molecules can be efficiently transferred into cells, including the ones present inside the spheroids, gene expression is limited to the external layers of cells (44). Taken together, these results, in agreement with the ones obtained by the group of R. Heller (45), indicate that the spheroid model is more relevant to an *in vivo* situation than cells cultured as monolayers (46, 47).

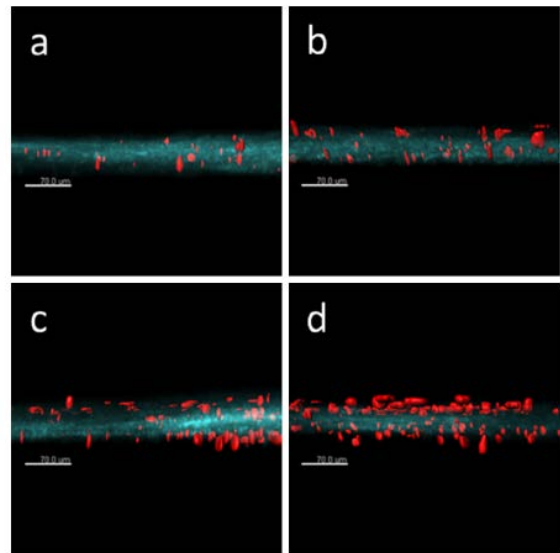


Figure 4: 3D dermal tissue electroporabilization. Reconstructed human dermal tissue was electroporabilized in the presence of propidium iodide (red) with 8 pulses of 5 ms duration at 1 Hz. Electric field intensity was 0 V/cm (a), 200 V/cm (b), 300 V/cm (c), 400 V/cm (d) and observed under a fluorescent biphoton microscope. Collagens are blue. From (49).

In order to assess the effects of ECM composition and organization, as well as intercellular junctions and communication, in normal tissue response to electric pulses, we are now developing an innovative three-dimensional (3D) reconstructed human connective tissue model (48). 3D human dermal tissue is reconstructed *in vitro* by a tissue engineering approach. This human cell model present multiple layers of primary dermal fibroblasts embedded in a native, collagen-rich ECM and can be a useful tool to study skin DNA electrotransfer mechanisms. We just showed that the cells within this standardized 3D tissue can be efficiently electroporabilized by milliseconds electric pulses (Figure 4).

We believe that a better comprehension of gene electrotransfer in such a model tissue would help improve electrogene therapy approaches such as the systemic delivery of therapeutic proteins and DNA vaccination.

CONCLUSIONS

Classical theories of electroporabilization present some limits to give a full description of the transport of molecules through membranes. There is still a need to clearly define the terms “Electroporabilization” and “Electrotransfer”. Certain effects of the electric field parameters on membrane permeabilization, and the associated transport of molecules, are well established but a great deal of what happens at the molecular level remains speculative. Molecular dynamics simulations are giving interesting new insight into the process (35, 50).

Electroinduced destabilisation of the membrane includes both lateral and transverse redistribution of lipids and proteins, leading to mechanical and electrical modifications which are not yet fully understood. One may suggest that such modifications can be involved in the subsequent transport of molecules interacting with them such as the DNA molecules. Experimental verification of the basic mechanisms leading to the electropermeabilization and other changes in the membrane, cells and tissues remain a priority given the importance of these phenomena for processes in cell biology and in medical applications.

REFERENCES

- [1] Gothelf, A., L. M. Mir, and J. Gehl. 2003. Electrochemotherapy: results of cancer treatment using enhanced delivery of bleomycin by electroporation. *Cancer Treat Rev* 29:371-387.
- [2] Rols, M. P. 2010. Gene transfer by electrical fields. *Curr Gene Ther* 10:255.
- [3] Andre, F. M., and L. M. Mir. 2010. Nucleic acids electrotransfer in vivo: mechanisms and practical aspects. *Curr Gene Ther* 10:267-280.
- [4] Mir, L. M. 2008. Application of electroporation gene therapy: past, current, and future. *Methods Mol Biol* 423:3-17.
- [5] Yarmush, M. L., A. Golberg, G. Sersa, T. Kotnik, and D. Miklavcic. 2014. Electroporation-based technologies for medicine: principles, applications, and challenges. *Annual review of biomedical engineering* 16:295-320.
- [6] Sersa, G., J. Teissie, M. Cemazar, E. Signori, U. Kamensek, G. Marshall, and D. Miklavcic. 2015. Electrochemotherapy of tumors as in situ vaccination boosted by immunogene electrotransfer. *Cancer immunology, immunotherapy : CII*.
- [7] Vandermeulen, G., K. Vanvarenberg, A. De Beuckelaer, S. De Koker, L. Lambrecht, C. Uyttenhove, A. Reschner, A. Vanderplasschen, J. Grooten, and V. Preat. 2015. The site of administration influences both the type and the magnitude of the immune response induced by DNA vaccine electroporation. *Vaccine* 33:3179-3185.
- [8] Cemazar, M., T. Jarm, and G. Sersa. 2010. Cancer electrogene therapy with interleukin-12. *Curr Gene Ther* 10:300-311.
- [9] Heller, L. C., and R. Heller. 2010. Electroporation gene therapy preclinical and clinical trials for melanoma. *Curr Gene Ther* 10:312-317.
- [10] Escoffre, J. M., and M. P. Rols. 2012. Electrochemotherapy: Progress and Prospects. *Curr Pharm Des*.
- [11] Daud, A. I., R. C. DeConti, S. Andrews, P. Urbas, A. I. Riker, V. K. Sondak, P. N. Munster, D. M. Sullivan, K. E. Ugen, J. L. Messina, and R. Heller. 2008. Phase I trial of interleukin-12 plasmid electroporation in patients with metastatic melanoma. *J Clin Oncol* 26:5896-5903.
- [12] Tamzali, Y., L. Borde, M. P. Rols, M. Golzio, F. Lyazrhi, and J. Teissie. 2011. Successful treatment of equine sarcoids with cisplatin electrochemotherapy: A retrospective study of 48 cases. *Equine veterinary journal*.
- [13] Neumann, E., M. Schaefer-Ridder, Y. Wang, and P. H. Hofschneider. 1982. Gene transfer into mouse lymphoma cells by electroporation in high electric fields. *Embo J* 1:841-845.
- [14] Escoffre, J. M., T. Portet, L. Wasungu, J. Teissie, D. Dean, and M. P. Rols. 2009. What is (Still not) Known of the Mechanism by Which Electroporation Mediates Gene Transfer and Expression in Cells and Tissues. *Mol Biotechnol* 41:286-295.
- [15] Cemazar, M., M. Golzio, G. Sersa, M. P. Rols, and J. Teissie. 2006. Electrically-assisted nucleic acids delivery to tissues in vivo: where do we stand? *Curr Pharm Des* 12:3817-3825.
- [16] Paganin-Gioanni, A., E. Bellard, J. M. Escoffre, M. P. Rols, J. Teissie, and M. Golzio. 2011. Direct visualization at the single-cell level of siRNA electrotransfer into cancer cells. *Proc Natl Acad Sci U S A* 108:10443-10447.
- [17] Escoffre, J. M., M. Hubert, J. Teissie, M. P. Rols, and C. Favard. 2014. Evidence for electro-induced membrane defects assessed by lateral mobility measurement of a GPI anchored protein. *Eur Biophys J*.
- [18] Escoffre, J. M., E. Bellard, C. Faurie, S. C. Sebai, M. Golzio, J. Teissie, and M. P. Rols. 2014. Membrane disorder and phospholipid scrambling in electropermeabilized and viable cells. *Biochim Biophys Acta* 1838:1701-1709.
- [19] Chopinet, L., C. Roduit, M. P. Rols, and E. Dague. 2013. Destabilization induced by electropermeabilization analyzed by atomic force microscopy. *Biochim Biophys Acta* 1828:2223-2229.
- [20] Chopinet, L., C. Formosa, M. P. Rols, R. E. Duval, and E. Dague. 2013. Imaging living cells surface and quantifying its properties at high resolution using AFM in QI (TM) mode. *Micron* 48:26-33.
- [21] Golzio, M., J. Teissie, and M. P. Rols. 2002. Direct visualization at the single-cell level of electrically mediated gene delivery. *Proc Natl Acad Sci U S A* 99:1292-1297.
- [22] Rosazza, C., S. H. Meglic, A. Zumbusch, M. P. Rols, and D. Miklavcic. 2016. Gene Electrotransfer: A Mechanistic Perspective. *Curr Gene Ther* 16:98-129.
- [23] Faurie, C., M. Rebersek, M. Golzio, M. Kanduser, J. M. Escoffre, M. Pavlin, J. Teissie, D. Miklavcic, and M. P. Rols. 2010. Electro-mediated gene transfer and expression are controlled by the life-time of DNA/membrane complex formation. *J Gene Med* 12:117-125.
- [24] Escoffre, J. M., T. Portet, C. Favard, J. Teissie, D. S. Dean, and M. P. Rols. 2011. Electromediated formation of DNA complexes with cell membranes and its consequences for gene delivery. *Biochim Biophys Acta* 1808:1538-1543.
- [25] Rosazza, C., A. Buntz, T. Riess, D. Woll, A. Zumbusch, and M. P. Rols. 2013. Intracellular tracking of single-plasmid DNA particles after delivery by electroporation. *Mol Ther* 21:2217-2226.
- [26] Rosazza, C., H. Deschout, A. Buntz, K. Braeckmans, M. P. Rols, and A. Zumbusch. 2016. Endocytosis and Endosomal Trafficking of DNA After Gene Electrotransfer In Vitro. *Molecular therapy. Nucleic acids* 5:e286.
- [27] Rosazza, C., E. Phez, J. M. Escoffre, L. Cezanne, A. Zumbusch, and M. P. Rols. 2012. Cholesterol implications in plasmid DNA electrotransfer: Evidence for the involvement of endocytotic pathways. *Int J Pharm* 423:134-143.
- [28] Rosazza, C., J. M. Escoffre, A. Zumbusch, and M. P. Rols. 2011. The actin cytoskeleton has an active role in the electrotransfer of plasmid DNA in mammalian cells. *Mol Ther* 19:913-921.
- [29] Faurie, C., M. Rebersek, M. Golzio, M. Kanduser, J. M. Escoffre, M. Pavlin, J. Teissie, D. Miklavcic, and M. P. Rols. 2010. Electro-mediated gene transfer and expression are controlled by the life-time of DNA/membrane complex formation. *Journal of Gene Medicine* 12:117-125.
- [30] Haberl, S., M. Kanduser, K. Flisar, D. Hodzic, V. B. Bregar, D. Miklavcic, J. M. Escoffre, M. P. Rols, and M. Pavlin.

2013. Effect of different parameters used for in vitro gene electrotransfer on gene expression efficiency, cell viability and visualization of plasmid DNA at the membrane level. *J Gene Med* 15:169-181.

[31] Lechardeur, D., and G. L. Lukacs. 2006. Nucleocytoplasmic Transport of Plasmid DNA: A Perilous Journey from the Cytoplasm to the Nucleus. *Hum Gene Ther* 17:882-889.

[32] Rosazza, C., A. Buntz, T. Riess, D. Woll, A. Zumbusch, and M. P. Rols. 2013. Intracellular tracking of single plasmid DNA-particles after delivery by electroporation. *Mol Ther*.

[33] Vaughan, E. E., and D. A. Dean. 2006. Intracellular trafficking of plasmids during transfection is mediated by microtubules. *Mol Ther* 13:422-428.

[34] Beebe, S. J., J. White, P. F. Blackmore, Y. Deng, K. Somers, and K. H. Schoenbach. 2003. Diverse effects of nanosecond pulsed electric fields on cells and tissues. *DNA Cell Biol* 22:785-796.

[35] Vernier, P. T., Y. Sun, and M. A. Gundersen. 2006. Nanoelectropulse-driven membrane perturbation and small molecule permeabilization. *BMC Cell Biol* 7:37.

[36] Chopinet, L., T. Batista-Napotnik, A. Montigny, M. Rebersek, J. Teissie, M. P. Rols, and D. Miklavcic. 2013. Nanosecond Electric Pulse Effects on Gene Expression. *J Membr Biol*.

[37] Escoffre, J. M., K. Kaddur, M. P. Rols, and A. Bouakaz. 2010. In vitro gene transfer by electrosonoporation. *Ultrasound Med Biol* 36:1746-1755.

[38] Phez, E., L. Gibot, and M. P. Rols. 2016. How transient alterations of organelles in mammalian cells submitted to electric field may explain some aspects of gene electrotransfer process. *Bioelectrochemistry*.

[39] Portet, T., C. Favard, J. Teissie, D. Dean, and M. P. Rols. 2011. Insights into the mechanisms of electromediated gene delivery and application to the loading of giant vesicles with negatively charged macromolecules. *Soft Matter* 7:3872-3881.

[40] Portet, T., F. Camps i Febrer, J. M. Escoffre, C. Favard, M. P. Rols, and D. S. Dean. 2009. Visualization of membrane loss during the shrinkage of giant vesicles under electropulsation. *Biophys J* 96:4109-4121.

[41] Mauroy, C., P. Castagnos, M. C. Blache, J. Teissie, I. Rico-Lattes, M. P. Rols, and M. Blanzat. 2012. Interaction between GUVs and catanionic nanocontainers: new insight into spontaneous membrane fusion. *Chem Commun (Camb)* 48:6648-6650.

[42] Frandsen, S. K., L. Gibot, M. Madi, J. Gehl, and M. P. Rols. 2015. Calcium Electroporation: Evidence for Differential Effects in Normal and Malignant Cell Lines, Evaluated in a 3D Spheroid Model. *PLoS One* 10:e0144028.

[43] Gibot, L., L. Wasungu, J. Teissie, and M. P. Rols. 2013. Antitumor drug delivery in multicellular spheroids by electroporation. *J Control Release* 167:138-147.

[44] Wasungu, L., J. M. Escoffre, A. Valette, J. Teissie, and M. P. Rols. 2009. A 3D in vitro spheroid model as a way to study the mechanisms of electroporation. *Int J Pharm* 379:278-284.

[45] Marrero, B., and R. Heller. 2012. The use of an in vitro 3D melanoma model to predict in vivo plasmid transfection using electroporation. *Biomaterials*.

[46] Chopinet, L., L. Wasungu, and M. P. Rols. 2011. First explanations for differences in electrotransfection efficiency in vitro and in vivo using spheroid model. *Int J Pharm*.

[47] Gibot, L., and M. P. Rols. 2013. Progress and Prospects: The Use of 3D Spheroid Model as a Relevant Way to Study and Optimize DNA Electrotransfer. *Current Gene Therapy* 13:175-181.

[48] Madi, M., M. P. Rols, and L. Gibot. 2016. Gene Electrotransfer in 3D Reconstructed Human Dermal Tissue. *Curr Gene Ther* 16:75-82.

[49] Madi, M., M. P. Rols, and L. Gibot. 2015. Efficient In Vitro Electroporation of Reconstructed Human Dermal Tissue. *J Membr Biol*.

[50] Polak, A., D. Bonhenry, F. Dehez, P. Kramar, D. Miklavcic, and M. Tarek. 2013. On the electroporation thresholds of lipid bilayers: molecular dynamics simulation investigations. *J Membr Biol* 246:843-850.

ACKNOWLEDGEMENT

This research was performed in the scope of the EBAM European Associated Laboratory (LEA) and is a result of networking efforts within COST TD1104. We were supported by the Centre National de la Recherche Scientifique (CNRS), the Agence Nationale de la Recherche (ANR), Projet PIERGEN ANR-12-ASTR-0039, the Direction Générale de l'Armement (DGA), and the Midi-Pyrénées Région. Experiments are due to the works of the PhD students and post-docs I have/had the pleasure to supervise and/or work with: Muriel Golzio, Cécile Faurie, Emilie Phez, Jean-Michel Escoffre, Thomas Portet, Chloé Mauroy, Louise Chopinet, Elisabeth Bellard, Christelle Rosazza, Amar Tamra, Moinecha Madi, Luc Wasungu, Flavien Pillet and Laure Gibot and Nathalie Joncker.



Marie-Pierre Rols was born in Decazeville, the “gueules noires” city of the Duc Decazes, France, in 1962. She received a Masters in Biochemistry, a Ph.D. in Cell Biophysics and the Habilitation à Diriger les Recherches from the Paul Sabatier University of Toulouse in 1984, 1989 and 1995, respectively. She is currently Director of Research at the IPBS-CNRS laboratory in Toulouse, group leader of the Cellular Biophysics team and head of the Biophysical and Structural Biology Department. She is secretary of the French Society for Nanomedicine. Her research interests lie in the fields of membrane electroporation in cells and tissues, mainly on the mechanism of nucleic acids electrotransfer. Marie-Pierre Rols is the author of 100 articles in peer-reviewed journals. In 1993 she received the Galvani Prize of the Bioelectrochemical Society, in 2006 a joined prize of the Midi-Pyrénées Région.

NOTES

Gene electrotransfer *in vivo*

Maja Čemažar

Institute of Oncology Ljubljana, Slovenia

Abstract: Gene electrotransfer consists of administration of nucleic acids (DNA, RNA oligonucleotides...) followed by application of electric pulses to the specific tissue in order to enable delivery of nucleic acids into cells and consequently the therapeutic action of delivered genetic material. Due to the size of nucleic acids the electrical parameters of gene electrotransfer vary greatly depending on the tissue to be transfected and also on the desired level and duration of expression as well as accompanied tissue damage. Besides optimization of electrical parameters for specific application, design of therapeutic plasmid DNA or RNA molecules can also influence the therapeutic outcome. Initial studies on gene electrotransfer were mainly focused on the evaluation of electrical parameters for efficient gene delivery to different tissues, such as skin, muscle, liver and tumors using various reporter genes encoding fluorescent proteins, luciferase and β -galactosidase. Therapeutic field of gene electrotransfer is mainly divided into two fields: DNA vaccination and cancer gene therapy. DNA vaccination against infectious diseases and cancer on one hand and antiangiogenic and immunomodulating gene therapies against cancer on the other hand are the prevalent areas of research. Furthermore, increasing number of clinical trials, especially in USA, are registered using electroporation for delivery of therapeutic plasmid DNA. The perspectives of therapeutic gene electrotransfer for cancer therapy lie mainly in different combination with standard local therapies, such as radiation therapy or electrochemotherapy, with the aim to turn local treatments into systemic ones. In addition, a lot of preclinical work is dedicated to optimization of therapeutic plasmid DNAs, development of new electrodes and evaluation of electrical parameters, which will lead to better planning and design of clinical trials.

INTRODUCTION

The *in vitro* application of electroporation for the introduction of DNA into the cells was evaluated and tested in 1982 by Neumann et al [1], 6 years before the use of electroporation for delivery of antitumor chemotherapeutic drugs (electrochemotherapy) into the tumor cells [2]. However, *in vivo* studies only slowly followed and the first *in vivo* study was performed in 1991 by Titomirov et al [3], evaluating the usefulness of exponentially decaying pulses for delivery of genes to the mouse skin. Later on, the transfection of brain, liver, tumor and muscle using different reporter genes were successfully demonstrated using different types of electric pulses [3–7]. Due to the physicochemical properties and the size of nucleic acids compared to small chemotherapeutic drugs, the mechanism of entry of nucleic acids is different than that of small molecules. In tissues, other, tissue and cell related parameters also influence the transfection efficiency, such as cell size, shape and organization in the tissues, presence of the extracellular matrix and tissue heterogeneity (presence of different types of cells in the particular tissue). In addition, the construction of plasmid and its administration can also influence the level of transfection as well as its duration. Therefore, a vast amount of studies in the field of *in vivo* gene electrotransfer were dedicated to evaluation of different parameters of electric pulses for different tissue type as well as for different application (Figure 1). Currently,

therapeutic use of gene electrotransfer is focused in mainly two fields: DNA vaccination and cancer gene therapy [8,9].

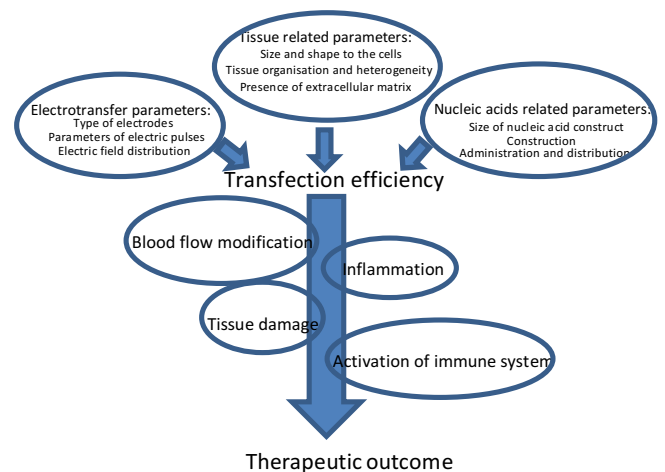


Figure 1: Different parameters can influence the transfection efficiency and therapeutic outcome of gene electrotransfer.

PRECLINICAL GENE ELECTROTRANSFER OF REPORTER GENES

Reporter genes used in preclinical studies on gene electrotransfer were mainly encoding either different fluorescent proteins or luciferase. Both enable to visualize the transfection of tissues (gene expression in cells in tissues) *in vivo* using different types of *in vivo* imaging, either whole body imaging or at the cellular level [10,11]. Most of the studies were performed in muscle and skin, as these tissues are easily accessible

and therefore represent an obvious target tissue for DNA vaccination. Besides easy accessibility for gene electrotransfer, muscle cells are long lived and they can produce relatively high quantities of therapeutic proteins that are also released into the blood stream, thus acting systemically. On the other hand, skin also represent a great target tissue, not only due to the easy accessibility, but mainly because of the numerous immune cells present in the skin that can elicit effective immune response of the organisms needed for DNA vaccination [12,13](Figure 2).

As mentioned in the introduction, numerous different parameters of electric pulses were used, either short ($\sim 100\mu\text{s}$) high voltage (in the range of $\sim 1000\text{ V}$) electric pulses or long (up to 100 ms) low voltage (up to few 100 V) pulses were used. Moreover, even a combination of high voltage and low voltage pulses were tested and showed improved transfection in skin and muscle compared to single type of pulses used for transfection [14–16]. In tumors, the combination of pulses did not result in improved transfection [18]. In addition, the influence of orientation and polarity of the applied electric pulses were also evaluated in tumors, demonstrating that increased transfection efficiency is obtained only by changing the electrode orientation, but not pulse polarity[19].

The main type of electrodes used in the studies was either plate or needle and more recently also non-invasive multielectrode arrays [15,19,20]. Other types of electrodes that were tested for gene electrotransfer were spatula electrodes for gene delivery to muscle [22] and other types of noninvasive electrodes, such as needle free, meander and contact electrodes for skin delivery [21–24]. Selection of electrode is very important for appropriate electric field distribution in the tissue which is a prerequisite for effective gene electrotransfer[24, 25].

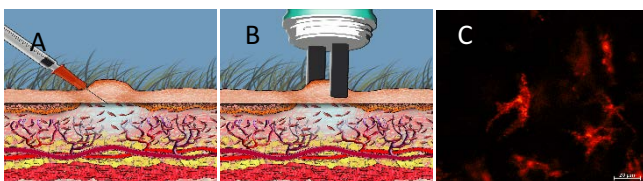


Figure 2: Gene electrotransfer to skin. **A** injection of plasmid DNA subcutaneously. A bubble on the skin will be formed. **B** If using plate electrodes, they are positioned in a way that the bubble is encompassed between the two plates. **C** Intravital confocal microscopy of cells in mouse skin expressing DsRED fluorescent protein at the depth of 30 μm .

Besides electrical parameters, the type of the nucleic acid used for electrotransfer can also affect the transfection efficiency. Namely, it was shown that smaller siRNA can more easily cross the plasma membrane compared to larger plasmid DNA

molecules, however the duration of the expression (or effect) is shorter [26–28]. Therefore, the plasmid DNA are still the most often used in gene electrotransfer studies. To improve the safety and targeting of the plasmid DNA delivery as well as to minimize the undesired tissue damage, the plasmids with tissue specific promoters, devoid of antibiotic resistance gene and with minimal or no bacterial backbone were constructed and evaluated in combination with electroporation [29–32].

Due to the size of plasmid DNA and the presence of nucleases in the blood and also tissues, the most suitable way of plasmid DNA administration is local injection. The distribution of the plasmid DNA in different tissues has different time frame, therefore it is also very important the timing between the injection of plasmid DNA and application of electric pulses. For muscle it was shown that it should be as soon as possible, while for the tumors, depending on the histological type, it can be up to 30 min after the injection of the plasmid [33–35]. Improved distribution and consequently better transfection efficiency can be achieved also by pretreatment of muscles and tumors with extracellular matrix degrading enzymes, such as hyaluronidase and collagenase [36,37].

In vitro, it was shown that size, orientation and shape of the cells influence the permeabilisation of the cell membranes and thus also transfection efficiency. The same is also valid *in vivo*. Tissues with more organized structure, such as muscle are more easy to transfect than highly heterogenic tissue, such as tumors [16]. In addition, in tumors with large cells higher transfection efficiency was obtained compared to tumors with smaller cells [38,39].

The importance of careful selection of plasmid DNA and electrical parameters for specific application, was recently reinforced by experiments showing that gene electrotransfer of plasmids devoid of therapeutic gene can induced complete regression of tumors and that cytosolic DNA sensors activating innate immune response were upregulated following gene electrotransfer [42]. The inflammation and induction of immune response was demonstrated also for muscle and skin transfection [41,42].

PRECLINICAL AND CLINICAL GENE ELECTROTRANSFER OF THERAPEUTIC GENES

The preclinical studies using therapeutic genes were mainly dedicated to evaluation of gene electrotransfer for DNA vaccination or treatment of various diseases, such as cancer, where therapies are targeted either directly to tumor cells or aim to increase the immune response of the organism against cancer cells.

In general, gene therapy can be performed using two different approaches. The first one is *ex vivo* gene therapy, where cells, including stem cells, are removed from patient, transfected *in vitro* with the plasmid or viral vector, selected, amplified, and then reinjected back into the patient. The other approach is *in vivo* gene therapy, where exogenous DNA is delivered directly into host's target tissue e.g. locally to tumor or peritumorally and for systemic release of the therapeutic molecule into skeletal muscle depending on the type of therapeutic molecules and intent of treatment [45].

Gene electrotransfer was first used for DNA vaccination in 1996 [46]. Currently, numerous studies, using gene electrotransfer mainly to muscle and skin for DNA vaccination against infectious diseases, arthritis, multiple sclerosis, inflammation are undergoing. In addition, several clinical trials, against infectious diseases, such as HIV, hepatitis are going on. Gene electrotransfer of plasmid DNA resulted in stimulation of both arms of adaptive immune system, humoral and cellular [8,9].

In cancer gene therapy, gene electrotransfer of therapeutic genes directly into tumors facilitates local intratumoral production of therapeutic proteins, enabling sufficient therapeutic concentration and thus therapeutic outcome. This is especially important in case of cytokines, where high systemic concentrations are associated with severe toxicity.

The first evaluation of intratumoral electrogene therapy for cancer treatment was performed 3 years after the first DNA vaccination study in 1999 in murine melanoma tumor model [47]. Since then, a variety of therapeutic genes, mostly encoding cytokines, but also tumor suppressor proteins, siRNA molecules against various targets, such as oncogenes, have been tested in a numerous animal tumor models. Overall, results of preclinical studies indicate, that intratumoral therapeutic gene electrotransfer enables efficient transgene expression with sufficient production of therapeutic proteins, which can lead to even complete tumor regression and in some cases to induction of long-term antitumor immunity in treated animals.

Some of the most significant antitumor effect to date in cancer gene therapy have been achieved with employment of active nonspecific immunotherapy, i.e. use of cytokines. Gene electrotransfer of genes, encoding different cytokines, has already shown promising results in preclinical trials on different animal tumor models. Cytokine genes, which showed the most potential for cancer therapy, are interleukin (IL)-2, IL-12, IL-18, interferon (IFN) α , and GM-CSF[47–52]. Currently, the most advanced therapy is using IL-12, which plays important role in the induction of cellular immune response through

stimulation of T-lymphocyte differentiation and production of IFN- γ and activation of natural killer cells[54]. Antitumor effect of IL-12 gene electrotransfer, has already been established in various tumor models, e.g. melanoma, lymphoma, squamous cell carcinoma, urinary bladder carcinoma, mammary adenocarcinoma and hepatocellular carcinoma[53]. Results of preclinical studies show that beside regression of tumor at primary and distant sites, electrogene therapy with IL-12 also promotes induction of long-term antitumor memory and therapeutic immunity, suppresses metastatic spread and increases survival time of experimental animals[53]. On preclinical level, gene electrotransfer to tumors was also employed in suicide gene therapy of cancer, replacement of oncogenes therapies, introduction of wild type tumor suppressor genes etc [47,54–56]. Another approach in cancer gene therapy, which is currently being widely investigated, is based on inhibition of angiogenesis of tumors. The basic concept of antiangiogenic gene therapy is transfection of cells with genes, encoding inhibitors of tumor angiogenesis. Electrotransfer of plasmids encoding antiangiogenic factors (angiostatin and endostatin) was demonstrated to be effective in inhibition of tumor growth and metastatic spread of different tumors[57–59]. Recently, RNA interference approach was evaluated, using siRNA molecule against endoglin, which is a co-receptor of transforming growth factor β and is overproduced in activated endothelial and also certain tumor cells. Gene electrotransfer of either siRNA or shRNA molecules against endoglin resulted in vascular targeted effect in mammary tumors as well as antitumor and antivascular effect in melanoma tumors that are expressing high level of endoglin [60,61].

Muscle tissue is, besides in DNA vaccination, used also as a target tissues due to the possibility of high production and secretion of therapeutic proteins. Gene electrotransfer to muscle was evaluated with the aim to treat various muscle diseases, for local secretion of angiogenic or neurotrophic factors or for systemic secretion of different therapeutic proteins, such as erythropoietin, coagulation factors, cytokines, monoclonal antibodies, etc. [62–64]. In cancer gene therapy, gene electrotransfer of plasmid DNA encoding cytokines IL-12, IL-24, and antiangiogenic factors was evaluated with encouraging results.

Clinical studies on gene electrotransfer with plasmid DNA encoding cytokine IL-12 in patients with melanoma, as well as in veterinary patients show great promise for further development of this therapy[65,66]. In human clinical study, 24 patients with malignant melanoma subcutaneous metastases were treated 3 times. The response to therapy was observed in treated as well as in distant non-treated tumor nodules. In 53%

of patients a systemic response was observed resulting in either stable disease or an objective response. The major adverse side-effect was transient pain after application of electric pulses. In post-treatment biopsies, tumor necrosis and immune cell infiltration was observed. This first human clinical trial with IL-12 electrogene therapy in metastatic melanoma proved that this therapy is safe and effective [66]. In veterinary oncology, 8 dogs with mastocytoma were treated with IL-12 gene electrotransfer. A good local antitumor effect with significant reduction of treated tumors' size, ranging from 15% to 83% (mean 52%) of the initial tumor volume was obtained. Additionally, a change in the histological structure of treated nodules was seen as reduction in the number of malignant mast cells and inflammatory cell infiltration of treated tumors. Furthermore, systemic release of IL-12 and IFN- γ in treated dogs was detected, without any noticeable local or systemic side-effects [67]. Again, the data suggest that intratumoral IL-12 electrogene therapy could be used for controlling local as well as systemic disease.

For example, results of intramuscular IL-12 gene electrotransfer in canine patients indicate that it is a safe procedure, which can result in systemic shedding of hIL-12 and possibly trigger IFN- γ response in treated patients, leading to prolonged disease free period and survival of treated animals [68].

PERSPECTIVES

In oncology, local ablative treatments are very effective, however they lack a systemic component. Therefore, much effort is dedicated to development of treatments, that would act systemically or that would add a systemic component to the local treatment. With the progress of knowledge in tumor immunology, new immunomodulating therapies were developed for treatment of cancer and are currently combined with standard treatment with great success. DNA vaccination and immune gene therapies with cytokines aim to stimulate antitumor immunity and are thus good candidates to be combined with local therapies [68,69].

Several studies combining electrochemotherapy or radiotherapy with gene electrotransfer have been evaluated preclinically. The most promising immune-gene therapy that already reached clinical trials in veterinary and human oncology, is gene electrotransfer of IL-12. In the preclinical studies IL-12 gene electrotransfer was combined with electrochemotherapy and radiotherapy in different tumor models. Intramuscular gene electrotransfer of IL-12 combined with electrochemotherapy with cisplatin increased the percentage of complete regression of fibrosarcoma SA-1 tumors to 60% compared to 17% complete regression after

electrochemotherapy alone [71]. When combined with radiotherapy even 100% complete response of LPB tumors was obtained [72]. Intratumoral IL-12 gene electrotransfer resulted in ~2.0 radiation dose modifying factor [73].

Clinically, only several studies were performed in client owned dogs, combining electrochemotherapy with either bleomycin or cisplatin and intratumoral or peritumoral application of IL-12 gene electrotransfer [73–76]. The results of these clinical studies are very promising and further studies, hopefully also in human oncology are foreseen.

Gene electrotransfer holds big potential for further development, which might lead to new clinical trials in both DNA vaccination and gene therapy application. Plasmid design is crucial for appropriate therapeutic protein production and effect, therefore the research is focused on codon optimization, the use of various promoters (tissue specific and inducible), the incorporation of various immunostimulatory motifs in the plasmid sequence and the use of plasmids devoid of antibiotic resistance gene, which is in compliance with Regulatory Agencies. In addition, physical factor, such as elevated temperature can also lead to improved gene electrotransfer. Furthermore, new types of electrodes, such as microneedles and non-invasive multi-electrode arrays with carefully selected parameters of electric pulses are evaluated and will lead to efficient gene electrotransfer with minimal side effects and discomfort for the patients.

REFERENCES

- [1] E. Neumann, M. Schaeffer, Y. Wang, and P. H. Hofschneider, "GENE-TRANSFER INTO MOUSE LYOMA CELLS BY ELECTROPORATION IN HIGH ELECTRIC-FIELDS," *Embo J.*, vol. 1, no. 7, pp. 841–845, 1982.
- [2] S. Orłowski, J. Belehradek J., C. Paoletti, and L. M. Mir, "Transient electroporation of cells in culture. Increase of the cytotoxicity of anticancer drugs," *Biochem Pharmacol*, vol. 37, no. 24, pp. 4727–4733, 1988.
- [3] A. V Titomirov, S. Sukharev, and E. Kistanova, "In vivo electroporation and stable transformation of skin cells of newborn mice by plasmid DNA.," *Biochim Biophys Acta*, vol. 1088, no. 1, pp. 131–134, 1991.
- [4] T. Nishi, K. Yoshizato, S. Yamashiro, H. Takeshima, K. Sato, K. Hamada, I. Kitamura, T. Yoshimura, H. Saya, J. Kuratsu, and Y. Ushio, "High-efficiency in vivo gene transfer using intraarterial plasmid DNA injection following in vivo electroporation.," *Cancer Res*, vol. 56, no. 5, pp. 1050–1055, 1996.
- [5] R. Heller, M. Jaroszeski, A. Atkin, D. Moradpour, R. Gilbert, J. Wands, and C. Nicolau, "In vivo gene electroinjection and expression in rat liver.," *FEBS Lett*, vol. 389, no. 3, pp. 225–228, 1996.
- [6] M. P. Rols, C. Delteil, M. Golzio, P. Dumond, S. Cros, and J. Teissie, "In vivo electrically mediated protein and gene transfer in murine melanoma.," *Nat Biotechnol*, vol. 16, no. 2, pp. 168–171, 1998.

- [7] L. M. Mir, M. F. Bureau, R. Rangara, B. Schwartz, and D. Scherman, "Long-term, high level *in vivo* gene expression after electric pulse-mediated gene transfer into skeletal muscle.," *CR Acad Sci III*, vol. 321, no. 11, pp. 893–899, 1998.
- [8] H. Aihara and J. Miyazaki, "Gene transfer into muscle by electroporation *in vivo*," *Nat Biotechnol*, vol. 16, no. 9, pp. 867–870, 1998.
- [9] L. Lambrecht, A. Lopes, S. Kos, G. Sersa, V. Pr eat, and G. Vandermeulen, "Clinical potential of electroporation for gene therapy and DNA vaccine delivery.," *Expert Opin. Drug Deliv.*, vol. 13, no. 2, pp. 295–310, 2016.
- [10] R. Heller and L. C. Heller, "Gene electrotransfer clinical trials.," *Adv. Genet.*, vol. 89, pp. 235–62, 2015.
- [11] E. Kinnear, L. J. Caproni, and J. S. Tregoning, "A Comparison of Red Fluorescent Proteins to Model DNA Vaccine Expression by Whole Animal *In Vivo* Imaging.," *PLoS One*, vol. 10, no. 6, p. e0130375, 2015.
- [12] A. Gothelf, J. Eriksen, P. Hojman, and J. Gehl, "Duration and level of transgene expression after gene electrotransfer to skin in mice.," *Gene Ther.*, vol. 17, no. 7, pp. 839–45, Jul. 2010.
- [13] A. Gothelf and J. Gehl, "Gene electrotransfer to skin; review of existing literature and clinical perspectives," *Curr Gene Ther*, vol. 10, no. 4, pp. 287–299, 2010.
- [14] C. Trollet, D. Scherman, and P. Bigey, "Delivery of DNA into muscle for treating systemic diseases: advantages and challenges.," *Methods Mol. Biol.*, vol. 423, pp. 199–214, 2008.
- [15] M. Cemazar, M. Golzio, G. Sersa, M. P. Rols, and J. Teissi e, "Electrically-assisted nucleic acids delivery to tissues *in vivo*: where do we stand?," *Curr Pharm Des*, vol. 12, no. 29, pp. 3817–3825, 2006.
- [16] F. M. Andre, J. Gehl, G. Sersa, V. Preat, P. Hojman, J. Eriksen, M. Golzio, M. Cemazar, N. Pavselj, M. P. Rols, D. Miklavcic, E. Neumann, J. Teissie, and L. M. Mir, "Efficiency of High- and Low-Voltage Pulse Combinations for Gene Electrotransfer in Muscle, Liver, Tumor, and Skin," *Hum. Gene Ther.*, vol. 19, no. 11, pp. 1261–1271, 2008.
- [17] N. Pavselj and V. Pr eat, "DNA electrotransfer into the skin using a combination of one high- and one low-voltage pulse.," *J. Control. Release*, vol. 106, no. 3, pp. 407–15, Sep. 2005.
- [18] M. Cemazar, M. Golzio, G. Sersa, P. Hojman, S. Kranjc, S. Mesojednik, M. P. Rols, and J. Teissie, "Control by pulse parameters of DNA electrotransfer into solid tumors in mice," *Gene Ther.*, vol. 16, no. 5, pp. 635–644, 2009.
- [19] V. Todorovic, U. Kamensek, G. Sersa, and M. Cemazar, "Changing electrode orientation, but not pulse polarity, increases the efficacy of gene electrotransfer to tumors *in vivo*," *Bioelectrochemistry*, vol. 100, pp. 119–127, 2014.
- [20] R. Heller, Y. Cruz, L. C. Heller, R. A. Gilbert, and M. J. Jaroszeski, "Electrically mediated delivery of plasmid DNA to the skin, using a multielectrode array.," *Hum. Gene Ther.*, vol. 21, no. 3, pp. 357–62, Mar. 2010.
- [21] S. Kos, T. Blagus, M. Cemazar, U. Lamprecht Tratar, M. Stimac, L. Prosen, T. Dolinsek, U. Kamensek, S. Kranjc, L. Steinstraesser, G. Vandermeulen, V. Pr eat, and G. Sersa, "Electrotransfer parameters as a tool for controlled and targeted gene expression in skin.," *Mol. Ther. Nucleic Acids*, vol. 5, no. 8, p. e356, Aug. 2016.
- [22] M. Don a, M. Sandri, K. Rossini, I. Dell'Aica, M. Podhorska-Okolow, and U. Carraro, "Functional *in vivo* gene transfer into the myofibers of adult skeletal muscle.," *Biochem. Biophys. Res. Commun.*, vol. 312, no. 4, pp. 1132–8, Dec. 2003.
- [23] L. Zhang, E. Nolan, S. Kreitschitz, and D. P. Rabussay, "Enhanced delivery of naked DNA to the skin by non-invasive *in vivo* electroporation.," *Biochim. Biophys. Acta*, vol. 1572, no. 1, pp. 1–9, Aug. 2002.
- [24] S. Babiuk, M. E. Baca-Estrada, M. Foldvari, L. Baizer, R. Stout, M. Storms, D. Rabussay, G. Widera, and L. Babiuk, "Needle-free topical electroporation improves gene expression from plasmids administered in porcine skin.," *Mol. Ther.*, vol. 8, no. 6, pp. 992–8, Dec. 2003.
- [25] L. Daugimont, N. Baron, G. Vandermeulen, N. Pavselj, D. Miklavcic, M. C. Jullien, G. Cabodevila, L. M. Mir, and V. Pr eat, "Hollow microneedle arrays for intradermal drug delivery and DNA electroporation," *J Membr Biol*, vol. 236, no. 1, pp. 117–125, 2010.
- [26] S. Maz eres, D. Sel, M. Golzio, G. Pucihar, Y. Tamzali, D. Miklavcic, and J. Teissi e, "Non invasive contact electrodes for *in vivo* localized cutaneous electropulsation and associated drug and nucleic acid delivery," *J Control Release*, vol. 134, no. 2, pp. 125–131, 2009.
- [27] S. Corovic, I. Lackovic, P. Sustaric, T. Sustar, T. Rodic, and D. Miklavcic, "Modeling of electric field distribution in tissues during electroporation," *Biomed Eng Online*, vol. 12, p. 16, 2013.
- [28] A. Paganin-Gioanni, E. Bellard, J. M. Escoffre, M. P. Rols, J. Teissi e, and M. Golzio, "Direct visualization at the single-cell level of siRNA electrotransfer into cancer cells," *Proc Natl Acad Sci U S A*, vol. 108, no. 26, pp. 10443–10447, 2011.
- [29] J.-M. Escoffre, A. Debin, J.-P. Reynes, D. Drocourt, G. Tiraby, L. Hellaudais, J. Teissie, and M. Golzio, "Long-lasting *in vivo* gene silencing by electrotransfer of shRNA expressing plasmid.," *Technol. Cancer Res. Treat.*, vol. 7, no. 2, pp. 109–16, Apr. 2008.
- [30] K. E. Broderick, A. Chan, F. Lin, X. Shen, G. Kichaev, A. S. Khan, J. Aubin, T. S. Zimmermann, and N. Y. Sardesai, "Optimized *in vivo* transfer of small interfering RNA targeting dermal tissue using *in vivo* surface electroporation," *Mol Ther Nucleic Acids*, vol. 1, p. e11, 2012.
- [31] C. Marie, G. Vandermeulen, M. Quiviger, M. Richard, V. Pr eat, and D. Scherman, "pFARs, plasmids free of antibiotic resistance markers, display high-level transgene expression in muscle, skin and tumour cells.," *J. Gene Med.*, vol. 12, no. 4, pp. 323–32, Apr. 2010.
- [32] G. Vandermeulen, H. Richiardi, V. Escriou, J. Ni, P. Fournier, V. Schirmacher, D. Scherman, and V. Pr eat, "Skin-specific promoters for genetic immunisation by DNA electroporation.," *Vaccine*, vol. 27, no. 32, pp. 4272–7, Jul. 2009.
- [33] N. Tesic and M. Cemazar, "In vitro targeted gene electrotransfer to endothelial cells with plasmid DNA containing human endothelin-1 promoter," in *Journal of Membrane Biology*, 2013, vol. 246, no. 10, pp. 783–791.
- [34] S. Chabot, J. Orio, M. Schmeer, M. Schleef, M. Golzio, and J. Teissi e, "Minicircle DNA electrotransfer for efficient tissue-targeted gene delivery.," *Gene Ther.*, vol. 20, no. 1, pp. 62–8, Jan. 2013.
- [35] G. Tevz, S. Kranjc, M. Cemazar, U. Kamensek, A. Coer, M. Krzan, S. Vidic, D. Pavlin, and G. Sersa, "Controlled systemic release of interleukin-12 after gene electrotransfer to muscle for cancer gene therapy alone or in combination with ionizing radiation in murine sarcomas," *J Gene Med*, vol. 11, no. 12, pp. 1125–1137, 2009.
- [36] M. Cemazar, D. Pavlin, S. Kranjc, A. Grosel, S. Mesojednik, and G. Sersa, "Sequence and time dependence of transfection

- efficiency of electrically-assisted gene delivery to tumors in mice," *Curr. Drug Deliv.*, vol. 3, no. 1, 2006.
- [37] S. Mesojednik, D. Pavlin, G. Sersa, A. Coer, S. Kranjc, A. Grosel, G. Tevz, and M. Cemazar, "The effect of the histological properties of tumors on transfection efficiency of electrically assisted gene delivery to solid tumors in mice," *Gene Ther.*, vol. 14, no. 17, 2007.
- [38] J. M. McMahon, E. Signori, K. E. Wells, V. M. Fazio, and D. J. Wells, "Optimisation of electrotransfer of plasmid into skeletal muscle by pretreatment with hyaluronidase -- increased expression with reduced muscle damage.," *Gene Ther.*, vol. 8, no. 16, pp. 1264–1270, 2001.
- [39] M. Cemazar, M. Golzio, G. Sersa, P. Hojman, S. Kranjc, S. Mesojednik, M. P. Rols, and J. Teissie, "Control by pulse parameters of DNA electrotransfer into solid tumors in mice," *Gene Ther.*, vol. 16, no. 5, pp. 635–644, 2009.
- [40] S. Mesojednik, D. Pavlin, G. Sersa, A. Coer, S. Kranjc, A. Grosel, G. Tevz, and M. Cemazar, "The effect of the histological properties of tumors on transfection efficiency of electrically assisted gene delivery to solid tumors in mice," *Gene Ther.*, vol. 14, no. 17, pp. 1261–1269, 2007.
- [41] M. Cemazar, G. Sersa, J. Wilson, G. M. Tozer, S. L. Hart, A. Grosel, and G. U. Dachs, "Effective gene transfer to solid tumors using different nonviral gene delivery techniques: Electroporation, liposomes, and integrin-targeted vector," *Cancer Gene Ther.*, vol. 9, no. 4, 2002.
- [42] K. Znidar, M. Bosnjak, M. Cemazar, and L. C. Heller, "Cytosolic DNA Sensor Upregulation Accompanies DNA Electrotransfer in B16.F10 Melanoma Cells," *Mol. Ther. - Nucleic Acids*, vol. 5, no. 6, 2016.
- [43] P. Chiarella, E. Massi, M. De Robertis, A. Sibilio, P. Parrella, V. M. Fazio, and E. Signori, "Electroporation of skeletal muscle induces danger signal release and antigen-presenting cell recruitment independently of DNA vaccine administration.," *Expert Opin. Biol. Ther.*, vol. 8, no. 11, pp. 1645–57, Nov. 2008.
- [44] J. J. Drabick, J. Glasspool-Malone, A. King, and R. W. Malone, "Cutaneous transfection and immune responses to intradermal nucleic acid vaccination are significantly enhanced by in vivo electroporation.," *Mol. Ther.*, vol. 3, no. 2, pp. 249–55, Feb. 2001.
- [45] M. L. Yarmush, A. Golberg, G. Serša, T. Kotnik, and D. Miklavčič, "Electroporation-based technologies for medicine: principles, applications, and challenges.," *Annu. Rev. Biomed. Eng.*, vol. 16, pp. 295–320, Jul. 2014.
- [46] M. Nomura, Y. Nakata, T. Inoue, A. Uzawa, S. Itamura, K. Nerome, M. Akashi, and G. Suzuki, "In vivo induction of cytotoxic T lymphocytes specific for a single epitope introduced into an unrelated molecule.," *J. Immunol. Methods*, vol. 193, no. 1, pp. 41–9, Jul. 1996.
- [47] G. L. Niu, R. Heller, R. Catlett-Falcone, D. Coppola, M. Jaroszeski, W. Dalton, R. Jove, and H. Yu, "Gene therapy with dominant-negative Stat3 suppresses growth of the murine melanoma B16 tumor in vivo," *Cancer Res.*, vol. 59, no. 20, pp. 5059–5063, 1999.
- [48] F. M. Andre and L. M. Mir, "Nucleic acids electrotransfer in vivo: mechanisms and practical aspects," *Curr Gene Ther.*, vol. 10, no. 4, pp. 267–280, 2010.
- [49] T. Dolinsek, B. Markelc, G. Sersa, A. Coer, M. Stimac, J. Lavrencak, A. Brozic, S. Kranjc, and M. Cemazar, "Multiple Delivery of siRNA against Endoglin into Murine Mammary Adenocarcinoma Prevents Angiogenesis and Delays Tumor Growth," *PLoS One*, vol. 8, no. 3, 2013.
- [50] L. Heller, C. Pottinger, M. J. Jaroszeski, R. Gilbert, and R. Heller, "In vivo electroporation of plasmids encoding GM-CSF or interleukin-2 into existing B16 melanomas combined with electrochemotherapy induces long-term antitumor immunity," *Melanoma Res.*, vol. 10, no. 6, pp. 577–583, 2000.
- [51] S. L. Li, X. J. Zhang, and X. Q. Xia, "Regression of tumor growth and induction of long-term antitumor memory by interleukin 12 electro-gene therapy," *J. Natl. Cancer Inst.*, vol. 94, no. 10, pp. 762–768, 2002.
- [52] L. Heller, V. Todorovic, and M. Cemazar, "Electrotransfer of single-stranded or double-stranded DNA induces complete regression of palpable B16.F10 mouse melanomas," *Cancer Gene Ther.*, vol. 20, no. 12, pp. 695–700, 2013.
- [53] M. Cemazar, T. Jarm, and G. Sersa, "Cancer electrogene therapy with interleukin-12.," *Curr. Gene Ther.*, vol. 10, no. 4, pp. 300–311, 2010.
- [54] G. Trinchieri, "Interleukin-12 and the regulation of innate resistance and adaptive immunity," *Nat. Rev. Immunol.*, vol. 3, no. 2, pp. 133–146, 2003.
- [55] L. C. Heller and R. Heller, "In vivo electroporation for gene therapy," *Hum. Gene Ther.*, vol. 17, no. 9, pp. 890–897, 2006.
- [56] J. M. Escoffre, J. Teissie, and M. P. Rols, "Gene transfer: how can the biological barriers be overcome?," *J Membr Biol.*, vol. 236, no. 1, pp. 61–74, 2010.
- [57] M. Cemazar and G. Sersa, "Electrotransfer of therapeutic molecules into tissues," *Curr Opin Mol Ther.*, vol. 9, no. 6, pp. 554–562, 2007.
- [58] T. Cichoń, L. Jamroz, J. Glogowska, E. Missol-Kolka, and S. Szala, "Electrotransfer of gene encoding endostatin into normal and neoplastic mouse tissues: inhibition of primary tumor growth and metastatic spread.," *Cancer Gene Ther.*, vol. 9, no. 9, pp. 771–7, Oct. 2002.
- [59] M. Uesato, Y. Gunji, T. Tomonaga, S. Miyazaki, T. Shiratori, H. Matsubara, T. Kouzu, H. Shimada, F. Nomura, and T. Ochiai, "Synergistic antitumor effect of antiangiogenic factor genes on colon 26 produced by low-voltage electroporation.," *Cancer Gene Ther.*, vol. 11, no. 9, pp. 625–32, Sep. 2004.
- [60] J. M. Weiss, R. Shivakumar, S. Feller, L.-H. Li, A. Hanson, W. E. Fogler, J. C. Fratantoni, and L. N. Liu, "Rapid, in vivo, evaluation of antiangiogenic and antineoplastic gene products by nonviral transfection of tumor cells.," *Cancer Gene Ther.*, vol. 11, no. 5, pp. 346–53, May 2004.
- [61] N. Tesic, U. Kamensek, G. Sersa, S. Kranjc, M. Stimac, U. Lamprecht, V. Preat, G. Vandermeulen, M. Butinar, B. Turk, and M. Cemazar, "Endoglin (CD105) Silencing Mediated by shRNA Under the Control of Endothelin-1 Promoter for Targeted Gene Therapy of Melanoma," *Mol. Ther. Acids*, vol. 4, 2015.
- [62] T. Dolinsek, G. Sersa, L. Prosen, M. Bosnjak, M. Stimac, U. Razborsek, and M. Cemazar, "Electrotransfer of plasmid DNA encoding an anti-mouse endoglin (CD105) shRNA to B16 melanoma tumors with low and high metastatic potential results in pronounced anti-tumor effects," *Cancers (Basel)*, vol. 8, no. 1, 2015.
- [63] J. M. McMahon and D. J. Wells, "Electroporation for gene transfer to skeletal muscles: current status.," *BioDrugs*, vol. 18, no. 3, pp. 155–65, 2004.
- [64] P. Lefesvre, J. Attema, and D. van Bekkum, "A comparison of efficacy and toxicity between electroporation and adenoviral gene transfer.," *BMC Mol. Biol.*, vol. 3, p. 12, Aug. 2002.
- [65] N. Perez, P. Bigey, D. Scherman, O. Danos, M. Piechaczyk,

- and M. Pelegrin, "Regulatable systemic production of monoclonal antibodies by *in vivo* muscle electroporation.," *Genet. Vaccines Ther.*, vol. 2, no. 1, p. 2, Mar. 2004.
- [66] A. I. Daud, R. C. DeConti, S. Andrews, P. Urbas, A. I. Riker, V. K. Sondak, P. N. Munster, D. M. Sullivan, K. E. Ugen, J. L. Messina, and R. Heller, "Phase I Trial of Interleukin-12 Plasmid Electroporation in Patients With Metastatic Melanoma," *J. Clin. Oncol.*, vol. 26, no. 36, pp. 5896–5903, 2008.
- [67] D. Pavlin, M. Cemazar, A. Cor, G. Sersa, A. Pogacnik, and N. Tozon, "Electrogene therapy with interleukin-12 in canine mast cell tumors," *Radiol Oncol.*, vol. 45, no. 1, pp. 31–39, 2011.
- [68] D. Pavlin, M. Cemazar, G. Sersa, and N. Tozon, "IL-12 based gene therapy in veterinary medicine.," *J. Transl. Med.*, vol. 10, p. 234, 2012.
- [69] G. Sersa, J. Teissie, M. Cemazar, E. Signori, U. Kamensek, G. Marshall, and D. Miklavcic, "Electrochemotherapy of tumors as *in situ* vaccination boosted by immunogene electrotransfer.," *Cancer Immunol. Immunother.*, vol. 64, no. 10, pp. 1315–27, Oct. 2015.
- [70] C. Y. Calvet and L. M. Mir, "The promising alliance of anti-cancer electrochemotherapy with immunotherapy.," *Cancer Metastasis Rev.*, vol. 35, no. 2, pp. 165–77, Jun. 2016.
- [71] A. Sedlar, T. Dolinsek, B. Markelc, L. Prosen, S. Kranjc, M. Bosnjak, T. Blagus, M. Cemazar, and G. Sersa, "Potentiation of electrochemotherapy by intramuscular IL-12 gene electrotransfer in murine sarcoma and carcinoma with different immunogenicity," *Radiol. Oncol.*, vol. 46, no. 4, 2012.
- [72] S. Kranjc, G. Tevz, U. Kamensek, S. Vidic, M. Cemazar, and G. Sersa, "Radiosensitizing effect of electrochemotherapy in a fractionated radiation regimen in radiosensitive murine sarcoma and radioresistant adenocarcinoma tumor model," *Radiat Res.*, vol. 172, no. 6, pp. 677–685, 2009.
- [73] A. Sedlar, S. Kranjc, T. Dolinsek, M. Cemazar, A. Coer, and G. Sersa, "Radiosensitizing effect of intratumoral interleukin-12 gene electrotransfer in murine sarcoma," *BMC Cancer*, vol. 13, 2013.
- [74] J. Cutrera, M. Torrero, K. Shiomitsu, N. Mauldin, and S. Li, "Intratumoral bleomycin and IL-12 electrochemogenetherapy for treating head and neck tumors in dogs.," *Methods Mol. Biol.*, vol. 423, pp. 319–25, Jan. 2008.
- [75] J. Cutrera, G. King, P. Jones, K. Kicenuik, E. Gumpel, X. Xia, and S. Li, "Safety and efficacy of tumor-targeted interleukin 12 gene therapy in treated and non-treated, metastatic lesions.," *Curr. Gene Ther.*, vol. 15, no. 1, pp. 44–54, Jan. 2015.
- [76] S. D. Reed, A. Fulmer, J. Buckholz, B. Zhang, J. Cutrera, K. Shiomitsu, and S. Li, "Bleomycin/interleukin-12 electrochemogenetherapy for treating naturally occurring spontaneous neoplasms in dogs," *Cancer Gene Ther.*, vol. 17, no. 8, pp. 571–578, 2010.
- [77] M. Cemazar, J. Ambrozic Avgustin, D. Pavlin, G. Sersa, A. Poli, A. Krhac Levacic, N. Tesic, U. Lamprecht Tratar, M. Rak, and N. Tozon, "Efficacy and safety of electrochemotherapy combined with peritumoral IL-12 gene electrotransfer of canine mast cell tumours," *Vet. Comp. Oncol.*, 2016.

ACKNOWLEDGEMENT

This research was funded by research grants from Slovenian Research Agency and was conducted in the scope of the EBAM European Associated Laboratory (LEA) and COST Action TD1104.



Maja Čemazar received her PhD in basic medical sciences from the Medical Faculty, University of Ljubljana in 1998. She was a postdoctoral fellow and researcher at Gray Cancer Institute, UK from 1999 to 2001. She was an associate researcher at the Institute of Pharmacology and Structural Biology in Toulouse, France in 2004. Currently, she works at the Department of Experimental Oncology, Institute of Oncology

Ljubljana and teaches at the Faculty of Health Sciences, University of Primorska, Slovenia. Her main research interests are in the field of gene electrotransfer employing plasmid DNA encoding different immunomodulatory and antiangiogenic therapeutic genes. In 2006 she received the Award of the Republic of Slovenia for important achievements in scientific research and development in the field of experimental oncology.

She is the author of more than 150 articles in peer-reviewed journals.

NOTES

NOTES

Drug and gene delivery in the skin by electroporation

Véronique Pr at

Universit  catholique de Louvain, Louvain Drug research Institute, Brussels, Belgium

STRUCTURE OF THE SKIN

Skin is composed of three primary layers: the epidermis, the dermis and the hypodermis. The epidermis consists of stratified squamous epithelium. The epidermis contains no blood vessels, and cells in the deepest layers are nourished by diffusion from blood capillaries extending to the upper layers of the dermis. The main type of cells which make up the epidermis are keratinocytes, with melanocytes and Langerhans cells also present. The main barrier to drug permeation is the stratum corneum, the outermost layer of the skin made of corneocytes embedded in multiple lipid bilayers. The dermis is the layer of skin beneath the epidermis that consists of connective tissue. It also contains many nerve endings hair follicles, sweat glands, lymphatic vessels and blood vessels.

TRANSDERMAL AND TOPICAL DRUG DELIVERY

The easy accessibility and the large area of the skin make it a potential route of administration. Despite these potential advantages for the delivery of drugs across or into the skin, a significant physical barrier impedes the transfer of large molecules. First, transdermal transport of molecules is limited by the low permeability of the stratum corneum, the outermost layer of the skin. Only potent lipophilic low molecular weight (<500) drugs can be delivered by passive diffusion at therapeutic rates. Hence, the transdermal penetration of hydrophilic and/or high molecular-weight molecules, including DNA, requires the use of methods to enhance skin permeability and/or to provide a driving force acting on the permeant. Both chemical (e.g. penetration enhancer) and physical (e.g. iontophoresis, electroporation, or sonophoresis) methods have been used.

TRANSDERMAL DRUG DELIVERY BY ELECTROPORATION

It has been demonstrated that application of high voltage pulses permeabilizes the stratum corneum and enhances drug transport. Electroporation of skin was shown to enhance and expedite transport across and/or into skin for many different compounds. Within a few minutes of high-voltage pulsing, molecular transport across skin increased by several orders of magnitude.

In vitro, the transport of several conventional drugs (e.g., fentanyl, β blockers, peptides (e.g., LHRH or calcitonine) was shown to be enhanced. Few in vivo studies confirm the increased transport and rapid onset of action.

The parameters affecting the efficacy of transport have been extensively studied. The electrical parameters (voltage, number and duration of the pulses), the formulation parameters (ionic strength...) allow the control of drug delivery.

The mechanism of drug transport is mainly electrophoretic movement and diffusion through newly created aqueous pathways in the stratum corneum created by the "electroporation" of the lipid bilayers.

The alterations in skin induced by high-voltage pulsing are relatively minor (decrease in skin resistance, hydration, lipid organisation) and reversible. However, light pain and muscle contraction that can be reduced by developing better electrode design, have been observed.

TOPICAL DRUG DELIVERY BY ELECTROPORATION

Besides the permeabilization of the stratum corneum and the subsequent increased skin permeability, electroporation also enhances the permeability of the viable cells of the skin and the subcutaneous tissue. Hence, it is an efficient method to deliver molecules into the skin when these molecules are applied topically or more efficiently for macromolecules including DNA when they are injected intradermally.

SKIN GENE DELIVERY

The skin represents an attractive site for the delivery of nucleic acids-based drugs for the treatment of topical or systemic diseases and immunisation. It is the most accessible organ and can easily be monitored and removed if problems occur. It is the largest organ of the body (15% of total adult body weight) and delivery to large target area could be feasible. However attempts at therapeutic cutaneous gene delivery have been hindered by several factors. Usually, except for viral vectors, gene expression is transient and typically disappears with 1 to 2 weeks due to the continuous renewal of the epidermis. Moreover, DNA penetration

is limited by the barrier properties of the skin, rendering topical application rather inefficient.

The potential use of DNA-based drugs to the skin could be: (i) gene replacement by introducing a defective or missing gene, for the treatment of genodermatosis (ii) gene therapeutic by delivering a gene expressing protein with a specific pharmacological effect, or suicidal gene, (iii) wound healing, (iv) immunotherapy with DNA encoding cytokines and (v) DNA vaccine. As the skin is an immunocompetent organ, DNA delivery in the skin by electroporation seems particularly attractive for DNA vaccination. The gene encoding the protein of interest can be inserted in a plasmid that carries this gene under the control of an appropriate eukaryotic promoter (e.g., the CMV promoter in most cases).

Effective gene therapy requires that a gene encoding a therapeutic protein must be administered and delivered to target cells, migrate to the cell nucleus and be expressed to a gene product. DNA delivery is limited by: (i) DNA degradation by tissues or blood nucleases, (ii) low diffusion at the site of administration, (iii) poor targeting to cells, (iv) inability to cross membrane, (v) low cellular uptake and (vi) intracellular trafficking to the nucleus.

The methods developed for gene transfer into the skin are based on the methods developed for gene transfection *in vitro* and in other tissues *in vivo* as well as methods developed to enhance transdermal drug delivery. They include (i) topical delivery, (ii) intradermal injection, (iii) mechanical methods, (iv) physical methods and (v) biological methods.

Topical application of naked plasmid DNA to the skin is particularly attractive to provide a simple approach to deliver genes to large areas of skin. However, the low permeability of the skin to high molecular weight hydrophilic molecules limits the use of this approach. Gene expression after topical delivery of an aqueous solution of DNA on intact skin has been reported to induce gene expression but the expression is very low. Hence, topical DNA delivery into the skin can only be achieved if the barrier function of the stratum corneum is altered.

One of the simplest ways of gene delivery is injecting naked DNA encoding the therapeutic protein. In 1990, Wolff et al. observed an expression during several months after injection of naked DNA into the muscle. Expression following the direct injection of naked plasmid DNA has been then established for skin. The epidermis and the dermis can take up and transiently express plasmid DNA following direct injection into animal skin. However, the expression remains low and physical and/or mechanical methods have been developed to enhance gene expression.

ELECTROPORATION IN SKIN GENE DELIVERY

Electroporation has been widely used to introduce DNA into various types of cells *in vitro*. It allows efficient delivery of DNA into cells and tissues *in vivo*, thereby improving the expression of therapeutic or immunogenic proteins that are encoded by plasmid DNA. Electroporation involves plasmid injection in the target tissue and application of short high voltage electric pulses by electrodes. The intensity and the duration of pulses and the more appropriate type of electrodes must be evaluated for each tissue. It is generally accepted that the electric field plays a double role in DNA transfection: it transiently disturbs membranes and increases cells permeability and promotes electrophoresis of negatively charged DNA.

Electrotransfer may be used to increase transgene expression 10 to 1000-fold more than the injection of naked DNA into the skin. Local delivery combined with electrotransfer could result in a significant increase of serum concentrations of a specific protein. Neither long-term inflammation nor necroses are observed. After direct intradermal injection of plasmid, the transfected cells are typically restricted to the epidermis and dermis. However, when high voltage pulse are applied after this intradermal injection, other cells, including adipocytes, fibroblasts and numerous dendritic-like cells within the dermis and subdermal layers were transfected.

Duration of expression after electrotransfer depends on the targeted tissue. In contrast to the skeletal muscle where expression lasts for several months, gene expression is limited to only of few weeks into the skin. For example, after intradermal electrotransfer of plasmid coding erythropoietin, the expression persisted for 7 weeks at the DNA injection site, and hematocrit levels were increased for 11 weeks. With reporter gene, shorter expressions were reported, probably due to an immune response.

Several authors tried to increase the effectiveness of the electrotransfer into the skin. By co-injecting a nuclease inhibitor with DNA, transfection expression was significantly increased. For the skin, combination of one high-voltage pulse and one low-voltage pulse delivered by plate electrodes has been proven to be efficient and well tolerated. The design of electrodes and injection method can also be optimised. In particular, several groups have shown that microarray electrodes are more efficient to increase gene expression in the skin than plate electrodes.

Electrotransfer has no detrimental effect on wound healing. A single injection of a plasmid coding keratinocyte growth factor coupled with electrotransfer improved and accelerated wound closure in a wound-healing diabetic mouse model. Host defense peptides,

in particular LL-37, are emerging as potential therapeutics for promoting wound healing and inhibiting bacterial growth. However, effective delivery of the LL-37 peptide remains limiting. We have shown that skin-targeted electroporation of a plasmid encoding hCAP-18/LL-37 promote the healing of wounds.

Vaccination is another interesting application of electrotransfer into the skin. Intradermal electrotransfer enhanced the expression of DNA encoded antigens into the skin and both humoral and cellular immune responses have been induced. Robust antibody responses were elicited following vaccine delivery in several tested animal models. Hence, it is developed as a potential alternative for DNA vaccine delivery and is currently tested in clinical trials, including for DNA cancer vaccines.

Electrotransfer of DNA encoding either IL-2, IL-12 or an antiangiogenic protein for the treatment of melanoma is currently tested in clinical trials.

REFERENCES

References on skin structure and skin delivery

- [1] Prausnitz MR, Langer R. Transdermal drug delivery. *Nat Biotechnol.* 2008 Nov;26(11):1261-8. Review.
- [2] Engelke L, Winter G, Hook S, Engert J. Recent insights into cutaneous immunization: How to vaccinate via the skin. *Vaccine.* 2015 Sep 8;33(37):4663-74.
- [3] Schoellhammer CM, Blankschtein D, Langer R. Skin permeabilization for transdermal drug delivery: recent advances and future prospects. *Expert Opin Drug Deliv.* 2014 Mar;11(3):393-407.

References on transdermal drug delivery by electroporation

- [4] Denet A.R., Vanbever R. and Pr  at V., Transdermal drug delivery by electroporation, *Advanced drug delivery reviews*, 2004;56:659-74. Review.
- [5] Jadoul A., Bouwstra J., and Pr  at V., Effects of iontophoresis and electroporation on the stratum corneum – Review of the biophysical studies, *Advanced drug delivery reviews*, 35, 1999, 89-105
- [6] Prausnitz M.R., A practical assessment of transdermal drug delivery by skin electroporation, *Advanced drug delivery reviews*, 35, 1999, 61-76
- [7] Ita K. Perspectives on Transdermal Electroporation. *Pharmaceutics.* 2016 Mar 17;8(1). pii: E9. doi: 10.3390/pharmaceutics8010009.
- [8] Wong TW, Chen TY, Huang CC, Tsai JC, Hui SW. Painless skin electroporation as a novel way for insulin delivery. *Diabetes Technol Ther;* 2011. 13(9): 929-35

References on skin gene delivery

- [9] Hengge UR. Gene therapy progress and prospects: the skin--easily accessible, but still far away. *Gene Ther* 2006; 13(22):1555-1563.
- [10] Branski LK, Pereira CT, Herndon DN et al. Gene therapy in wound healing: present status and future directions. *Gene Ther* 2007; 14(1):1-10.

References on electroporation on skin gene delivery

- [11] Lambrecht L, Lopes A, Kos S, Sersa G, Pr  at V, Vandermeulen G. Clinical potential of electroporation for gene therapy and DNA vaccine delivery. *Expert Opin Drug Deliv.* 2016;13(2):295-310.
- [12] Gothelf A, Gehl J. Gene electrotransfer to skin; review of existing literature and clinical perspectives. *Curr Gene Ther.* 2010;10(4):287-99.
- [13] Drabick JJ, Glasspool-Malone J, King A et al. Cutaneous transfection and immune responses to intradermal nucleic acid vaccination are significantly enhanced by in vivo electroporation. *Mol Ther* 2001; 3(2):249-255.
- [14] Andr   FM, Gehl J, Sersa G, Pr  at V, Hojman P, Eriksen J, Golzio M, Cemazar M, Pavselj N, Rols MP, Miklavcic D, Neumann E, Teissi   J, Mir LM. Efficiency of high- and low-voltage pulse combinations for gene electrotransfer in muscle, liver, tumor, and skin. *Hum Gene Ther.* 2008;19(11):1261-71
- [15] Glasspool-Malone J, Somiari S, Drabick JJ et al. Efficient nonviral cutaneous transfection. *Mol Ther* 2000; 2(2):140-146.
- [16] Heller LC, Jaroszeski MJ, Coppola D et al. Optimization of cutaneous electrically mediated plasmid DNA delivery using novel electrode. *Gene Ther* 2007; 14(3):275-280.
- [17] Pavselj N, Pr  at V. DNA electrotransfer into the skin using a combination of one high- and one low-voltage pulse. *J Control Release* 2005; 106(3):407-415.
- [18] Vandermeulen G, Staes E, Vanderhaeghen ML, Bureau MF, Scherman D, Pr  at V. Optimisation of intradermal DNA electrotransfer for immunisation. *J Control Release.* 2007;124(1-2):81-7.
- [19] Byrnes CK, Malone RW, Akhter N et al. Electroporation enhances transfection efficiency in murine cutaneous wounds. *Wound Repair Regen* 2004; 12(4):397-403.
- [20] Steinstraesser L, Lam MC, Jacobsen F, Porporato PE, Chereddy KK, Becerikli M, Stricker I, Hancock RE, Lehnhardt M, Sonveaux P, Pr  at V, Vandermeulen G. Skin electroporation of a plasmid encoding hCAP-18/LL-37 host defense peptide promotes wound healing. *Mol Ther.* 2014;22(4):734-42.
- [21] Kos S, Blagus T, Cemazar M, Lamprecht Tratar U, Stimac M, Prosen L, Dolinsek T, Kamensek U, Kranjc S, Steinstraesser L, Vandermeulen G, Pr  at V, Sersa G. Electrotransfer parameters as a tool for controlled and targeted gene expression in skin. *Mol Ther Nucleic Acids.* 2016;5(8):e356.

NOTES

NOTES

Molecular Dynamics Simulations of Lipid Membranes Electroporation

Mounir Tarek

Theory, Simulations and Modeling
CNRS- Université de Lorraine France

Abstract: Currently, computational approaches enable to follow, at the atomic scale, the local perturbation lipid membranes undergo when they are subject to external electric field. We describe here the molecular dynamics simulation methods devised to perform *in silico* experiments of membranes subject to nanosecond, megavolt-per-meter pulsed electric fields and of membranes subject to charge imbalance, mimicking therefore the application of low voltage – long duration pulses. At the molecular level, the results show the two types of pulses produce similar effects: provided the TM voltage these pulses create are higher than a certain threshold, hydrophilic pores stabilized by the membrane lipid head groups form within the nanosecond time scale across the lipid core. The simulations are further used to characterize the transport of charged species through these pores. The results obtained are believed to capture the essence of the several aspects of the electroporation phenomena in bilayers' membranes, and could serve as an additional, complementary source of information to the current arsenal of experimental tools.

Electroporation disturbs transiently or permanently the integrity of cell membranes [1–3]. These membranes consist of an assembly of lipids, proteins and carbohydrates that self-organize into a thin barrier that separates the interior of cell compartments from the outside environment [4]. The main lipid constituents of natural membranes are phospholipids that arrange themselves into a two-layered sheet (a bilayer). Experimental evidence suggests that the effect of an applied external electric field to cells is to produce aqueous pores specifically in the lipid bilayer [5–9]. Information about the sequence of events describing the electroporation phenomenon can therefore be gathered from measurements of electrical currents through planar lipid bilayers along with characterization of molecular transport of molecules into (or out of) cells subjected to electric field pulses. It may be summarized as follows: Long and intense electrical pulses induce rearrangements of the membrane components (water and lipids) that ultimately lead to the formation of aqueous hydrophilic pores [5–10] whose presence increases substantially the ionic and molecular transport through the otherwise impermeable membranes [11].

In erythrocyte membranes, large pores could be observed using electron microscopy [12], but in general, the direct observation of the formation of nano-sized pores is not possible with conventional techniques. Furthermore, due to the complexity and heterogeneity of cell membranes, it is difficult to describe and characterize their electroporation in terms of atomically resolved processes. Atomistic simulations in general, and molecular dynamics (MD) simulations in particular, have proven to be effective for providing insights into both the structure and the

dynamics of model lipid membrane systems in general [13–18]. Several MD simulations have recently been conducted in order to model the effect of electric field on membranes [19–23], providing perhaps the most complete molecular model of the electroporation process of lipid bilayers.

MD SIMULATIONS OF LIPID MEMBRANES

Molecular dynamics (MD) refers to a family of computational methods aimed at simulating macroscopic behaviour through the numerical integration of the classical equations of motion of a microscopic many-body system. Macroscopic properties are expressed as functions of particle coordinates and/or momenta, which are computed along a phase space trajectory generated by classical dynamics [24,25]. When performed under conditions corresponding to laboratory scenarios, MD simulations can provide a detailed view of the structure and dynamics of a macromolecular system. They can also be used to perform “computer experiments” that cannot be carried out in the laboratory, either because they do not represent a physical behaviour, or because the necessary controls cannot be achieved.

MD simulations require the choice of a potential energy function, *i.e.* terms by which the particles interact, usually referred to as a force field. Those most commonly used in chemistry and biophysics, *e.g.* GROMOS [26] CHARMM [27] and AMBER [28], are based on molecular mechanics and a classical treatment of particle-particle interactions that precludes bond dissociation and therefore the simulation of chemical reactions. Classical MD force fields consist of a summation of bonded forces associated with chemical bonds, bond angles, and bond dihedrals, and non-bonded forces associated with van der Waals forces and

electrostatic interactions. The parameters associated with these terms are optimized to reproduce structural and conformational changes of macromolecular systems.

Conventional force fields only include point charges and pair-additive Coulomb potentials, which prevent them from describing realistic collective electrostatic effects, such as charge transfer, electronic excitations or electronic polarization, which is often considered as a major limitation of the classical force fields. Note that constant efforts are undertaken on the development of potential functions that explicitly treat electronic polarizability in empirical force fields [29–31] but none of these “polarizable” force fields is widely used in large-scale simulations for now, the main reasons for that being the dramatic increase of the computational time of simulation and additional complications with their parameterization. In this perspective, classical force fields provide an adequate description of the properties of membrane systems and allow semi-quantitative investigations of membrane electrostatics.

MD simulations use information (positions, velocities or momenta, and forces) at a given instant in time, t , to predict the positions and momenta at a later time, $t + \Delta t$, where Δt is the time step, of the order of a femtosecond, taken to be constant throughout the simulation. Numerical solutions to the equations of motion are thus obtained by iteration of this elementary step. Computer simulations are usually performed on a small number of molecules (few tens to few hundred thousand atoms), the system size being limited of course by the speed of execution of the programs, and the availability of computer power. In order to eliminate edge effects and to mimic a macroscopic system, simulations of condensed phase systems consider a small patch of molecules confined in a central simulation cell, and replicate the latter using periodic boundary conditions (PBCs) in the three directions of Cartesian space. For membranes for instance the simulated system would correspond to a small fragment of either a black film, a liposome or multilamellar oriented lipid stacks deposited on a substrate [32,33].

Traditionally, phospholipids have served as models for investigating *in silico* the structural and dynamical properties of membranes. From both a theoretical and an experimental perspective, zwitterionic

phosphatidylcholine (PC) lipid bilayers constitute the best characterized systems [34–37]. More recent studies have considered a variety of alternative lipids, featuring different, possibly charged, head groups [38][39–42], and more recently mixed bilayer compositions [43–49]. Despite their simplicity, bilayers built from PC lipids represent remarkable test systems to probe the computation methodology and to gain additional insight into the physical properties of membranes [14,17,50,51].

MODELING MEMBRANES ELECTROPORATION

The effects of an electric field on a cell may be described considering the latter as a dielectric layer (cell surface membrane) embedded in conductive media (internal: cytoplasm and external: extracellular media). When relatively low-field pulses of microsecond or millisecond duration are applied to this cell (by placing for instance the cell between two electrodes and applying a constant voltage pulse) the resulting current causes accumulation of electrical charges at both sides of the cell membrane. The time required to charge the surface membrane is dependent upon the electrical parameters of the medium in which it is suspended. For a spherical cell it is estimated using equivalent network RC circuits in the 100 ns time scale [19,52–55]. A charging time constant in the range of hundreds of nanoseconds was also obtained from derivations based on the Laplace equation (see e.g. [56] for the first-order analysis on a spherical vesicle; [57] for the second-order analysis; and [58] for the second-order analysis for two concentric spherical vesicles *i.e.* modeling an organelle). If on the other hand, the pulse duration is short enough relative to the charging time constant of the resistive-capacitive network formed by the conductive intracellular and extracellular fluids and the cell membrane dielectric, which is the case for nanosecond pulses, then the response of the system is mainly dielectric and is linked to the polarization of the interfacial water (see below).

Simulations allow ones to perform *in silico* experiments under both conditions, *i.e.* submitting the system either to Nanosecond, megavolt-per-meter pulsed electric fields or to charge imbalance, mimicking therefore the application of low voltage – long duration pulses. In the following we will describe the results of such simulations.

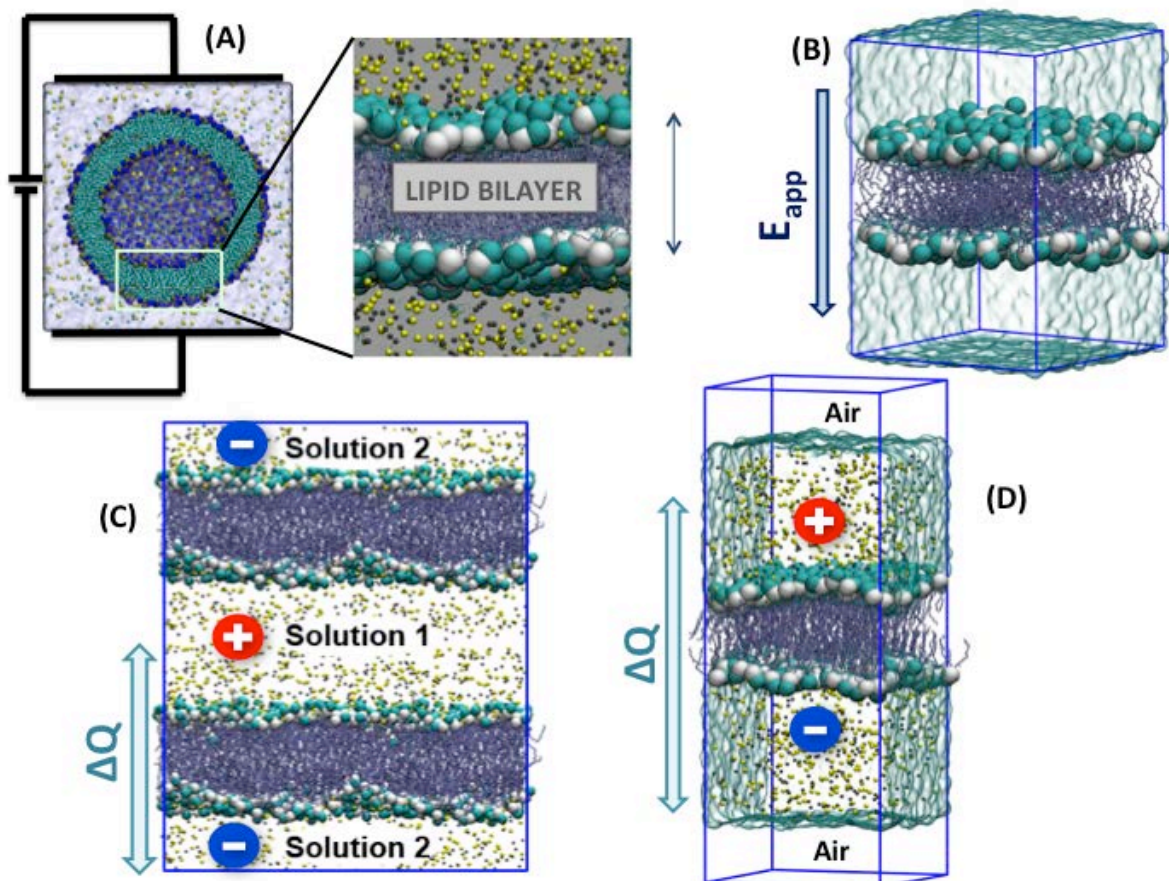


Figure 1 Protocols for atomistic modelling of cell membranes or liposomes lipid bilayers (A) electroporation; (B) nsPEFs protocol: the system is modeled in absence of salt, and subject to an electric field E_{app} perpendicular to the bilayer (z axis). Note that in some studies ions were also considered; (C) μ s- m sPEFs protocol introduced in the double bilayer setup: a charge imbalance ΔQ is set across each bilayer and the scheme is implemented using classical PBCs. To prevent ions from migrating through the periodic boundary conditions, the simulation box (in blue) is extended in the direction perpendicular to the bilayer (z axis) to create a vacuum slab in the air/water interface protocol (D).

A- ELECTROPORATION INDUCED BY DIRECT EFFECT OF AN ELECTRIC FIELD

In simulations, it is possible to apply “directly” a constant electric field \vec{E} perpendicular to the membrane (lipid bilayers) plane. In practice, this is done by adding a force $\vec{F} = q_i \vec{E}$ to all the atoms bearing a charge q_i [59–63]. MD simulations adopting such an approach have been used to study membrane electroporation [19–23], lipid externalization [64], to activate voltage-gated K^+ channels [65] and to determine transport properties of ion channels [66–69].

The consequence of such perturbation stems from the properties of the membrane and from the simulations set-up conditions: Pure lipid membranes exhibit a heterogeneous atomic distributions across the bilayer to which are associated charges and molecular dipoles distributions. Phospholipid head-groups adopt in general a preferential orientation. For hydrated PC

bilayers at temperatures above the gel to liquid crystal transition, the phosphatidyl-choline dipoles point on average 30 degrees away from the membrane normal [70]. The organization of the phosphate (PO_4^-), choline ($N(CH_3)_3^+$) and the carbonyl ($C=O$) groups of the lipid head group give hence rise to a permanent dipole and the solvent (water) molecules bound to the lipid head group moieties tend to orient their dipoles to compensate the latter [71]. The electrostatic characteristics of the bilayer may be gathered from estimates of the electrostatic profile $\phi(z)$ that stems from the distribution of all the charges in the system. $\phi(z)$ is derived from MD simulations using Poisson’s equation and expressed as the double integral of $\rho(z)$, the molecular charge density distributions:

$$\Delta\phi(z) = \phi(z) - \phi(0) = -\frac{1}{\epsilon_0} \iint_0^z \rho(z'') dz'' dz' .$$

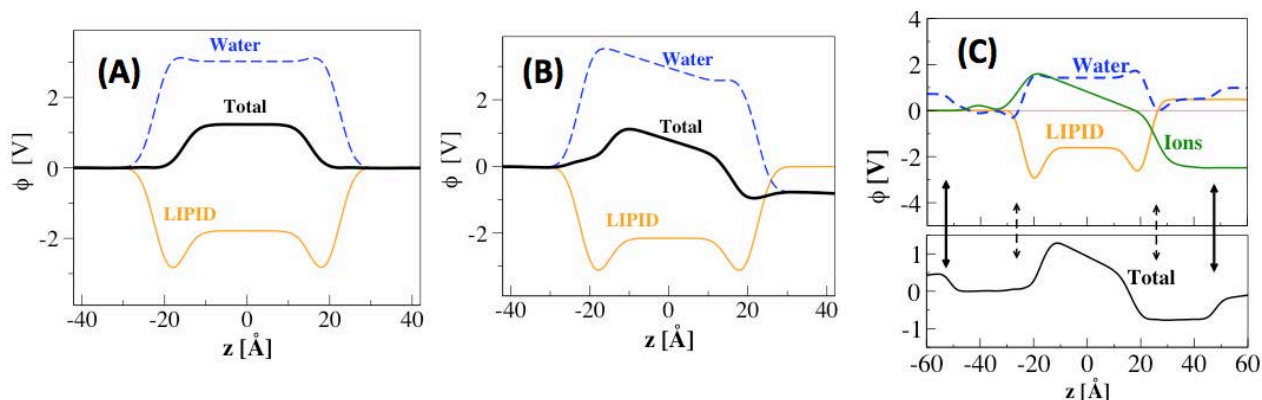


Figure. 2 Electrostatic potential profiles $\phi(z)$ along the membrane normal (z axis) of a POPC lipid bilayer. Bilayer (A) at rest, (B) subject to a transverse electric field (nsPEF protocol), and (C) bilayer set with a charge imbalance (μ s-msPEF protocol). $z=0$ represents the center of the lipid bilayer. The contributions to the electrostatic profile from water (blue), lipid (yellow), ions (green) are reported next to the total one (black). The dashed arrows in panel C indicate the positions of the lipid/water interfaces and the solid arrows the position of the water/air interfaces. Note that the TM voltage U_m (potential difference between the upper and lower water baths) in the nsPEF protocol is mainly due to water dipoles reorientation, while in the μ s-msPEF protocol it is mainly due to the charge (ions) distribution.

For lipid bilayers, most of which are modelled without consideration of a salt concentration, an applied electric field acts specifically and primarily on the interfacial water dipoles (small polarization of bulk water molecules). The reorientation of the lipid head groups appears not to be affected at very short time scales [21,72], and not exceeding few degrees toward the field direction at longer time scale [22]. Hence, within a very short time scale - typically few picoseconds [21] - a transverse field \vec{E} induces an overall TM potential ΔV (cf. Fig 2). It is very important to note here that, because of the MD simulation setup (and the use of PBCs), \vec{E} induces a voltage difference $\Delta V \approx |\vec{E}| \cdot L_z$ over the whole system, where L_z is the size of the simulation box in the field direction. In the example shown in Fig 2, L_z is ~ 10 nm. The electric field ($0.1 \text{ V} \cdot \text{nm}^{-1}$) applied to the POPC bilayer induces $\Delta V \sim 1 \text{ V}$.

MD simulations of pure lipid bilayers have shown that the application of electric fields of high enough magnitude leads to membrane electroporation, with a rather common poration sequence: The electric field

favours quite rapidly (within a few hundred picoseconds) formation of water defects and water wires deep into the hydrophobic core [20]. Ultimately water fingers forming at both sides of the membrane join up to form water channels (often termed pre-pores or hydrophobic pores) that span the membrane. Within nanoseconds, few lipid head-groups start to migrate from the membrane-water interface to the interior of the bilayer, stabilizing hydrophilic pores (~ 1 to 3 nm diameter).

All MD studies reported pore expansion as the electric field was maintained. In contrast, it was shown in one instance [21] that a hydrophilic pore could reseal within few nanoseconds when the applied field was switched off. Membrane complete recovery, i.e. migration of the lipid head group forming the hydrophilic pore toward the lipid/water interface, being a much longer process, was not observed. More recently systematic studies of pore creation and annihilation life time as a function of field strength have shed more light onto the complex dynamics of pores in simple lipid bilayers [22,73]. Quite interestingly, addition of salt has been shown to modulate these characteristic time scales [74].

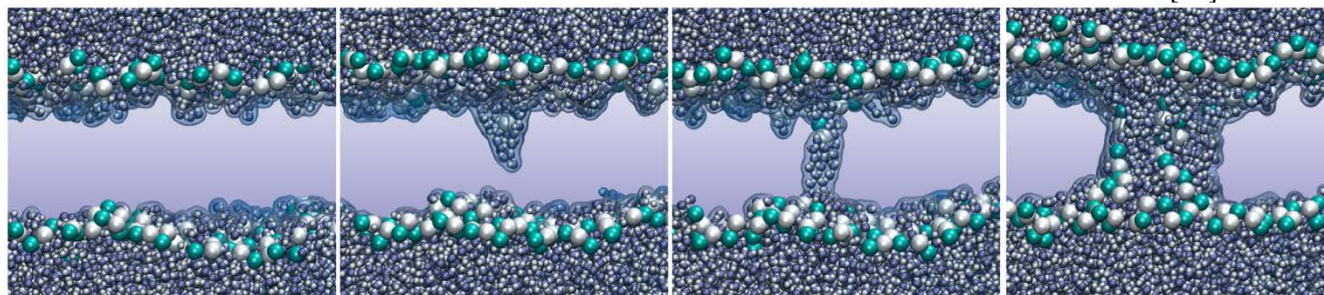


Figure. 3 Pore evolution in a POPC bilayer: The POPC headgroups are shown as cyan and white beads, the lipids tails are not show for clarity. The pore creation, in MD simulations, takes places in the range of nanoseconds.

For typical MD system sizes (128 lipids; 6 nm x 6 nm membrane cross section), most of the simulations reported a single pore formation at high field strengths. For much larger systems, multiple pore formation with diameters ranging from few to 10 nm could be witnessed [20,21]. Such pores are in principle wide enough to transport ions and small molecules. One attempt has so far been made to investigate such a molecular transport under electroporation [21]. In this simulation, partial transport of a 12 base pairs DNA strand across the membrane could be followed. The strand considered diffused toward the interior of the bilayer when a pore was created beneath it and formed a stable complex DNA/lipid in which the lipid head groups encapsulate the strand. The process provided support to the gene delivery model proposed by Golzio et al. [75] in which, an “anchoring step” connecting the plasmid to permeabilized cells membranes that takes place during DNA transfer assisted by electric pulses, and agrees with the last findings from the same group [76]. More recently, (see sections below) it was shown that even a single 10 ns electric pulses of high enough magnitude can enhance small siRNA transport through lipid membranes [77].

The electroporation process takes place much more rapidly under higher fields, without a major change in the pore formation characteristics. The lowest voltages reported to electroporate a PC lipid bilayer are ~ 2 V [22][72]. Ziegler and Vernier [23] reported minimum poration external field strengths for 4 different PC lipids with different chain lengths and composition (number of unsaturations). The authors find a direct correlation between the minimum porating fields (ranging from $0.26 \text{ V}\cdot\text{nm}^{-1}$ to $0.38 \text{ V}\cdot\text{nm}^{-1}$) and the membrane thickness (ranging from 2.92 nm to 3.92 nm). Note that estimates of electroporation thresholds from simulations should, in general be considered only as indicative since it is related to the time scale the pore formation may take. A field strength threshold is “assumed” to be reached when no membrane rupture is formed within the 100 ns time scale.

B- ELECTROPORATION INDUCED BY IONIC SALT CONCENTRATION GRADIENTS

Regardless of how low intensity millisecond electrical pulses are applied, the ultimate step is the charging of the membrane due to ions flow. The resulting ionic charge imbalance between both sides of the lipid bilayer is locally the main effect that induces the TM potential. In a classical set up of membrane simulations, due to the use of 3d PBCs, the TM voltage cannot be controlled by imposing a charge imbalance Q_s across the bilayer, even when ions are present in the electrolytes. Several MD simulations protocols that can

overcome this limitation have been recently devised (Fig. 1):

The double bilayer setup: It was indeed shown that TM potential gradients can be generated by a charge imbalance across lipid bilayers by considering a MD unit cell consisting of three salt-water baths separated by two bilayers and 3d-PBCs [78] (cf. Fig. 1.C). Setting up a net charge imbalance between the two independent water baths at time $t=0$ induces a TM voltage ΔV by explicit ion dynamics.

The single bilayer setup: Delemotte et al. [79] introduced a variant of this method where the double layer is not needed, avoiding therefore the over-cost of simulating a large system. The method consists in considering a unique bilayer surrounded by electrolyte baths, each of them terminated by an air/water interface [43]. The system is set-up as indicated in Fig. 1.D. First, a hydrated bilayer is equilibrated at a given salt concentration using 3d periodic boundary conditions. Air water interfaces are then created on both sides of the membrane, and further equilibration is undertaken at constant volume, maintaining therefore a separation between the upper and lower electrolytes. A charge imbalance Q_s between the two sides of the bilayer are generated by simply displacing at time $t=0$ an adequate number of ions from one side to the other. As far as the water slabs are thicker than 25-30 Å, the presence of air water interfaces has no incidence on the lipid bilayer properties and the membrane “feels” as if it is embedded in infinite baths whose characteristics are those of the modelled finite solutions.

Fig. 2 reports the electrostatic potential profiles along the normal to the membrane generated from MD simulations a POPC bilayer in contact with 1M NaCl salt water baths at various charge imbalances Q_s , using the single bilayer method. For all simulations, the profiles computed at the initial stage show plateau values in the aqueous regions and, for increasing Q_s , an increasing electrostatic potential difference between the two electrolytes indicative of a TM potential ΔV . Quite interestingly, the profiles show clearly that, in contrast to the electric field case where the TM voltage is mainly due to the water dipole reorientation, most of the voltage drop in the charge imbalance method is due to the contribution from the ions. Indeed the sole collapse of the electrostatic potential due to the charge imbalance separation by the membrane lipid core accounts for the largest part of ΔV .

Using the charge imbalance set-up, it was possible for the first time to directly demonstrate *in silico* that the simulated lipid bilayer behaves as a capacitor [79,80]. Simulations at various charge imbalances Q_s show a linear variation of ΔV from which the capacitance can be estimated as $C = Q_s \cdot \Delta V^{-1}$. The capacitance values extracted from simulations are

expected to depend on the lipid composition (charged or not) and on the force field parameters used and as such constitute a supplementary way of checking the accuracy of lipid force field parameters used in the simulation. Here, in the case of POPC bilayers embedded in a 1M solution of NaCl, the later amounts to $0.85 \mu\text{F}\cdot\text{cm}^{-2}$ which is in reasonable agreement with the value usually assumed in the literature *e.g.* $1.0 \mu\text{F}\cdot\text{cm}^{-2}$ [78,81] and with recent measurements for planar POPC lipid bilayers in a 100 mM KCl solution ($0.5 \mu\text{F}\cdot\text{cm}^{-2}$).

For large enough induced TM voltages, the three protocols lead to electroporation of the lipid bilayer. As in the case of the electric field method, for ΔV above

1.5-2.5 Volts, the electroporation process starts with the formation of water fingers that protrude inside the hydrophobic core of the membrane. Within nanoseconds, water wires bridging between the two sides of the membrane under voltage stress appear. If the simulations are further expanded, lipid head-groups migrate along one wire and form a hydrophilic connected pathway (Fig.3). Because salt solutions are explicitly considered in these simulations, ion conduction through the hydrophilic pores occurred following the electroporation of the lipid bilayers. Details about the ionic transport through the pores formed within the bilayer core upon electroporation could be gathered.

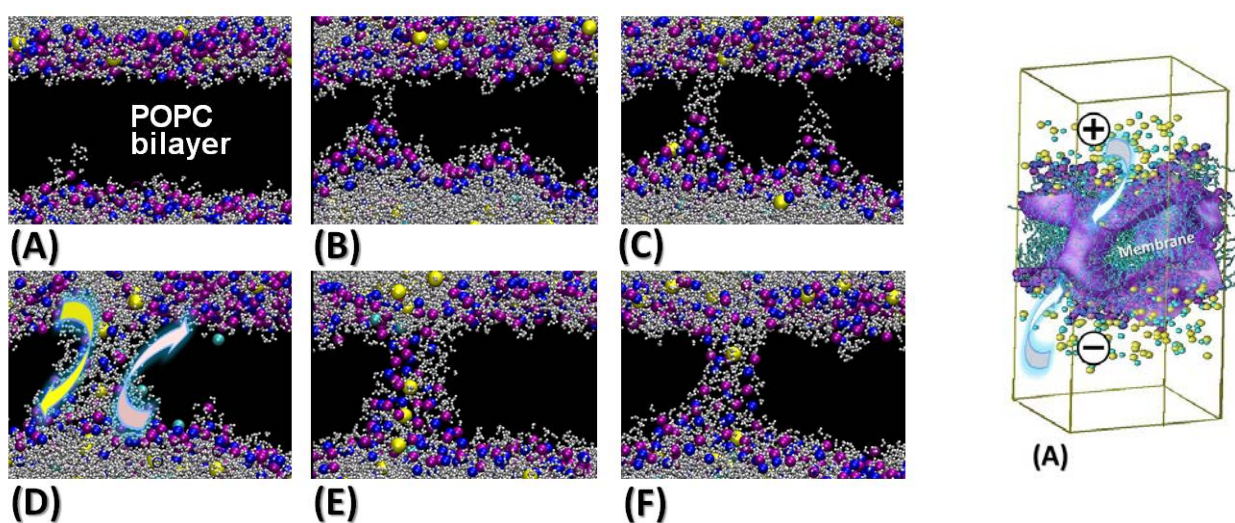


Figure. 4 Left Sequence of events following the application of a TM voltage to a POPC lipid bilayer using the charge imbalance method (panels A to F). Note the migration of Na^+ (yellow) and Cl^- (cyan) ions through the formed hydrophilic pores that are lined with lipid phosphate (magenta) and nitrogen (blue) head group atoms. Panel F represents the state of a non conducting pore reached when the exchange of ions between the two baths lowered Q_s and therefore ΔV to values ≈ 200 mV. Right Topology of the nanometer wide hydrophilic pores formed under high transmembrane ΔV imposed by the charge imbalance method in the planar bilayer (A). The arrows highlight the subsequent ionic flow through the pores.

The MD simulations of the double bilayer system [82,83], and the results presented here for the single bilayer set-up show that both cations and anions exchange through the pores between the two baths, with an overall flux of charges directed toward a decrease of the charge imbalance. Ions translocation through the pores from one bulk region to the other lasts from few tens to few hundreds picoseconds, and leads to a decrease of the charge imbalance and hence to the collapse of ΔV . Hence, for all systems, when the charge imbalance reached a level where the TM voltage was down to a couple of hundred mV, the hydrophilic pores “close” in the sense that no more ionic translocation occurs (Fig 4.F). The final topology of the pores toward the end of the simulations remain stable for time spans exceeding the 10 nanoseconds scale,

showing as reported in previous simulations [21] that the complete recovery of the original bilayer structure requires a much longer time scale.

Note that in order to maintain ΔV constant the modeler needs to maintain the initial charge imbalance by “injecting” charges (ions) in the electrolytes at a paste equivalent to the rate of ions translocation through the hydrophilic pore. This protocol is, in particular for the single bilayer setup, adequate for performing simulations under constant voltage (low voltage, ms duration) or constant current conditions, which is suitable for comparison to experiments undertaken under similar conditions [84].

C- INTERNAL ELECTRIC FIELD DISTRIBUTION AND ORIGIN OF MEMBRANES ELECTROPORATION

In order to determine the detailed mechanism of the pore creation, it is helpful to probe the electric field distribution across the bilayer, both at rest and under the effect of a TM voltage. Figure 5.A displays the electrostatic potential profiles for a lipid bilayer subject to increasing electric fields that generate TM potentials ranging from 0 V to ~ 3 V. At 0 V, the lipid bilayer is at rest and the profiles reveal, in agreement with experiment [85], the existence of a positive potential difference between the membrane interior and the adjacent aqueous phases.

At rest, the voltage change across the lipid water interfaces gives rise locally to large electric fields (in the present case up to $1.5 \text{ V}\cdot\text{nm}^{-1}$) oriented toward the bulk, while at the center of the bilayer, the local electric

field is null (Fig. 5.B,C). When external electric fields of magnitudes respectively of 0.06 and $0.30 \text{ V}\cdot\text{nm}^{-1}$ are applied, reorientation of the water molecules gives rise to TM potentials of respectively ~ 0.75 and 3 V . Figs 5.B and C reveal the incidence of such reorganization on the local electric field both at the interfacial region and within the bilayer core. In particular one notes that the field in the membrane core has risen to a value $\sim 1 \text{ V}\cdot\text{nm}^{-1}$ for the highest ΔV imposed.

For the charge imbalance method, the overall picture is similar, where again, the TM voltages created give rise to large electric fields within the membrane core, oriented perpendicular to the bilayer.

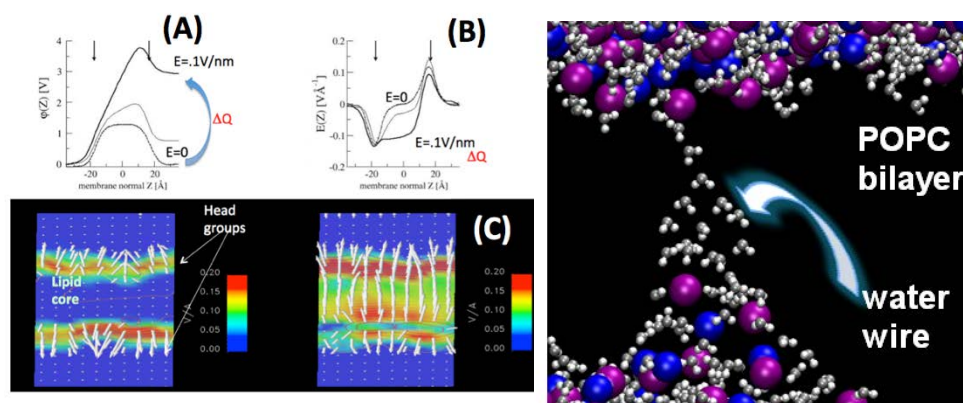


Figure 5 (A) Electrostatic potential profiles across a lipid bilayer subject to electric fields of 0 V/nm (dotted line) 0.06 V/nm (thin line) and 0.30 V/nm (bold line), or to a charge imbalance ΔQ . (B) Corresponding electric field profiles. (C) 2d (out of plane) maps of the electric field distribution. The local electric field direction and strength are displayed as white arrows. Note that at 0 mV , due to the bilayer dipole potential at rest, the larger electric fields are located at the lipid water interfaces and are oriented toward the solvent, and no electric field is present in the lipid core. When the bilayer is subject to a TM potential, a net electric field appears in the hydrocarbon region. The latter promotes dipolar orientation and penetration of water molecules (Right panel) inside the bilayer.

Qualitatively, in both methods, the cascade of events following the application of the TM voltage, and taking place at the membrane, is a direct consequence of such a field distribution. Indeed, water molecules initially restrained to the interfacial region, as they randomly percolate down within the membrane core, are subject to a high electric field, and are therefore inclined to orient their dipole along this local field. These molecules can then easily hydrogen bond among themselves, which results in the creation of single water files. Such fingers protrude through the hydrophobic core from both sides of the membrane. Finally, these fingers meet up to form water channels (often termed pre-pores or hydrophobic pores) that span the membrane. As the TM voltage is maintained, these water wires appear to be able to overcome the free energy barrier associated to the formation of a single file of water molecules spanning the bilayer (estimated to be $\sim 108 \text{ kJ/mol}$ in the absence of external electric field [86]). As the electrical stress is maintained, lipid head group migrate along the stable water wires and participate in the formation of larger “hydrophilic

pores”, able to conduct ions and larger molecules as they expand.

Ziegler et al. [23] have shown clearly that the orientation of the lipid headgroups (dipoles) is not a determinant factor in the EP process. The general assumption that the lipid headgroups have a marginal role in the formation of the electropores, is consistent with studies on octane [20] as well as vacuum slabs [87] electroporation: These works have shown that, as in lipid bilayers, water columns can form in any water/low-dielectric/water system subject to high electric fields.

Experimental evidence shows that pores do close when the PEF is turned off. The kinetics of this process determines how long leakage from or delivery to targeted cells can last. MD simulations indicate that this process initiates with a collapse of the pore (closure) due to a rapid leakage of water outwards to the bulk, followed by a much slower reorganization that leads to lipid headgroups re-partitioning toward the external hydrophilic leaflets. Resealing kinetics is independent of the magnitude of the pore initiation

electric fields. In general, complete recovery of the original bilayer structure requires a much longer time scale [21,87,88], spanning from nanoseconds to hundreds of nanoseconds, and depends critically on the structure of the bilayer [89]. Note that addition of salt to systems undergoing the nsPEF protocol has been shown to modulate the characteristic time scales of the whole pore life cycle [88,90].

COMPLEX BILAYER MODELS: EP THRESHOLDS AND PORE FEATURES

A- ELECTROPORATION THRESHOLDS

Since the pioneering simulations [21,91], which considered simple lipid bilayers of 1,2-dioleoyl-sn-glycero-3-phosphocholine (DOPC) and dimyristoyl-phosphatidylcholine (DMPC), a variety of lipid bilayers have been modeled in order to understand the key elements that might modulate their electroporation thresholds. The increase of the EP threshold upon addition of cholesterol [92–94] was studied using the E field [95] and charge imbalance protocols [93]. For the former, a steady increase of the EP threshold coincides with an increase in cholesterol concentration: a two folds higher electric field was necessary for the electroporation of bilayers with the addition of 50 mol% cholesterol. Under μ s-msPEFs conditions, the EP threshold was showed to level-off above 30 mol % cholesterol. Generally, the increase of the EP threshold has been linked to the increase of the stiffness of the bilayer [92,94].

In a series of papers [96,97] Tarek's group investigated the effect on the EP threshold of ester and ether linkages, of branched (phytanoyl) tails, and of bulky (glucosyl-myo and myo inositol) lipid head groups. The authors have found that the EP threshold of a lipid bilayer depends not only on the "electrical" properties of the membrane, i.e. its dipole potential or membrane capacitance, but also on the nature of lipids hydrophobic tails. The authors report that there is a correlation between the lateral pressure in the water/lipid interface and the EP threshold. They suggest that an increase of the lateral pressure (in the branched lipid membrane compared with the simple lipid bilayers) hinders the local diffusion of water molecules toward the interior of the hydrophobic core, which lowers the probability of pore formation, increasing therefore the electroporation threshold.

Comparing specifically the Archeal lipids (glucosyl-myo and myo inositol head groups) to normal PC lipid, the higher electroporation thresholds for the former was attributed [96,97] to the strong hydrogen-bonding network stabilizing the head-group head group interactions. Likewise, Gurtovenko et al. [98] reported higher EP threshold for

phosphatidylethanolamine (PE) lipid bilayers compared to phosphatidylcholine (PC) lipid bilayers. This effect was linked to inter-lipid hydrogen bonding taking place in the PE bilayer, which leads to a denser packed water/lipid interface and more ordered hydrocarbon lipid chains. Considering an asymmetric bilayer, composed by PC and PE lipid leaflets, the authors observed that the initial electroporation feature, i.e. the water column formation is also asymmetric, with initial steps taking place primarily at the PC leaflet. Studying more complex composition membranes, Piggot et al. [99] reported that the Gram-positive bacterial *S. aureus* cell membrane is less resistant to poration than the Gram-negative bacterial *E. coli* outer membrane (EcOM). The higher EP threshold of the EcOM was linked to the reduced mobility of the Lipopolysaccharide molecules that are located in the outer leaflet. Additional factors, such as cholesterol, the presence of impurities, and other compounds, can modify the permeation properties of membrane models by acting on their stability.

B- PORE FEATURES

The MD results support the hypothesis that following the application of a high transmembrane voltage, the cell membrane is permeabilized by the formation of conducting hydrophilic pores stabilized by the lipid headgroups. The properties of the lipids play a determinant role in the electropores life-time and in its structural characteristics (e.g. size, shape, morphology) [87]. Other studies, considering various lipid bilayers, challenged the standard pore morphology. Tarek and coauthors pointed out that a peculiar EP process may be possible in which large long living ion-conducting water columns are not stabilized by lipid headgroups [93,97,100]. These "hydrophobic" conducting pores originate from constraints of a different nature in the lipid bilayer. The first report [100] focused on a palmitoyl-oleyl-phosphatidylserine (POPS) bilayer characterized by negatively charged headgroups. When this system was subject to a charge imbalance high enough to electroporate the bilayer, the migration of lipids along the water column turn out to be largely hindered (Fig. 5, second panel [100]). Similar conclusions were drawn for PC lipid bilayers containing more than 30 mol % cholesterol [93] or for Archeal lipids [97] (Fig. 5). This peculiar morphology was ascribed to the repulsion of negatively charged headgroups in the first case [100], to the condensing effect of cholesterol in the second [93], and to the steric hindrance of the bulky headgroups coupled with the branched tails in the latter [97].

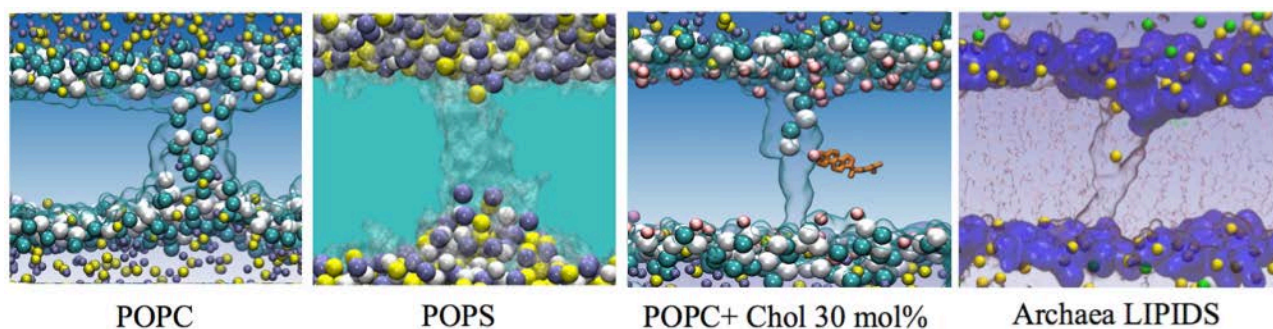


Figure 6. Various morphologies of conducting pores revealed by MD simulations. Note that beside the POPC zwitterionic lipids, pores formed in POPS, a negatively charged lipid, with addition of cholesterol, or in the complex Archaea lipids (sugar like head groups), the electropores are not stabilized by the lipid head groups.

C- PORES STABILIZATION

When dealing with the characteristics of electropores (e.g. size, conductance, transport of molecules) one would expect the pore to be in an energetically favorable state, i.e. one that corresponds to a stable configuration. In order to understand if the pore can be considered in a steady state for a given TM voltage and characterize its size and conductance, the two MD procedures, (introduced in previous sections) need to be improved. Indeed, the main drawback of these two protocols, as usually used, resides in the impossibility of maintaining a stable pore. In the electric field method, the pore tends to expand, leading to the breakdown of the bilayer, when it reaches the dimensions of the simulation cell box. The charge imbalance protocol, on the other hand, suffers from an important shortcoming: The imbalance is not re-set during the simulation. Thus, in the studies carried out both with the double and single bilayer schemes, the charge imbalance imposed at the beginning decreases significantly within several tens/hundreds ps (depending on the system size) of EP due to an exchange of ions through the pore. The decrease of the charge imbalance results in a TM voltage drop, which ultimately leads to pore collapse and resealing.

When using the nsPEF protocol, the lowering of the electric field intensity after pore creation was shown to result in its stabilization [22]. Using the same strategy, Fernández et al. [95] could modulate the size of the pore and showed that it depends only on the strength of the stabilizing electric field. More recently our group [101] used a scheme to maintain a constant charge imbalance, refining thereby the μ s-msPEFs approach to obtain size-controlled steady pores. The protocol used is identical to the procedure proposed by Kutzner et al. [84] to study the transport in ion channels using the double layer scheme. In this procedure, named “swapping”, the number of ions in the two solution baths is frequently estimated and, if the latter differs from the initial setup, a “swapping” event takes place: An ion of one solution is exchanged by a water

molecule of the other solution bath (see the supplementary material for more information). Note that to overcome the limitation of simulating the bilayer in the NVT ensemble (constant volume), the swapping procedure can be coupled with the NP γ T ensemble (constant surface tension) to maintain the bilayer surface tension constant (null) and mimic, therefore, experimental conditions [101].

D- PORE CHARACTERIZATION

A first attempt to link experimental evidence of pore conductance and radius estimation was carried out by Kramar et al. using a linear rising current technique combined with MD simulations performed under similar conditions [102]. Their findings suggest that the opening and closing of a single pore under conductance in the 100-nS scale would be possible for a pore diameter of \sim 5 nm.

More systematic investigations, using the nsPEF [95,103] and μ s-msPEF [101] modified protocols allowed to better characterize the conductance of electropores. For simulations carried out under the two protocols and when applying TM voltages below the EP threshold, the pore formed could be stabilized to different radii for tens of ns. Quite interestingly, the pore radii, and the pore conductance were found to vary almost linearly with the applied voltage. Moreover, the pores were found to be more selective to cations than to anions [101,103,104]. This selectivity arises from the nature of the lipid molecules constituting the pore: The negatively charged phosphate groups that form the walls of the pore attract sodium ions, which hinders their passage across the bilayer, but also makes the pore interior electrostatically unfavorable for other sodium ions [105]. This, already, suggests that the transport through electropores is sensitive to the type of solutes, showing a different affinity for different charged species.

TRANSPORT OF MOLECULES

Although numerous molecules are implicated in EP and/or concerned by its applications (e.g. drugs, genetic material, dyes, ...), very few have been investigated with MD simulations. Apart from few studies in which electropore-mediated flip-flop of zwitterionic PC lipids [106–108] was reported, most simulations concerned charged species for which transport involved electrophoresis [21,77,109]. In the following, we discuss the results obtained using the two simulations protocols.

A- nsPEFs

nsPEFs can induce externalization of phosphatidylserine (PS), a phospholipid usually confined to the inner leaflet of the plasma membrane that can trigger several recognition, binding and signaling functions. MD studies of PS bilayers [19,110] showed how PS externalization is a pore-mediated event occurring exclusively with an electrophoretic drift.

A decade ago, Tarek [21] reported the first MD simulation on the transport of a short DNA double strand using high intense electric fields. It was shown that the uptake occurred only in presence of the pore by electrophoretic drift. Since then, to our knowledge, only two MD studies have been reported on the transport of molecules under nsPEFs. In 2012 Breton et al. [77] showed that a single 10 ns high-voltage electric pulse can permeabilize giant unilamellar vesicles (GUVs) and allows the delivery of a double-stranded siRNA (-42e charge, 13.89 kDa) through the formed pore, by electrophoresis (Fig. 7 [77]). Comparing experimental evidence with MD simulations they could show in particular that: (i) following the application of an electric field, the siRNA is pushed toward the lipid headgroups forming an siRNA- phospholipids headgroups complex that remains stable even when the pulse is switched off; (ii) no transport is detected for electric fields applied below the EP threshold; (iii) when the E_{app} is above the EP threshold (E_{th}) the siRNA is electrophoretically pulled through the electropore and translocated within a 10 ns time scale; (iv) if the E_{th} is turned off before the complete transition, the pore collapses around the molecule which is, hence, trapped.

Recently, Salomone et al. [109] used a combination of nsPEFs and the chimeric peptides (CM18-Tat11) as efficient delivery vectors for plasmid DNA using endocytotic vesicles. To provide molecular details about the processes taking place, the authors modeled the peptide and its fragments. They reported from MD simulations that, when subject to high electric fields, Tat11, a small cationic peptide (residues 47-57 of HIV-1 Tat protein; +8e charge, 1.50 kDa) can translocate

through an electroporated bilayer within few nanoseconds without interacting with the phospholipid headgroups. In contrast, the amphipathic peptide CM18, even when located near a preformed pore, remains anchored to the lipid headgroups and does not translocate during a 12 ns high electric field pulse.

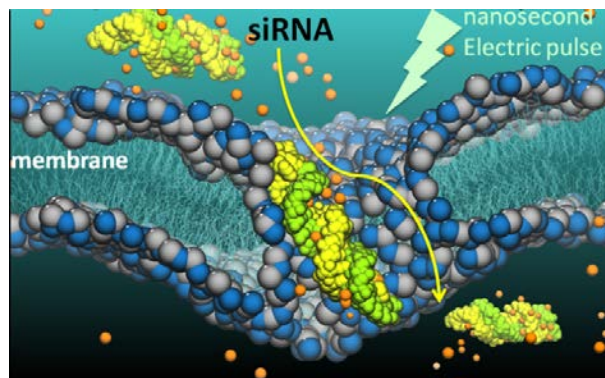


Figure 7: A single 10 ns high-voltage electric pulse can permeabilize lipid vesicles and allow the delivery of siRNA to the cytoplasm. Combining experiments and molecular dynamics simulations has allowed us to provide the detailed molecular mechanisms of such transport and to give practical guidance for the design of protocols aimed at using nanosecond-pulse siRNA electro-delivery in medical and biotechnological applications [77].

B- μ s-msPEFs

We present below the latest results from MD simulations of the uptake of molecules through lipids bilayers subject to μ s-msPEFs. We focus our attention on Tat11 and the siRNA double strand to compare their mechanism of transport to the one reported using the nsPEFs [77,109]. These data have been reported in [111].

Transport of siRNA

In 2011 Paganin-Gioanni et al. [76] investigated siRNA uptake by murine melanoma cells, when subject to electric pulses (1 Hz of repetition frequency) using time lapse fluorescence confocal microscopy. A direct transfer into the cell cytoplasm of the negatively charged siRNA was observed across the plasma membrane exclusively on the side facing the cathode. Noting that when added after electropulsation, the siRNA was inefficient for gene silencing because it did not penetrate the cell, the authors concluded that the siRNA transport takes place during the electric pulse and is due to electrophoresis through electropores. The same group reported also that 0.17 kV/cm - 5 ms pulses, named EGT, are more effective in terms of silencing than the more intense less lasting HV pulses (1.3 kV/cm - 0.1 ms). They showed on the other hand that a double pulse procedure, consisting of one HV followed by a long below-EP-threshold pulse does not increase the efficiency of the delivery. All together,

their evidence suggests that, for msPEFs, the key factors for an efficient delivery are the voltage above the EP threshold and the duration of the pulse.

In order to investigate the siRNA transfer into cells under conditions similar to the μ s-msPEFs experiments, we have performed a set of simulations where the system was subject to several voltages (see Table 1). We first electroporate a bilayer patch by submitting it to a high charge imbalance. Once the pore was large enough (arbitrary value of ~ 2 nm radius) we lowered ΔQ s to stabilize it to different radii as in [101]. These configurations were then used to start the simulations with siRNA placed near the pore mouth and were continued at the desired voltage.

Table 1 Pore radius R and crossing time t_c estimated at specific TM voltages (U_m) for the two molecules considered. The pore radius (diameter) is estimated as the minimum lipid to lipid distance along the pore lumen

System	t_s (ns)	U_m (V)	R (nm)	t_c (ns)
POPC_1024+siRNA	100	0.16 ± 0.16	2.0 ± 0.6	> 100
	35	0.55 ± 0.19	3.3 ± 0.2	32.5
POPC_1024+Tat ₁₁	40	0.43 ± 0.16	1.6 ± 0.2	32.8
	14	0.70 ± 0.24	2.0 ± 0.1	11.3

t_s – simulation time; U_m – transmembrane voltage create by the charge imbalance; R – minimum pore radius maintained by a given U_m (see SM); t_c – crossing time of the molecule through the electropore.

For the lowest transmembrane voltages U_m run, the siRNA approached the large pore (~ 4 nm diameter) mouth then started sliding through it while interacting with the lipid headgroups lining it. The complete translocation of the siRNA did not occur however within the first 100 ns of the run. In a completely independent run, we repeated the simulation by maintaining a higher voltage, namely 0.55 V. The siRNA approach, pore entry and sliding under these conditions (Fig. 7) were similar to the lower voltage run. However, at 0.55 V despite its anchoring to the lipid headgroups, a complete translocation from the upper to the lower water bath occurred in ~ 30 ns. Two factors contributed probably to this speed up. Compared to the previous conditions, not only the

electrophoretic force pulling the siRNA is indeed higher, but the pore size increases too under this higher voltage.

All together the simulations mimicking μ s-msPEFs experiments, demonstrate that the translocation of siRNA through the pore driven by the application of TM voltages above 0.5 V takes place in the nanosecond time scale, as reported for the nsPEFs. Noticeably, in both simulations carried out under electric field or under the charge imbalance, the siRNA remains anchored to the lower leaflet of the membrane after translocation without diffusing in the bulk solution even if the voltage is maintained.

Experiments performed on mouse melanoma cells applying ms-long pulses evidenced that tuning the duration of the pulse is essential for an efficient siRNA uptake. In fact the authors found more effective the EGT (0.17 kV/cm, 5 ms) class of pulses than the HV (1.3 kV/cm, 0.1 ms) one. No direct measurement of the TM voltage was carried out during these experiments and the authors assume that it is around 0.25 V, since it was observed that the EP threshold value is always about 0.20 mV for many different cell systems [112]. Corroborated by our findings, one can speculate that the transport of siRNA when subject to longer pulses could be facilitated by the formation of a pore population having larger diameters. This population of larger pores would allow siRNAs to flow through the pore and to access directly the cytoplasm increasing the transport efficiency.

Transport of Tat₁₁

The translocation for Tat₁₁ differs from the highly charged siRNA because no specific interactions between this peptide and the lipid headgroups take place during the process, resulting in a faster uptake. Under a TM voltage $U_m \sim 0.70$ V, the molecule, initially parallel to the membrane and located near the pore opening, first rotates to align its dipole along the local electric field (Fig. 10, $t = 0$ ns), then drifts though the center of the pore with a radius of 2 nm (Fig. 10, $t = 8$ ns), over the same time scale reported by the nsPEFs procedure [109]. The Tat₁₁ reaches the lower bath where it freely diffuses (Fig. 8, $t = 12$ ns). At lower U_m (~ 0.43 V) Tat₁₁ translocates in 32.8 ns (see Table 1), presumably as a consequence of a higher hindrance of the pore (the pore radius decreases to 0.4 nm) and of a reduction of the electrophoretic drift.

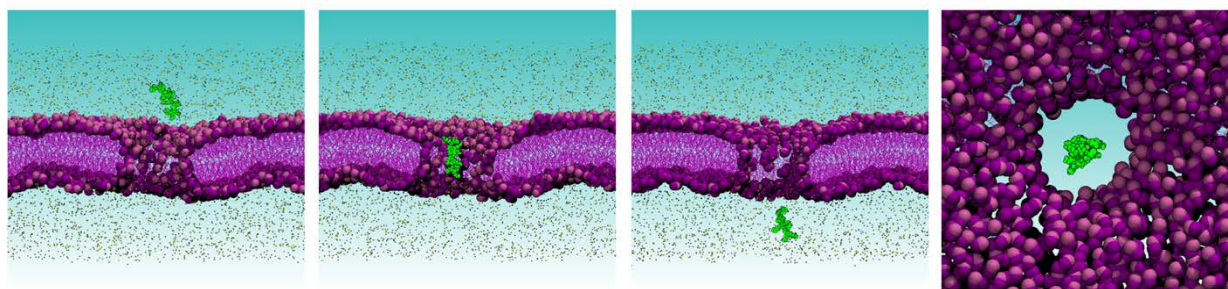


Figure. 8 The process of Tat₁₁ transport in three frames corresponding to 0, 8, and 12 ns. In the right panel the top view clearly shows no interactions between the molecule and the pore walls. The POPC headgroups are shown as mauve and violet beads, the tails as purple lines; sodium and chloride ions are colored in yellow and gray; Tat₁₁ is green (adapted from [111]).

Considering a patch of 256 lipids, and applying an electric field that generates a 1.6 V across the bilayer, Salomone et al. [109] reported that Tat11 translocates through an electropore within 10 ns. This seems inconsistent with our results since one should expect that under our conditions, i.e. subject to a voltage U_m of ~ 0.43 V, the time needed for Tat11 transport would be much longer. Indeed, if one considers only the ratio of electrophoresis, translocation of Tat11 should be three times slower at the lower voltage. In addition, a second inconsistency concerns the sizes of the pores created. Indeed in [109] the pore created has a radius of ~ 1.7 nm, much smaller than one expected from our results: we generated a pore of radius ~ 1.6 nm under $U_m \sim 0.43$ V (Table 1). We have recently reported size effects in simulations of lipid bilayers electroporation, and shown specifically that patches of 256 lipids are too small to study electroporation: Pores generated in MD simulations using such patches are much smaller than those generated using larger patches (1024 lipid).

Despite these discrepancies, it is very interesting to note that both when applying both an electric field and charge imbalance, the translocation of a small charged molecule such as Tat11 occurs on the tens of nanosecond time scale.

DISCUSSION AND PERSPECTIVES

A current goal in improving our understanding of EP is the development of a comprehensive microscopic description of the phenomenon, not an easy task due to the nanoscale dimensions of the lipid electropore and the short time scale (nanoseconds) of pore creation, which present challenges to direct experimental observations. For these reasons, molecular dynamics simulations have become extremely important to study EP in atomic detail. In the last decade, a large number of MD simulations have hence been conducted in order to model the effect of electric fields on membranes, providing perhaps the most complete molecular model of the EP process of lipid bilayers.

Our investigation of the electrotransfer of small charged molecules, siRNA ($-42e$) and Tat11 ($+8e$)

through a cell membrane model subject to microsecond pulse electric fields (μ s-msPEFs) provided a novel insight. For transmembrane voltages of few hundred millivolts we report for siRNA a complete crossing translocation from one side of the bilayer to the other within several tens of nanoseconds despite its strong anchoring with the zwitterionic phospholipids headgroups. Tat11 on the other hand, is transported (within ~ 10 ns) without any interaction with the pore. Interestingly, for both molecules, we found that the transport process takes place at the same time scale (nanosecond) as much shorter pulses (nsPEFs) that we previously reported. Importantly, we recall that experiments are performed on cells, while our investigation concerns lipid bilayers. In cells, one should also consider the cytoskeleton and possible interactions with molecules e.g. siRNA in its way to the cytosol, slowing down the process of translocation.

In summary, we have designed MD protocols suitable for the characterization of the transport of uncharged and charged species driven by μ s-msPEFs that can help to shed light on the uptake mechanism of drugs by cell membranes. Systematic studies carried out with this protocol in presence of other relevant drugs (e.g. bleomycin) or dyes (e.g. propidium iodide, YO-PRO,...) are expected to drastically broaden our understanding of the uptake mechanism, thus providing further insights may lead to improvements in related experimental techniques and therapeutic effectiveness.

It is worth mentioning another aspect that needs to be considered as well when studying electric field effect on cells. It has been suggested over a decade ago, that membranes can be oxidized upon electroporation. Experimental evidence reports, indeed, that pulsed electric fields can increase the extent at which lipid acyl chain peroxidation occurs. In particular, it has been demonstrated that the application of external electric fields alters the phospholipid composition and properties of liposomes, vesicles and cells [113–119]. The presence of oxidized lipids within biomembranes is known to modify their physical properties and, in particular, their permeability [120–123]. We cannot

therefore exclude that uptake under PEFs experiments may be, at least partially, taking place through diffusion across oxidized/permeabilized lipid bilayers and not uniquely across electropores. Simulations along these lines should improve our characterization of the electro-transport of molecules across membranes driven by electric fields.

REFERENCES

- [1] N. Eberhard, A. E. Sowers, and C. A. Jordan, *Electroporation and electrofusion in cell biology*. New York: Plenum Press, 1989.
- [2] J. A. Nickoloff, *Animal cell electroporation and electrofusion protocols*, vol. 48. Totowa, NJ: Humana Press, 1995.
- [3] S. Li, *Electroporation protocols: preclinical and clinical gene medicine*, vol. 423. Totowa, NJ.: Humana press, 2008.
- [4] R. B. Gennis, *Biomembranes: molecular structure and function*. Heidelberg: Spring Verlag, 1989.
- [5] I. G. Abidor, V. B. Arakelyan, L. V. Chernomordik, Y. A. Chizmadzhev, V. F. Pastushenko, and M. P. Tarasevich, "Electric breakdown of bilayer lipid membranes. I. The main experimental facts and their qualitative discussion," *J. Electroanal. Chem.*, vol. 104, no. C, pp. 37–52, 1979.
- [6] R. Benz, F. Beckers, and U. Zimmerman, "Reversible electrical breakdown of lipid bilayer membranes - Charge-pulse relaxation study," *J. Membr. Biol.*, vol. 48, pp. 181–204, 1979.
- [7] J. C. Weaver and Y. A. Chizmadzhev, "Theory of electroporation: A review," *Bioelectrochemistry and Bioenergetics*, vol. 41, no. 2. Elsevier Science S.A., pp. 135–160, 1996.
- [8] J. C. Weaver, "Electroporation of biological membranes from multicellular to nano scales," *IEEE Trans. Dielectr. Electr. Insul.*, vol. 10, pp. 754–768, 2003.
- [9] C. Chen, S. W. Smye, M. P. Robinson, and J. A. Evans, "Membrane electroporation theories: A review," *Medical and Biological Engineering and Computing*, vol. 44, no. 1–2. pp. 5–14, 2006.
- [10] G. Pucihar, T. Kotnik, B. Valic, and D. Miklavcic, "Numerical determination of transmembrane voltage induced on irregularly shaped cells," *Ann. Biomed. Eng.*, vol. 34, pp. 642–652, 2006.
- [11] G. Pucihar, T. Kotnik, D. Miklavcic, and T. J., "Kinetics of transmembrane transport of small molecules into electroporeabilized cells," *Biophys. J.*, vol. 95, pp. 2837–2848, 2008.
- [12] D. C. Chang, "Structure and dynamics of electric field-induced membrane pores as revealed by rapid-freezing electron microscopy," in *Guide to Electroporation and Electrofusion*, Orlando, Florida: Academic Press, 1992, pp. 9–27.
- [13] D. P. Tieleman, S.-J. Marrink, and H. J. C. Berendsen, "A Computer Perspective of Membranes: Molecular Dynamics Studies of Lipid Bilayer Systems," *Biochim. Biophys. Acta*, vol. 1331, no. 3, pp. 235–270, 1997.
- [14] D. J. Tobias, K. Tu, and M. L. Klein, "Assessment of all-atom potentials for modeling membranes: Molecular dynamics simulations of solid and liquid alkanes and crystals of phospholipid fragments," *J. Chim. Phys.*, vol. 94, pp. 1482–1502, 1997.
- [15] L. R. Forrest and M. S. P. Sansom, "Membrane simulations: bigger and better," *Curr. Opin. Struct. Biol.*, vol. 10, pp. 174–181, 2000.
- [16] S. E. Feller, "Molecular dynamics simulations of lipid bilayers," *Curr. Opin. Coll. In.*, vol. 5, pp. 217–223, 2000.
- [17] C. Chipot, M. L. Klein, M. Tarek, and S. Yip, "Modeling lipid membranes," in *Handbook of Materials Modeling*, S. Yip, Ed. Dordrecht, The Netherlands: Springer, 2005, pp. 929–958.
- [18] S. J. Marrink, A. H. de Vries, and D. P. Tieleman, "Lipids on the move: Simulations of membrane pores, domains, stalks and curves," *Biochim. Biophys. Acta. Biomembr.*, vol. 1788, pp. 149–168, 2009.
- [19] Q. Hu, S. Viswanadham, R. P. Joshi, K. H. Schoenbach, S. J. Beebe, and P. F. Blackmore, "Simulations of transient membrane behavior in cells subjected to a high-intensity ultrashort electric pulse," *Phys. Rev. E - Stat. Nonlinear, Soft Matter Phys.*, vol. 71, no. 3, p. 31914, 2005.
- [20] D. P. Tieleman, "The molecular basis of electroporation," *BMC Biochem.*, vol. 5, no. 1, p. 10, Jan. 2004.
- [21] M. Tarek, "Membrane electroporation: a molecular dynamics simulation," *Biophysical journal*, vol. 88, no. 6. pp. 4045–4053, 2005.
- [22] R. A. Böckmann, B. L. de Groot, S. Kakorin, E. Neumann, and H. Grubmüller, "Kinetics, statistics, and energetics of lipid membrane electroporation studied by molecular dynamics simulations," *Biophys. J.*, vol. 95, no. 4, pp. 1837–1850, 2008.
- [23] M. J. Ziegler and P. T. Vernier, "Interface water dynamics and porating electric fields for phospholipid bilayers," *J. Phys. Chem. B*, vol. 112, pp. 13588–13596, 2008.
- [24] M. P. Allen and D. J. Tildesley, *Computer simulation of liquids*. Oxford: Clarendon Press, 1987.
- [25] A. R. Leach, *Molecular modelling: principles and applications*, Second Edi. Prentice Hall, 2001.
- [26] L. D. Schuler, X. Daura, and W. F. van Gunsteren, "An improved GROMOS96 force field for aliphatic hydrocarbons in the condensed phase," *J. Comp. Chem*, vol. 22, pp. 1205–1218, 2001.
- [27] A. D. MacKerell Jr., D. Bashford, M. Bellott, R. L. Dunbrack Jr., J. Evanseck, M. J. Field, S. Fischer, J. Gao, H. Guo, S. Ha, D. Joseph-McCarthy, L. Kuchnir, K. Kuczera, F. T. K. Lau, C. Mattos, S. Michnick, T. Ngo, D. T. Nguyen, B. Prodhom, W. E. Reiher III, B. Roux, M. Schlenkerich, J. C. Smith, R. Stote, J. Straub, M. Watanabe, J. Wiorkiewicz-Kuczera, D. Yin, and M. Karplus, "All-atom empirical potential for molecular modeling and dynamics studies of proteins," *J. Phys. Chem. B*, vol. 102, pp. 3586–3616, 1998.
- [28] D. A. Case, D. A. Pearlman, J. W. Caldwell, T. E. Cheatham III, W. S. Ross, C. L. Simmerling, T. A. Darden, K. M. Merz, R. V. Stanton, A. L. Cheng, J. J. Vincent, M. Crowley, V. Tsui, R. J. Radmer, Y. Duan, J. Pitera, I. Massova, G. L. Seibel, and U. C. Singh, *AMBER6*. San Francisco: University of California, 1999.
- [29] K. Vanommeslaeghe, E. Hatcher, C. Acharya, S. Kundu, S. Zhong, J. Shim, E. Darian, O. Guvench, P. Lopes, I. Vorobyov, and A. and Mackerell, "CHARMM General Force Field: A Force Field for Drug-Like Molecules Compatible With the CHARMM All-Atom Additive Biological Force Fields," *J. Comp. Chem.*, vol. 31, no. 4, pp. 671–690, 2010.
- [30] A. Warshel, M. Kato, and A. V. Pislakov, "Polarizable force fields: history, test cases, and prospects," *J. Chem. Theory Comput.*, vol. 3, pp. 2034–2045, 2007.

- [31] T. A. Halgren and W. Damm, "Polarizable force fields," *Curr. Opin. Struct. Biol.*, vol. 11, pp. 236–242, 2001.
- [32] E. Lindahl and O. Edholm, "Mesoscopic undulations and thickness fluctuations in lipid bilayers from molecular dynamics simulations," *Biophys. J.*, vol. 79, pp. 426–433, 2000.
- [33] S. J. Marrink and A. E. Mark, "Effect of undulations on surface tension in simulated bilayers," *J. Phys. Chem. B*, vol. 105, pp. 6122–6127, 2001.
- [34] S. W. Chiu, M. Clark, E. Jakobsson, S. Subramaniam, and H. L. Scott, "Optimization of hydrocarbon chain interaction parameters: Application to the simulation of fluid phase lipid bilayers," *J. Phys. Chem. B*, vol. 103, pp. 6323–6327, 1999.
- [35] T. Rög, K. Murzyn, and M. Pasenkiewicz-Gierula, "The dynamics of water at the phospholipid bilayer: A molecular dynamics study," *Chem. Phys. Lett.*, vol. 352, pp. 323–327, 2002.
- [36] L. Saiz and M. L. Klein, "Computer simulation studies of model biological membranes," *Acc. Chem. Res.*, vol. 35, pp. 482–489, 2002.
- [37] S. E. Feller, K. Gawrisch, and A. D. MacKerell, "Polyunsaturated fatty acids in lipid bilayers: intrinsic and environmental contributions to their unique physical properties," *J. Am. Chem. Soc.*, vol. 124, pp. 318–326, 2002.
- [38] M. L. Berkowitz and M. J. Raghavan, "Computer simulation of a water/membrane interface," *Langmuir*, vol. 7, pp. 1042–1044, 1991.
- [39] K. V. Damodaran and K. M. Merz, "A comparison of dmpc and dlpe based lipid bilayers," *Biophys. J.*, vol. 66, pp. 1076–1087, 1994.
- [40] J. J. L. Cascales, J. G. de la Torre, S. J. Marrink, and H. J. C. Berendsen, "Molecular dynamics simulation of a charged biological membrane," *J. Chem. Phys.*, vol. 104, pp. 2713–2720, 1996.
- [41] P. Mukhopadhyay, L. Monticelli, and D. P. Tieleman, "Molecular dynamics simulation of a palmitoyl-oleoyl phosphatidylserine bilayer with Na⁺ Counterions and NaCl," *Biophys. J.*, vol. 86, pp. 1601–1609, 2004.
- [42] S. W. Chiu, S. Vasudevan, E. Jakobsson, R. J. Mashl, and H. L. Scott, "Structure of sphingomyelin bilayers: A simulation study," *Biophys. J.*, vol. 85, pp. 3624–3635, 2003.
- [43] A. S. Pandit, D. Bostick, and M. L. Berkowitz, "Molecular dynamics simulation of a dipalmitoylphosphatidylcholine bilayer with NaCl," *Biophys. J.*, vol. 84, pp. 3743–3750, 2003.
- [44] R. Y. Patel and P. V. Balaji, "Characterization of symmetric and asymmetric lipid bilayers composed of varying concentrations of ganglioside GM1 and DPPC," *J. Phys. Chem. B*, vol. 112, pp. 3346–3356, 2008.
- [45] M. Dahlberg and A. Maliniak, "Molecular dynamics simulations of cardiolipin bilayers," *J. Phys. Chem. B*, vol. 112, pp. 11655–11663, 2008.
- [46] A. A. Gurtovenko and I. Vattulainen, "Effect of NaCl and KCl on phosphatidylcholine and phosphatidylethanolamine lipid membranes: Insight from atomic-scale simulations for understanding salt-induced effects in the plasma membrane," *J. Phys. Chem. B*, vol. 112, pp. 1953–1962, 2008.
- [47] R. Vacha, M. L. Berkowitz, and P. Jungwirth, "Molecular model of a cell plasma membrane with an asymmetric multicomponent composition: Water permeation and ion effects," *Biophys. J.*, vol. 96, pp. 4493–4501, 2009.
- [48] T. Rog, H. Martinez-Seara, N. Munck, M. Oresic, M. Karttunen, and I. Vattulainen, "Role of cardiolipins in the inner mitochondrial membrane: Insight gained through atom-scale simulations," *J. Phys. Chem. B*, vol. 113, pp. 3413–3422, 2009.
- [49] Z. Li, R. M. Venable, L. A. Rogers, D. Murray, and R. W. Pastor, "Molecular dynamics simulations of PIP2 and PIP3 in lipid bilayers: Determination of ring orientation, and the effects of surface roughness on a poisson-boltzmann description," *Biophys. J.*, vol. 97, pp. 155–163, 2009.
- [50] M. Tarek, D. J. Tobias, S. H. Chen, and M. L. Klein, "Short wavelength collective dynamics in phospholipid bilayers: a molecular dynamics study," *Phys. Rev. Lett.*, vol. 87, p. 238101, 2001.
- [51] C. Anézo, A. H. de Vries, H. D. Höltje, D. P. Tieleman, and S. J. Marrink, "Methodological issues in lipid bilayer simulations," *J. Phys. Chem. B*, vol. 107, pp. 9424–9433, 2003.
- [52] S. J. Beebe and K. H. Schoenbach, "Nanosecond pulsed electric fields: A new stimulus to activate intracellular signaling," *J. Biomed. Biotech.*, vol. 4, pp. 297–300, 2005.
- [53] Z. Vasilkoski, A. T. Esser, T. R. Gowrishankar, and J. C. Weaver, "Membrane electroporation: The absolute rate equation and nanosecond time scale pore creation," *Phys. Rev. E - Stat. Nonlinear, Soft Matter Phys.*, vol. 74, no. 2, 2006.
- [54] R. Sundararajan, "Nanosecond electroporation: another look," *Mol. Biotech.*, vol. 41, pp. 69–82, 2009.
- [55] J. Deng, K. H. Schoenbach, E. Stephen Buescher, P. S. Hair, P. M. Fox, and S. J. Beebe, "The Effects of Intense Submicrosecond Electrical Pulses on Cells," *Biophys. J.*, vol. 84, no. 4, pp. 2709–2714, Apr. 2003.
- [56] H. Pauly and H. P. Schwan, "Über Die Impedanz Einer Suspension Von Kugelförmigen Teilchen Mit Einer Schale - Ein Modell Für Das Dielektrische Verhalten Von Zellsuspensionen Und Von Proteinlösungen," *Z Naturforsch B*, vol. 14, no. 2, pp. 125–131, 1959.
- [57] T. Kotnik, D. Miklavcic, and T. Slivnik, "Time course of transmembrane voltage induced by time-varying electric fields - a method for theoretical analysis and its application," *Bioelectrochem. Bioenerg.*, vol. 45, no. 1, pp. 3–16, 1998.
- [58] T. Kotnik and D. Miklavcic, "Theoretical evaluation of voltage inducement on internal membranes of biological cells exposed to electric fields," *Biophys. J.*, vol. 90, no. 2, pp. 480–491, 2006.
- [59] Q. Zhong, Q. Jiang, P. B. Moore, D. M. Newns, and M. L. Klein, "Molecular dynamics simulation of a synthetic ion channel," *Biophys. J.*, vol. 74, pp. 3–10, 1998.
- [60] Y. Yang, D. Henderson, P. Crozier, R. L. Rowley, and D. D. Busath, "Permeation of ions through a model biological channel: effect of periodic boundary condition and cell size," *Molec. Phys.*, vol. 100, pp. 3011–3019, 2002.
- [61] D. P. Tieleman, J. H. C. Berendsen, and M. S. P. Sansom, "Voltage-dependent insertion of alamethicin at phospholipid/water and octane water interfaces," *Biophys. J.*, vol. 80, pp. 331–346, 2001.
- [62] P. S. Crozier, D. Henderson, R. L. Rowley, and D. D. Busath, "Model channel ion currents in NaCl extended simple point charge water solution with applied-field molecular dynamics," *Biophys. J.*, vol. 81, pp. 3077–3089, 2001.
- [63] B. Roux, "The membrane potential and its representation by a constant electric field in computer simulations," *Biophys. J.*, vol. 95, pp. 4205–4216, 2008.
- [64] P. T. Vernier, M. J. Ziegler, Y. Sun, W. V. Chang, M. A. Gundersen, and D. P. Tieleman, "Nanopore formation and phosphatidylserine externalization in a phospholipid bilayer at high transmembrane potential," *J. Am. Chem. Soc.*, vol. 128, no. 19, pp. 6288–6289, 2006.

- [65] W. Treptow, B. Maigret, C. Chipot, and M. Tarek, "Coupled motions between pore and voltage-sensor domains: a model for Shaker B, a voltage-gated potassium channel.," *Biophys. J.*, vol. 87, pp. 2365–2379, 2004.
- [66] A. Aksimentiev and K. Schulten, "Imaging a-hemolysin with molecular dynamics: ionic conductance, osmotic permeability, and the electrostatic potential map," *Biophys. J.*, vol. 88, pp. 3745–3761, 2005.
- [67] F. Khalili-Araghi, E. Tajkhorshid, and K. Schulten, "Dynamics of K⁺ ion conduction through Kv1.2.," *Biophys. J.*, vol. 91, pp. L72–L74, 2006.
- [68] M. Sotomayor, V. Vasquez, E. Perozo, and K. Schulten, "Ion conduction through MscS as determined by electrophysiology and simulation," *Biophys. J.*, vol. 92, pp. 886–902, 2007.
- [69] C. Chimere, L. Movileanu, S. Pezeshki, M. Winterhalter, and U. Kleinekathofer, "Transport at the nanoscale: temperature dependence of ion conductance," *Eur. Biophys. J. Biophys. Lett.*, vol. 38, pp. 121–125, 2008.
- [70] D. J. Tobias, "Electrostatic calculations: recent methodological advances and applications to membranes," *Curr. Opin. Struct. Biol.*, vol. 11, pp. 253–261, 2001.
- [71] K. Gawrisch, D. Ruston, J. Zimmerberg, V. Parsegian, R. Rand, and N. Fuller, "Membrane dipole potentials, hydration forces, and the ordering of water at membrane surfaces," *Biophys. J.*, vol. 61, pp. 1213–1223, 1992.
- [72] P. T. Vernier and M. J. Ziegler, "Nanosecond field alignment of head group and water dipoles in electroporating phospholipid bilayers," *J. Phys. Chem. B*, vol. 111, no. 45, pp. 12993–12996, 2007.
- [73] Z. A. Levine and P. T. Vernier, "Life cycle of an electropore: Field-dependent and field-independent steps in pore creation and annihilation," *J. Membr. Biol.*, vol. 236, no. 1, pp. 27–36, 2010.
- [74] Z. A. Levine and P. T. Vernier, "Calcium and phosphatidylserine inhibit lipid electropore formation and reduce pore lifetime," *J. Membr. Biol.*, vol. 245, no. 10, pp. 599–610, 2012.
- [75] M. Golzio, J. Teissie, and M.-P. Rols, "Direct visualization at the single-cell level of electrically mediated gene delivery," *Proc. Natl. Acad. Sci. U.S.A.*, vol. 99, pp. 1292–1297, 2002.
- [76] a Paganin-Gioanni, E. Bellard, J. M. Escoffre, M. P. Rols, J. Teissie, and M. Golzio, "Direct visualization at the single-cell level of siRNA electrotransfer into cancer cells.," *Proc. Natl. Acad. Sci. U. S. A.*, vol. 108, no. 26, pp. 10443–10447, 2011.
- [77] M. Breton, L. Delemotte, A. Silve, L. M. Mir, and M. Tarek, "Transport of siRNA through lipid membranes driven by nanosecond electric pulses: an experimental and computational study.," *J. Am. Chem. Soc.*, vol. 134, no. 34, pp. 13938–13941, Aug. 2012.
- [78] J. N. Sachs, P. S. Crozier, and T. B. Woolf, "Atomistic simulations of biologically realistic transmembrane potential gradients," *J. Chem. Phys.*, vol. 121, pp. 10847–10851, 2004.
- [79] L. Delemotte, F. Dehez, W. Treptow, and M. Tarek, "Modeling membranes under a transmembrane potential," *J. Phys. Chem. B*, vol. 112, no. 18, pp. 5547–5550, 2008.
- [80] L. Delemotte and M. Tarek, "Molecular dynamics simulations of lipid membrane electroporation," *J. Membr. Biol.*, vol. 245, no. 9, pp. 531–543, 2012.
- [81] B. Roux, "Influence of the membrane potential on the free energy of an intrinsic protein," *Biophys. J.*, vol. 73, pp. 2980–2989, 1997.
- [82] A. A. Gurtovenko and I. Vattulainen, "Pore Formation Coupled to Ion Transport through Lipid Membranes as Induced by Transmembrane Ionic Charge Imbalance: Atomistic Molecular Dynamics Study," *J. Am. Chem. Soc.*, vol. 127, no. 50, pp. 17570–17571, 2005.
- [83] S. K. Kandasamy and R. G. Larson, "Cation and anion transport through hydrophilic pores in lipid bilayers," *J. Chem. Phys.*, vol. 125, p. 74901, 2006.
- [84] Kutzner C, Grubmüller H, de Groot BL, and Z. U., "Computational electrophysiology: the molecular dynamics of ion channel permeation and selectivity in atomistic detail," *Biophys J*, vol. 101, pp. 809–817, 2011.
- [85] Y. A. Liberman and V. P. Topaly, "Permeability of biomolecular phospholipid membranes for fat-soluble ions," *Biophys. USSR*, vol. 14, p. 477, 1969.
- [86] S. J. Marrink, F. Jähnig, and H. J. Berendsen, "Proton transport across transient single-file water pores in a lipid membrane studied by molecular dynamics simulations," *Biophys. J.*, vol. 71, pp. 632–647, 1996.
- [87] M.-C. Ho, Z. A. Levine, and P. T. Vernier, "Nanoscale, Electric Field-Driven Water Bridges in Vacuum Gaps and Lipid Bilayers," *J. Membr. Biol.*, vol. 246, no. 11, pp. 793–801, May 2013.
- [88] Z. A. Levine and P. T. Vernier, "Life cycle of an electropore: Field-dependent and field-independent steps in pore creation and annihilation," *J. Membr. Biol.*, vol. 236, no. 1, pp. 27–36, Jul. 2010.
- [89] W. F. D. Bennett and D. P. Tieleman, "The importance of membrane defects-lessons from simulations.," *Acc. Chem. Res.*, vol. 47, no. 8, pp. 2244–51, 2014.
- [90] U. Pliquet, R. P. Joshi, V. Sridhara, and K. H. Schoenbach, "High electrical field effects on cell membranes.," *Bioelectrochemistry*, vol. 70, no. 2, pp. 275–282, 2007.
- [91] D. P. Tieleman, H. Leontiadou, A. E. Mark, and S. J. Marrink, "Simulation of pore formation in lipid bilayers by mechanical stress and electric fields," *J. Am. Chem. Soc.*, vol. 125, no. 21, pp. 6382–6383, 2003.
- [92] S. Koronkiewicz and S. Kalinowski, "Influence of cholesterol on electroporation of bilayer lipid membranes: chronopotentiometric studies," *Biochim. Biophys. Acta - Biomembr.*, vol. 1661, no. 2, pp. 196–203, Mar. 2004.
- [93] M. Casciola, D. Bonhenry, M. Liberti, F. Apollonio, and M. Tarek, "A molecular dynamic study of cholesterol rich lipid membranes: comparison of electroporation protocols.," *Bioelectrochemistry*, vol. 100, pp. 11–17, Dec. 2014.
- [94] S. Kakorin, U. Brinkmann, and E. Neumann, "Cholesterol reduces membrane electroporation and electric deformation of small bilayer vesicles," *Biophys. Chem.*, vol. 117, no. 2, pp. 155–171, 2005.
- [95] M. L. Fernández, M. Risk, R. Reigada, and P. T. Vernier, "Size-controlled nanopores in lipid membranes with stabilizing electric fields," *Biochem. Biophys. Res. Commun.*, vol. 423, no. 2, pp. 325–330, 2012.
- [96] A. Polak, D. Bonhenry, F. Dehez, P. Kramar, D. Miklavčič, and M. Tarek, "On the electroporation thresholds of lipid bilayers: molecular dynamics simulation investigations.," *J. Membr. Biol.*, vol. 246, no. 11, pp. 843–850, Nov. 2013.
- [97] A. Polak, M. Tarek, M. Tomšič, J. Valant, N. P. Ulrih, A. Jamnik, P. Kramar, and D. Miklavčič, "Electroporation of archaeal lipid membranes using MD simulations," *Bioelectrochemistry*, vol. 100, pp. 18–26, 2014.

- [98] A. A. Gurtovenko and A. S. Lyulina, "Electroporation of asymmetric phospholipid membranes," *J. Phys. Chem. B*, vol. 118, no. 33, pp. 9909–9918, 2014.
- [99] T. J. Piggot, D. A. Holdbrook, and S. Khalid, "Electroporation of the *E. coli* and *S. aureus* membranes: Molecular dynamics simulations of complex bacterial membranes," *J. Phys. Chem. B*, vol. 115, no. 45, pp. 13381–13388, 2011.
- [100] F. Dehez, L. Delemotte, P. Kramar, D. Miklavčič, and M. Tarek, "Evidence of conducting hydrophobic nanopores across membranes in response to an electric field," *J. Phys. Chem. C*, vol. 118, no. 13, pp. 6752–6757, 2014.
- [101] M. Casciola, M. A. Kasimova, L. Rems, S. Zullino, F. Apollonio, and M. Tarek, "Properties of lipid electropores I: Molecular dynamics simulations of stabilized pores by constant charge imbalance Properties of lipid electropores I: Molecular dynamics simulations of stabilized pores by constant charge imbalance," *Bioelectrochemistry*, vol. 109, pp. 108–116, 2016.
- [102] P. Kramar, L. Delemotte, A. Maček Lebar, M. Kotulska, M. Tarek, and D. Miklavčič, "Molecular-level characterization of lipid membrane electroporation using linearly rising current," *J. Membr. Biol.*, vol. 245, no. 10, pp. 651–659, Oct. 2012.
- [103] M. C. Ho, M. Casciola, Z. A. Levine, and P. T. Vernier, "Molecular dynamics simulations of ion conductance in field-stabilized nanoscale lipid electropores," *J. Phys. Chem. B*, vol. 117, no. 39, pp. 11633–11640, 2013.
- [104] H. Leontiadou, A. E. Mark, and S.-J. Marrink, "Ion transport across transmembrane pores," *Biophys. J.*, vol. 92, no. 12, pp. 4209–4215, Jun. 2007.
- [105] A. A. Gurtovenko and I. Vattulainen, "Ion leakage through transient water pores in protein-free lipid membranes driven by transmembrane ionic charge imbalance," *Biophys. J.*, vol. 92, no. 6, pp. 1878–1890, 2007.
- [106] A. A. Gurtovenko and I. Vattulainen, "Molecular mechanism for lipid flip-flops," *J. Phys. Chem. B*, vol. 111, no. 48, pp. 13554–13559, 2007.
- [107] A. A. Gurtovenko, J. Anwar, and I. Vattulainen, "Defect-Mediated Trafficking across Cell Membranes: Insights from in Silico Modeling," 2010.
- [108] V. Sridhara and R. P. Joshi, "Numerical study of lipid translocation driven by nanoporation due to multiple high-intensity, ultrashort electrical pulses," *Biochim. Biophys. Acta - Biomembr.*, vol. 1838, no. 3, pp. 902–909, 2014.
- [109] F. Salomone, M. Breton, I. Leray, F. Cardarelli, C. Boccardi, D. Bonhenry, M. Tarek, L. M. Mir, and F. Beltram, "High-yield nontoxic gene transfer through conjugation of the CM 18-Tat11 chimeric peptide with nanosecond electric pulses," *Mol. Pharm.*, vol. 11, no. 7, pp. 2466–2474, 2014.
- [110] P. T. Vernier, M. J. Ziegler, Y. Sun, M. A. Gundersen, and D. P. Tieleman, "Nanopore-facilitated, voltage-driven phosphatidylserine translocation in lipid bilayers- in cells and in silico," *Phys. Biol.*, vol. 3, pp. 233–247, 2006.
- [111] M. Casciola and M. Tarek, "A molecular insight into the electro-transfer of small molecules through electropores driven by electric fields," *Biochim. Biophys. Acta - Biomembr.*, 2016.
- [112] J. Teissie and M. P. Rols, "An Experimental Evaluation of the Critical Potential Difference Inducing Cell-Membrane Electroporation," *Biophys. J.*, vol. 65, no. 1, pp. 409–413, 1993.
- [113] L. C. Benov, P. A. Antonov, and S. R. Ribarov, "Oxidative damage of the membrane-lipids after electroporation," *Gen. Physiol. Biophys.*, vol. 13, no. 2, pp. 85–97, Apr. 1994.
- [114] B. Gabriel and J. Teissie, "Generation of reactive-oxygen species induced by electroporation of Chinese hamster ovary cells and their consequence on cell viability," *Eur. J. Biochem.*, vol. 223, no. 1, pp. 25–33, Jul. 1994.
- [115] M. Maccarrone, M. R. Bladergroen, N. Rosato, and A. F. Agro, "Role of Lipid Peroxidation in Electroporation-Induced Cell Permeability," *Biochem. Biophys. Res. Commun.*, vol. 209, no. 2, pp. 417–425, Apr. 1995.
- [116] M. Maccarrone, N. Rosato, and A. F. Agrò, "Electroporation enhances cell membrane peroxidation and luminescence," *Biochem. Biophys. Res. Commun.*, vol. 206, no. 1, pp. 238–245, Jan. 1995.
- [117] Y. Zhou, C. K. Berry, P. A. Storer, and R. M. Raphael, "Peroxidation of polyunsaturated phosphatidyl-choline lipids during electroformation," *Biomaterials*, vol. 28, no. 6, pp. 1298–1306, Feb. 2007.
- [118] O. N. Pakhomova, V. A. Khorokhorina, A. M. Bowman, R. Rodaitė-Riševičienė, G. Saulis, S. Xiao, and A. G. Pakhomov, "Oxidative effects of nanosecond pulsed electric field exposure in cells and cell-free media," *Arch. Biochem. Biophys.*, vol. 527, no. 1, pp. 55–64, Nov. 2012.
- [119] M. Breton, M. Amirkavei, and L. M. Mir, "Optimization of the Electroformation of Giant Unilamellar Vesicles (GUVs) with Unsaturated Phospholipids," *J. Membr. Biol.*, vol. 248, no. 5, pp. 827–835, Oct. 2015.
- [120] P. Jurkiewicz, A. Olżyńska, L. Cwiklik, E. Conte, P. Jungwirth, F. M. Megli, and M. Hof, "Biophysics of Lipid Bilayers Containing Oxidatively Modified Phospholipids: Insights from Fluorescence and EPR Experiments and from MD Simulations," *Biochim. Biophys. Acta*, vol. 1818, no. 10, pp. 2388–2402, 2012.
- [121] P. T. Vernier, Z. A. Levine, Y.-H. Wu, V. Joubert, M. J. Ziegler, L. M. Mir, and D. P. Tieleman, "Electroporating fields target oxidatively damaged areas in the cell membrane," *PLoS One*, vol. 4, no. 11, p. e7966, Jan. 2009.
- [122] L. Beranova, L. Cwiklik, P. Jurkiewicz, M. Hof, and P. Jungwirth, "Oxidation changes physical properties of phospholipid bilayers: fluorescence spectroscopy and molecular simulations," *Langmuir*, vol. 26, no. 9, pp. 6140–6144, May 2010.
- [123] S. Kalghatgi, C. S. Spina, J. C. Costello, M. Liesa, J. R. Morones-Ramirez, S. Slomovic, A. Molina, O. S. Shirihai, and J. J. Collins, "Bactericidal antibiotics induce mitochondrial dysfunction and oxidative damage in Mammalian cells," *Sci. Transl. Med.*, vol. 5, no. 192, p. 192ra85, 2013.

ACKNOWLEDGEMENT

Simulations presented in this work benefited from access to the HPC resources of the Centre Informatique National de l'Enseignement Supérieur (CINES) FRANCE. The authors would like to acknowledge very fruitful and insightful discussion with Damijan Miklavcic, Luis Mir and Thomas Vernier. Research conducted in the scope of the EBAM European Associated Laboratory (LEA). M.T acknowledges the support of the French Agence Nationale de la Recherche, under grant (ANR-10- BLAN-916-03-INTCELL), and the support from the "Contrat Plan État-Region Lorraine 2015-2020" sub-project MatDS.



Mounir Tarek born in Rabat-Morocco. He received a Ph.D. in Physics from the University of Paris in 1994. He is a senior research scientist (Directeur de Recherches) at the CNRS. For the last few years, he worked on large-scale state-of-the-art molecular simulations of lipid membranes and TM proteins probing their structure and dynamics.

NOTES

NOTES

Nanoscale and Multiscale Electropulsation

P. Thomas Vernier

Frank Reidy Research Center for Bioelectrics,
Old Dominion University, Norfolk, VA, USA

INTRODUCTION

To utilize the diverse *effects* of electric fields on biological systems we must understand the *causes*. In particular, we want to know the details of the *interactions* between electric fields and biomolecular structures. By looking at very short time scales (nanoseconds) and at single events (non-repetitive stimuli), we reduce the number of larger-scale disturbances and concentrate on reversible perturbations. The analysis is primarily in the time domain, but pulse spectral content may be important for some applications.

Of course, some important *effects* of electropulsation may be a consequence of irreversible processes driven by longer electric field exposures (microseconds, milliseconds). Short-pulse studies can help to dissect these processes.

Although modeling is of necessity a significant component of bioelectrics investigations, experimental observations are fundamental, and to conduct experiments in **nanosecond** bioelectrics, one must be able to generate and accurately monitor the appropriate electrical stimuli, a non-trivial engineering challenge. We will discuss cause and effect here from both **scientific and engineering perspectives**, using data from experiments and simulations. It is commonplace in electrical engineering, and increasingly so in biology, to attack a problem with a combination of modeling and experimental tools. In nanosecond bioelectrics, observations (in vitro and in vivo) give rise to models (molecular and continuum), which drive experiments, which adjust and calibrate the models, which feed back again to empirical validation. This feedback loop focuses investigations of a very large parameter space on the critical ranges of values for the key variables.

NANOSECOND BIOELECTRICS

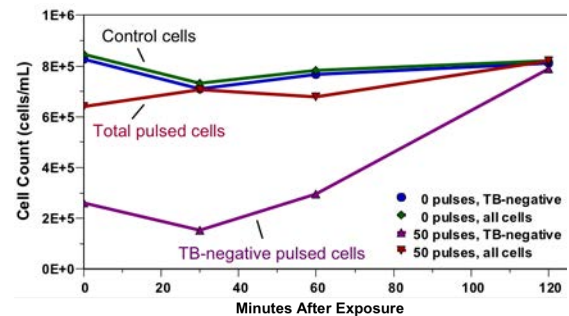


Figure 1. Nanoelectropulsed Jurkat T lymphoblasts recover over 2 hrs from initial Trypan blue permeabilization after exposure to 50, 20 ns, 4 MV/m pulses at 20 Hz.



Figure 2. Timeline representing the sequence of events following electrical polarization of a biological tissue or aqueous suspension of cells. The sub-nanosecond regime can be modeled by the dielectric properties of the system. For longer times the distribution of fields and potentials is dominated by the migration of charged species.

From longstanding theory that models the cell as a dielectric shell [1–4] came the notion that sub-microsecond electric pulses could “bypass” the cell membrane, depositing most of their energy inside the cell instead of in the plasma membrane, the primary target of longer pulses. This idea was investigated experimentally beginning in the late 1990s, and apparently confirmed [5–6]. Even though one early report indicated that the electric field-driven conductive breakdown of membranes can occur in as little as 10 ns [7], and a theoretical analysis demonstrated that pulses with field amplitudes greater than about 1 MV/m will produce porating transmembrane potentials within about 2 ns [8], and a well-grounded model predicted “poration everywhere” in the nanosecond regime [9], procedures used to detect electroporation of the plasma membrane (and the loss of membrane integrity in general) produced negative results for pulses with durations less than the charging time constant of a small cell in typical media (< 100 ns).

In addition to highlighting the limitations of traditional experimental methods for observing membrane permeabilization, this apparent discrepancy between model and observation points

also to inadequacies in the dielectric shell model itself, at time scales below the membrane (cell) charging time. Higher-frequency effects associated with the dielectric properties of high-permittivity aqueous media and low-permittivity biological membranes [10–13] are negligible for the electropermeabilizing conditions that are most commonly studied (μs , kV/m pulses), but for nanosecond pulses they cannot be ignored.

Several lines of experimental evidence indicate that nanosecond electric pulses cause changes in the integrity and organization of the cell membrane.

Trypan blue permeabilization. While remaining propidium-negative, the cell volume of Jurkat T lymphoblasts exposed to a series of 50, 20 ns, 4 MV/m pulses increases, and they become permeable to Trypan blue (TB) (Figure 1). With increasing time after pulse exposure, these weakly TB-positive cells become again impermeable to TB. Similar observations have been reported for B16 murine melanoma cells exposed to sub-nanosecond (800 ps) pulses at very high fields [14].

Nanosecond porating transmembrane potentials. Fluorescence imaging with a membrane potential-sensitive dye indicates that porating transmembrane potentials are generated during nanoelectropulse exposure [15].

Nanoelectropulse-induced PS externalization. Loss of asymmetry in membrane phospholipid distribution resulting from phosphatidylserine (PS) externalization occurs immediately after nanoelectropulse exposure [16], consistent with membrane reorganization driven directly by nanosecond-duration electric fields and a mechanism in which nanometer-diameter pores provide a low-energy path for electrophoretically facilitated diffusion of PS from the cytoplasmic leaflet of the plasma membrane to the external face of the cell [8].

Simulations link PS externalization and nanoporation. In molecular dynamics (MD) simulations of electroporation, hydrophilic pores appear within a few nanoseconds [17], and PS migrates electrophoretically along the pore walls to the anode-facing side of the membrane [18–19], an *in silico* replication of experimental observations in living cells [20].

Nanoelectropermeabilization. The first direct evidence for nanoelectropermeabilization was obtained by monitoring influx of YO-PRO-1 (YP1) [21], a more sensitive indicator of membrane permeabilization than propidium (PPD) [22]. Additional direct evidence comes from patch clamp experiments, which reveal long-lasting increases in

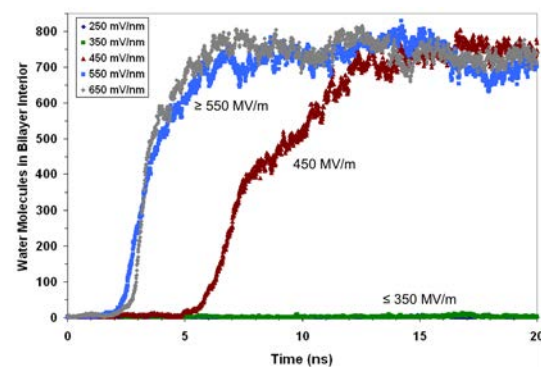


Figure 3. Electric field-driven intrusion of water into a simulated lipid bilayer.

membrane conductance following exposure to 60 ns pulses [23–25].

Nanosecond activation of electrically excitable cells. Electrically excitable cells provide a highly responsive environment for nanoelectropulse biology. Adrenal chromaffin cells [26] and cardiomyocytes [27] react strongly to a single 4 ns pulse, and muscle fiber has been shown to respond to a 1 ns stimulus [28].

Nanosecond bioelectrics and the dielectric stack model. Figure 2 depicts a time line of events in an aqueous suspension of living cells and electrolytes between two electrodes after an electric pulse is applied. Water dipoles re-orient within about 8 ps. The field also alters the electro-diffusive equilibrium among charged species and their hydrating water, with a time constant that ranges from 0.5 to 7 ns, depending on the properties of the media. Pulses shorter than the electrolyte relaxation time do not generate (unless the field is very high) enough interfacial charge to produce porating transmembrane potentials. The dielectric shell model in this regime can be replaced with a simpler, dielectric stack model, in which the local electric field depends only on the external (applied) electric

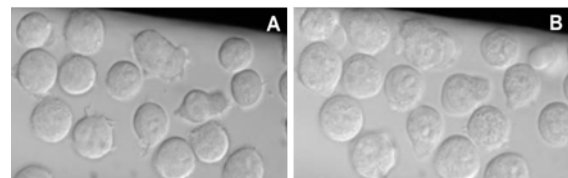


Figure 4. Differential interference contrast (DIC) images of Jurkat T lymphoblasts before (A) and 30 s after (B) exposure to 5 ns, 10 MV/m electric pulses (30 pulses, 1 kHz). Note swelling, blebbing, and intracellular granulation and vesicle expansion, results of the osmotic imbalance caused by electropermeabilization of the cell membrane.

field and the dielectric permittivity of each component of the system.

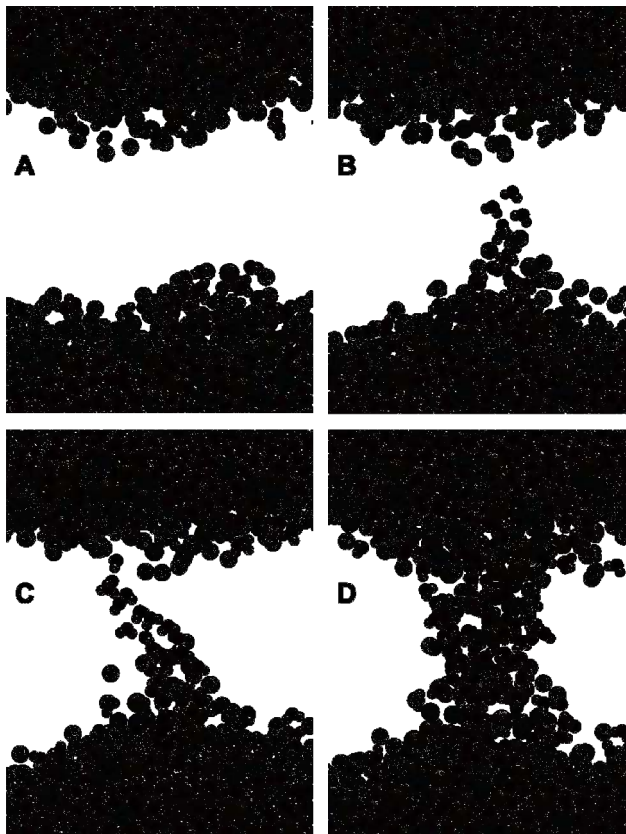


Figure 5. Electropore creation sequence. (A) Molecular dynamics representation of a POPC lipid bilayer. Small red and white spheres at the top and bottom of the panel are water oxygen and hydrogen atoms. Gold and blue spheres are head group phosphorus and nitrogen, respectively, and grey spheres are phospholipid acyl oxygens. For clarity, atoms of the hydrocarbon chains in the interior of the bilayer are not shown. In the presence of a porating electric field, a water intrusion appears (B) and extends across the bilayer (C). Head groups follow the water to form a hydrophilic pore (D). The pore formation sequence, from the initiation of the water bridge to the formation of the head-group-lined pore takes less than 5 ns.

Nanoelectropermeabilization and continuum models. MD simulations at present provide the only available molecular-scale windows on electropore formation in lipid bilayers. Current models perform reasonably well, but simulations of electroporation still contain many assumptions and simplifications. To validate these models, we look for intersections between all-atom molecular assemblies, continuum representations of cell suspensions and tissues, and experimental observations of cells and whole organisms. For example, a leading continuum model assumes an exponential relation between the transmembrane potential and several indices of electropore formation [29]. The MD results in Figure 3, showing water intrusion into the membrane interior as a function of applied electric field, qualitatively demonstrate this same non-linear

relation between field and poration. The challenge is to achieve a quantitative congruency of the coefficients.

NANOSECOND EXPERIMENTS AND MODELS

Experiments and molecular models of membrane permeabilization. Figure 4 shows a simple and direct response of cells to pulse exposure — swelling [25,30,31]. Electropermeabilization of the cell membrane results in an osmotic imbalance that is countered by water influx into the cell and an increase in cell volume. This phenomenon, initiated by electrophysical interactions with basic cell constituents — ions, water, and phospholipids — on a much shorter time scale (a few nanoseconds) than usually considered by electrophysiologists and cell biologists, provides a simple, direct, and well-defined connection between simulations and experimental systems. By correlating observed kinetics of permeabilization and swelling with rates of pore formation and ion and water transport obtained from molecular simulations and continuum representations, we are improving the accuracy and applicability of the models.

Molecular dynamics and macroscale (continuum) models. Figure 5 shows the main steps in the electric field-driven formation of a nanopore in a typical MD simulation of a porating phospholipid bilayer, part of a larger scheme for the step-by-step development (and dissolution) of the electrically conductive defects that contribute at least in part to what we call a permeabilized membrane [32]. These molecular simulations permit us to conduct virtual experiments across a wide parameter space currently inaccessible in practice to direct observation. Although we cannot yet align the detailed energetics and kinetics that can be extracted from MD simulations with laboratory results, it is possible to compare MD data with the predictions of the macroscale models used to describe electroporation.

Figure 6 shows how pore initiation time (time between application of porating electric field and the appearance of a membrane-spanning water column (Fig. 5C)) varies with the magnitude of the electric field in MD simulations [32]. The value of the electric field in the membrane interior, extracted from simulations by integrating the charge density across the system, is used as a normalizing quantity.

This membrane internal field results from the interaction of the applied external field with the interface water and head group dipoles, which also create the large dipole potential found in the membrane interior even in the absence of an applied field [33]. The nonlinear decrease in pore initiation time with increased electric field may be interpreted as a lowering of the activation energy for the

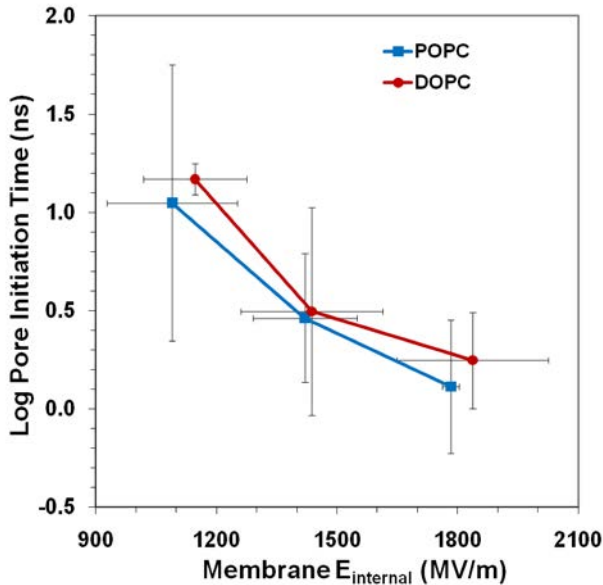


Figure 6. Electropore initiation time is a nonlinear function of the magnitude of the porating electric field. Pore initiation time (time required to form the water bridge shown in Fig. 1C) is exponentially dependent on the applied electric field, expressed here as the electric field observed in the lipid bilayer interior in molecular dynamics simulations. Error bars are standard error of the mean from at least three independent simulations. Data are from Tables 4 and 5 of [32].

formation of the pore-initiating structures described above. We can use simulation results like those in Fig. 6 to reconcile molecular dynamics representations with continuum models, and ultimately both of these to experiment. For example, the relation between electric field and pore creation rate is described in the Krassowska-Weaver stochastic pore model in the following expression,

$$K_{pore} = Ae^{-E(r,V_m)/k_B T}, \quad (1)$$

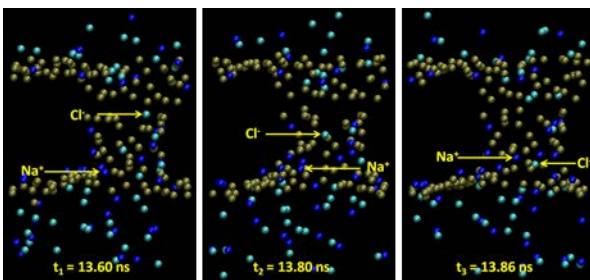


Figure 7. Sodium and chloride ions migrating through a lipid nanopore in the presence of an external electric field.

where K_{pore} is the pore creation rate, A is a rate constant, $E(r, V_m)$ is the energy of a pore with radius r at transmembrane potential V_m , and k_B , and T are the Boltzmann constant and the absolute temperature [29,34–36]. One of our objectives is to reconcile the pore creation rate in (1) with our simulated pore initiation times, reconciling the two models. We are in the process also of validating the stochastic pore model expression for pore density,

$$\frac{dN}{dt} = \alpha e^{\beta(\Delta\psi_m^2)} \left(1 - \frac{N}{N_{eq}} \right), \quad (2)$$

where N and N_{eq} are pores per unit area, instantaneous and equilibrium values, α and β are empirical electroporation model parameters, and $\Delta\psi_m$ is the transmembrane potential.

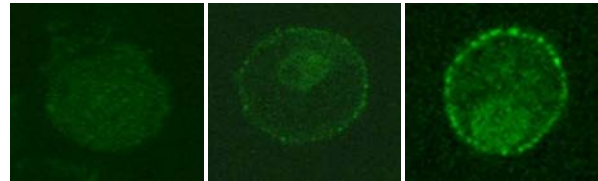


Figure 8. Immunocytochemical labeling of dopamine- β -hydroxylase (DBH) using an anti-DBH antibody coupled with a fluorescently-tagged 2° antibody. DBH is externalized by exocytotic fusion of vesicles with plasma membrane. Left panel, control. Center panel, 2 min after treatment with the pharmacological stimulant DMPP. Right panel, 2 min after a single, 5 ns, 5 MV/m pulse.

Computing power is needed not only to enable simulations of larger systems. The large variability in pore initiation time indicated by the error bars in Fig. 6 means that independent simulations of each condition must be repeated many times to ensure valid results. (A surprising number of conclusions in the existing literature have been published on the basis of single simulations.)

Because of the complexity of all of the structures, systems, and processes which comprise the permeabilized membrane of a living cell (the electropermeome), a comprehensive analytical understanding of permeabilization (pore?) lifetime remains a major challenge for both models and experimental approaches.

Better models can contribute also to our understanding of practical problems in bioelectrics. For example, despite years of study, controversy remains regarding the effects, or lack of effects, of exposures to low levels of radio-frequency (RF) electromagnetic fields [37,38]. Part of the reason for failure to establish certainty on this issue arises from the difficulty of conducting experiments with a sufficient number of variables and a sufficient

number of samples to generate reliable data sets. With accurate simulation tools, honed by reconciliation with experiment, we can explore the large variable and statistical space in which suspected biophysical effects might occur, narrowing the range of experimental targets and focusing on systems in which effects are most likely and in which mechanisms will be clear.

Experiments and molecular models of ion conductance. The earliest identified and most direct indicators of electric field-driven membrane permeabilization are changes in electrical properties, including an increase in ion conductance [39,40]. Data from careful experimental work can be interpreted as measured values corresponding to the conductance of a single pore [41–44]. By combining continuum models of electroporation with this experimental data and with established values for ion electrophoretic mobilities and affinities between ions and phospholipids, we can draw conclusions about pore geometry and areal density. But the inaccessibility (so far) of membrane electropores to direct observation and manipulation of their physical structure prevents us from definitively bridging the gap between model and experiment.

A recently developed method for stabilizing electropores in molecular dynamics simulations of phospholipid bilayers [45] allows extraction of ion conductance from these model systems and thus provides a new and independent connection between models and experiments, in this case from the atomically detailed models of lipid electropores constructed with molecular dynamics. Figure 7 shows one of these stabilized pores with electric field-driven ions passing through it.

Although the magnitude of the conductance measured in these simulations is highly dependent on the accuracy of the ion and water models and their interactions with the phospholipid bilayer interface (and there is much room for improvement in this area), initial results are consistent with expectations from both continuum models and experimental observations.

NANOSECOND EXCITATION

Nanoelectrostimulation of neurosecretory and neuromuscular cells. Applications of pulsed electric fields in the clinic, particularly in electrochemotherapy and gene electrotransfer, are well known and described in detail in other parts of this course. We note here a potential biomedical application specifically of nanosecond electric pulses, the activation and modulation of the activity

of neurosecretory and neuromuscular processes, an area which remains relatively unexplored. The sensitivity of electrically excitable cells to nanoelectropulses raises the possibility that very low energy (nanosecond, megavolt-per-meter pulses are high power, but low total energy because of their brief duration) devices for cardiac regulation (implanted pacemakers and defibrillators), remote muscle activation (spinal nerve damage), and neurosecretory modulation (pain management) can be constructed with nanoelectropulse technology. Figure 8 demonstrates functional activation of an adrenal chromaffin cell after a single 5 ns, 5 MV/m pulse [46,47].

ACKNOWLEDGMENT

Collaborative insights from Francesca Apollonio, Delia Arnaud-Cormos, Gale Craviso, Rumiana Dimova, M. Laura Fernández, Wolfgang Frey, Julie Gehl, Martin Gundersen, Volker Knecht, Malgorzata Kotulska, Philippe Leveque, Micaela Liberti, Carmela Marino, Caterina Merla, Damijan Miklavčič, Lluís Mir, Andrei Pakhomov, Uwe Pliquet, Ramon Reigada, Marcelo Risk, Marie-Pierre Rols, Maria Rosaria Scarfi, Aude Silve, Mounir, Tarek, Justin Teissié, Peter Tieleman, Mayya Tokman, and Jim Weaver (and very important to me but too many to name members of their research groups), and modeling and experimental expertise from Maura Casciola, Federica Castellani, Ming-Chak Ho, Zachary Levine, Paolo Marracino, Stefania Romeo, Esin Sözer, and Yu-Hsuan Wu contributed to this work. Funding is provided by the Frank Reidy Research Center for Bioelectrics at Old Dominion University and the Air Force Office of Scientific Research (FA9550-15-1-0517, FA9550-14-1-0123). Computing resources were provided by the USC Center for High-Performance Computing and Communications (<http://www.usc.edu/hpcc/>) and Old Dominion University High-Performance Computing (<http://www.odu.edu/hpc/>).

REFERENCES

- [1] Sher, L. D., E. Kresch, and H. P. Schwan. 1970. On the possibility of nonthermal biological effects of pulsed electromagnetic radiation. *Biophys. J.* 10:970-979.
- [2] Drago, G. P., M. Marchesi, and S. Ridella. 1984. The frequency dependence of an analytical model of an electrically stimulated biological structure. *Bioelectromagnetics* 5:47-62.
- [3] Plonsey, R., and K. W. Altman. 1988. Electrical stimulation of excitable cells - a model approach. *Proceedings of the IEEE* 76:1122-1129.
- [4] Schoenbach, K. H., R. P. Joshi, J. F. Kolb, N. Y. Chen, M. Stacey, P. F. Blackmore, E. S. Buescher, and S. J. Beebe. 2004. Ultrashort electrical pulses open a new gateway into biological cells. *Proceedings of the IEEE* 92:1122-1137.
- [5] Hofmann, F., H. Ohnimus, C. Scheller, W. Strupp, U. Zimmermann, and C. Jassoy. 1999. Electric field pulses can induce apoptosis. *J. Membr. Biol.* 169:103-109.
- [6] Schoenbach, K. H., S. J. Beebe, and E. S. Buescher. 2001. Intracellular effect of ultrashort electrical pulses. *Bioelectromagnetics* 22:440-448.
- [7] Benz, R., and U. Zimmermann. 1980. Pulse-length dependence of the electrical breakdown in lipid bilayer membranes. *Biochim. Biophys. Acta* 597:637-642.

- [8] Vernier, P. T., Y. Sun, L. Marcu, C. M. Craft, and M. A. Gundersen. 2004. Nanoelectropulse-induced phosphatidylserine translocation. *Biophys. J.* 86:4040-4048.
- [9] Gowrishankar, T. R., and J. C. Weaver. 2006. Electrical behavior and pore accumulation in a multicellular model for conventional and supra-electroporation. *Biochem. Biophys. Res. Commun.* 349:643-653.
- [10] Grosse, C., and H. P. Schwan. 1992. Cellular membrane potentials induced by alternating fields. *Biophys. J.* 63:1632-1642.
- [11] Gowrishankar, T. R., and J. C. Weaver. 2003. An approach to electrical modeling of single and multiple cells. *Proc. Natl. Acad. Sci. U. S. A.* 100:3203-3208.
- [12] Kotnik, T., and D. Miklavcic. 2000. Second-order model of membrane electric field induced by alternating external electric fields. *IEEE Trans. Biomed. Eng.* 47:1074-1081.
- [13] Timoshkin, I. V., S. J. MacGregor, R. A. Fouracre, B. H. Crichton, and J. G. Anderson. 2006. Transient electrical field across cellular membranes: pulsed electric field treatment of microbial cells. *Journal of Physics D-Applied Physics* 39:596-603.
- [14] Schoenbach, K. H., S. Xiao, R. P. Joshi, J. T. Camp, T. Heeren, J. F. Kolb, and S. J. Beebe. 2008. The effect of intense subnanosecond electrical pulses on biological cells. *IEEE Trans. Plasma Sci.* 36:414-422.
- [15] Frey, W., J. A. White, R. O. Price, P. F. Blackmore, R. P. Joshi, R. Nuccitelli, S. J. Beebe, K. H. Schoenbach, and J. F. Kolb. 2006. Plasma membrane voltage changes during nanosecond pulsed electric field exposure. *Biophys. J.* 90:3608-3615.
- [16] Vernier, P. T., Y. Sun, L. Marcu, C. M. Craft, and M. A. Gundersen. 2004. Nanosecond pulsed electric fields perturb membrane phospholipids in T lymphoblasts. *FEBS Lett.* 572:103-108.
- [17] Tieleman, D. P. 2004. The molecular basis of electroporation. *BMC Biochem* 5:10.
- [18] Hu, Q., R. P. Joshi, and K. H. Schoenbach. 2005. Simulations of nanopore formation and phosphatidylserine externalization in lipid membranes subjected to a high-intensity, ultrashort electric pulse. *Phys Rev E Stat Nonlin Soft Matter Phys* 72:031902.
- [19] Vernier, P. T., M. J. Ziegler, Y. Sun, W. V. Chang, M. A. Gundersen, and D. P. Tieleman. 2006. Nanopore formation and phosphatidylserine externalization in a phospholipid bilayer at high transmembrane potential. *J. Am. Chem. Soc.* 128:6288-6289.
- [20] Vernier, P. T., M. J. Ziegler, Y. Sun, M. A. Gundersen, and D. P. Tieleman. 2006. Nanopore-facilitated, voltage-driven phosphatidylserine translocation in lipid bilayers - in cells and in silico. *Physical Biology* 3:233-247.
- [21] Vernier, P. T., Y. Sun, and M. A. Gundersen. 2006. Nanoelectropulse-driven membrane perturbation and small molecule permeabilization. *BMC Cell Biol.* 7:37.
- [22] Idziorek, T., J. Estaquier, F. De Bels, and J. C. Ameisen. 1995. YOPRO-1 permits cytofluorometric analysis of programmed cell death (apoptosis) without interfering with cell viability. *J. Immunol. Methods* 185:249-258.
- [23] Pakhomov, A. G., J. F. Kolb, J. A. White, R. P. Joshi, S. Xiao, and K. H. Schoenbach. 2007. Long-lasting plasma membrane permeabilization in mammalian cells by nanosecond pulsed electric field (nsPEF). *Bioelectromagnetics* 28:655-663.
- [24] Pakhomov, A. G., R. Shevin, J. A. White, J. F. Kolb, O. N. Pakhomova, R. P. Joshi, and K. H. Schoenbach. 2007. Membrane permeabilization and cell damage by ultrashort electric field shocks. *Arch. Biochem. Biophys.* 465:109-118.
- [25] Pakhomov, A. G., A. M. Bowman, B. L. Ibey, F. M. Andre, O. N. Pakhomova, and K. H. Schoenbach. 2009. Lipid nanopores can form a stable, ion channel-like conduction pathway in cell membrane. *Biochem. Biophys. Res. Commun.* 385:181-186.
- [26] Vernier, P. T., Y. Sun, M. T. Chen, M. A. Gundersen, and G. L. Craviso. 2008. Nanosecond electric pulse-induced calcium entry into chromaffin cells. *Bioelectrochemistry* 73:1-4.
- [27] Wang, S., J. Chen, M. T. Chen, P. T. Vernier, M. A. Gundersen, and M. Valderrabano. 2009. Cardiac myocyte excitation by ultrashort high-field pulses. *Biophys. J.* 96:1640-1648.
- [28] Rogers, W. R., J. H. Merritt, J. A. Comeaux, C. T. Kuhnel, D. F. Moreland, D. G. Teltschik, J. H. Lucas, and M. R. Murphy. 2004. Strength-duration curve for an electrically excitable tissue extended down to near 1 nanosecond. *IEEE Trans. Plasma Sci.* 32:1587-1599.
- [29] DeBruin, K. A., and W. Krassowska. 1998. Electroporation and shock-induced transmembrane potential in a cardiac fiber during defibrillation strength shocks. *Ann. Biomed. Eng.* 26:584-596.
- [30] F. M. Andre, M. A. Rassokhin, A. M. Bowman, and A. G. Pakhomov, "Gadolinium blocks membrane permeabilization induced by nanosecond electric pulses and reduces cell death," *Bioelectrochemistry*, vol. 79, pp. 95-100, Aug 2010.
- [31] O. M. Nesin, O. N. Pakhomova, S. Xiao, and A. G. Pakhomov, "Manipulation of cell volume and membrane pore comparison following single cell permeabilization with 60- and 600-ns electric pulses," *Biochim Biophys Acta*, vol. 1808, pp. 792-801, Dec 20 2010.
- [32] Z. A. Levine and P. T. Vernier, "Life cycle of an electropore: field-dependent and field-independent steps in pore creation and annihilation," *J Membr Biol*, vol. 236, pp. 27-36, Jul 2010.
- [33] R. J. Clarke, "The dipole potential of phospholipid membranes and methods for its detection," *Adv Colloid Interface Sci*, vol. 89-90, pp. 263-81, Jan 29 2001.
- [34] I. P. Sugar and E. Neumann, "Stochastic model for electric field-induced membrane pores. Electroporation," *Biophys Chem*, vol. 19, pp. 211-25, May 1984.
- [35] S. A. Freeman, M. A. Wang, and J. C. Weaver, "Theory of electroporation of planar bilayer membranes: predictions of the aqueous area, change in capacitance, and pore-pore separation," *Biophys J*, vol. 67, pp. 42-56, Jul 1994.
- [36] R. W. Glaser, S. L. Leikin, L. V. Chernomordik, V. F. Pastushenko, and A. I. Sokirko, "Reversible electrical breakdown of lipid bilayers: formation and evolution of pores," *Biochim Biophys Acta*, vol. 940, pp. 275-87, May 24 1988.
- [37] J. M. S. McQuade, J. H. Merritt, S. A. Miller, T. Scholin, M. C. Cook, A. Salazar, O. B. Rahimi, M. R. Murphy, and P. A. Mason, "Radiofrequency-radiation exposure does not induce detectable leakage of albumin across the blood-brain barrier," *Radiation Research*, vol. 171, pp. 615-621, May 2009.
- [38] N. D. Volkow, D. Tomasi, G. J. Wang, P. Vaska, J. S.

- Fowler, F. Telang, D. Alexoff, J. Logan, and C. Wong, "Effects of cell phone radiofrequency signal exposure on brain glucose metabolism," *JAMA*, vol. 305, pp. 808-13, Feb 23 2011.
- [39] Stämpfli, R., and M. Willi. 1957. Membrane potential of a Ranvier node measured after electrical destruction of its membrane. *Experientia* 13:297-298.
- [40] Coster, H. G. L. 1965. A quantitative analysis of the voltage-current relationships of fixed charge membranes and the associated property of "punch-through". *Biophys. J.* 5:669-686.
- [41] Chernomordik, L. V., S. I. Sukharev, S. V. Popov, V. F. Pastushenko, A. V. Sokirko, I. G. Abidor, and Y. A. Chizmadzhev. 1987. The electrical breakdown of cell and lipid membranes: the similarity of phenomenologies. *Biochim. Biophys. Acta* 902:360-373.
- [42] Kalinowski, S., G. Ibrón, K. Bryl, and Z. Figaszewski. 1998. Chronopotentiometric studies of electroporation of bilayer lipid membranes. *Biochim. Biophys. Acta* 1369:204-212.
- [43] Melikov, K. C., V. A. Frolov, A. Shcherbakov, A. V. Samsonov, Y. A. Chizmadzhev, and L. V. Chernomordik. 2001. Voltage-induced nonconductive pre-pores and metastable single pores in unmodified planar lipid bilayer. *Biophys. J.* 80:1829-1836.
- [44] Koronkiewicz, S., S. Kalinowski, and K. Bryl. 2002. Programmable chronopotentiometry as a tool for the study of electroporation and resealing of pores in bilayer lipid membranes. *Biochim. Biophys. Acta* 1561:222-229.
- [45] Fernandez, M. L., M. Risk, R. Reigada, and P. T. Vernier. 2012. Size-controlled nanopores in lipid membranes with stabilizing electric fields. *Biochem. Biophys. Res. Commun.* 423:325-330.
- [46] G. L. Craviso, P. Chatterjee, G. Maalouf, A. Cerjanic, J. Yoon, I. Chatterjee, and P. T. Vernier, "Nanosecond electric pulse-induced increase in intracellular calcium in adrenal chromaffin cells triggers calcium-dependent catecholamine release," *Ieee Transactions on Dielectrics and Electrical Insulation*, vol. 16, pp. 1294-1301, Oct 2009.
- [47] G. L. Craviso, S. Choe, P. Chatterjee, I. Chatterjee, and P. T. Vernier, "Nanosecond electric pulses: a novel stimulus for triggering Ca^{2+} influx into chromaffin cells via voltage-gated Ca^{2+} channels," *Cell Mol Neurobiol*, vol. 30, pp. 1259-65, Nov 2010.



P. Thomas Vernier is Research Professor at the Frank Reidy Research Center for Bioelectrics at Old Dominion University and Adjunct Research Professor in the Ming Hsieh Department of Electrical Engineering at the University of Southern California. His research and industrial experience includes ultraviolet microscopy analysis of S-adenosylmethionine metabolism in the yeast *Rhodotorula glutinis*, molecular biology of the temperature-sensitive host restriction of bacterial viruses in *Pseudomonas aeruginosa*, low-level environmental gas monitoring, wide-band instrumentation data recording, and semiconductor device modeling and physical and electrical characterization. He currently concentrates on the effects of nanosecond, megavolt-per-meter electric fields on biological systems, combining experimental observations with molecular dynamics simulations, and on the integration of cellular and biomolecular sensors, carbon nanotubes, and quantum dots with commercial integrated electronic circuit fabrication processes. Vernier received his Ph.D. in Electrical Engineering from the University of Southern California in 2004, and is a member of the American Chemical Society, American Society for Gene and Cell Therapy, American Society for Microbiology, Bioelectromagnetics Society, Biophysical Society, and Institute of Electrical and Electronics Engineers.

NOTES

NOTES

Electrochemotherapy from bench to bedside: principles, mechanisms and applications

Gregor Serša

Institute of Oncology Ljubljana, Slovenia

Abstract: Electrochemotherapy consists of administration of the chemotherapeutic drug followed by application of electric pulses to the tumour, in order to facilitate the drug uptake into the cells. Only two chemotherapeutics are currently used in electrochemotherapy, bleomycin and cisplatin, which both have hampered transport through the plasma membrane without electroporation of tumours. Preclinical studies elaborated on the treatment parameters, route of drug administration and proved its effectiveness on several experimental tumour models. Based on the known mechanisms of action, electrochemotherapy has been successfully tested in the clinics and is now in standard treatment of cutaneous tumours and metastases. Electrochemotherapy as a platform technology, is now being translated also into the treatment of bigger and deep seated tumours. With new electrodes and new electric pulse generators, clinical trials are on-going for treatment of liver metastases and primary tumours, of pancreas, bone metastases and soft tissue sarcomas, as well as brain metastases, tumours in in oesophagus or in rectum.

INTRODUCTION

Electrochemotherapy protocols were optimized in preclinical studies *in vitro* and *in vivo*, and basic mechanisms elucidated, such as electroporation of cells, tumour drug entrapment (vascular lock), vascular-disrupting effect and involvement of the immune response. Based on all these data, electrochemotherapy with bleomycin and cisplatin was promptly evaluated in clinical trials. Recent reviews elaborate on its technology and biomedical applications in medical practice [1,2].

PRECLINICAL STUDIES

In vitro studies

Electroporation proved to be effective in facilitating transport of different molecules across the plasma membrane for different biochemical and pharmacological studies. However, when using chemotherapeutic drugs, this facilitated transport increases intracellular drug accumulation with the aim to increase their cytotoxicity. Since electroporation can facilitate drug transport through the cell membrane only for molecules which are poorly permeant or non-permeant, suitable candidates for electrochemotherapy are limited to those drugs that are hydrophilic and/or lack a transport system in the membrane. Several chemotherapeutic drugs were tested *in vitro* for potential application in combination with electroporation of cells. Among the tested drugs, only two were identified as potential candidates for electrochemotherapy of cancer patients. The first is bleomycin, which is hydrophilic and has very restricted transport through the cell membrane, but its cytotoxicity can be potentiated up to several 1000 times by electroporation of cells. A few hundred internalized

molecules of bleomycin are sufficient to kill the cell. The second is cisplatin, whose transport through the cell membrane is also hampered. Early studies suggested that cisplatin is transported through the plasma membrane mainly by passive diffusion, while recent studies have demonstrated that transporters controlling intracellular copper homeostasis are significantly involved in influx (Ctr1) and efflux (ATP7A and ATP7B) of cisplatin [3]. Electroporation of the plasma membrane enables greater flux and accumulation of the drug in the cells, which results in an increase of cisplatin cytotoxicity by up to 80-fold [4-7]. This promising preclinical data obtained *in vitro* on a number of different cell lines has paved the way for testing these two drugs in electrochemotherapy *in vivo* on different tumor models.

In vivo studies

Bleomycin and cisplatin were tested in an electrochemotherapy protocol in animal models *in vivo* (Fig 1). Extensive studies in different animal models with different types of tumors, either transplantable or spontaneous, were performed [4-7,8,9].

In these studies, different factors controlling antitumor effectiveness were determined:

- ❖ The drugs can be given by different *routes of administration*, they can be injected either intravenously or intratumorally. The prerequisite is that, at the time of application of electric pulses to the tumour, a sufficient amount of drug is present in the tumour. Therefore, after intravenous drug administration into small laboratory animals (for example 4 mg/kg of cisplatin or 0.5 mg/kg bleomycin), only a few minutes interval is needed

to reach the maximal drug concentration in the tumours. After intratumoural administration, this interval is even shorter and the application of electric pulses has to follow the administration of the drug as soon as possible (within a minute) [4-7].

- ❖ Good antitumor effectiveness may be achieved by good tissue electroporation. Electroporation of the plasma membrane is obtained if the cell is exposed to a sufficiently high electric field. This depends on the *electric field distribution in the tissue* which is controlled by the electrode geometry and tissue composition. The electric field distribution in the tissue and cell electroporation can be improved by rotating the electric field. Surface tumours can be effectively treated by plate electrodes, whereas appropriate electric field distribution in the deeper parts of the tumour is assured by using needle electrodes [10-12].

- ❖ The antitumor effectiveness depends on the *amplitude, number, frequency and duration of the electric pulses applied*. Several studies in which parallel plate electrodes were used for surface tumours showed that amplitude over distance ratio above 1000 V/cm is needed for tumour electroporation, and that above 1500 V/cm, irreversible changes in the normal tissues adjacent to the tumour occur. For other types of electrodes, the electric field distribution and thus, also the necessary amplitude of electric pulses, need to be determined by numerical calculations. *Repetition frequencies of the pulses* for electrochemotherapy are either 1 Hz or 5 kHz with equal effect if the concentration of drug present in the tumour is high enough. The minimal number of pulses used is 4; most studies use 8 electric pulses of 100 μ s [4,7,11,13-15].

All the experiments conducted *in vivo* in animals provided sufficient data to demonstrate that electrochemotherapy with either bleomycin or cisplatin is effective in the treatment of solid tumours, using drug concentrations which have no or minimal antitumor effect without application of electric pulses. A single treatment by electrochemotherapy already induces partial or complete regression of tumours, whereas treatment with bleomycin or cisplatin alone or application of electric pulses alone has no or minimal antitumour effect.

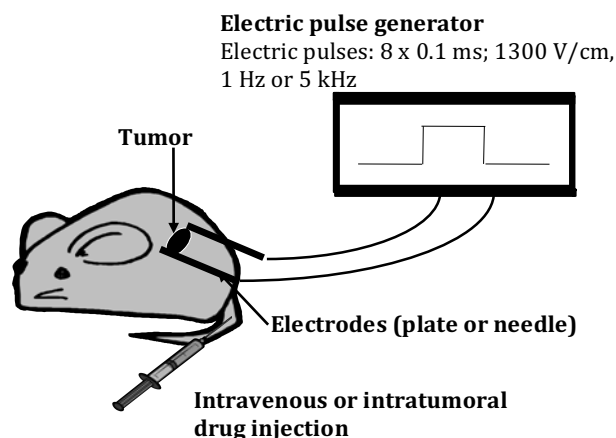


Figure 1: Protocol of electrochemotherapy of experimental tumours presented schematically. The drug is injected either intravenously or intratumourally at doses which do not usually exert an antitumor effect. After an interval which allows sufficient drug accumulation in the tumours, electric pulses are applied to the tumor either by plate or needle electrodes. The electrodes are placed in such a way that the whole tumor is encompassed between the electrodes, providing good electric field distribution in the tumours for optimal electroporation of cells in the tumours.

Mechanisms of action

The principal mechanism of electrochemotherapy is *electroporation* of cells in the tumours, which increases the drug effectiveness by enabling the drug to reach the intracellular target. This was demonstrated in studies which measured the intratumoural drug accumulation and the amount of drug bound to DNA. Basically, the amounts of bleomycin and cisplatin in the electroporated tumours were up to 2-4 fold higher than in those without application of electric pulses [4-7]. Besides membrane electroporation, which facilitates drug transport and its accumulation in the cell, other mechanisms that are involved in the antitumor effectiveness of electrochemotherapy were described. The application of electric pulses to tissues induces a transient, but reversible *reduction of blood flow* [16,17]. Restoration of the blood flow in normal tissue is much faster than that in tumours [18,19]. The vascular lock in the tumour induces *drug entrapment* in the tissue, providing more time for the drug to act.

The cytotoxic effect of electrochemotherapy is not limited only to tumour cells in the tumours. Electrochemotherapy also acts on stromal cells, including endothelial cells in the lining of tumour blood vessels, which undergo cell death [19]. Consequently, by vascular-disrupting action of electrochemotherapy, a cascade of tumour cell death occurs due to long-lasting hypoxia in the affected vessels. This represents yet another mechanism involved in the antitumor effectiveness of electrochemotherapy, i.e. a *vascular-*

disrupting effect [20-22]. This vascular-disrupting action of electrochemotherapy is important in clinical situations where haemorrhagic tumour nodules need to be treated [23].

A difference in the antitumor effectiveness of electrochemotherapy was observed between immunocompetent and immunodeficient experimental animals, indicating on involvement of the *immune response* in antitumor effectiveness [24]. Due to massive tumour antigen shedding in organisms after electrochemotherapy, systemic immunity can be induced and also up-regulated by additional treatment with biological response modifiers like IL-2, IL-12, GM-CSF and TNF- α [24-28].

To sum up, the electrochemotherapy protocol was optimized in preclinical studies *in vitro* and *in vivo*, and basic mechanisms were elucidated. In addition to the electroporation of cells, vascular lock leading to drug entrapment in tumours, a vascular- disrupting effect and involvement of the immune response were also demonstrated. Based on all this data, electrochemotherapy with bleomycin and cisplatin was promptly evaluated in clinical trials and is now in routine use in human and veterinary oncology.

CLINICAL STUDIES

The first clinical study was published in 1991 on head and neck tumour nodules [29], which was thereafter followed by several others [2]. These clinical studies demonstrated the antitumor effectiveness of electrochemotherapy using either bleomycin or cisplatin, given intravenously or intratumorally. In addition to single or multiple cutaneous or subcutaneous melanoma nodules, a response was demonstrated in breast and head and neck cancer nodules, as well as Kaposi's sarcoma, hypernephroma, chondrosarcoma and basal cell carcinoma. However, these clinical studies were performed with slightly variable treatment protocols, different electrodes and different electric pulse generators. Thus, there was a need for a prospective multi-institutional study, which was conducted by a consortium of four cancer centres gathered in the ESOPE project funded under the European Commission's 5th Framework Programme. In this study, the treatment response after electrochemotherapy according to tumour type, drug used, route of administration and type of electrodes, was tested [30]. The results of this study can be summarized as follows:

- An objective response rate of 85% (73.7% complete response rate) was achieved for electrochemotherapy-treated tumour nodules,

regardless of tumour histology and drug or route of administration used.

- At 150 days after treatment, the local tumour control rate for electrochemotherapy was 88% with bleomycin given intravenously, 73% with bleomycin given intratumorally and 75% with cisplatin given intratumorally, demonstrating that all three approaches were equally effective in local tumour control.
- Side effects of electrochemotherapy were minor and tolerable (muscle contractions and pain sensation).

The results of the ESOPE study confirmed previously reported results on the effectiveness of electrochemotherapy and Standard Operating Procedures (SOP) for electrochemotherapy were prepared [31].

The ESOPE study set the stage for introduction of electrochemotherapy in Europe. After the encouraging results of the ESOPE study, several cancer centers have started to use electrochemotherapy and reported the results of their studies. Collectively, the results were again similar as reported in the ESOPE study. However some advances in the treatment were reported. Predominantly it was reported that tumours bigger than 3 cm in diameter can be successfully treated by electrochemotherapy in successive electrochemotherapy sessions [32,33]. In general, electrochemotherapy provides a benefit to patients especially in quality of life [33], because electrochemotherapy is nowadays used predominantly in palliative intent [32,33].

CLINICAL USE AND TREATMENT PROCEDURES FOR ELECTROCHEMOTHERAPY

Based on all these reports, electrochemotherapy has been recognized as a treatment option for disseminated cutaneous disease in melanoma, and accepted in many national and also international guidelines for treatment of melanoma [34].

Treatment advantages and clinical use for electrochemotherapy can be summarized as follows:

- Effective in treatment of tumours of different histology in the cutaneous or subcutaneous tissue.
- Palliative treatment with improvement of patient's quality of life.
- Treatment of choice for tumours refractory to conventional treatments.
- Cytoreductive treatment before surgical resection in an organ sparing effect.

- Treatment of bleeding metastases.

The treatment procedure is as follows: based on SOP, tumour nodules can be treated by electrochemotherapy with injection of bleomycin intravenously or intratumourally and by electrochemotherapy with cisplatin given intratumourally. The choice of the chemotherapeutic drug is not based on tumour histology, but depends on the number and size of the nodules. After drug injection, the tumour nodules are exposed to electric pulses. The interval between intravenous drug injection and application of electric pulses is 8-28 min, and after intratumoural injection, as soon as possible. Different sets of electrodes are available for application; plate electrodes for smaller tumour nodules and needle electrodes for the treatment of larger (3 cm) and thicker tumour nodules. The treatment can be performed in a single session or can be repeated in case of newly emerging nodules or on those nodules which relapsed in some regions which were not treated well in the first treatment [30-33].

The treatment after a single electrochemotherapy session in most cases results in complete tumour eradication. When necessary, treatment can be repeated at 4-8 week intervals with equal antitumor effectiveness. The treatment has a good cosmetic effect without scarring of the treated tissue

In summary, electrochemotherapy has been recognized as a valid treatment approach; over 140 cancer centers have started to use it and have reported positive results. So far the effectiveness of the therapy is on case based evidence and further controlled and randomized studies are needed for the translation of this technology into broader and standard clinical practice. For further acceptance of electrochemotherapy in medical community, the first important step has been made, since electrochemotherapy for treatment of melanoma skin metastases and for treatment of primary basal cell and primary squamous cell carcinoma was recently listed in NICE guidelines.

Recently all published studies up to 2012 on electrochemotherapy in treatment of superficial nodules were reviewed in systematic review and meta-analysis [35]. Data analysis confirmed that electrochemotherapy had a significantly ($p < 0.001$) higher effectiveness (by more than 50%) than bleomycin or cisplatin alone, where only 8% of the tumors were in CR. After a single electro-chemotherapy, the treatment can be repeated with similar effectiveness. The overall effectiveness of electrochemotherapy was 84.1% objective responses (OR), from these 59.4% complete responses (CR). Another recent review and a clinical study suggested that SOP may need refinement; since the currently used

SOP for electrochemotherapy may not be suitable for tumors bigger than 3 cm in diameter, but such tumors are suitable for the multiple consecutive electrochemotherapy sessions [36].

NEW CLINICAL APPLICATIONS OF ELECTROCHEMOTHERAPY

Based on clinical experience that electrochemotherapy can be effectively used in treatment of cancer with different histology, when appropriately executed, the treatment could be used also for treatment of deep seated tumors. Prerequisite for that is further development of the technology in order to reach and effectively treat the tumors located either in the muscle, liver, bone, esophagus, rectum, brain or other internal organs.

The first reports have already been published in treatment of colorectal liver metastases (*Figure 2*), pancreatic tumors, and bone metastases. However, the technology can be implemented also in treatment of other localizations, such as head and neck tumors.

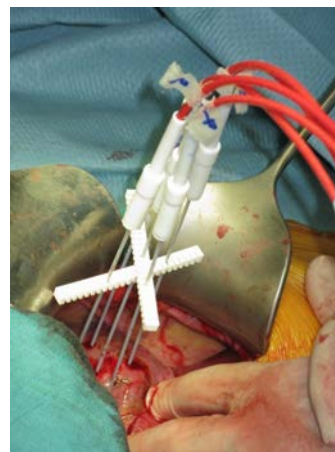


Figure 2: Electrochemotherapy of liver metastasis. Electrodes were inserted into the tumor and around the tumor in healthy liver tissue and connected to electric pulse generator. Electric pulses were delivered between the pairs of electrodes according to the treatment plan.

CONCLUSION

Electrochemotherapy is one of the biomedical applications of electroporation. Its development has reached clinical application and is an example of successful translational medicine. However its development is not finished yet; new technical developments will certainly enable further clinical uses and eventually clinical benefit for the patients. Another application of electroporation is still awaiting such translation, gene therapy based on gene electrotransfer.

REFERENCES

- [1] Yarmush ML, Goldberg A, Sersa G, Kotnik T, Miklavcic D. Electroporation-based technologies for medicine: principles, applications, and challenges. *Ann Rev Biomed Eng* 2014; **16**: 295-320.
- [2] Miklavcic D, Mali B, Kos B, Heller R, Sersa G. Electrochemotherapy: from the drawing board into medical practice. *BioMedical OnLine* 2014; **13**: 29.
- [3] Howell SB, Safaei R, Larson CA, Sailor MJ. Sopper transporters and the cellular pharmacology of the Platinum-containing cancer drugs. *Mol Pharmacol* 2010; **77**:887-94.
- [4] Sersa G. Electrochemotherapy: animal work review. In: Jaroszeski MJ, Heller R, Gilbert R, editors. *Electrochemotherapy, electrogenetherapy, and transdermal drug delivery. Electrically mediated delivery of molecules to cells*. Totowa, New Jersey: Humana Press, 2000. p. 119-36.
- [5] Mir LM. Therapeutic perspectives of in vivo cell electropermeabilization. *Bioelectrochem* 2001; **53**: 1-10.
- [6] Gehl J. Electroporation: theory and methods, perspectives for drug delivery, gene therapy and research. *Acta Physiol Scand* 2003; **177**: 437-47.
- [7] Mir LM. Bases and rationale of the electrochemotherapy. *EJC Suppl* 2006; **4**: 38-44.
- [8] Agerholm-larsen B, Iversen HK, Ibsen P, Moller JM, Mahmood F, Jansen KS, Gehl J. Preclinical validation of electrochemotherapy as an effective treatment for brain tumors. *Cancer Res* 2011; **71**:3753-62.
- [9] Vásquez JL, Ibsen P, Lindberg H, Gehl J. In vitro and in vivo experiments on electrochemotherapy for bladder cancer. *J Urol* 2015; **193**: 1009-15.
- [10] Miklavcic D, Beravs K, Semrov D, Cemazar M, Demsar F, Sersa G. The importance of electric field distribution for effective in vivo electroporation of tissues. *Biophys J* 1998; **74**: 2152-8.
- [11] Miklavcic D, Corovic S, Pucihar G, Pavselj N. Importance of tumor coverage by sufficiently high local electric field for effective electrochemotherapy. *EJC Suppl* 2006; **4**: 45-51.
- [12] Corovic S, Al Hakere B, Haddad V, Miklavcic D, Mir LM. Importance of the contact surface between electrodes and treated tissue in electrochemotherapy. *Tech Cancer Res Treat* 2008; **7**: 292—99.
- [13] Sersa G, Miklavcic D, Cemazar M, Rudolf Z, Pucihar G, Snoj M. Electrochemotherapy in treatment of tumours. *Eur J Surg Oncol* 2008; **34**: 232-40.
- [14] Miklavcic D, Pucihar G, Pavlovec M, Ribaric S, Mali M, Macek-Lebar A, Petkovsek M, Nastran J, Kranjc S, Cemazar M, Sersa G. The effect of high frequency electric pulses on muscle contractions and antitumor efficiency in vivo for a potential use in clinical electrochemotherapy. *Bioelectrochemistry* 2005; **65**: 121-8.
- [15] Sersa G, Kranjc S, Cemazar M, Scancar J, Krzan M, Neumann E. Comparison of antitumor effectiveness of electrochemotherapy using different electric pulse repetition frequencies. *J membrane biology* 2010; **236**: 155-162.
- [16] Sersa G, Cemazar M, Parkins CS, Chaplin DJ. Tumour blood flow changes induced by application of electric pulses. *Eur J Cancer* 1999; **35**: 672-7.
- [17] Bellard E, Markelc B, Pelofy S, Le Guerroué F, Sersa G, Teissie J, Cemazar M, Golzio M. Intravital microscopy at the single vessel level brings new insights of vascular modification mechanisms induced by electropermeabilization. *J Control Release* 2012; **163**: 396-403.
- [18] Gehl J, Skovsgaard T and Mir LM. Vascular reactions to in vivo electroporation: characterization and consequences for drug and gene delivery. *Biochim Biophys Acta* 2002; **1569**: 51-8.
- [19] Cemazar M, Parkins CS, Holder AL, Chaplin DJ, Tozer GM and Sersa G. Electroporation of human microvascular endothelial cells: evidence for anti-vascular mechanism of electrochemotherapy. *Br J Cancer* 2001; **84**: 556-70
- [20] Jarm T, Cemazar M, Miklavcic D, Sersa G. Antivascular effects of electrochemotherapy: implications in treatment of bleeding metastases. *Exp Rev Anticancer Ther* 2010; **10**: 729-746.
- [21] Sersa G, Jarm T, Kotnik T, Coer A, Podkrajsek M, Sentjurc M, Miklavcic D, Kadivec M, Kranjc S, Secerov A, Cemazar M. Vascular disrupting action of electroporation and electrochemotherapy with bleomycin in murine sarcoma. *Brit J Cancer*, 2008, **98**: 388-98
- [22] Markelc B, Bellard E, Sersa G, Pelofy S, Teissie J, Coer A, Golzio M, Cemazar. In vivo molecular imaging and histological analysis of changes induced by electric pulses used for plasmid DNA electrotransfer to the skin: a study in a dorsal window chamber in mice. *J Membrane Biol* 2012; **245**: 545-554.
- [23] Gehl J, Geertsen PF. Palliation of haemorrhaging and ulcerated cutaneous tumours using electrochemotherapy. *EJC Suppl* 2006; **4**: 35-37.
- [24] Sersa G, Miklavcic D, Cemazar M, Belehradek JJr, Jarm T, Mir LM. Electrochemotherapy with CDDP on LPB sarcoma: comparison of the anti-tumor effectiveness in immunocompetent and immunodeficient mice. *Bioelectrochem Bioener* 1997; **43**: 279-283.
- [25] Sersa G, Cemazar M, Menart V, Gaberc-Porekar V, Miklavčič D. Antitumor effectiveness of electrochemotherapy is increased by TNF- α on SA-1 tumors in mice. *Cancer Letters* 1997; **116**: 85-92.
- [26] Mir LM, Roth C, Orłowski S, Quintin-Colona F, Fradelizi D, Belahradek J, Kourilsky P. Systemic antitumor effects of electrochemotherapy combined with histoincompatible cells secreting interleukin 2. *J Immunother* 1995; **17**: 30-8.
- [27] Heller L, Pottinger C, Jaroszeski MJ, Gilbert R, Heller R. In vivo electroporation of plasmids encoding GM-CSF or interleukin-2 into existing B16 melanoma combined with electrochemotherapy inducing long-term antitumour immunity. *Melanoma Res* 2000; **10**: 577-83.
- [28] Cemazar M, Todorovic V, Scancar, J Lamprecht U, Stimac M, Kamensek U, Kranjc S, Coer A, Sersa G. Adjuvant INF- α therapy to electrochemotherapy with intravenous cisplatin in murine sarcoma exerts synergistic antitumor effectiveness. *Radiol Oncol* 2015; **49**:32-40
- [29] Mir LM, Belehradek M, Domenge C, Orłowski S, Poddevin B, Belehradek J Jr, Schwaab G, Luboinski B, Paoletti C. Electrochemotherapy, a new antitumor treatment: first clinical trial. *C R Acad Sci III* 1991; **313**: 613-8.
- [30] Marty M, Sersa G, Garbay JR, Gehl J, Collins CG, Snoj M, et al. Electrochemotherapy – An easy, highly effective and safe treatment of cutaneous and subcutaneous metastases: Results of ESOPE (European Standard Operating Procedures of Electrochemotherapy) study. *EJC Suppl* 2006; **4**: 3-13.
- [31] Mir LM, Gehl J, Sersa G, Collins CG, Garbay JR, Billard V, et al. Standard operating procedures of the electrochemotherapy:

Instructions for the use of bleomycin or cisplatin administered either systemically or locally and electric pulses delivered by Cliniporator™ by means of invasive or non-invasive electrodes. *EJC Suppl* 2006; **4**: 14-25.

- [32] Campana LG, Mocellin S, et al. Bleomycin-based electrochemotherapy: clinical outcome from a single institution's experience with 52 patients. *Ann Surg Oncol* 2008; **16**: 191-9.
- [33] Quaglino P, Mortera C, et al. Electrochemotherapy with intravenous bleomycin in the local treatment of skin melanoma metastases. *Ann Surg Oncol* 2008; **15**: 2215-22.
- [34] Testori A, Rutkowski P, Marsden J, Bastholt L, Chiarion-Sileni V, Hauschild A, Eggermont AM, Surgery and radiotherapy in the treatment of cutaneous melanoma, *Ann Oncol* 2009; **20 Suppl 6**: 22-9.
- [35] Mali B, Jarm T, Snoj M, Sersa G, Miklavcic D. Antitumor effectiveness of electrochemotherapy: a systematic review and meta-analysis. *Eur J Surg Oncol* 2013; **39**: 4-16.
- [36] Mali B, Miklavcic D, Campana L, Cemazar M, Sersa G, Snoj M, Jarm T. Tumor size and effectiveness of electrochemotherapy. *Radiol Oncol* 2013; **47**: 32-41.

ACKNOWLEDGEMENT

This research was funded by a research grant from the Research Agency of the Republic of Slovenia and was conducted in the scope of the EBAM European Associated Laboratory (LEA) and resulted from the networking efforts of the COST Action TD1104 (www.electroporation.net).



Gregor Sersa, graduated from the Biotechnical Faculty at the University of Ljubljana in 1978, where he is currently a professor of molecular biology. He is employed at the Institute of Oncology in Ljubljana as Head of the Department of Experimental Oncology. His specific field of interest is the effect of electric field on tumor cells and tumors as drug and gene

delivery system in different therapeutic approaches. Besides experimental work, he is actively involved in the education of undergraduate and postgraduate students at the University of Ljubljana.

NOTES

Electrochemotherapy in clinical practice; Lessons from development and implementation - and future perspectives

Julie Gehl

Center for Experimental Drug and Gene Electrotransfer, Department of Oncology, Herlev and Gentofte Hospital, University of Copenhagen, Denmark.

Abstract: In just two decades electrochemotherapy has developed from an experimental treatment to standard therapy. This paper describes this development and also goes into the details of how a new technology can become implemented, to benefit patients. Electrochemotherapy is a technology that involves the use of electric pulses and chemotherapy. Thus the development of this technology has required specialists in biology, engineering and medicine to pull together, in order to achieve this accomplishment. This paper describes the development of equipment, as well as standard operating procedures, for treatment with electrochemotherapy. This chapter also deals with sharing knowledge about the use of the technology, and ensuring access for patients.

DEVELOPMENT OF ELECTROCHEMOTHERAPY

Initial studies on the organization of the cell membrane, and on deformation of this membrane by electric forces, were performed through the particularly the 1960s and 70s. In 1977 rupture of erythrocytes was described in a Nature paper [1], and another highly influential paper was Neumanns study from 1982 [2], demonstrating DNA electrotransfer which is now one of the most frequently used laboratory methods in molecular biology.

A very active field in cancer therapy in the 1970s and 80s was resistance to drug therapy, and there was great optimism that understanding resistance to therapy could ultimately lead to a cure for cancer. Different important cellular resistance systems were discovered, e.g. the multidrug transporter p-glycoprotein, that enables cancer cells to export chemotherapy [3]. In this landscape electroporation was a new technology that allowed circumvention of membrane based resistance by simply plowing a channel through cell membrane, allowing non-permeant drugs inside.

A number of studies were published about enhancement of cytotoxicity by electroporation [4,5] in vitro, and also in vivo [6], principally from Lluís Mir's group at Institut Gustave-Roussy. It was also here that, in a remarkable short time-frame, the first clinical study was reported, preliminary results in French in 1991, and the final publication in 1993 [7]. A few years later [8], the first studies from the US came out, as well as studies from Slovenia [9], and Denmark [10].

Out of a wish to create electroporation equipment for clinical use, which would be able to perform both gene therapy and electrochemotherapy, which could be adapted by the user to accommodate developments, and which was a useful instrument for the treating physician, i.e. by showing precise recordings of voltage and current along with the treatment, the Cliniporator

consortium was formed. This European consortium developed and tested the Cliniporator [11,12].

A subsequent European consortium, named ESOPE (European Standard Operating Procedures for Electrochemotherapy) set out to get the Cliniporator approved for clinical use, to produce electrodes for it, to test the system in a clinical protocol, as well as to make concluding standard operating procedures.

Four groups went into the clinical study of which three had previous experience with electrochemotherapy. And the methods used differed between those three centers.

In France, a hexagonal electrode was used, with 7.9 mm between electrodes and a firing sequence allowing each of seven electrodes to be pairwise activated 8 times, a total of 96 pulses delivered at high frequency, with a voltage of 1.3 kV/cm (voltage to electrode distance ratio). Patients were sedated, bleomycin was given iv, and the procedure took place in an operating theatre [7].

In the Slovenian studies, patients were treated with cisplatin intratumorally, and with plate electrodes using 1.3 kV/cm, anesthesia not described. Pulses were administered as two trains of each four pulses [9].

In Denmark we used intratumoral bleomycin, a linear array electrode of two opposing rows of needles activated against each other using 1.2 kV/cm, 8 pulses at 1 Hz. Local anesthesia with lidocaine was used [10].

In other words, there was agreement about the overall purpose, but three different approaches. The ESOPE study [13] brought these three approaches together, and on the technical side, the three different electrodes were manufactured, and the final conclusion of the different methods and electrodes were defined in collaboration.

The standard operating procedures [14] are very detailed, allowing a newcomer to the field to immediately implement the procedure. Thus it is described how to administer the drug and pulses, how

to make treatment decisions, and how to evaluate response and perform follow-up.

The standard operating procedures, together with the availability of certified equipment, marked a dramatic change in the use of electrochemotherapy. Thus when the standard operating procedures were published in 2006 only few European centers were active, and after the publication of the procedures the number of centers quickly rose and is today over 140. It would be estimated that this number will continue to grow, and also that the generators now being placed in various institutions will be increasingly used also for new indications.

IMPLEMENTATION

In an ideal world, new developments in cancer therapy become immediately available to patients. But experience shows that from the development of the technology, and the emergence of the first results, there is still quite a road to be traveled in order for the individual patient to be able to be referred, if the treatment is relevant to the particular case. First of all, equipment must be present at the individual institution, along with knowledgeable surgeons and oncologists trained to provide the treatment. The logistical set up must be in place, and this includes availability of time in the operating rooms and competent nursing support. Patients need to know that the treatment is an option. As electrochemotherapy is an option for patients suffering from different types of cancer, it requires continuous work to address specialists in the different fields. Information available on the internet can be an important resource for patients, as well as professionals.

Various countries have different approval mechanisms for new treatments, and endorsement can be a time-consuming affair. The most renowned national agency is the National Institute of Health and Care Excellence (NICE) in the UK, which has a rigorous scrutinization of new technologies and where central documents are freely available. NICE has guidances for electrochemotherapy for cutaneous metastases, and primary skin cancers respectively [15,16]. These national recommendations, as well as the integration of electrochemotherapy into specific guidelines (see e.g. [17]) are very important for the improving accessibility to treatment.

RESEARCH

A very important point is that the standard operating procedures were a very important foundation – but must be followed up with more detailed experience and

further developments. Several groups have published further studies on electrochemotherapy, broadening the knowledge base and answering specific questions of clinical importance [18-26].

Furthermore, electrochemotherapy is now being developed for a number of new indications, including mucosal head and neck cancer, gastro-intestinal cancers, lung cancer (primary and secondary), gynecological cancers, sarcoma, bone metastases, as well as brain metastases. For each of these indications standard operating procedures will need to be developed, in order to allow dissemination of the treatment.

REFERENCES

- [1] Kinoshita K, Tsong TY. Formation and resealing of pores of controlled sizes in human erythrocyte membrane. *Nature* 1977;268:438-41.
- [2] Neumann E, Schaefer-Ridder M, Wang Y, Hofschneider PH. Gene transfer into mouse lyoma cells by electroporation in high electric fields. *EMBO J* 1982;1(7):841-45.
- [3] Skovsgaard T, Nissen NI. Membrane transport of anthracyclines. *Pharmacol Ther* 1982;18(3):293-311.
- [4] Okino M, Mohri H. Effects of a high-voltage electrical impulse and an anticancer drug on in vivo growing tumors. *JpnJ Cancer Res* 1987;78(0910-5050 SB - M SB - X):1319-21.
- [5] Orłowski S, Belehradec Jr J, Paoletti C, Mir LM. Transient electroporation of cells in culture. Increase of the cytotoxicity of anticancer drugs. *Biochemical Pharmacology* 1988;37(24):4727-33.
- [6] Mir LM, Orłowski S, Belehradec J, Jr., Paoletti C. Electrochemotherapy potentiation of antitumor effect of bleomycin by local electric pulses. *Eur J Cancer* 1991;27(1):68-72.
- [7] Belehradec M, Domenge C, Luboinski B, Orłowski S, Belehradec Jr J, Mir LM. Electrochemotherapy, a new antitumor treatment. First clinical phase I-II trial. *Cancer* 1993;72(12):3694-700.
- [8] Heller R. Treatment of cutaneous nodules using electrochemotherapy. [Review] [32 refs]. *Journal of the Florida Medical Association* 1995;82(2):147-50.
- [9] Sersa G, Stabuc B, Cemazar M, Jancar B, Miklavcic D, Rudolf Z. Electrochemotherapy with cisplatin: Potentiation of local cisplatin antitumor effectiveness by application of electric pulses in cancer patients. *European Journal of Cancer* 1998;34(8):1213-18.
- [10] Gehl J, Geertsen PF. Efficient palliation of haemorrhaging malignant melanoma skin metastases by electrochemotherapy. *Melanoma Res* 2000;10(6):585-9.
- [11] Andre FM, Gehl J, Sersa G, Preat V, Hojman P, Eriksen J, et al. Efficiency of High- and Low-Voltage Pulse Combinations for Gene Electrotransfer in Muscle, Liver, Tumor, and Skin. *Human Gene Therapy* 2008;19(11):1261-71.
- [12] Hojman P, Gissel H, Andre F, Courmil-Henrionnet C, Eriksen J, Gehl J, et al. Physiological effect of high and low voltage pulse combinations for gene electrotransfer in muscle. *HumGene Ther* 2008(1557-7422 (Electronic)).
- [13] Marty M, Sersa G, Garbay JR, Gehl J, Collins CG, Snoj M, et al. Electrochemotherapy - An easy, highly effective and safe treatment of cutaneous and subcutaneous metastases: Results of

- ESOPE (European Standard Operating Procedures of Electrochemotherapy) study. *Ejc Supplements* 2006;4(11):3-13.
- [14] Mir LM, Gehl J, Sersa G, Collins CG, Garbay JR, Billard V, et al. Standard operating procedures of the electrochemotherapy: Instructions for the use of bleomycin or cisplatin administered either systemically or locally and electric pulses delivered by the Cliniporator™ by means of invasive or non-invasive electrodes. *European Journal of Cancer Supplements* 2006;4(11):14-25.
- [15] National Institute for Health Care. Electrochemotherapy for metastases in the skin from tumours of non-skin origin and melanoma. <http://publicationsnice.org.uk/electrochemotherapy-for-metastases-in-the-skin-from-tumours-of-non-skin-origin-and-melanoma-ipg446> 2013.
- [16] (NICE) NifHaCE. Electrochemotherapy for primary basal cell carcinoma and primary squamous cell carcinoma. www.nice.org.uk 2014.
- [17] Stratigos A, Garbe C, Lebbe C, Malvehy J, Del Marmol V, Pehamberger H, et al. Diagnosis and treatment of invasive squamous cell carcinoma of the skin: European consensus-based interdisciplinary guideline. *Eur J Cancer* 2015;51(14):1989-2007.
- [18] Matthiessen LW, Chalmers RL, Sainsbury DC, Veeramani S, Kessell G, Humphreys AC, et al. Management of cutaneous metastases using electrochemotherapy. *Acta Oncol* 2011;50:621-29.
- [19] Matthiessen LW, Johannesen HH, Hendel HW, Moss T, Kamby C, Gehl J. Electrochemotherapy for large cutaneous recurrence of breast cancer: A phase II clinical trial. *Acta Oncologica* 2012;51(6):713-21.
- [20] Campana LG, Valpione S, Falci C, Mocellin S, Basso M, Corti L, et al. The activity and safety of electrochemotherapy in persistent chest wall recurrence from breast cancer after mastectomy: a phase-II study. *Breast Cancer Res Treat* 2012;134:1169-78.
- [21] Campana LG, Bianchi G, Mocellin S, Valpione S, Campanacci L, Brunello A, et al. Electrochemotherapy treatment of locally advanced and metastatic soft tissue sarcomas: results of a non-comparative phase II study. *World JSurg* 2014;38:813-22.
- [22] Campana LG, Mali B, Sersa G, Valpione S, Giorgi CA, Stojan P, et al. Electrochemotherapy in non-melanoma head and neck cancers: a retrospective analysis of the treated cases. *BrJ Oral Maxillofac Surg* 2014.
- [23] Curatolo P, Mancini M, Clerico R, Ruggiero A, Frascione P, Di Marco P, et al. Remission of extensive merkel cell carcinoma after electrochemotherapy. *Arch Dermatol* 2009;145(4):494-5.
- [24] Curatolo P, Quaglino P, Marengo F, Mancini M, Nardo T, Mortera C, et al. Electrochemotherapy in the treatment of Kaposi sarcoma cutaneous lesions: a two-center prospective phase II trial. *Ann Surg Oncol* 2012;19(1):192-8.
- [25] Quaglino P, Mortera C, Osella-Abate S, Barberis M, Illengo M, Rissone M, et al. Electrochemotherapy with intravenous bleomycin in the local treatment of skin melanoma metastases. *Ann Surg Oncol* 2008;15:2215-22.
- [26] Quaglino P, Matthiessen LW, Curatolo P, Muir T, Bertino G, Kunte C, et al. Predicting patients at risk for pain associated with electrochemotherapy. *Acta Oncol* 2015;54(3):298-306.



Julie Gehl heads the Center for Experimental drug and gene Electrotransfer at Department of Oncology, Herlev Hospital at the University of Copenhagen. The center undertakes both preclinical and clinical investigations of the use of electrotransfer in drug and gene delivery. Julie Gehl is an MD, and specialist in Oncology. Dr. Gehl has an extensive publication record, is an experienced principal investigator and has guided numerous ph.d. students and students.

NOTES

NOTES

Development of devices and electrodes

Damijan Miklavčič, Matej Reberšek

University of Ljubljana, Faculty of Electrical Engineering, Ljubljana, Slovenia

Abstract: Since first reports on electroporation, numerous electroporation based biotechnological and biomedical applications have emerged. The necessary pulse generators are characterized by the shape of the pulses and their characteristics: pulse amplitude and duration. In addition, the electrodes are the important “connection” between the cells/tissue and pulse generator. The geometry of the electrodes together with the cell/tissue sample properties determine the necessary output power and energy that the electroporators need to provide. The choice of electroporator – the pulse generator depends on biotechnological and biomedical application but is inherently linked also to the electrodes choice.

INTRODUCTION

Since first reports on electroporation (both irreversible and reversible), a number of applications has been developed and list of applications which are based on electroporation is still increasing. First pulse generators have been simple in construction and have provided an exponentially decaying pulse of up to several thousands of volts. Also the electrodes were very simple in their design – usually parallel plate electrodes with couple of millimeters distance between them was used, and cells in suspension were placed in-between [1]. Later, new pulse generators were developed which were/are able to provide almost every shape of pulse, and also electrodes which can be bought are extremely diverse [2]–[6]. It is important to note that most often nowadays devices that generate rectangular pulses are being used.

The amplitude of pulses and their duration depend strongly on biotechnological/biomedical application. For electrochemotherapy most often a number of 1000 V pulses of 100 μ s duration are needed. For effective gene transfer longer pulses 5-20 ms pulses but of lower amplitude, or a combination of short high- and longer low-voltage pulses are used. For other applications like tissue ablation by means of irreversible electroporation, or liquid-food or water sterilization, thousands of volts pulses are needed. In addition to the pulse amplitude and duration, an important parameter to be taken into account is also the power and energy that need to be provided by the generator.

The energy that needs to be provided is governed by the voltage, current and pulse duration and/or number of pulses. The current if the voltage is set is governed by the load, and this is determined by the geometry of the load, and the load is determined by geometry of the tissue/cell sample and its electrical conductivity. The geometry of the tissue to be exposed to electric pulses are predominantly determined by the shape of the electrodes, the distance between them, depth of electrode penetration/immersion into the sample. Tissue/cell suspension electrical conductivity depends on tissue type or cell sample properties and can be

considerably increased while tissue/cells are being exposed to electrical pulses of sufficient amplitude.

Based on the above considerations not a single pulse generator will fit all applications and all needs of a researcher [7]. One can either seek for a specialized pulse generator which will only provide the pulses for this specific biotechnological or biomedical application, or for a general purpose pulse generator which will allow to generate “almost” all what researcher may find interesting in his/her research. Irrespective of the choice, it has to be linked also to the electrodes choice [8]–[10].

THERAPEUTIC AND TECHNOLOGICAL APPLICATIONS OF ELECTROPORATION

Nowadays electroporation is widely used in various biological, medical, and biotechnological applications [11]–[16]. Tissue ablation relying on irreversible electroporation is less than a decade old, but its efficacy is promising especially in treating non-malignant tissue, in the field of water treatment where efficacy of chemical treatment is enhanced with electroporation, in food preservation where electroporation has proven, in some cases, to be as effective as pasteurization [17]. In contrast, applications based on reversible electroporation are currently more widespread and established in different experimental and/or practical protocols. Probably the most important of them is the introduction of definite amount of small or large molecules to cytoplasm through the plasma membrane. Furthermore, slight variation of electric field parameters results in an application where molecules can be directly inserted into the plasma membrane or cells can be effectively fused.

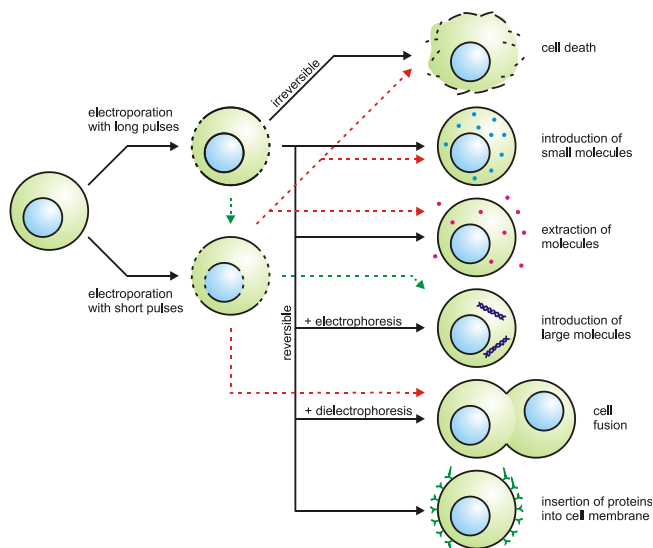


Figure 1: Exposure of a cell to an electric field may result either in permeabilization of cell membrane or its destruction. In this process the electric field parameters play a major role. If these parameters are within certain range, the permeabilization is reversible; therefore it can be used in applications such as introduction of small or large molecules into the cytoplasm, insertion of proteins into cell membrane or cell fusion.

ELECTROCHEMOTHERAPY

The most representative application of delivery of small molecules through electroporated membrane is electrochemotherapy. It was demonstrated in several preclinical and clinical studies, both on humans and animals, that electrochemotherapy can be used as treatment of choice in local cancer treatment [18], [19]. Most often a number of short rectangular 100 μ s long pulses with amplitudes up to 1000 V, are applied. Number of pulses that are usually delivered is 8. These can be delivered at pulse repetition frequency of 1 Hz or 5 kHz [20]. New technological developments were made available for in treating deep seated tumours, where 3000 V, 50 A and 100 μ s pulses are being delivered [21]. Recent advances in treating liver metastasis, bone metastasis and soft tissue sarcoma have been reported [22]–[24].

TISSUE ABLATION BY NON-THERMAL IREVERSIBLE ELECTROPORATION

The ablation of undesirable tissue through the use of irreversible electroporation has recently been suggested as a minimally invasive method for tumor removal but could also be used in cardiac tissue ablation instead of RF heating tissue ablation or other tissue ablation techniques [12], [25], [26]. Similarly as in electrochemotherapy pulses of 50 or 100 μ s with amplitudes up to 3000 V are used [27]. The number of pulses delivered to the target tissue is however considerably higher. If in electrochemotherapy 8 pulses are delivered, here 96 pulses are used. Pulse repetition

frequency needs to be low 1 or 4 Hz in order to avoid excessive heating [28].

GENE ELECTROTRANSFER

Exogenous genetic material can be delivered to cells by using non-viral methods such as electropermeabilization [29]. Electrotransfection can be achieved using: exponentially decaying pulses; square wave pulses with superimposed RF signals; or only long square wave pulses up to 20 ms and with amplitudes ranging from 200 to 400 V [30]. Although no consensus can be reached, it can however be stated that longer pulses are generally used in gene transfection than in electrochemotherapy. Furthermore, two distinct roles of electric pulses were described. In experiments where several short high voltage pulses (e.g. $8 \times 100 \mu$ s of 1000 V) were followed by long low voltage pulses (e.g. 1×100 ms of 80 V) [31]. It was demonstrated that short high voltage pulses are permeabilizing the membrane while the longer lower voltage pulses have an electrophoretic effect on DNA itself facilitating interaction of plasmid with the membrane [32]. Skin can be an excellent target for gene transfer protocols due to its accessibility [33].

ELECTROFUSION

So far we have presented applications of electroporation that are used to introduce different molecules either to the cytosol or to the cell plasma membrane. But electroporation of cell plasma membrane can also result in fusion of cells. This process has been termed electrofusion. First reports of *in vitro* electrofusion of cells date back into 1980s. In the reports it has been shown that fusion between two cells can proceed only if the cells are in contact prior or immediately after electroporation. The contact between the cells can be achieved either by dielectrophoretic connection of neighboring cells, which is followed by electroporation or by centrifugation of cell suspension after exposure to electric field. In both cases cells must be reversibly permeabilized, otherwise they lose viability and there is no electrofusion [34]. Electrofusion in *in vitro* environment is possible due to high possibility of cell movement while cells in tissues are more or less fixed, nevertheless *in vivo* electrofusion has been observed in B16 melanoma tumors as well as cells to tissue fusion [35], [36]. Electrofusion of cells of different sizes can be achieved by nanosecond pulsed electric fields [37].

ELECTROEXTRACTION

Electroporation can be used to extract substances (e.g. juice, sugar, pigments, lipid and proteins) from

biological tissue or cells (e.g. fruits, sugar beets, microalgae, wine and yeast). Electroextraction can be more energy and extraction efficient, and faster than classical extraction methods (pressure, thermal denaturation and fermentation) [38]–[42]. An economic assessment of microalgae-based bioenergy production was recently made [43]. Recommendations guidelines on the key information to be reported in biotechnological studies because of variability in results obtained in different laboratories [44].

ELECTRO- PASTEURIZATION AND STERILIZATION

Irreversible electroporation can be used in applications where permanent destruction of microorganisms is required, i.e. food processing and water treatment [45]. Still, using irreversible electroporation in these applications means that substance under treatment is exposed to a limited electric field since it is desirable that changes in treated substance do not occur (e.g. change of food flavor) and that no by-products emerge due to electric field exposure (e.g. by-products caused by electrolysis). This is one of the reasons why short (in comparison to medical applications) in the range of 1-3 μ s are used. Especially industrial scale batch or flowthrough exposure systems may require huge power generators with amplitudes up to 40 kV and peak currents up to 500 A. Although batch and flow-through processes are both found on industrial scale, flow-through is considered to be superior as it allows treatment of large volumes. Such mode of operation requires constant operation requiring higher output power of pulse generators [13], [46].

ELECTRIC FIELD DISTRIBUTION *IN VIVO*

In most applications of tissue permeabilization it is required to expose the volume of tissue to E intensities between the two “thresholds” i.e. to choose in advance a suitable electrode configuration and pulse parameters for the effective tissue electroporation [47]. Therefore electric field distribution in tissue has to be estimated before the treatment, which can be achieved by combining results of rapid tests or *in situ* monitoring [48] with models of electric field distribution [49]–[53]. However, modeling of electric field distribution in tissue is demanding due to heterogeneous tissue properties and usually complex geometry. Analytical models can be employed only for simple geometries. Usually they are developed for 2D problems and tissue with homogenous electrical properties. Therefore in most cases numerical modeling techniques are still more acceptable as they can be used for modeling 3D geometries and complex tissue properties. For that purpose mostly finite element method and finite

difference method are applied. Both numerical methods have been successfully applied and validated by comparison of computed and measured electric field distribution. Furthermore, advanced numerical models were build, which take into consideration also tissue conductivity increase due to tissue or cell electroporation. These advanced models describe E distribution as a function of conductivity $\sigma(E)$. In this way models represent electroporation tissue conductivity changes according to distribution of electric field intensities [54], [55].

ELECTRODES FOR *IN VITRO* AND *IN VIVO* APPLICATIONS

Effectiveness of electroporation in *in vitro*, *in vivo* or clinical environment depends on the distribution of electric field inside the treated sample. Namely, the most important parameter governing cell membrane permeabilization is the local electric field to which the cell is exposed [47]. To achieve this we have to use an appropriate set of electrodes and an electroporation device – electroporator that generates required voltage or current signals. Although both parts of the mentioned equipment are important and necessary for effective electroporation, electroporator has a substantially more important role since it has to be able to deliver the required signal to its output loaded by impedance of the sample between electrodes.

Nowadays there are numerous types of electrodes that can be used for electroporation in any of the existing applications [56]–[60]. According to the geometry, electrodes can be classified into several groups, i.e. parallel plate electrodes, needle arrays, wire electrodes, tweezers electrodes, coaxial electrodes, etc (Fig. 2). Each group comprises several types of electrodes that can be further divided according to the applications, dimensions, electrode material etc. In any case selection of electrode type plays an important role in characterization of the load that is connected to the output of the electroporator. During the design of the electroporator load characterization represents the starting point and represents a considerable engineering problem, because electrical characteristics of substance between electrodes (e.g. cell suspension, tissue, etc.) vary from experiment to experiment and even during the course of experiment. In general the load between electrodes has both a resistive and a capacitive component. The value of each component is defined by geometry and material of electrodes and by electrical and chemical properties of the treated sample. In *in vitro* conditions these parameters that influence the impedance of the load can be well controlled since size and geometry of sample are known especially if cuvettes are used. Furthermore, by using specially prepared cell media, electrical and chemical properties

are defined or can be measured. On the other hand, in *in vivo* conditions, size and geometry can still be controlled to a certain extent but electrical and chemical properties can only be estimated, especially if needle electrodes are used that penetrate through different tissues. However, even if we manage to reliably define these properties during the development of the device, it is practically impossible to predict changes in the electrical and chemical properties of the sample due to exposure to high-voltage electric pulses [61]. Besides electroporation of cell membranes which increases electrical conductivity of the sample, electric pulses also cause side effects like Joule heating and electrolytic contamination of the sample [62], which further leads to increased sample conductivity [63].

ELECTRIC PULSES

For better understanding and critical reading of various reports on electroporation phenomenon and electroporation based applications, complete disclosure of pulse parameters needs to be given. Electric pulses are never “square” or “rectangular”, but they are characterized by their rise time, duration/width, fall time, pulse repetition frequency. Rise time and fall time are determined as time needed to rise from 10% to 90%

of the amplitude, drop from 90% to 10% of amplitude, respectively. Pulse width is most often defined as time between 50% amplitude on the rise and 50% amplitude on the fall. Pulse repetition frequency is the inverse of the sum of pulse width and pause between two consecutive pulses. These may seem trivial when discussing pulses of 11 ms, but become an issue when discussing ns or even ps pulses [64]. The cell membrane damage and uptake of ions is significantly reduced when using bipolar ns pulses instead of monopolar [65]. Shapes other than “rectangular” have been investigated with respect to electroporation efficiency [66]. It was suggested exposure of cells to pulse amplitudes above given critical amplitude and duration of exposure to this above critical value seem to be determining level of membrane electroporation irrespective of pulse shape. Exponentially decaying pulses are difficult to be considered as such but were predominantly used in 80s for gene electrotransfer. Their shape was convenient as the first peak part of the pulses acts as the permeabilizing part, and the tail of the pulse acts as electrophoretic part pushing DNA as towards and potentially through the cell membrane [31].

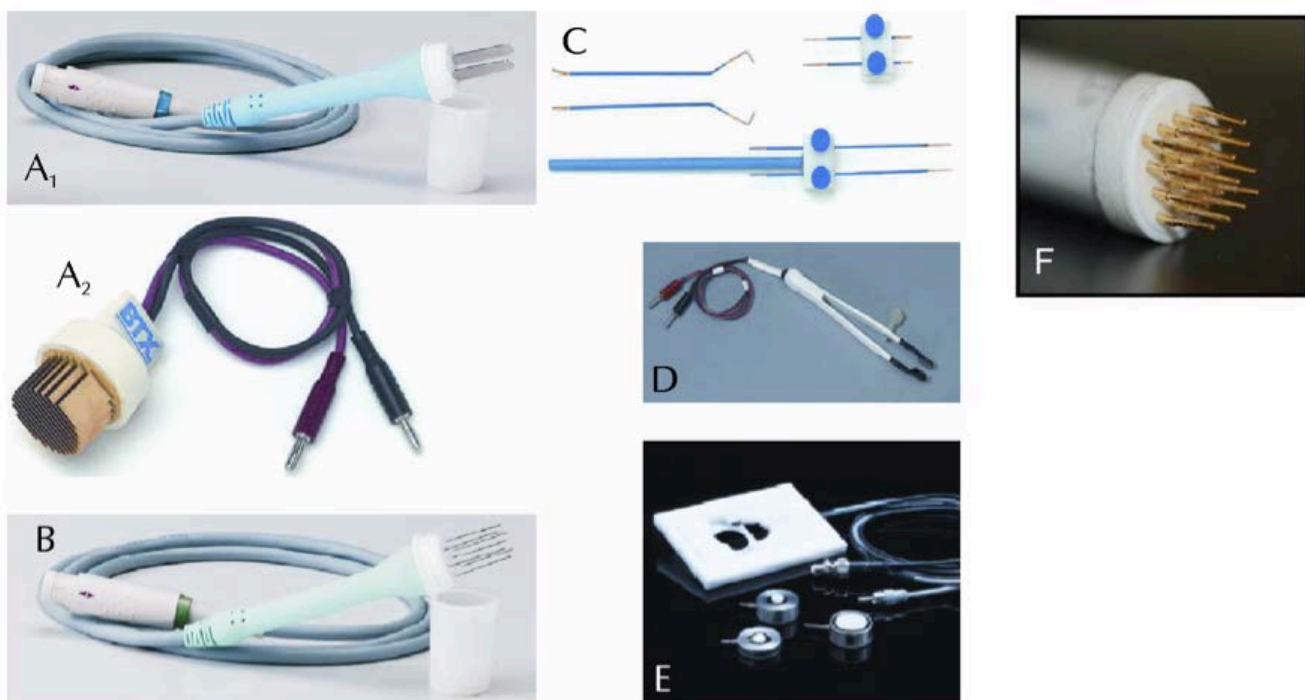


Figure 2: Examples of commercially available electrode for electroporation. Electrodes belong to the following group: A₁ and A₂ –parallel plate electrodes, B – needle arrays, C – wire electrodes, D – tweezers electrodes, E – coaxial electrodes and F – multiple electrodes array. Electrodes A₁ and B are produced by IGEA, Italy and are used for clinical applications of electrochemotherapy and electrotransfection. Electrodes A₂, C and E are used for different *in vitro* applications and are produced by: E – Cyto Pulse Sciences, U.S.A.; A₂, C and also D that are used for *in vivo* applications, are produced by BTX Hardware division, U.S.A, F are used for skin gene electrotransfer [33].

ELECTROPORATORS – THE NECESSARY PULSE GENERATORS

Electroporator is an electronic device that generates signals, usually square wave or exponentially decaying pulses, required for electroporation [1]. Parameters of the signal delivered to electrodes with the treated sample vary from application to application. Therefore, in investigating of electroporation phenomenon and development of electroporation based technologies and treatments it is important that electroporator is able to deliver signals with the widest possible range of electrical parameters if used in research. If however used for a specific application only, e.g. clinical treatment such as electrochemotherapy, pulse generator has to provide exactly required pulse parameters in a reliable manner. Moreover, electroporator must be safe and easy to operate and should offer some possibilities of functional improvements. Clinical electroporators used in electrochemotherapy of deep-seated tumors or in non-thermal tissue ablation are also equipped with ECG synchronization algorithms which minimizes possible influence of electric pulse delivery on heart function [67].

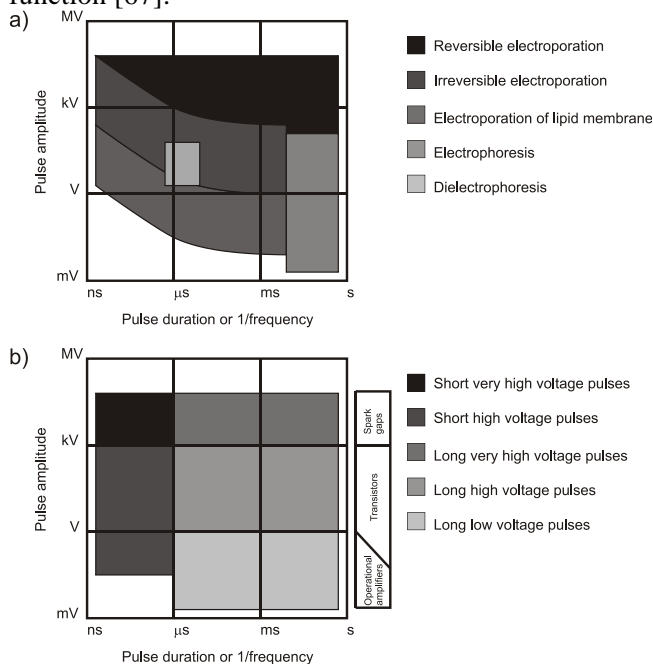


Figure 3: Areas of amplitude and duration of electrical pulses which are used in the research of electroporation and related effects (a). Five different areas of electroporation pulse generation (b). To amplify or to generate very-high-voltage electroporation pulses (over a few kV) spark gaps and similar elements are used, for high-voltage (a few V to a few kV) transistors and for low-voltage operational amplifiers are used. Nanosecond (short) pulses are generated with different techniques than pulses longer than 1 μ s. Originally published in Advanced electroporation techniques in biology and medicine by Reberšek and Miklavčič 2010 [3].

In principle, electroporators can be divided in several groups depending on biological applications, but from the electrical point of view only two types of

electroporators exist: devices with voltage output (output is voltage signal $U(t)$) and devices with current output (output is current signal $I(t)$). Both types of devices have their advantages and disadvantages, but one point definitely speaks in favor of devices with voltage output. For example, if we perform *in vitro* experiments with parallel plate electrodes with plate sides substantially larger than the distance between them, the electric field strength E that is applied to the sample can be approximated by the voltage-to-distance ratio U/d , where d is the electrode distance and U the amplitude of applied signal obtained from an electroporator with voltage output. On the other hand, if an electroporator with current output is used, the same approximation could be used only if additional measurement of voltage difference between electrodes is performed or if the impedance Z of the sample is known, measured or approximated and voltage difference between electrodes is estimated using Ohm's law $U = I \cdot Z$. Nevertheless, there are several commercially available electroporators that fulfill different ranges of parameters and can be used in different applications. A list of commercially available electrodes and electroporators has been presented in 2004 by Puc and colleagues [68], updated in 2010 [3] in a manuscripts that describe techniques of signal generation required for cell/tissue electroporation, and is now again being updated [6].

To be sure the applied pulses are adequate we have to measure the applied voltage and current during the pulse delivery.

In nanosecond applications rise time of the pulse is sometimes shorter than the electrical length (the time in which an electrical signal travels through the line) between the source and the load. In this case, the impedance of the load and the transmission line has to match the impedance of the generator, so that there are no strong pulse reflections and consequently pulse prolongations.

Based on the studies reported in the literature it is very difficult to extract a general advice how to design experiments or treatments with electroporation. In principle we can say that pulse amplitude (voltage-to-distance ratio) should typically be in the range from 200 V/cm up to 2000 V/cm. Pulse durations should be in the range of hundreds of microseconds for smaller molecules and from several milliseconds up to several tens of milliseconds for macromolecules such as plasmid DNA (in the latter case, due to the very long pulse duration, optimal pulse amplitude can even be lower than 100 V/cm). If there is any possibility to obtain the equipment that generates bipolar pulses or have a possibility to change electric field orientation in the sample, these types of pulses/electroporators should

be used because bipolar pulses yield a lower poration threshold, higher uptake, reduce electrolyte wear and electrolytic contamination of the sample, and an unaffected viability compared to unipolar pulses of the same amplitude and duration. Better permeabilisation or gene transfection efficiency and survival can also be obtained by changing field orientation in the sample using special commutation circuits that commute electroporation pulses between the electrodes [56], [58], [69]. Short bipolar pulses were also investigated as they mitigate nerve/muscle stimulation [70]–[72].

This general overview of electrical parameters should however only be considered as a starting point for a design of experiments or treatments. Optimal values of parameters namely also strongly depend on the cell type used, on the molecule to be introduced, and on specific experimental conditions. The pulse characteristics determined as optimal or at least efficient and the tissue/sample will than determine the architecture of the pulse generator, whether it will be a Marx generator, Blumlein, or... [7].

CONCLUSIONS

Electroporation has been studied extensively until now, and a number of applications has been developed. Electrochemotherapy has been demonstrated as an effective local treatment of solid tumors and is the most mature therapeutic application right now. Electroporation for gene transfection however has been long used in *in vitro* situation. With a hold on viral vectors electroporation represents a viable non-viral alternative also for *in vivo* gene transfection. Clinical applications and expansion of electrochemotherapy and tissue ablation have been hindered by the lack of adequate electroporators and their certification in Europe (CE Medical Device) and limited approval by FDA in USA [73]. Cliniporator (IGEA, s.r.l. Carpi, Italy) was certified in EU (CE mark) as a medical device and is offered on the market along with standard operating procedures for electrochemotherapy of cutaneous and subcutaneous tumors. NanoKnife (AngioDynamics, Queensbury, USA) was certified in EU and approved by the FDA for surgical ablation of soft tissue, including cardiac and smooth muscle. Some electroporators are now available under the license for clinical evaluation purposes: Collectra, Elgen, Medpulser, Cliniporator VITAE, BetaTech, DermaVax, EasyVax, Ellisphere, TriGrid [4].

Development of new applications warrants further development of pulse generators and electrodes. Based on the above considerations however, a single pulse generator will not fit all applications and all needs of researchers. One can either seek for a specialized pulse generator which will only provide the pulses for his/her specific biotechnological or biomedical application, or

for a general purpose pulse generator which will allow to generate “almost” all what researcher may find interesting/necessary in his/her research. Irrespective of the choice, this has to be linked also to the electrodes choice and tissue/sample conductivity.

REFERENCES

- [1] M. Reberšek, D. Miklavčič, C. Bertacchini, and M. Sack, “Cell membrane electroporation-Part 3: the equipment,” *Electr. Insul. Mag. IEEE*, vol. 30, no. 3, pp. 8–18, 2014.
- [2] K. Flisar, M. Puc, T. Kotnik, and D. Miklavcic, “Cell membrane electropermeabilization with arbitrary pulse waveforms,” *IEEE Eng. Med. Biol. Mag. Q. Mag. Eng. Med. Biol. Soc.*, vol. 22, no. 1, pp. 77–81, Feb. 2003.
- [3] M. Reberšek and D. Miklavčič, “Concepts of Electroporation Pulse Generation and Overview of Electric Pulse Generators for Cell and Tissue Electroporation,” in *Advanced Electroporation Techniques in Biology and Medicine*, A. G. Pakhomov, D. Miklavčič, and M. S. Markov, Eds. Boca Raton: CRC Press, 2010, pp. 323–339.
- [4] L. G. Staal and R. Gilbert, “Generators and Applicators: Equipment for Electroporation,” in *Clinical Aspects of Electroporation*, S. T. Kee, J. Gehl, and E. W. Lee, Eds. New York: Springer, 2011, pp. 45–65.
- [5] G. A. Hofmann, “Instrumentation and electrodes for *in vivo* electroporation,” in *Electrochemotherapy, Electrogenotherapy, and Transdermal Drug Delivery*, M. J. Jaroszeski, R. Heller, and R. Gilbert, Eds. Totowa: Humana Press, 2000, pp. 37–61.
- [6] E. Pirc, M. Reberšek, and D. Miklavčič, “Dosimetry in electroporation based technologies and treatments,” in *Dosimetry in bioelectromagnetics*, M. S. Markov, Ed. London: Taylor & Francis, In press.
- [7] M. Reberšek and D. Miklavčič, “Advantages and Disadvantages of Different Concepts of Electroporation Pulse Generation,” *Automatika*, vol. 52, no. 1, pp. 12–19, Mar. 2011.
- [8] M. Reberšek *et al.*, “Electroporator with automatic change of electric field direction improves gene electrotransfer *in-vitro*,” *Biomed. Eng. Online*, vol. 6, p. 25, 2007.
- [9] P. Kramar, D. Miklavcic, and A. M. Lebar, “A system for the determination of planar lipid bilayer breakdown voltage and its applications,” *NanoBioscience IEEE Trans. On*, vol. 8, no. 2, pp. 132–138, 2009.
- [10] J. M. Sanders, A. Kuthi, Yu-Hsuan Wu, P. T. Vernier, and M. A. Gundersen, “A linear, single-stage, nanosecond pulse generator for delivering intense electric fields to biological loads,” *IEEE Trans. Dielectr. Electr. Insul.*, vol. 16, no. 4, pp. 1048–1054, Aug. 2009.
- [11] S. Haberl, J. Teissié, W. Frey, and D. Miklavčič, “Cell Membrane Electroporation – Part 2: The Applications,” *IEEE Electr. Insul. Mag.*, vol. 29, no. 1, pp. 19–27, Feb. 2013.
- [12] C. Jiang, R. V. Davalos, and J. C. Bischof, “A Review of Basic to Clinical Studies of Irreversible Electroporation Therapy,” *IEEE Trans. Biomed. Eng.*, vol. 62, no. 1, pp. 4–20, Jan. 2015.
- [13] S. Mahnič-Kalamiza, E. Vorobiev, and D. Miklavčič, “Electroporation in Food Processing and Biorefinery,” *J. Membr. Biol.*, vol. 247, no. 12, pp. 1279–1304, Dec. 2014.
- [14] M. L. Yarmush, A. Golberg, G. Serša, T. Kotnik, and D. Miklavčič, “Electroporation-Based Technologies for Medicine: Principles, Applications, and Challenges,” *Annu. Rev. Biomed. Eng.*, vol. 16, no. 1, pp. 295–320, Jul. 2014.

- [15] T. Kotnik, W. Frey, M. Sack, S. Haberl Meglič, M. Peterka, and D. Miklavčič, "Electroporation-based applications in biotechnology," *Trends Biotechnol.*, vol. 33, no. 8, pp. 480–488, Aug. 2015.
- [16] A. Golberg *et al.*, "Energy-efficient biomass processing with pulsed electric fields for bioeconomy and sustainable development," *Biotechnol. Biofuels*, vol. 9, no. 1, Dec. 2016.
- [17] M. Morales-de la Peña, P. Elez-Martínez, and O. Martín-Belloso, "Food Preservation by Pulsed Electric Fields: An Engineering Perspective," *Food Eng. Rev.*, vol. 3, no. 2, pp. 94–107, Mar. 2011.
- [18] D. Miklavčič, B. Mali, B. Kos, R. Heller, and G. Serša, "Electrochemotherapy: from the drawing board into medical practice," *Biomed. Eng. Online*, vol. 13, no. 1, p. 29, 2014.
- [19] D. E. Spratt *et al.*, "Efficacy of Skin-Directed Therapy for Cutaneous Metastases From Advanced Cancer: A Meta-Analysis," *J. Clin. Oncol.*, vol. 32, no. 28, pp. 3144–3155, Oct. 2014.
- [20] B. Mali, T. Jarm, M. Snoj, G. Sersa, and D. Miklavcic, "Antitumor effectiveness of electrochemotherapy: A systematic review and meta-analysis," *Eur. J. Surg. Oncol. EJSO*, vol. 39, no. 1, pp. 4–16, Jan. 2013.
- [21] L. G. Campana *et al.*, "Recommendations for improving the quality of reporting clinical electrochemotherapy studies based on qualitative systematic review," *Radiol. Oncol.*, vol. 50, no. 1, pp. 1–13, Feb. 2016.
- [22] D. Miklavčič *et al.*, "Electrochemotherapy: technological advancements for efficient electroporation-based treatment of internal tumors," *Med. Biol. Eng. Comput.*, vol. 50, no. 12, pp. 1213–1225, Dec. 2012.
- [23] I. Edhemovic *et al.*, "Intraoperative electrochemotherapy of colorectal liver metastases: Electrochemotherapy of Liver Metastases," *J. Surg. Oncol.*, vol. 110, no. 3, pp. 320–327, Sep. 2014.
- [24] A. Gasbarrini, W. K. Campos, L. Campanacci, and S. Boriani, "Electrochemotherapy to Metastatic Spinal Melanoma: A Novel Treatment of Spinal Metastasis?," *Spine*, vol. 40, no. 24, pp. E1340–1346, Dec. 2015.
- [25] J. Lavee, G. Onik, P. Mikus, and B. Rubinsky, "A novel nonthermal energy source for surgical epicardial atrial ablation: irreversible electroporation," *Heart Surg. Forum*, vol. 10, no. 2, pp. E162–167, 2007.
- [26] P. G. Wagstaff *et al.*, "Irreversible electroporation: state of the art," *OncoTargets Ther.*, vol. 9, pp. 2437–2446, Apr. 2016.
- [27] C. Bertacchini, P. M. Margotti, E. Bergamini, A. Lodi, M. Ronchetti, and R. Cadossi, "Design of an irreversible electroporation system for clinical use," *Technol. Cancer Res. Treat.*, vol. 6, no. 4, pp. 313–320, Aug. 2007.
- [28] R. E. Neal, P. A. Garcia, J. L. Robertson, and R. V. Davalos, "Experimental Characterization and Numerical Modeling of Tissue Electrical Conductivity during Pulsed Electric Fields for Irreversible Electroporation Treatment Planning," *IEEE Trans. Biomed. Eng.*, vol. 59, no. 4, pp. 1076–1085, Apr. 2012.
- [29] L. Lambrecht, A. Lopes, S. Kos, G. Sersa, V. Prát, and G. Vandermeulen, "Clinical potential of electroporation for gene therapy and DNA vaccine delivery," *Expert Opin. Drug Deliv.*, vol. 13, no. 2, pp. 295–310, 2016.
- [30] A. Gothelf and J. Gehl, "What you always needed to know about electroporation based DNA vaccines," *Hum. Vaccines Immunother.*, vol. 8, no. 11, pp. 1694–1702, Nov. 2012.
- [31] S. Satkauskas *et al.*, "Mechanisms of in vivo DNA electrotransfer: respective contributions of cell electropermeabilization and DNA electrophoresis," *Mol. Ther. J. Am. Soc. Gene Ther.*, vol. 5, no. 2, pp. 133–140, Feb. 2002.
- [32] M. Kandušer, D. Miklavčič, and M. Pavlin, "Mechanisms involved in gene electrotransfer using high- and low-voltage pulses — An in vitro study," *Bioelectrochemistry*, vol. 74, no. 2, pp. 265–271, Feb. 2009.
- [33] R. Heller, Y. Cruz, L. C. Heller, R. A. Gilbert, and M. J. Jaroszeski, "Electrically mediated delivery of plasmid DNA to the skin, using a multielectrode array," *Hum. Gene Ther.*, vol. 21, no. 3, pp. 357–362, Mar. 2010.
- [34] M. Usaj, K. Flisar, D. Miklavcic, and M. Kanduser, "Electrofusion of B16-F1 and CHO cells: The comparison of the pulse first and contact first protocols," *Bioelectrochemistry*, vol. 89, pp. 34–41, Feb. 2013.
- [35] H. Mekid and L. M. Mir, "In vivo cell electrofusion," *Biochim. Biophys. Acta BBA - Gen. Subj.*, vol. 1524, no. 2–3, pp. 118–130, Dec. 2000.
- [36] R. Heller and R. J. Grasso, "Reproducible layering of tissue culture cells onto electrostatically charged membranes," *J. Tissue Cult. Methods*, vol. 13, no. 1, pp. 25–29.
- [37] L. Rems, M. Ušaj, M. Kandušer, M. Reberšek, D. Miklavčič, and G. Pucihar, "Cell electrofusion using nanosecond electric pulses," *Sci. Rep.*, vol. 3, Nov. 2013.
- [38] M. Zakhartsev, C. Momeu, and V. Ganeva, "High-Throughput Liberation of Water-Soluble Yeast Content by Irreversible Electropermeation (HT-irEP)," *J. Biomol. Screen.*, vol. 12, no. 2, pp. 267–275, Jan. 2007.
- [39] M. Sack *et al.*, "Electroporation-Assisted Dewatering as an Alternative Method for Drying Plants," *IEEE Trans. Plasma Sci.*, vol. 36, no. 5, pp. 2577–2585, Oct. 2008.
- [40] M. Sack *et al.*, "Research on Industrial-Scale Electroporation Devices Fostering the Extraction of Substances from Biological Tissue," *Food Eng. Rev.*, vol. 2, pp. 147–156, Mar. 2010.
- [41] E. Puértolas, G. Saldaña, S. Condón, I. Álvarez, and J. Raso, "Evolution of polyphenolic compounds in red wine from Cabernet Sauvignon grapes processed by pulsed electric fields during aging in bottle," *Food Chem.*, vol. 119, no. 3, pp. 1063–1070, Apr. 2010.
- [42] S. Haberl, M. Jarc, A. Štrancar, M. Peterka, D. Hodžič, and D. Miklavčič, "Comparison of Alkaline Lysis with Electroextraction and Optimization of Electric Pulses to Extract Plasmid DNA from *Escherichia coli*," *J. Membr. Biol.*, Jul. 2013.
- [43] A. L. Gonçalves, M. C. M. Alvim-Ferraz, F. G. Martins, M. Simões, and J. C. M. Pires, "Integration of Microalgae-Based Bioenergy Production into a Petrochemical Complex: Techno-Economic Assessment," *Energies*, vol. 9, no. 4, p. 224, Mar. 2016.
- [44] J. Raso *et al.*, "Recommendations guidelines on the key information to be reported in studies of application of PEF technology in food and biotechnological processes," *Innov. Food Sci. Emerg. Technol.*, Aug. 2016.
- [45] J. R. Beveridge, S. J. MacGregor, L. Marsili, J. G. Anderson, N. J. Rowan, and O. Farish, "Comparison of the effectiveness of biphasic and monophasic rectangular pulses for the inactivation of micro-organisms using pulsed electric fields," *IEEE Trans. Plasma Sci.*, vol. 30, no. 4, pp. 1525–1531, Aug. 2002.
- [46] S. Toepfl, "Pulsed electric field food processing industrial equipment design and commercial applications," *Stewart Postharvest Rev.*, vol. 8, no. 2, pp. 1–7, 2012.

- [47] T. Kotnik, P. Kramar, G. Pucihar, D. Miklavcic, and M. Tarek, "Cell membrane electroporation- Part 1: The phenomenon," *IEEE Electr. Insul. Mag.*, vol. 28, no. 5, pp. 14–23, Oct. 2012.
- [48] M. Kranjc *et al.*, "In Situ Monitoring of Electric Field Distribution in Mouse Tumor during Electroporation," *Radiology*, vol. 274, no. 1, pp. 115–123, Jan. 2015.
- [49] D. Miklavcic, K. Beravs, D. Semrov, M. Cemazar, F. Demsar, and G. Sersa, "The importance of electric field distribution for effective in vivo electroporation of tissues.," *Biophys. J.*, vol. 74, no. 5, pp. 2152–2158, May 1998.
- [50] N. Pavselj, Z. Bregar, D. Cukjati, D. Batiuskaite, L. M. Mir, and D. Miklavcic, "The Course of Tissue Permeabilization Studied on a Mathematical Model of a Subcutaneous Tumor in Small Animals," *IEEE Trans. Biomed. Eng.*, vol. 52, no. 8, pp. 1373–1381, Aug. 2005.
- [51] D. Sel, D. Cukjati, D. Batiuskaite, T. Slivnik, L. M. Mir, and D. Miklavcic, "Sequential Finite Element Model of Tissue Electroporability," *IEEE Trans. Biomed. Eng.*, vol. 52, no. 5, pp. 816–827, May 2005.
- [52] D. Miklavcic, S. Corovic, G. Pucihar, and N. Pavselj, "Importance of tumour coverage by sufficiently high local electric field for effective electrochemotherapy," *Eur. J. Cancer Suppl.*, vol. 4, no. 11, pp. 45–51, Nov. 2006.
- [53] D. Miklavcic *et al.*, "Towards treatment planning and treatment of deep-seated solid tumors by electrochemotherapy," *Biomed Eng Online*, vol. 9, no. 10, pp. 1–12, 2010.
- [54] S. Corovic, I. Lackovic, P. Sustaric, T. Sustar, T. Rodic, and D. Miklavcic, "Modeling of electric field distribution in tissues during electroporation," *Biomed. Eng. Online*, vol. 12, no. 1, p. 16, 2013.
- [55] J. Langus, M. Kranjc, B. Kos, T. Šuštar, and D. Miklavčič, "Dynamic finite-element model for efficient modelling of electric currents in electroporated tissue," *Sci. Rep.*, vol. 6, p. 26409, May 2016.
- [56] R. A. Gilbert, M. J. Jaroszeski, and R. Heller, "Novel electrode designs for electrochemotherapy," *Biochim. Biophys. Acta*, vol. 1334, no. 1, pp. 9–14, Feb. 1997.
- [57] S. Mazères *et al.*, "Non invasive contact electrodes for in vivo localized cutaneous electropulsation and associated drug and nucleic acid delivery," *J. Control. Release Off. J. Control. Release Soc.*, vol. 134, no. 2, pp. 125–131, Mar. 2009.
- [58] M. Reberšek, S. Čorović, G. Serša, and D. Miklavčič, "Electrode commutation sequence for honeycomb arrangement of electrodes in electrochemotherapy and corresponding electric field distribution," *Bioelectrochemistry*, vol. 74, no. 1, pp. 26–31, Nov. 2008.
- [59] J. Čemažar, D. Miklavčič, and T. Kotnik, "Microfluidic devices for manipulation, modification and characterization of biological cells in electric fields - a review," *Inf. MIDEM*, vol. 43, no. 3, pp. 143–161, Sep. 2013.
- [60] P. F. Forde *et al.*, "Preclinical evaluation of an endoscopic electroporation system," *Endoscopy*, vol. 48, no. 5, pp. 477–483, May 2016.
- [61] M. Pavlin *et al.*, "Effect of Cell Electroporation on the Conductivity of a Cell Suspension," *Biophys. J.*, vol. 88, no. 6, pp. 4378–4390, Jun. 2005.
- [62] M. Phillips, L. Rubinsky, A. Meir, N. Raju, and B. Rubinsky, "Combining Electrolysis and Electroporation for Tissue Ablation," *Technol. Cancer Res. Treat.*, vol. 14, no. 4, pp. 395–410, Aug. 2015.
- [63] I. Lackovic, R. Magjarevic, and D. Miklavcic, "Three-dimensional finite-element analysis of joule heating in electrochemotherapy and in vivo gene electrotransfer," *Dielectr. Electr. Insul. IEEE Trans. On*, vol. 16, no. 5, pp. 1338–1347, 2009.
- [64] K. Mitsutake, A. Satoh, S. Mine, K. Abe, S. Katsuki, and H. Akiyama, "Effect of pulsing sequence of nanosecond pulsed electric fields on viability of HeLa S3 cells," *Dielectr. Electr. Insul. IEEE Trans. On*, vol. 19, no. 1, pp. 337–342, 2012.
- [65] B. L. Ibey *et al.*, "Bipolar nanosecond electric pulses are less efficient at electroporability and killing cells than monopolar pulses," *Biochem. Biophys. Res. Commun.*, vol. 443, no. 2, pp. 568–573, Jan. 2014.
- [66] T. Kotnik, D. Miklavčič, and L. M. Mir, "Cell membrane electroporability by symmetrical bipolar rectangular pulses: Part II. Reduced electrolytic contamination," *Bioelectrochemistry*, vol. 54, no. 1, pp. 91–95, Aug. 2001.
- [67] B. Mali *et al.*, "Electrochemotherapy of colorectal liver metastases-an observational study of its effects on the electrocardiogram," *Biomed. Eng. Online*, vol. 14, no. Suppl 3, p. S5, 2015.
- [68] M. Puc, S. Čorović, K. Flisar, M. Petkovšek, J. Nastran, and D. Miklavčič, "Techniques of signal generation required for electroporability: Survey of electroporability devices," *Bioelectrochemistry*, vol. 64, no. 2, pp. 113–124, Sep. 2004.
- [69] M. Reberšek, M. Kanduđer, and D. Miklavčič, "Pipette tip with integrated electrodes for gene electrotransfer of cells in suspension: a feasibility study in CHO cells," *Radiol. Oncol.*, vol. 45, no. 3, pp. 204–208, 2011.
- [70] C. B. Arena *et al.*, "High-frequency irreversible electroporation (H-FIRE) for non-thermal ablation without muscle contraction," *Biomed. Eng. OnLine*, vol. 10, p. 102, Nov. 2011.
- [71] M. B. Sano *et al.*, "Bursts of Bipolar Microsecond Pulses Inhibit Tumor Growth," *Sci. Rep.*, vol. 5, p. 14999, Oct. 2015.
- [72] D. C. Sweeney, M. Reberšek, J. Dermol, L. Rems, D. Miklavčič, and R. V. Davalos, "Quantification of cell membrane permeability induced by monopolar and high-frequency bipolar bursts of electrical pulses," *Biochim. Biophys. Acta BBA - Biomembr.*, vol. 1858, no. 11, pp. 2689–2698, Nov. 2016.
- [73] M. Reberšek, C. Bertacchini, M. Sack, and D. Miklavčič, "Cell Membrane Electroporation – Part 3: The Equipment," *IEEE Electr. Insul. Mag.*, In press.

ACKNOWLEDGEMENT

This research was in part supported by Slovenian Research Agency, and by Framework Programs of European Commission through various grants. Research was conducted in the scope of the EBAM European Associated Laboratory (LEA).



Damijan Miklavčič was born in Ljubljana, Slovenia, in 1963. He received a Masters and a Doctoral degree in Electrical Engineering from University of Ljubljana in 1991 and 1993, respectively. He is currently Professor and the Head of the Laboratory of Biocybernetics at the Faculty of Electrical Engineering, University of Ljubljana.

His research areas are biomedical engineering and study of the interaction of electromagnetic fields with biological systems. In the last years he has focused on the engineering aspects of electroporation as the basis of drug delivery into cells in tumor models *in vitro* and *in vivo*. His research includes biological experimentation, numerical modeling and hardware development for electrochemotherapy, irreversible electroporation, transdermal drug delivery and gene electrotransfer.



Matej Reberšek, was born in Ljubljana, Slovenia, in 1979. He received the Ph.D. degree in electrical engineering from the University of Ljubljana, Slovenia.

He is an Assistant Professor and a Research Associate in the Laboratory of Biocybernetics, at the Faculty of Electrical Engineering, University of Ljubljana.

His main research interests are in the field of electroporation, especially design

of electroporation devices and investigation of biological responses to different electric pulse parameters.

NOTES

NOTES

Electroporation and electropermeabilisation - pieces of puzzle put together

Lluís M Mir^{1,2}

¹*Vectorology and Anticancer Therapies, UMR 8203, CNRS, Univ. Paris-Sud, Université Paris-Saclay, Gustave-Roussy, 114, Rue Edouard Vaillant, F-94805 Villejuif Cédex, France* ²*European Associated Laboratory (LEA) on the pulsed Electric fields in Biology And Medicine (LEA EBAM).*

Until now, two main generic approaches have been used to detect the cell permeabilization after the application of electric pulses to cells or tissues. They were based either on the detection of electrical changes of the tissue/cells (bioimpedance measurements, or simply conductance determinations) or on molecular exchanges across the membrane (diffusion or electrotransfer of markers, like fluorescent small molecules, radioactive compounds, plasmids coding for reporter genes, etc.).

The models built to describe the phenomena occurring at the cell membrane (even at artificial membranes, whether these artificial membranes were planar membranes or membranes of vesicles of different sizes and compositions) have been based on the physical principles that could explain the transport of molecules across the membrane. The input of the bioimpedance measurements, while very useful in practical terms, has brought a limited contribution to the understanding of these phenomena. However, in the transport phenomena there are parameters not related to the structural features of the membrane before, during and after the pulses. Indeed, there is an impact of the size of the molecules, their charge, the gradient of concentration between the inside and the outside, the sensitivity of their detection inside the cells, etc. There are a number of examples, whatever the duration of the pulses, nanosecond pulses or microseconds pulses, that can be reported.

Several new techniques have been recently applied recently to explore the changes in the membrane itself, independently of any transport phenomenon. Some of these techniques come from technologies that were not previously used to analyse the effects of the electric pulses on the lipid bilayers or the cell membranes.

On the one hand, the use of Giant Unilamellar Vesicles (composed of a defined lipid species and of the size of an animal cell) has allowed analysing chemical changes occurring in the lipid bilayers during the delivery of the pulses; molecular dynamics has started to bring the explanations for these reactions to occur. It is important to note that these two approaches (experimental and in silico) restrain their analysis to the lipid part of the complex cell membranes.

On the other hand, using cells in culture, non linear optical methods are producing new elements of the puzzle. Spontaneous Raman microspectroscopy is bringing information about the modifications of proteins that could occur during the delivery of the electric pulses. Because biological objects are immersed in water-based media, Confocal Raman microscopes must be used to eliminate the non-resonant contribution of the water.

Coherent Raman microspectroscopy, like the Coherent AntiStokes Raman Scattering microspectroscopy, seems more attractive because of the enhancement of the signal caused by the “coherence” provided by the use of two or three lasers accordingly tuned. Enhancement with respect to spontaneous Raman signal can reach 10^8 times. Coherent AntiStokes Raman Scattering microspectroscopy has recently provided us with information on changes in the interfacial water (the few layers of water molecules organized at the surface of the membranes) and even of the interstitial water. After the pulses delivery, an important loss of the interfacial water signal has been recorded, which means that the alterations of the membrane structure consecutive to the pulses application also affects the water surrounding the membrane. We are thus acquiring information on the changes occurring in the membranes independently of any transport phenomenon. This information has now to be introduced into the models that tentatively describe the phenomena occurring at the membranes.

However, there is another level of perturbations that has also to be taken into account, for which information is rapidly accumulating: the cell reactions to the stress caused by the electric pulses delivery. It corresponds to the ensemble of the biological aspects linked to the electric pulses delivery, with kinetics that can be orders of magnitude longer than the duration of the electric pulses and even of the duration of the recovery of the cells impermeability to classical electropermeabilization markers..

The construction of any new model is therefore becoming incredibly complex. This just reflects the complexity of the phenomena that have been presented in the Electroporation-Based Technologies and Treatments school. The viscous, elastic and viscoelastic models of membranes electrical breakdown are far behind us. The models describing the generation of stable pores are also insufficient nowadays. Models including several terms to explain the evolution of the permeability and the conductivity of the cell membranes are arising. It is a hope that they will be able to give clues about the many questions that are still unsolved. For example, considering the “irreversible electroporation”, it is still unknown what the “irreversible” event is ...

All the aspects developed here above will be discussed in the frame of a new model of the phenomena occurring in the membranes of the cells exposed to the electric pulses. This model will be presented, and terminology will be delivered for a correct use of terms that have been used indistinctly until now. Therefore a distinction

between “electroporation” and “electropermeabilization” will be brought in the context of the cells “electropulsation”, as parts of a puzzle that collectively we want to put together.



Lluís M. Mir was born in Barcelona, Spain, in 1954. He received a Masters in Biochemistry in 1976 from Ecole Normale Supérieure, Paris, and a Doctorate (D.Sc.) in Cell Biology in 1983. In 1978 he entered CNRS as Attaché de Recherches in the Laboratory of Basic Pharmacology and Toxicology, Toulouse. In 1983 he was promoted to Chargé de Recherches at CNRS, and in 1985 he moved to the Laboratory of

Molecular Oncology CNRS-Institut Gustave-Roussy and Univ. Paris Sud, Villejuif). In 1989 he moved to the Laboratory of Molecular Pharmacology (Villejuif), and in 2002 to the Laboratory of Vectorology and Gene Transfer (Villejuif). In 1999, he was promoted to Directeur de Recherches at CNRS.

Lluís M. Mir was one of the pioneers of the research of electropermeabilization (electroporation) and the applications of

this technique for antitumor electrochemotherapy and DNA electrotransfer. He is the author of 193 articles in peer-reviewed journals, 21 chapters in books, and over 500 presentations at national and international meetings, invited lectures at international meetings and seminars. He received the Award for the medical applications of electricity of the Institut Electricité Santé in 1994, the Annual Award of Cancerology of the Ligue contre le Cancer (committee Val-de-Marne) in 1996, and Award of the Research of Rhône-Poulenc-Rorer in 1998 and the medal of the CNRS under the auspices of the Sciences Academy in 2012. He is an Honorary Senator of the University of Ljubljana (2004). He is also fellow of the American Institute of Biological and Medical Engineering. He has been visiting professor of the Universities of Berkeley (USA), Bielefeld (Germany) and Jerusalem (Israel). He is the director of the laboratory of Vectorology (UMR 8203 of CNRS, University Paris-Sud and Institut Gustave-Roussy), and he is also the founder and co-director of the European Associated Laboratory on Electroporation in Biology and Medicine of the CNRS, the Universities of Ljubljana, Primorska, Toulouse and Limoges, the Institute of Oncology Ljubljana and the Institut Gustave-Roussy

NOTES

INVITED LECTURERS

Detecting changes of membrane properties with electrical and optical diagnostics

Aude Silve

Karlsruhe Institute of Technology, Eggenstein-Leopoldshafen, Germany

Abstract: Electric pulses can modify properties of cells membrane and especially make it permeable to molecules that normally are non-permeant. One way to study this effect is therefore to study transport of molecules using for example fluorescence techniques or viability essays. Such an approach is not only extremely important for basic studies but it is also extremely relevant when one intends to develop an application which requires either penetration of a foreign molecules inside cells (like drugs or DNA), or extraction of molecules for industrial purposes. The outcome of such experiments however not only depends on damages induced to the membrane but also on properties of the transported molecules which are investigated i.e size, conformation, polarity etc. and it also depends on the transport mechanisms which are involved i.e. diffusion, electrophoresis, ... Some other approaches which are independent of molecular transport, are however available and can provide more straight forward information on the state of a membrane. Electrical diagnostics, in particular such as bioimpedance or patch-clamp, can provide direct information on the modification of the conductance of the cells membrane. Additionally, some optical diagnostics such as measurement of transmembrane voltage using voltage sensitive dyes can also be used to study modification of membrane conductance induced by pulsed electric fields. Each technique provides different information. The benefits and drawbacks of each of them will be discussed.

ABOUT EXPERIMENTAL APPROACHES TO STUDY EFFECTS OF ELECTRIC PULSES ON BIOLOGICAL CELLS

In the last decades, many applications of electroporation have been developed and proven to be successful both in the medical domain and in the food industry. In parallel, tremendous efforts have been made to provide quantitative data that could help to understand the electroporation phenomenon especially at the membrane level. For example, several studies have looked at the size of the molecules that can be transported through a permeabilized membrane [1], [2] or on the mechanisms of large molecule uptake [3]. Most of these studies, however, are focused on the consequences of electropermeabilisation i.e. transport of molecules. Other studies, using electrical measurements provide quantitative data on the changes of conductance of the membrane. The two most popular approaches in the literature are bio-impedance and micro-electrodes techniques. Bio-impedance measurements are usually performed on tissues [4]–[6] or on suspension of cells [7], while micro-electrodes are used on lipid bilayers [8]–[12] or on cells (patch-clamp technique) [13]–[16]. Bioimpedance approaches exhibit the advantage of being performed in an open-field configuration and are therefore representative for the situation encountered in all applications. This is not the case for micro-electrodes approaches which, nevertheless, have the great advantage of simultaneously providing values of the conductance of the membrane as well as values of transmembrane voltage (TMV). Micro-electrodes approaches are thus extremely valuable to understand

the basic mechanisms which relate TMV to membrane's conductance increase. However, since the electrodes always impose the TMV on a membrane (or the current flowing across it), it is not possible to evaluate the behaviour of a membrane in an open-field configuration. Moreover, both bio-impedance and micro-electrodes approaches cannot render the spatial distribution of the TMV or of the conductance change and only average changes can be evaluated. One possible solution to combine the benefit of the two types of approaches is to study cells in an open field configuration and to follow their transmembrane voltage by using non-invasive methods like the use of a fluorescence voltage sensitive dye (VSD). In such an approach, single cells are stained with a VSD and variations of the TMV translate into a change of fluorescence [17], [18]. Analysis of fluorescence signal can in return provide information on the conductance of the cell membrane.

Each of the methods mentioned above has benefits and drawbacks. This course will try to address those aspects and show how the different techniques might be used to increase the knowledge about electroporation.

BIOIMPEDANCE

Bioimpedance is a discipline which consists in measuring passive electrical properties of biological samples. Those passive properties can be understood by considering the simplest description of a biological cell i.e. it consists of a membrane which delimits an intracellular and an extracellular space. Internal and external media are ionic solutions and the presence of

the ions makes those media electrically conductive. Typical conductivity values are around 1 S/m. On the contrary, the membrane of cells, behaves almost as a pure dielectric and has a very low conductance of typically 1 S.m⁻². By extrapolating this basic description to a biological tissue, which is an assembly of individual cells, it is possible to construct a simple electrical model that represents the electrical behaviour of tissue [19]. This electrical model consists in a resistor (R_{ext} [Ohm, Ω]) in parallel with a series association of a capacitor (C_m [farad, F]) and a resistor (R_{int} [ohm, Ω]) (see Figure 1). The resistors R_{ext} and R_{int} describe the conductive properties of the extracellular and intracellular media, respectively, and the capacitor represents the dielectric properties of the membranes of cells. To be closer to reality, it should be noted that the properties of the membranes should not be represented by a pure capacitor but should include a cole-cole element α [20], [21].

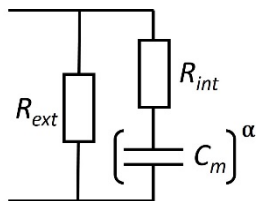


Figure 1: Most simple electrical model of a biological tissue. The resistors R_{ext} and R_{int} describe the electrical properties of the extracellular and intracellular media. The capacitor C_m and the cole-cole element α represent the properties of the membranes of cells.

A typical measurement result of the bioimpedance of a biological tissue (in this case a potato sample) is depicted on Figure 2. The magnitude of the impedance is plotted versus the frequency. The black line represents an intact sample, while the dotted line represents the same sample after performing electroporation. The main effect of electroporation on the impedance waveform is a drop of the magnitude which appears to be more pronounced at low frequencies. Such changes can be interpreted from an electrical point of view as partial short circuiting of the capacitor representing the membrane. This is in agreement with the idea that electroporation generates conductive structures in cell membranes [19].

Bioimpedance can therefore be used as a tool to measure the intensity of damages induced by pulsed electric fields on biological sample. Studying the impact of pulse magnitude, pulse duration, number of pulses or repetition rate [6] is one common application of this technique. Additionally this approach has very concrete applications. For example it can be used to evaluate the efficiency of a pulse protocol to induce electroporation of a tumour and therefore predict the treatment outcome [5]. It can also be used in the food

industry to control the efficiency of electroporation of the treated matter [15].

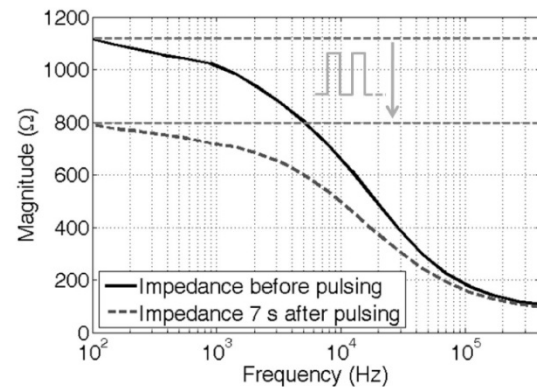


Figure 2: Typical magnitude of the bioimpedance of a potato sample before and after applying pulses which induce electroporation (In this case 4 pulses of 100 μ s, 300 V/cm were applied at 1 Hz)

Bioimpedance measurements can therefore be beneficial both for basic and for applied research by providing very precise quantitative parameters of passive electrical properties of a tissue. However, one of its limits is that it cannot provide local electric properties such as membrane conductance. For example, the value of C_m as described in Figure 1, is an image of membrane conductance but it does to calculate the value of this conductance. In order to access such parameters, other methods are therefore required, such as patch-clamp.

PATCH CLAMP APPROACH

The patch-clamp technique is one of the most powerful tool for studying electrophysiology on single cells. A typical protocol consists in creating a direct electrical access to the inside of a cell using a fine-tipped glass capillary filled with an electrolyte solution. An electrode inside the glass capillary provides the electric potential inside the cell. A counter electrode is placed inside the buffer surrounding the cell and enables to impose a known TMV across the cell's membrane. This configuration, known as whole-cell configuration, is illustrated on Figure 3.

This technique was initially developed to study physiological TMV and currents passing through the membrane. However, such a technique can also be used to study membranes' response to suprphysiological voltages [13]–[15]. Indeed, suprphysiological TMV can directly be imposed on the membrane thanks to the two electrodes. In that sense, it is very close to techniques applied on artificial planar lipid bilayers [8]–[12].

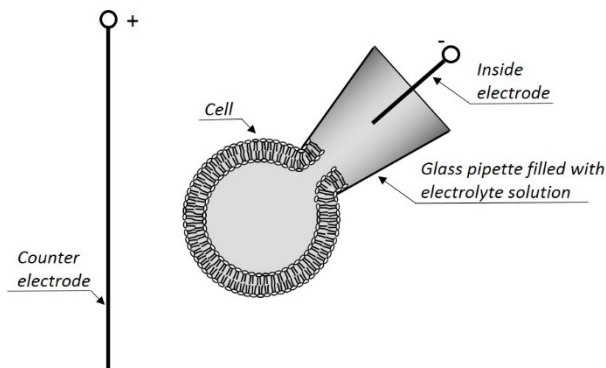


Figure 3: Illustration of the whole cell configuration of patch-clamp. Illustration adapted from [22], with authorization of Lars Wegner.

The main benefit of the patch-clamp approach is that the TMV is directly imposed through two electrodes and therefore is known and controlled. Additionally, the TMV is homogeneous over the whole surface of the membrane.

While imposing a voltage, it is possible to monitor the ionic current flowing through the membrane and therefore to measure the conductance of the membrane. Figure 4 shows typical results of a whole cell experiment performed on a DC3F cell. Voltage pulses of 10 ms were applied directly on the membrane. The currents across the membrane of one cell were measured, for applied TMV ranging from -300 mV to +350 mV. For voltages ranging between -235 mV and +190 mV, it appears that the current increases linearly with the TMV. Outside of this voltage range, the current increases dramatically, indicating an increase of the membrane's conductance. The average thresholds obtained from experiments on 18 individuals cells, are $+201 \pm 7$ mV for depolarisation and -231 ± 8 mV for hyperpolarisation [16].

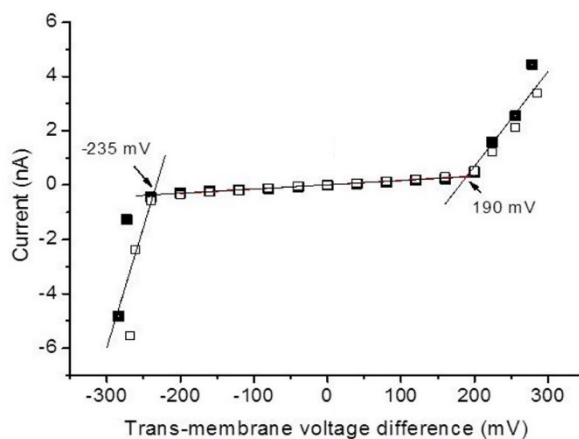


Figure 4: Current-voltage relations of a DC3F cell exposed to a train of 10-ms pulses in the whole cell configuration of the patch clamp technique. Currents were plotted against the trans-membrane voltage difference obtained by taking the voltage drop at the access resistance into account.

Additional experiments have shown that the state of high conductivity of the membrane induced by suprphysiological TMV has a life time of approximately 100 ms which can therefore be described as a “transient permeabilisation”. When the TMV is turned back to physiological values, conductivity of the membrane returns to value close, but not equal, to the initial one, before the conductivity increase. Indeed one observes a low but persistent permeabilisation which prevails after a permeabilising pulse for at least 40 min. Observations therefore support the idea that permeabilisation is a two-step phenomenon.

Patch-clamp therefore enables to provide quantitative measurements of membrane's properties. The results given above are just some example of what can be obtained with patch-clamp. However some limitations remain. The two main ones are the following:

- Since the TMV is equally distributed on the whole membrane, results cannot reflect the spatial distribution of the conductance increase which appears when a cell is exposed to electric pulses in an open field configuration
- Additionally, patch-clamp dynamics is relatively slow and it does not allow to apply TMV pulses which are shorter than a few milliseconds.

APPROACH USING VOLTAGE SENSITIVE DYES

One possibility to overcome those limitations consists in using voltage sensitive dyes (VSD). These molecules, insert into cell's membrane and emit a fluorescence signal which is related to the local transmembrane voltage. By comparing the fluorescence of stained cells before and during an electric pulse, it is possible to study the induced transmembrane voltage (see Figure 5). Such a strategy was already used in the past and proven to be very successful to study the spatial distribution of TMV or the charging time of the TMV [23]–[25].

The main difficulty of experiments using VSD lies in the interpretation of the data and in the calibration of the fluorescence signal. Indeed, it is very difficult to give an absolute value of the TMV. Nevertheless, even without absolute calibration it is possible to obtain quantitative results regarding the properties of the membrane.

By studying the kinetic of the TMV during pulses of 100 μ s of different field magnitudes it can be observed that during the application of an external electric pulse with a magnitude ranging from 60 $\text{kV}\cdot\text{m}^{-1}$ to 200 $\text{kV}\cdot\text{m}^{-1}$ the induced TMV remains constant for several microseconds and then starts to decrease. The duration of the stable phase depends on the magnitude

of the electric field: the higher the electric field, the shorter the stable phase. Similar observations have already been mentioned by Hibino and colleagues [6-7] using similar experimental approaches but other types of VSD.

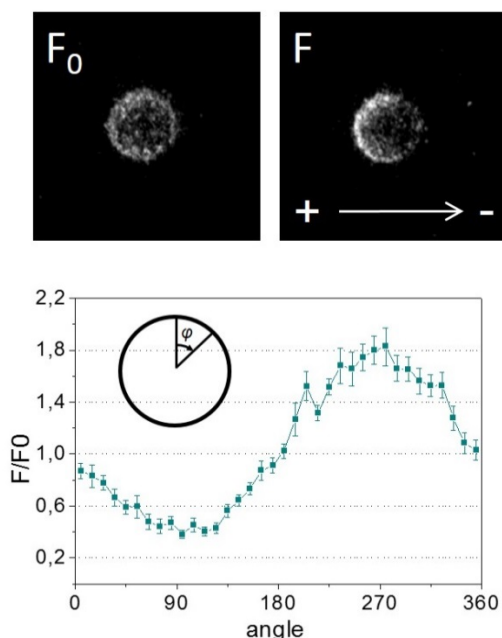


Figure 5: Fluorescence images of DC3F cells stained with the voltage sensitive dye ANNINE-6. The image on the left provides the fluorescence F_0 in the absence of external electric field. The image on the right gives the fluorescence F , 1 μ s after the onset of an electric field of 100 kV/m. It is visible on the picture that the fluorescence is not homogeneous over the whole membrane. The graph displays the fluorescence ratio F/F_0 as a function of the position on the membrane φ (average signal of 10 cells). The variation in fluorescence intensity can thereafter be interpreted in terms of TMV induced by the external electric field.

Therefore, VSD dyes can provide information that is not accessible with other techniques. However, it should be kept in mind that it remains an indirect measurement of the TMV in comparison with data provided by patch clamp. One of its main advantage is the time resolution which in principal can go down to a few nanoseconds provided that appropriate dyes are used [18], [26]. Some intrinsic limitation of this approach like limited sensitivity or uncertainty of fluorescence calibration, however, should be kept in mind before starting an experimental campaign.

CONCLUSION

The three methods mentioned above are all precious tools to study modifications of cells membrane during electroporation. None of them is sufficient on its own and all three of them together will also not be sufficient to fully understand electroporation. Providing thorough models of electroporation will therefore require the

ability to synthesize all information provided by all different techniques always keeping in mind the range in which a given method remains valid.

REFERENCES

- [1] A. Silve, I. Leray, and L. M. Mir, "Demonstration of cell membrane permeabilization to medium-sized molecules caused by a single 10ns electric pulse," *Bioelectrochemistry Amst. Neth.*, Oct. 2011.
- [2] O. M. Nesin, O. N. Pakhomova, S. Xiao, and A. G. Pakhomov, "Manipulation of cell volume and membrane pore comparison following single cell permeabilization with 60- and 600-ns electric pulses," *Biochim. Biophys. Acta*, vol. 1808, no. 3, pp. 792–801, Mar. 2011.
- [3] M. Breton, L. Delemotte, A. Silve, L. M. Mir, and M. Tarek, "Transport of siRNA through Lipid Membranes driven by Nanosecond Electric Pulses: an Experimental and Computational Study," *J. Am. Chem. Soc.*, Aug. 2012.
- [4] A. Ivorra and B. Rubinsky, "In vivo electrical impedance measurements during and after electroporation of rat liver," *Bioelectrochemistry Amst. Neth.*, vol. 70, no. 2, pp. 287–295, May 2007.
- [5] A. Ivorra, B. Al-Sakere, B. Rubinsky, and L. M. Mir, "In vivo electrical conductivity measurements during and after tumor electroporation: conductivity changes reflect the treatment outcome," *Phys. Med. Biol.*, vol. 54, no. 19, pp. 5949–5963, Oct. 2009.
- [6] A. Silve, A. Guimerà Brunet, B. Al-Sakere, A. Ivorra, and L. M. Mir, "Comparison of the effects of the repetition rate between microsecond and nanosecond pulses: Electroporation-induced electro-desensitization?," *Biochim. Biophys. Acta BBA - Gen. Subj.*, vol. 1840, no. 7, pp. 2139–2151, Jul. 2014.
- [7] U. Pliquett, R. P. Joshi, V. Sridhara, and K. H. Schoenbach, "High electrical field effects on cell membranes," *Bioelectrochemistry*, vol. 70, no. 2, pp. 275–282, Mai 2007.
- [8] M. Robello and A. Gliozzi, "Conductance transition induced by an electric field in lipid bilayers," *Biochim. Biophys. Acta BBA - Biomembr.*, vol. 982, no. 1, pp. 173–176, Jun. 1989.
- [9] M. Naumowicz and Z. A. Figaszewski, "Pore formation in lipid bilayer membranes made of phosphatidylcholine and cholesterol followed by means of constant current," *Cell Biochem. Biophys.*, vol. 66, no. 1, pp. 109–119, May 2013.
- [10] I. G. Abidor, V. B. Arakelyan, L. V. Chernomordik, Y. A. Chizmadzhev, V. F. Pastushenko, and M. P. Tarasevich, "Electric breakdown of bilayer lipid membranes: I. The main experimental facts and their qualitative discussion," *J. Electroanal. Chem. Interfacial Electrochem.*, vol. 104, pp. 37–52, 1979.
- [11] R. Benz and K. Janko, "Voltage-induced capacitance relaxation of lipid bilayer membranes Effects of membrane composition," *Biochim. Biophys. Acta BBA - Biomembr.*, vol. 455, no. 3, pp. 721–738, Dezember 1976.
- [12] P. Kramar, D. Miklavcic, and A. M. Lebar, "Determination of the lipid bilayer breakdown voltage by means of linear rising signal," *Bioelectrochemistry Amst. Neth.*, vol. 70, no. 1, pp. 23–27, Jan. 2007.
- [13] L. H. Wegner, B. Flickinger, C. Eing, T. Berghöfer, P. Hohenberger, W. Frey, and P. Nick, "A patch clamp study on the electro-permeabilization of higher plant cells: Supraphysiological voltages induce a high-conductance, K+

- selective state of the plasma membrane," *Biochim. Biophys. Acta BBA - Biomembr.*, vol. 1808, no. 6, pp. 1728–1736, Jun. 2011.
- [14] L. H. Wegner and S. Schönwälder, "Electroporation of plant cells studied with the patch clamp technique," presented at the EAPPC/BEAMS, Karlsruhe, Germany, 2012.
- [15] L. H. Wegner, "Cation selectivity of the plasma membrane of tobacco protoplasts in the electroporated state," *Biochim. Biophys. Acta*, vol. 1828, no. 8, pp. 1973–1981, Aug. 2013.
- [16] L. H. Wegner, W. Frey, and A. Silve, "Electroporation of DC-3F is a Dual Process," *Biophys. J.*, vol. 108, no. In press, Mar. 2015.
- [17] B. Kuhn and P. Fromherz, "Anellated Hemicyanine Dyes in a Neuron Membrane: Molecular Stark Effect and Optical Voltage Recording," *J. Phys. Chem. B*, vol. 107, no. 31, pp. 7903–7913, Aug. 2003.
- [18] W. Frey, J. A. White, R. O. Price, P. F. Blackmore, R. P. Joshi, R. Nuccitelli, S. J. Beebe, K. H. Schoenbach, and J. F. Kolb, "Plasma membrane voltage changes during nanosecond pulsed electric field exposure," *Biophys. J.*, vol. 90, no. 10, pp. 3608–3615, May 2006.
- [19] A. Ivorra, "Tissue Electroporation as a Bioelectric Phenomenon: Basic Concepts," in *Irreversible Electroporation*, B. Rubinsky, Ed. Berlin, Heidelberg: Springer Berlin Heidelberg, 2010, pp. 23–61.
- [20] K. S. Cole, "Electric phase angle of cell membranes," *J. Gen. Physiol.*, vol. 15, no. 6, pp. 641–649, Jul. 1932.
- [21] S. Grimnes and Ø. G. Martinsen, *Bioimpedance and bioelectricity basics*. Academic Press, 2008.
- [22] L. H. Wegner, "La Technique de Patch-Clamp dans la recherche sur l'Electroporation.," *3EI*, vol. 75, 2014.
- [23] M. Hibino, H. Itoh, and K. Kinoshita Jr, "Time courses of cell electroporation as revealed by submicrosecond imaging of transmembrane potential," *Biophys. J.*, vol. 64, no. 6, pp. 1789–1800, Jun. 1993.
- [24] M. Hibino, M. Shigemori, H. Itoh, K. Nagayama, and K. Kinoshita Jr, "Membrane conductance of an electroporated cell analyzed by submicrosecond imaging of transmembrane potential," *Biophys. J.*, vol. 59, no. 1, pp. 209–220, Jan. 1991.
- [25] D. Gross, L. M. Loew, and W. W. Webb, "Optical imaging of cell membrane potential changes induced by applied electric fields," *Biophys. J.*, vol. 50, no. 2, pp. 339–348, Aug. 1986.
- [26] W. Frey, K. Baumung, J. F. Kolb, N. Chen, J. White, M. A. Morrison, S. J. Beebe, and K. H. Schoenbach, "Real-time imaging of the membrane charging of mammalian cells exposed to nanosecond pulsed electric fields," in *Power Modulator Symposium, 2004 and 2004 High-Voltage Workshop. Conference Record of the Twenty-Sixth International*, 2004, pp. 216–219.



Aude Silve was born in France, some years ago. She received her M.S. degree in "physics and biology interactions", from the University of Paris 11, France. She then obtained her Ph.D. degree in the UMR 8203 CNRS-Institute Gustave-Roussy, Villejuif, France under the supervision of Lluís M. Mir. Since 2012 she works at the Institute for Pulsed Power and Microwave

Technology at Karlsruhe Institute of Technology, Germany. Her current research interests include effects of nanosecond duration pulses on living cells, study of transmembrane voltage and voltage sensitive dyes. Since one year she has been working on the application of pulses for down processing of microalgae, especially for purposes of lipid extraction.

NOTES

NOTES

Giant vesicles in electric fields: What can we learn about membrane properties and electroporation

Rumiana Dimova

Max Planck Institute of Colloids and Interfaces, Science Park Golm, 14424 Potsdam, Germany

Abstract: Giant vesicles provide exceptional biomembrane models for systematic studies on the effect of electric fields on lipid bilayers. They have typical sizes of tens of micrometers and thus, their main advantage is that the membrane response to AC and DC fields can be directly visualized under the optical microscope. This lecture will give an overview of research activities spanning a decade of investigations. Particular emphasis will be placed on experimental approaches for deducing the membrane properties based on exposing giant vesicles to AC fields and DC pulses. We will consider the dependence of the vesicle morphology on both field frequency and media conductivity when exposed to AC fields. When the conductivity of the external solution is higher than the internal conductivity, the vesicles undergo prolate-oblate transition at field frequencies of several kHz. Theoretical descriptions of this transition provide an analytical expression for the transition frequency. We used this prediction to develop a method for measuring the membrane capacitance. At a fixed field frequency in the low frequency regime and increasing field strength, the degree of vesicle deformation increases and can be used to deduce the bending rigidity of the membrane. Inhomogeneous AC fields trigger flows on the membrane surface visualized by domain movement. We have also studied the vesicle response to DC pulses of duration in the range 50 μ s – 5 ms. When exposed to strong pulses, giant vesicles porate. Using the dynamics of the pore closure we established an approach to measure the edge tension and evaluate the membrane stability. We also explored the application of giant vesicle electrofusion for synthesis of nanoparticles and for establishing a protocol for creating multicomponent giant vesicles with precisely known composition.

INTRODUCTION

Giant lipid vesicles [1, 2] provide biomembrane models suitable for systematic studies on the behavior of lipid bilayers exposed to external factors. The membrane response to AC fields or DC pulses can be directly visualized under the microscope [3-8]. AC fields induce stationary deformation of the vesicles, while the response to short DC pulses is very dynamic and difficult to resolve with standard video recording. Using fast digital imaging, we were able to capture the immediate response of giant lipid vesicles to electric fields [4, 9-13]. The vesicle response and relaxation dynamics was recorded with a high temporal resolution using phase contrast microscopy.

This report summarizes our observations on electro-deformation, -poration and -fusion of giant vesicles. We first introduce some basic relations describing the interaction between electric fields and membranes. Then, we consider the shape transitions observed when vesicles are subjected to AC fields with different frequencies and/or media conductivities. The response of vesicles to DC pulses is considered in terms of vesicle deformation and poration.

SOME EQUATIONS

Lipid membranes are essentially impermeable to ions. Thus, in the presence of an electric field, charges accumulate on both sides of the bilayer. For a spherical vesicle of radius R and tilt angle θ between the electric

field and the surface normal, the charge accumulation gives rise to the transmembrane potential [14]

$$\Delta\Psi_m = 1.5R |\cos \theta| E [1 - \exp(-t/\tau_{\text{charg}})] \quad (1)$$

as a function of time t . Here E is the amplitude of the applied electric field and τ_{charg} is the membrane charging time given by [14]:

$$\tau_{\text{charg}} = R C_m [1/\lambda_{\text{in}} + 1/(2\lambda_{\text{ex}})] \quad (2)$$

where C_m is the membrane capacitance, of the order of 1 μ F/cm² for fluid lipid membranes [15], and λ_{in} and λ_{ex} are the conductivities of the internal and external vesicle solutions, respectively. Above some electroporation threshold, the transmembrane potential $\Delta\Psi_m$ cannot be further increased, the membrane porates, thus becoming conductive and permeable.

The electroporation phenomenon can also be understood in terms of a stress in the bilayer created by the electric field. The transmembrane potential, $\Delta\Psi_m$, induces an effective electrical tension σ_{el} , as defined by the Maxwell stress tensor [9, 15, 16]. This tension is given by

$$\sigma_{\text{el}} = \epsilon\epsilon_0 [h/(2h_e^2)] \Delta\Psi_m^2 \quad (3)$$

where ϵ is the dielectric constant of the aqueous solution, ϵ_0 the vacuum permittivity, h is the total bilayer thickness, (~ 4 nm), and h_e the dielectric thickness (~ 2.8 nm for lecithin bilayers [17]). For vesicles with some initial tension σ_0 , the total tension reached during the pulse is

$$\sigma = \sigma_0 + \sigma_{\text{el}} \quad (4)$$

The total membrane tension cannot exceed the tension of rupture. For lipid membranes, the tension of rupture is in the range 5 – 10 mN/m and is also known as lysis tension, σ_{lys} ; see e.g. references [13, 15, 18]. The lysis tension can be reached either by applying an overall mechanical tension to the vesicle, for example using micropipettes or osmotic pressure, and/or by locally building up an electric stress. In the latter case, electroporation occurs when the membrane tension reaches the lysis tension. This corresponds to building up a certain critical transmembrane potential, $\Delta\Psi_m = \Delta\Psi_c$, which for cell membranes is $\Delta\Psi_c \approx 1$ V. Similarly, for tension-free giant vesicles, the critical potential $\Delta\Psi_c \approx 1$ V [13]. The value of the critical poration potential decreases when the initial membrane tension increases. It also depends strongly on the membrane composition [13].

In the next sections we first consider the response of the vesicle membrane when subjected to “mild” AC fields before considering the cases of membrane deformation and poration induced by DC pulses.

VESICLE DEFORMATION IN AC FIELDS

The shape deformation of vesicles in AC fields has been studied for decades, but the dependence of the morphology of giant vesicle on both field frequency and media conductivity has been fully characterized only recently [4, 19–21]. At low field frequencies (few kHz), vesicles in water deform into prolates with the longer axis oriented along the field direction [22]. At intermediate frequencies (several kHz), again for vesicles in water medium, prolate-oblate transitions are observed [4, 19, 23, 24] as theoretically predicted [25–28]. This behavior is observed also when the conductivity of the external vesicle solution, λ_{ex} is higher than the internal conductivity λ_{in} . Interestingly, when the conductivity of the internal solution is raised so that it exceeds the external conductivity, i.e. at $\lambda_{\text{in}} > \lambda_{\text{ex}}$, the prolate-oblate transition is suppressed. With increasing field frequency, the vesicles undergo only the prolate-to-sphere transition. Two examples for the shape evolution of vesicles at different conductivity conditions are provided in Fig. 1.

The prolate-to-sphere transition frequency, ν_c , depends on the membrane charging time [20, 27, 28] and has the following form

$$\nu_c = \frac{\lambda_{\text{in}}}{2\pi RC_m} \left[\left(1 - \frac{\lambda_{\text{in}}}{\lambda_{\text{ex}}} \right) \left(\frac{\lambda_{\text{in}}}{\lambda_{\text{ex}}} + 3 \right) \right]^{-1/2} \quad (5)$$

Thus, knowing the conductivities of the solutions inside and outside the vesicles, and after measuring the vesicle size, one can infer the membrane capacitance from the dependence of the prolate–oblate transition frequency ν_c on the inverse vesicle diameter [29].

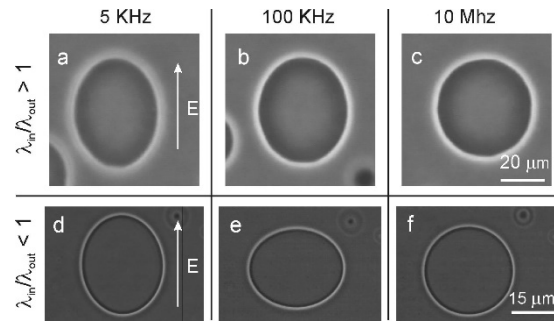


Figure 1: Two giant vesicles (phase contrast microscopy) in different conductivity conditions subjected to AC field of 20 kV/m and various field frequencies as indicated above the images. The field direction is indicated with an arrow in (a, d). The conductivity conditions are $\lambda_{\text{in}} > \lambda_{\text{ex}}$ for (a–c) where only prolate-to-sphere transformation is observed, and $\lambda_{\text{in}} < \lambda_{\text{ex}}$ for (d–f) where prolate-to-oblate and oblate-to-sphere transitions are detected. Reproduced from [3].

At a fixed frequency (in the range 25 kHz and 300 kHz), the degree of deformation of the vesicle as a function of the field strength can be used to deduce the bending rigidity of the membrane [30] (note that at relatively low field frequencies around 1 - 2 kHz and strong fields, one may observe the formation of large pores of several micrometres [31], or protrusions of long membrane tubules [32]). The bending rigidity is a material property of the lipid bilayer characterizing how soft the membrane is. It is typically of the order of $10 k_B T$, $k_B T$ being the thermal energy. Apart from the lipid composition, a number of factors can influence the bending rigidity [33]. For example, introducing a small fraction of the ganglioside GM1 in the membrane was shown to decrease the membrane bending rigidity as measured from electrodeformation analysis [34].

AC electric fields induce lateral forces at the vesicle interface, which may even lead to fluid flows when the field is inhomogeneous. Such surface lipid flows have been observed on multicomponent giant vesicles with domains when exposed to asymmetric AC field [35].

VESICLE RESPONSE TO DC PULSES

While the discussion on vesicles exposed to AC fields is limited to stationary shapes, DC pulses induce short-lived shape deformations. Because the application of both AC fields and DC pulses creates a transmembrane potential, vesicle deformations of similar nature are to be expected in both cases. When charged vesicles are close to the electrode, the application of weak DC fields provides us with a mean to study reversible vesicle adhesion [36, 37].

In the following subsections, we will consider the response of vesicles with membrane in the fluid state. The mechanical and rheological properties of membranes in the gel phase differ significantly from those of fluid membranes. These differences introduce new features in the response of gel-phase membranes

to electric fields, for example, the vesicle surface may wrinkle. We refer the reader to reference [38], where the deformation and poration of giant vesicles in the gel phase has been discussed.

Electrodeformation of vesicles in water

In the absence of salt, spherical vesicles subjected to electric pulses adopt ellipsoidal shapes, which relax back to the initial vesicle shapes after the end of the pulse. The degree of deformation of an ellipsoidal vesicle can be characterized by the aspect ratio of the two principal radii, a and b . For $a/b = 1$, the vesicle is a sphere, for $a/b > 1$ the vesicle is a prolate (like in Fig. 1a) with the long axis a oriented in the direction of the field. The relaxation dynamics of this aspect ratio depends on whether the vesicle has been porated or not.

The typical decay time for the relaxation of non-porated vesicles, τ_1 , is on the order of 100 μs [9]. It is defined by the relaxation of the total membrane tension attained at the end of the pulse, which is the sum of the electrotension σ_{el} and the initial tension σ_0 ; see Eq. 4. Thus, τ_1 relates mainly to the relaxation of membrane stretching: $\tau_1 \sim \eta_m/\sigma$, where η_m is the surface viscosity of the membrane, $\eta_m \approx 3.5 \times 10^{-7}$ N.s/m (the surface viscosity of a membrane has units [bulk viscosity] \times [bilayer thickness]). For membrane tensions of the order of 5 mN/m (which should be around the maximum tension before the membrane ruptures) one obtains $\tau_1 \sim 100$ μs corresponding well to experimentally measured values [9].

The relaxation dynamics of porated vesicles is significantly different from the one of non-porated vesicles [9]. Indeed, two different types of dynamic response can be distinguished for porated vesicles. The relaxation of vesicles with no excess area is described by a single exponential decay, while vesicles with excess area exhibit two characteristic decay times. These two cases for vesicles above the poration limit are illustrated in Fig. 2. Naturally, vesicles with excess area deform much more than those without (compare the two curves in Fig. 2). The relaxation of porated vesicles completes over a much longer time than that of nonporated ones. For vesicles with no excess area, the relaxation time is $\tau_2 \cong 7 \pm 3$ ms. When the vesicles have some excess area, the relaxation proceeds in two steps, fast relaxation characterized by τ_2 , and a second, longer, relaxation with decay time, τ_3 : $0.5 \text{ s} < \tau_3 < 3 \text{ s}$.

The relaxation time τ_3 is related to the presence of some excess area available for shape changes; for more details see Ref. [9]. The relaxation process associated with τ_2 , takes place during the time interval when pores are present (see shaded region in Fig. 2). Thus, τ_2 is determined by the closing of the pores: $\tau_2 \sim \eta_d r_{\text{pore}} / (2\gamma)$. Here r_{pore} is the pore radius and γ is the pore edge

tension, $\gamma \cong 10$ pN [13]. For a typical pore radius of 1 μm one obtains $\tau_2 \sim 10$ ms.

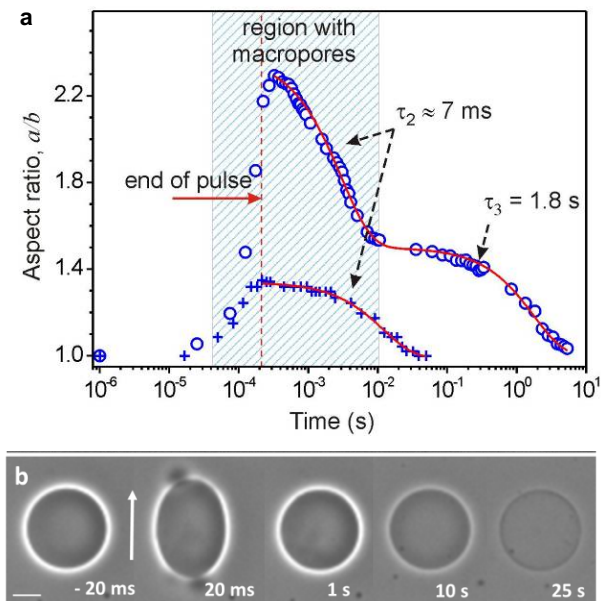


Figure 2: Electroporation of giant vesicles. (a) Data from the response and relaxation of two vesicles, in which macropores were observed. One of the vesicles (crosses) did not have excess area and the relaxation is described by a single exponential fit (solid curve) with a decay time τ_2 . The other vesicle (open circles) had excess area and its relaxation is described by a double exponential fit (solid curve) with decay times τ_2 and τ_3 as described in the text and in reference [9]. In both cases, the pulse strength was $E = 200$ kV/m and the pulse duration was $t_p = 200$ μs (the end of the pulse is indicated with a vertical dashed line). The time $t = 0$ was set as the beginning of the pulse. The shaded area indicates the time interval when macropores were optically detected. The radii of the vesicles were around 10 μm . Reproduced from reference [3]. (b) Pores and contrast loss in a giant vesicle after poration. The macropores (see second snapshot) reseal within tens of milliseconds, but long-lived submicroscopic pores stabilized by pore-spanning macromolecules (see e.g. [39]) can persist and the vesicle loses the original sugar asymmetry seconds after the pulse. The scale bars represent 20 μm .

Macropores (with sizes of a few microns) in electroporated giant vesicles can be directly observed with phase contrast microscopy if the vesicles possess sugar asymmetry (e.g. sucrose solution inside and isotonic glucose solution outside), which makes the vesicle appear dark on a lighted background. When a pore forms, the light halo around the vesicle appears broken (see second snapshot in Fig. 2b). These pores can attain sizes of up to 4-5 μm in diameter and reseal within tens of milliseconds. Long-lasting submicroscopic pores can lead to loss of the sugar asymmetry (see loss of contrast as observed in Fig. 2b) or loss of fluorescence contrast if water-soluble fluorophores are preloaded in the vesicles [40].

The electroporation of giant vesicles and the observation of the pore closure can be employed to deduce another material property of the membrane, namely the edge tension γ [13]. The edge tension

reflects the energetic penalty per unit length for reorganizing the lipid molecules in the bilayer so that their polar heads can line the pore walls and form a hydrophilic pore. The analysis of the process or pore dynamics was further developed in [41].

The vesicle relaxation dynamics can be considered using a droplet-based model [42, 43], which yielded a way of deducing the initial tension of the vesicle and the membrane bending rigidity [43].

In fluid vesicles, occasionally, DC pulses can induce macropores that remain stably open or even never reseal followed by vesicle destabilization and collapse. Stable and long-lived pores can be observed in the presence of cone-shaped molecules in the bilayer reducing the edge tension [44, 45], or in the presence of hydrogel polymers (agarose) physically hindering pore closure [39]. When DC pulses are applied to giant vesicles containing a large fraction of negatively charged lipids, vesicle burst/collapse is often observed [46].

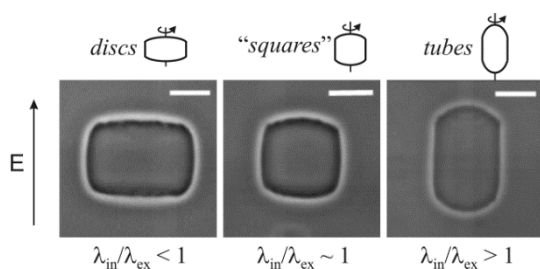


Figure 3: DC-pulse induced deformation of vesicles containing salt in the vesicle exterior at different conductivity conditions. Schematic illustrations of the cross sections of the vesicles are given above every snapshot. The field direction is indicated with an arrow on the left. The presence of salt in the vesicle exterior causes flattening of the vesicle membrane into disc-like, “square”-like, and tube-like shapes, whereby the overall vesicle morphology depends on the conductivity ratio. The scale bars correspond to 15 μm . Reproduced from reference [3].

Electrodeformation of vesicles in salt solutions

As discussed above, vesicles in aqueous solutions adopt ellipsoidal shapes when exposed to electric fields. However, in the presence of salt in the vesicle exterior (e.g. NaCl solution with concentration above 0.1 mM), unusual shape changes were observed [10]. The vesicles adopt spherocylindrical shapes (cylinders with spherical caps) during the pulse; see Fig. 3. These deformations are short-lived (their lifetime is about 1 ms) and occur only in the presence of salt outside the vesicles, irrespective of their inner content. Theoretical description of the unusual spherocylindrical deformations was recently developed and the flat and curved regions in the vesicle interpreted as coexistence of porated and nonporated regions [47].

ELECTROFUSION

When a DC pulse is applied to a couple of fluid-phase vesicles, which are in contact and oriented in the direction of the field, electrofusion can be observed. The necessary condition is that membrane poration is induced in the contact area between the two vesicles. Membrane fusion is fast. The time needed for the formation of a fusion neck can be rather short as demonstrated by electrophysiological methods applied to the fusion of small vesicles with cell membranes [48-51]. The time evolution of the observed membrane capacitance indicates that the formation of the fusion neck is presumably faster than 100 μs . Direct observation of the fusion of giant vesicles confirm this finding suggesting that this time is even shorter [11, 12]. From optical microscopy micrographs, one can measure the fusion neck diameter and follow the dynamics of its expansion as shown in Fig. 4.

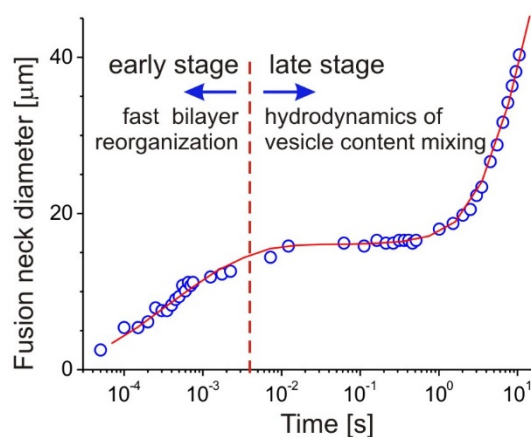


Figure 4: Time evolution of the fusion neck diameter formed between two vesicles with radii of about 15 μm . The solid curve is a guide to the eye. The vertical dashed line indicates the border between the two stages in the fusion dynamics. Reproduced from reference [3].

From the data, two stages of the fusion process can be distinguished (note that the data in Fig. 4 are displayed in a semi logarithmic plot): an early one, which is very fast and with average expansion velocity of about $2 \times 10^4 \mu\text{m/s}$, followed by a later slower one with an expansion rate, which is orders or magnitude smaller ($\sim 2 \mu\text{m/s}$). The early stage is governed by fast relaxation of the membrane tension built during the pulse, whereby the dissipation occurs in the bilayer. Essentially, the driving forces here are the same as those responsible for the relaxation dynamics of nonporated vesicles (as characterized by τ_1 in the previous section). In the later stage of fusion, the dynamics is mainly governed by the displacement of the volume of fluid around the fusion neck between the fused vesicles. The restoring force is related to the bending elasticity of the lipid bilayer [11, 12].

Electrofusion of giant vesicles has some practical applications. Giant vesicles formed from multicomponent (e.g. ternary) lipid mixtures have the disadvantage of exhibiting compositional heterogeneity between vesicles in the batch. Electrofusion of two giant vesicles, each made of "simple" bilayer composition (e.g. single- or two-component), can be employed to create vesicles with precisely known membrane composition. Furthermore, these vesicles can be used to deduce tie lines in the phase diagram of ternary mixtures [52]. Tie lines show the composition of domains in phase separated vesicles.

Another application of electrofusion of giant vesicles goes in the direction of their use as microcompartments or microreactors. Electrofusion of two giant vesicles in order to initiate content mixing reactions has been employed previously [53]. We have demonstrated how vesicle electrofusion can be applied for the synthesis of quantum-dot-like CdS nanoparticles in closed compartments [54, 55].

CONCLUDING REMARKS

Giant vesicles as cell-size systems provide a very useful model for resolving the effect of electric fields on lipid membranes. They allow for direct optical microscopy observation of membrane deformations in the micrometer range. We examined the behavior of giant vesicles exposed to AC fields of various frequencies. The solution conductivity appeared to be a major factor determining the overall deformation of the vesicles. It remains to be seen whether similar behavior is found for cells. In many cases, the cell deformation will be mainly determined by the cytoskeleton flexibility rather than the membrane stiffness. However, for cells like leukocytes, it would be interesting to explore the influence of solution conductivity and field frequency on the cell shape.

Until recently, the temporal limit of optical microscopy observations with analogue video technology was in the range of milliseconds. Using fast digital imaging, we revealed the dynamics of electrodeformation and electroporation of vesicles subjected to DC pulses, as well as electrofusion events with microsecond resolution [1, 3, 4, 9-13]. New shape deformations, such as cylindrical ones with square cross section have been detected [4, 10]. In addition, the dynamics of vesicle fusion became accessible. The expansion of the fusion neck is extremely fast in the beginning and is characterized by rates on the order of a couple of cm/s. For membranes whose thickness is only several nanometers, such a velocity is tremendous. Electrofusion of vesicles with different bilayer composition has been demonstrated to be a feasible method for creating multidomain vesicles and provides

new opportunities for studying the dynamics of domain formation and stability [3, 4, 12, 52]. Fusing vesicles loaded with different internal solutions has also provided us with an approach for synthesis of nanoparticles in microreactors represented by giant vesicles [54].

REFERENCES

- [1] R. Dimova, S. Aranda, N. Bezlyepkina, V. Nikolov, K.A. Riske, R. Lipowsky, A practical guide to giant vesicles. Probing the membrane nanoregime via optical microscopy, *J Phys: Condens Matter*, 18(2006) S1151-S76.
- [2] R. Dimova, Giant Vesicles: A Biomimetic Tool for Membrane Characterization, in: A. Iglič (Ed.) *Advances in Planar Lipid Bilayers and Liposomes*, Academic Press 2012, pp. 1-50.
- [3] R. Dimova, K.A. Riske, S. Aranda, N. Bezlyepkina, R.L. Knorr, R. Lipowsky, Giant vesicles in electric fields, *Soft Matter*, 3(2007) 817-27.
- [4] R. Dimova, N. Bezlyepkina, M.D. Jordo, R.L. Knorr, K.A. Riske, M. Staykova, et al., Vesicles in electric fields: Some novel aspects of membrane behavior, *Soft Matter*, 5(2009) 3201-12.
- [5] R. Dimova, Electrodeformation, Electroporation, and Electrofusion of Cell-Sized Lipid Vesicles, in: A.G. Pakhomov, D. Miklavcic, M. Markov (Eds.), *Advanced Electroporation Techniques in Biology and Medicine*, CRC Press, Boca Raton, 2010, pp. 97-122.
- [6] R. Dimova, Membrane Electroporation in High Electric Fields, in: R.C. Alkire, D.M. Kolb, J. Lipkowski (Eds.), *Bioelectrochemistry Fundamentals, Applications and Recent Developments*, Wiley-VCH Verlag GmbH & Co. KGaA, Weinheim, 2011, pp. 335-67.
- [7] T. Portet, R. Dimova, D.S. Dean, M.-P. Rols, Electric Fields and Giant Vesicles, *Biophys J*, 98(2010) 77a-a.
- [8] T. Portet, F.C.I. Febrer, J.M. Escoffre, C. Favard, M.P. Rols, D.S. Dean, Visualization of Membrane Loss during the Shrinkage of Giant Vesicles under Electropulsation, *Biophys J*, 96(2009) 4109-21.
- [9] K.A. Riske, R. Dimova, Electro-deformation and poration of giant vesicles viewed with high temporal resolution, *Biophys J*, 88(2005) 1143-55.
- [10] K.A. Riske, R. Dimova, Electric pulses induce cylindrical deformations on giant vesicles in salt solutions, *Biophys J*, 91(2006) 1778-86.
- [11] C.K. Haluska, K.A. Riske, V. Marchi-Artzner, J.M. Lehn, R. Lipowsky, R. Dimova, Time scales of membrane fusion revealed by direct imaging of vesicle fusion with high temporal resolution, *Proc Natl Acad Sci U S A*, 103(2006) 15841-6.
- [12] K.A. Riske, N. Bezlyepkina, R. Lipowsky, R. Dimova, Electrofusion of model lipid membranes viewed with high temporal resolution, *Biophys Rev Lett*, 1(2006) 387-400.
- [13] T. Portet, R. Dimova, A New Method for Measuring Edge Tensions and Stability of Lipid Bilayers: Effect of Membrane Composition, *Biophys J*, 99(2010) 3264-73.
- [14] K. Kinoshita, I. Ashikawa, N. Saita, H. Yoshimura, H. Itoh, K. Nagayama, et al., Electroporation of cell-membrane visualized under a pulsed-laser fluorescence microscope, *Biophys J*, 53(1988) 1015-9.
- [15] D. Needham, R.M. Hochmuth, Electro-Mechanical Permeabilization of Lipid Vesicles - Role of Membrane Tension and Compressibility, *Biophys J*, 55(1989) 1001-9.
- [16] I.G. Abidor, V.B. Arakelyan, L.V. Chernomordik, Y.A. Chizmadzhev, V.F. Pastushenko, M.R. Tarasevich, Electrical breakdown of bilayer lipid-membranes. 1. Main experimental

- facts and their qualitative discussion, *Bioelectrochem Bioenerg*, 6(1979) 37-52.
- [17] S.A. Simon, T.J. McIntosh, Depth of water penetration into lipid bilayers, *Methods Enzymol*, 127(1986) 511-21.
- [18] K. Olbrich, W. Rawicz, D. Needham, E. Evans, Water permeability and mechanical strength of polyunsaturated lipid bilayers, *Biophys J*, 79(2000) 321-7.
- [19] S. Aranda, K.A. Riske, R. Lipowsky, R. Dimova, Morphological transitions of vesicles induced by alternating electric fields, *Biophys J*, 95(2008) L19-L21.
- [20] P. Peterlin, Frequency-dependent electrodeformation of giant phospholipid vesicles in AC electric field, *J Biol Phys*, DOI: 10.1007/s10867-010-9187-3(2010).
- [21] P. Peterlin, S. Svetina, B. Zeks, The prolate-to-oblate shape transition of phospholipid vesicles in response to frequency variation of an AC electric field can be explained by the dielectric anisotropy of a phospholipid bilayer, *J Phys: Condens Matter*, 19(2007) 136220.
- [22] G. Niggemann, M. Kummrow, W. Helfrich, The Bending Rigidity of Phosphatidylcholine Bilayers - Dependences on Experimental-Method, Sample Cell Sealing and Temperature, *J Phys II*, 5(1995) 413-25.
- [23] M.D. Mitov, P. Meleard, M. Winterhalter, M.I. Angelova, P. Bothorel, Electric-field-dependent thermal fluctuations of giant vesicles, *Phys Rev E*, 48(1993) 628-31.
- [24] P. Peterlin, S. Svetina, B. Zeks, The frequency dependence of phospholipid vesicle shapes in an external electric field, *Pfluegers Arch/Eur J Physiol*, (2000) R139-R40.
- [25] H. Hyuga, K. Kinoshita, N. Wakabayashi, Transient and steady-state deformations of a vesicle with an insulating membrane in response to step-function or alternating electric-fields, *Jpn J Appl Phys, Part 1*, 30(1991) 2649-56.
- [26] H. Hyuga, K. Kinoshita, N. Wakabayashi, Steady-state deformation of a vesicle in alternating electric-fields, *Bioelectrochem Bioenerg*, 32(1993) 15-25.
- [27] P.M. Vlahovska, R.S. Gracia, S. Aranda-Espinoza, R. Dimova, Electrohydrodynamic Model of Vesicle Deformation in Alternating Electric Fields, *Biophys J*, 96(2009) 4789-803.
- [28] T. Yamamoto, S. Aranda-Espinoza, R. Dimova, R. Lipowsky, Stability of Spherical Vesicles in Electric Fields, *Langmuir*, 26(2010) 12390-407.
- [29] P.F. Salipante, R.L. Knorr, R. Dimova, P.M. Vlahovska, Electrodeformation method for measuring the capacitance of bilayer membranes, *Soft Matter*, 8(2012) 3810-6.
- [30] R.S. Gracià, N. Bezlyepkina, R.L. Knorr, R. Lipowsky, R. Dimova, Effect of cholesterol on the rigidity of saturated and unsaturated membranes: fluctuation and electrodeformation analysis of giant vesicles, *Soft Matter*, 6(2010) 1472-82.
- [31] W. Harbich, W. Helfrich, Alignment and Opening of Giant Lecithin Vesicles by Electric-Fields, *Z Naturforsch, A: Phys Sci*, 34(1979) 1063-5.
- [32] K. Antonova, V. Vitkova, C. Meyer, Membrane tubulation from giant lipid vesicles in alternating electric fields, *Phys Rev E*, 93(2016) 012413.
- [33] R. Dimova, Recent developments in the field of bending rigidity measurements on membranes, *Adv Colloid Interface Sci*, 208(2014) 225-34.
- [34] N. Fricke, R. Dimova, GM1 softens POPC membranes and induces the formation of micron-sized domains, Submitted, (2016).
- [35] M. Staykova, R. Lipowsky, R. Dimova, Membrane flow patterns in multicomponent giant vesicles induced by alternating electric fields, *Soft Matter*, 4(2008) 2168-71.
- [36] J. Steinkuehler, J. Agudo-Canalejo, R. Lipowsky, R. Dimova, Variable Adhesion Strength for Giant Unilamellar Vesicles Controlled by External Electrostatic Potentials, *Biophys J*, 108(2015) 402a-a.
- [37] J. Steinkuehler, J. Agudo-Canalejo, R. Lipowsky, R. Dimova, Modulating vesicle adhesion by electric fields, *Biophys J*, (2016) in press.
- [38] R.L. Knorr, M. Staykova, R.S. Gracia, R. Dimova, Wrinkling and electrodeformation of giant vesicles in the gel phase, *Soft Matter*, 6(2010) 1990-6.
- [39] Rafael B. Lira, R. Dimova, Karin A. Riske, Giant Unilamellar Vesicles Formed by Hybrid Films of Agarose and Lipids Display Altered Mechanical Properties, *Biophys J*, 107(2014) 1609-19.
- [40] R.B. Lira, J. Steinkuehler, R.L. Knorr, R. Dimova, K.A. Riske, Posing for a picture: vesicle immobilization in agarose gel, *Scientific Reports*, 6(2016) 25254.
- [41] R. Ryham, I. Berezovik, F.S. Cohent, Aqueous Viscosity Is the Primary Source of Friction in Lipidic Pore Dynamics, *Biophys J*, 101(2011) 2929-38.
- [42] J. Zhang, J.D. Zahn, W.C. Tan, H. Lin, A transient solution for vesicle electrodeformation and relaxation, *Phys Fluids*, 25(2013).
- [43] M. Yu, R.B. Lira, K.A. Riske, R. Dimova, H. Lin, Ellipsoidal Relaxation of Deformed Vesicles, *Phys Rev Lett*, 115(2015).
- [44] E. Karatekin, O. Sandre, H. Guitouni, N. Borghi, P.H. Puech, F. Brochard-Wyart, Cascades of transient pores in giant vesicles: Line tension and transport, *Biophys J*, 84(2003) 1734-49.
- [45] N. Rodriguez, S. Cribier, F. Pincet, Transition from long- to short-lived transient pores in giant vesicles in an aqueous medium, *Phys Rev E*, 74(2006) 061902.
- [46] K.A. Riske, R.L. Knorr, R. Dimova, Bursting of charged multicomponent vesicles subjected to electric pulses, *Soft Matter*, 5(2009) 1983-6.
- [47] P.F. Salipante, M.L. Shapiro, P.M. Vlahovska, Electric Field Induced Deformations of Biomimetic Fluid Membranes, *Procedia IUTAM*, 16(2015) 60-9.
- [48] R. Llinas, I.Z. Steinberg, K. Walton, Relationship between presynaptic calcium current and postsynaptic potential in squid giant synapse, *Biophys J*, 33(1981) 323-51.
- [49] M. Lindau, G.A. de Toledo, The fusion pore, *Biochim Biophys Acta*, 1641(2003) 167-73.
- [50] I. Hafez, K. Kisler, K. Berberian, G. Dernick, V. Valero, M.G. Yong, et al., Electrochemical imaging of fusion pore openings by electrochemical detector arrays, *Proc Natl Acad Sci U S A*, 102(2005) 13879-84.
- [51] J.C. Shillcock, R. Lipowsky, Tension-induced fusion of bilayer membranes and vesicles, *Nat Mater*, 4(2005) 225-8.
- [52] N. Bezlyepkina, R.S. Gracià, P. Shchelokovskyy, R. Lipowsky, R. Dimova, Phase Diagram and Tie-Line Determination for the Ternary Mixture DOPC/eSM/Cholesterol, *Biophys J*, 104(2013) 1456-64.
- [53] D.T. Chiu, C.F. Wilson, F. Ryttsen, A. Stromberg, C. Farre, A. Karlsson, et al., Chemical transformations in individual ultrasmall biomimetic containers, *Science*, 283(1999) 1892-5.
- [54] P. Yang, R. Lipowsky, R. Dimova, Nanoparticle Formation in Giant Vesicles: Synthesis in Biomimetic Compartments, *Small*, 5(2009) 2033-7.
- [55] P. Yang, R. Dimova, Nanoparticle Synthesis in Vesicle Microreactors, in: A. George (Ed.) *Biomimetic Based Applications*, InTech2011, pp. 523-52.

ACKNOWLEDGEMENTS

The experimental work on vesicles in electric fields was initiated together with Karin A. Riske. I would also like to thank Roland L. Knorr, Natalya Bezlyepkina, Thomas Portet, Margarita Staykova, Peng Yang, Said Aranda, Marie Domange Jordö, Benjamin Klasczyk, and Jan Steinkuehler and D. Duda. I also wish to acknowledge the valuable insight I got from the enlightening

discussions with theoreticians such as Reinhard Lipowsky, Petia M. Vlahovska, Tetsuya Yamamoto, and Rubèn S. Gracià.



Rumiana Dimova was born in Dobrich, Bulgaria, in 1971. She studied chemical physics and theoretical chemistry at Sofia University. In 1999, she obtained her PhD degree at Bordeaux University, France. Since 2000, she is a group leader at the Max Planck Institute of Colloids and Interfaces in Potsdam, Germany. Her research interests are in the field of biophysics of model membranes, their interactions with various molecules, and response to external fields.

Rumiana Dimova is the author of 90 articles in SCI-ranked journals that have been cited over 2360 times to date. According to Web of Science, her current H-index is 30. In 2014, the European Physical Society awarded her with the Emmy Noether distinction for women in physics.

NOTES

NOTES

PEF-Processing in Microalgae Valorization

Wolfgang Frey

Karlsruhe Institute of Technology, Institute for Pulsed Power and Microwave Technology, Karlsruhe, Germany

Abstract: Microalgae, often referred to as third generation biomass, very efficiently produce a large variety of valuable components, e.g. antioxidants, lipids, proteins and carbohydrates, at high intracellular concentration, and are considered as a promising feedstock for energetic utilization, as a future source of fine chemicals and for food and feed industry. Conventional downstream processing path-ways involve mechanical cell disruption and in some cases drying steps which are energy-intensive. PEF treatment can considerably reduce the required treatment energy demand and in addition allows subsequent recovery of different component fractions which allows establishing biorefinery concepts for economic future component recovery and utilization.

INTRODUCTION

Microalgae biomass is one of the most efficiently growing biomass. Due to its high content of exploitable components microalgae are a promising and sustainable resource of lipids, proteins vitamins and antioxidants.

Unfortunately most microalgae protect their cell interior by a very rigid cell wall which impedes component recovery. Membrane permeabilization by PEF treatment has been demonstrated to be an advantageous tool for energy-efficient extraction of microalgal cell components.

SOME BASICS ABOUT MICROALGAE BIOMASS

When grown in closed photobioreactor systems, realistic yields of microalgae biomass are in the order of 40 – 80 t·ha⁻¹·yr⁻¹ [1]. This value is about 2-5 times higher than yields achieved with agriculturally grown biomass. High performance energy crops, e.g. Miscanthus can only deliver 20 t·ha⁻¹·yr⁻¹ at most [2].

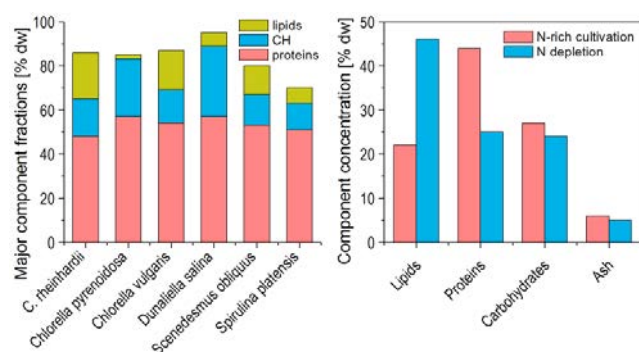


Figure 1: Major component composition of various microalgae strains for nitrogen-sufficient cultivation conditions, reproduced from [3], left and major component fractions of *Chlorella vulgaris* for N-rich and N-depleted cultivation conditions, reproduced from [4].

Photobioreactor cultivation can be done on barren lands, thus microalgae biomass production doesn't compete with agricultural food industry and avoids impoverishment of soil. The content of valuable products, i.e. lipids, proteins, carbohydrates exceeds 80% of the biomass, Figure 1, left. For nitrogen-sufficient cultivation conditions with satisfactory biomass growth rates, the protein content amounts to 50% on average. The lipid fraction accounts for 20% of the biomass.

Higher lipid yields of 50% and more can be obtained from microalgae under nitrogen-depleted cultivation conditions, Figure 1, right. In that case microalgae switch their metabolism from biomass growth to nutrient storage for survival. For *Chlorella vulgaris*, the CH³ content is hardly affected by the nitrogen concentration in the growth medium, Figure 1, right.

Under nitrogen starvation, microalgae growth is low. For this reason oil yield values of 50 t·ha⁻¹·yr⁻¹ and higher sometimes stated in older literature references, e.g. [5, 6], have to be considered carefully, since their calculation bases on maximum oil content and maximum growth values which cannot be obtained simultaneously. A feasible oil yield from microalgae biomass obtained under satisfactory growth conditions is about 10-14 t·ha⁻¹·yr⁻¹, which is still considerably higher than oil yields of 1.2 t·ha⁻¹·yr⁻¹, obtainable from rape seed cultivation.

Besides lipids, microalgae are also considered as a promising source of proteins. The amino acid profile of microalgal proteins matches very well the profiles of egg or soya and satisfies the human nutrition requirements recommended by FAO/WHO⁴ [7, 8]. Thus nowadays research efforts more and more focus on recovery of microalgal proteins.

Despite all convincing advantages, microalgae component and biomass utilization faces economic and

³ CH: carbohydrates

⁴ FAO: Food and Agriculture Organization of the United Nations;
WHO: World Health Organization

technological challenges to be overcome for broad market launch.

Microalgae cultivation in closed photobioreactor systems consume almost half of the energy which is chemically stored in the biomass. The lowest energy consumption for cultivation of 10 MJ/kg_{dw}⁵ is reported for flat panel systems [9], whereas the stored energy ranges between 20 – 27 MJ/kg_{dw} [10], depending on the lipid content of the biomass.

Microalgae processing consumes energy for dewatering, cell disruption and component extraction. Lowest values for microalgae biomass centrifugation from cultivation cell density (2 g_{dw}/l – 10 g_{dw}/l) to wet processing density (100 g_{dw}/l – 200 g_{dw}/l) are between 3-4 MJ/kg_{dw} [www.evodos.eu]. Conventional mechanical cell disruption [11] by ball milling [12] or high pressure homogenisation are in the same order of magnitude or slightly higher. In the case that dry processing is required for component extraction, as evident for some lipid extraction routes, additional 7 MJ/kg_{dw} have to be expended for biomass drying. This narrows the possible net energy gain for an energetic use of microalgae, e.g. as a future source of biofuels.

Nowadays costs for cultivation of 1 kg of dry microalgae biomass are between 4-5 €, when produced on large scale [13]. When marketed for biofuels, the achievable price is 0.5 €/kg [1]. This immediately makes clear that nowadays a sole energetic use of microalgae is not economic. Besides lipids for biofuel, higher value products have to be marketed. Water-soluble proteins can achieve values of 5 €/kg on the food market [1]. Market prices for glucans and antioxidants are considerably higher, >300 \$/kg [14], but the market volume is small. Nevertheless, for a mid-term and broad market launch of microalgal products R&D efforts nowadays have to focus on reducing cultivation costs on one hand and on optimizing downstream processing in terms of recovery of multiple components and energy efficiency on the other hand.

PEF-PROCESSING OF MICROALGAE BIOMASS

A first indication of successful membrane permeabilization of microalgal cells in suspension is the immediate increase of suspension conductivity during continuous flow treatment of *Auxenochlorella protothecoides*. After start-up of the setup with tap water until $t = 20$ s, the conductivity rises to 1 mS/cm, when the unwashed and concentrated microalgae suspension, pre-concentrated to 100 g_{dw}/l, filled the treatment volume. A subsequent and slower-rising increase up to 1.6 mS/cm results from release of ions

from inside the microalgae cells. Please note, that this conductivity value represents an average conductivity of the suspension in the treatment volume calculated from voltage and current measurements at the treatment chamber during continuous flow treatment and includes conductivity values of cell-suspension volume-elements which just have entered the chamber and also of volume elements close to the outlet of the chamber. The conductivity of the treated sample at the output of the chamber is 2,2 mS/cm and higher.

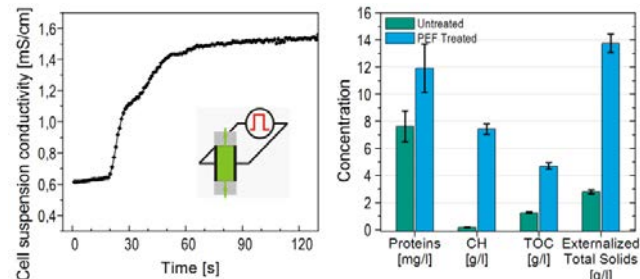


Figure 2: Increase of the conductivity of microalgae suspensions during PEF treatment, left, and component yield increase after PEF treatment, right.

Besides ionic release, also an increase in CH concentration can be detected in the supernatant after PEF treatment [15]. The total mass of released products after PEF treatment amounts to 14% of the dry cell weight in suspension, Figure 2, right. The spontaneous release of proteins is low.

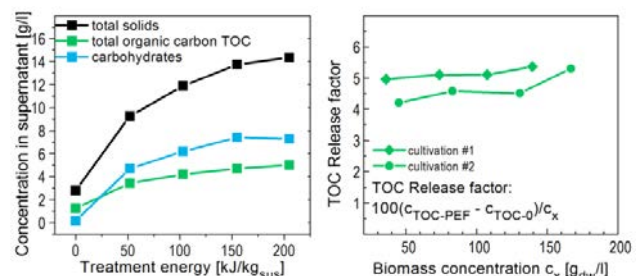


Figure 3: Increase of externalized water-soluble components over treatment energy after PEF treatment with 1 μs square pulses, left. The diagram to the right shows the externalization of total organic carbon normalized on biomass density. Component release is not impaired at high biomass densities.

The required energy for PEF-processing of microalgae is shown in Figure 3, left diagram. The component yield starts to saturate at a specific treatment energy value of 150 kJ/kg_{sus} of treated suspension. In case that the biomass concentration in suspension was 100 g_{dw}/l, the required energy for PEF-processing of 1 kg of dry biomass is 1.5 MJ/kg_{dw}.

In the microalgae community, treatment energy values are always normalized to the dry weight of the

⁵ dw: dry weight

treated biomass. In the case of wet PEF-processing of microalgae biomass the biomass concentration in the treated suspension is an important factor.

In the PEF community there is general consensus that the measurable result of PEF treatment, e.g. component yield or bacterial inactivation, for square pulses scales with the overall treatment time $N \cdot T$, i.e. the product of number of pulses N and pulse duration T , provided that the electric field is high enough for whole membrane surface permeabilization and the pulse duration is long compared to the charging time constant of membrane [16]. Consequently, for constant conductivities κ of the suspension to be treated, the resulting effect of PEF treatment scales with the specific treatment energy delivered to the cell suspension. For microalgae treatment this means that the relative component yield can be expected to be the same for a suspension exhibiting a conductivity of $\kappa = 1$ mS/cm and for cell densities of e.g. 20 g_{dw}/l and 100 g_{dw}/l, when being treated with the same specific energy of e.g. 100 kJ/kg_{sus}. For this example, the same treatment result can be expected for treatment energies related to the dry biomass weight of 5 MJ/kg_{dw} in the first case and 1 MJ/kg_{dw} in the second case. When treatment energy values are normalized to dry biomass weight, the effect of PEF treatment does *not* necessarily scale with this specific energy value.

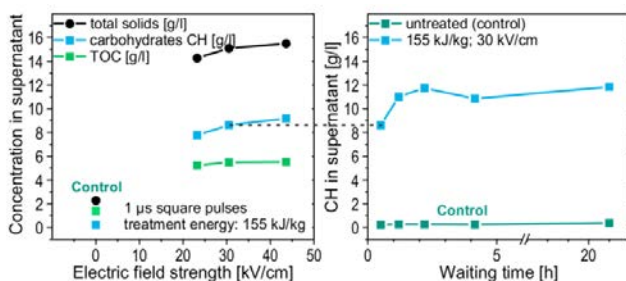


Figure 4: Component release from microalgae only weakly depends on the electric field strength between 20 kV/cm and 45 kV/cm, left, whereas an additional waiting time after PEF treatment can increase component yield, e.g. carbohydrates, considerably, right.

For constant treatment energy delivered to the suspension, the component yield only weakly depends on the electric field magnitude within a range of 20 kV/cm and 45 kV/cm, Figure 4, left, whereas an additional waiting time of 2 hours improves component release by more than 40%, Figure 4, right [15].

In consequence of above considerations, the energy consumption for PEF-treatment can be decreased by increasing the biomass density in the suspension to be treated. Usually, microalgae suspensions up to a concentration of 200 g_{dw}/l are satisfactorily pumpable through the treatment chamber. The CH-yield, Figure 3, right, and also final conductivity value were found to

be invariant of biomass concentration c_x for processing with constant treatment energy of 150 kJ/kg_{sus}. For the highest concentration of 170 g_{dw}/l selected for this experiment, Figure 3, the required treatment energy was 0.88 MJ/kg_{dw} [15]. This is 4 times lower as required for conventional mechanical cell disruption. For cross reference please note that in literature energy values are often given in kWh. 1 kWh is equivalent to 3.6 MJ.

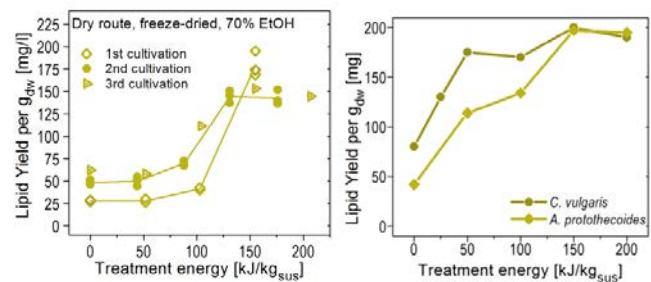


Figure 5: Lipid yield from PEF-treated microalgae biomass for dry-route processing, left. The biomass was freeze dried after PEF treatment. Lipid yield after EtOH extraction was 3-4 times higher for samples treated at 150 kJ/kg_{sus}. The same increase in EtOH extraction efficiency could be obtained for wet-route processing, right. In that case, the solvent was added to the wet pellet of microalgae after PEF-treatment. The required treatment energy for PEF-assisted lipid recovery from *C. vulgaris* is lower than for *A. protothecoides*, right.

Up to here, all results discussed were obtained from PEF treatment of *Auxenochlorella protothecoides*, exhibiting a strong cell wall. Although the release of water-soluble products was considerable, no lipids could be detected in the supernatant after PEF treatment. The current hypothesis for this observation is, that the lipid droplets stored intracellularly cannot pass the cell wall due to their large diameter of about 1 μ m, Figure 6, left [17]. However, a combination of PEF treatment and subsequent solvent extraction of lipids with Ethanol was shown to increase lipid yield by a factor of 3-4, Figure 5, left, if the sample was treated with PEFs prior to lipid extraction [18]. This lipid yield increase could also be obtained for *Chlorella vulgaris*, Figure 5, right.

The energy demand for satisfactory lipid extraction yields depends on the strain to be treated. The required treatment energy for *Auxenochlorella protothecoides* amounts to 150 kJ/kg_{sus}, whereas for *Chlorella vulgaris* already 50 kJ/kg_{sus} are sufficient to obtain extraction values close to the maximum, Figure 5, left.

Interestingly, the extraction yield for solvent extraction from wet biomass more or less linearly increases with treatment energy, whereas for dry route processing a considerable yield increase only could be observed at energy values higher than 100 kJ/kg_{sus}.

Currently there is no consistent explanation for this behaviour.

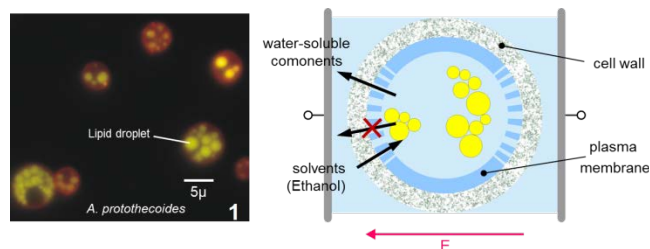


Figure 6: Intracellular lipid droplets accumulated in *A. protothecoides*, left. The schematic to the right illustrates the selectivity of PEF-assisted component recovery: after PEF treatment, water-soluble components can pass the permeabilized cell membrane and cell wall, but not lipid droplets. Solvent access to the cell interior is improved, thus increasing the lipid yield of a subsequent solvent extraction step.

This leads to our current understanding on the effect of PEF-treatment of microalgae for component recovery, graphically summarized in Figure 6, right: PEF treatment enables a yield increase of water-soluble components right after treatment. It also improves solvent access to the cell interior. Lipids are detained by the cell wall, but can be recovered at high efficiencies by subsequent solvent extraction. This opens processing opportunities for microalgae cascade processing, i.e. the recovery of multiple component fractions.

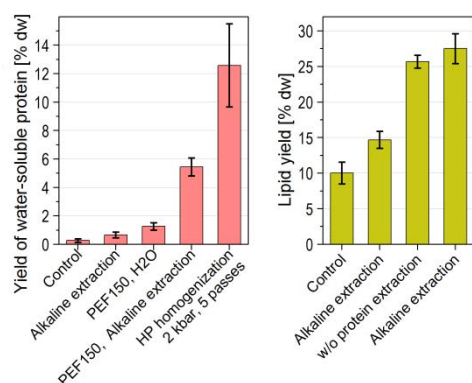


Figure 7: PEF-assisted cascade processing of *Chlorella vulgaris*: The application of an alkaline protein extraction buffer containing DDT considerably can increase protein yield after PEF treatment, left. Subsequent ethanolic extraction of lipids is not impaired by previous protein extraction.

Besides lipids, the second major product fraction to be recovered from microalgae is protein. The total protein content of microalgae is about 50%. Microalgal proteins exhibit excellent techno-functional properties, e.g. emulsifying capability, which is of high relevance in food technology [19]. Conventionally processed, protein extraction requires mechanical cell disruption. As most efficient conventional methods nowadays ball

milling [12] and high pressure homogenization [20] are discussed.

Important for PEF-assisted protein extraction is the fact, that the variety of microalgal proteins exhibit different water-solubility. About 20% of the proteins of microalgae are assumed to be water-soluble [1]. Protein solubility in water is higher in alkaline media [7]. Furthermore, proteins are bound to organelles and to the cell wall (~30% [7]) which above all impedes PEF-assisted recovery. In particular, protein extraction from chlorella-type microalgae is discussed to be challenging because of their tight and rigid cell wall.

Since proteins are comparatively large molecules, it is not surprising, that the protein release from *Chlorella vulgaris* after PEF treatment is low, Figure 7, “PEF150 H2O”, for sole aqueous extraction [21] without applying additional measures to enhance extraction. When using an extraction buffer at higher pH containing dithiothreitol (DTT) [22], i.e. a reducing agent capable of breaking disulfide bonds, the protein yield after PEF treatment increases considerably, Figure 7, “PEF150, alkaline extraction”. This procedure allows PEF-assisted recovery of more than 40% of the overall water-soluble protein content obtained after high-pressure homogenization. Importantly, subsequent lipid recovery by solvent extraction is not impaired at all by previous protein extraction, Figure 7, right. Another big advantage of PEF-processing of microalgae is preservation of excellent mechanical separability of the biomass, since cell morphology is not affected by PEF treatment. No cell debris is generated.

These advantages of PEF-processing, such as preservation of biomass separability, enhancement of component yields and the opportunity of a subsequent recovery of several component fractions at low expenditures of treatment energy may open new biorefinery pathways for future economic microalgae utilization [23, 24].

ACKNOWLEDGEMENTS

This work was supported by the Helmholtz-Program on Renewable Energies and by the KIT Microalgae Platform, <http://bvt.blk.kit.edu/english/599.php>.

REFERENCES

- [1] R. H. Wijffels, M. J. Barbosa, and M. H. M. Eppink, "Microalgae for the production of bulk chemicals and biofuels," *Biofuels, Bioproducts and Biorefining*, vol. 4, pp. 287-295, 2010.
- [2] I. Lewandowski and A. Heinz, "Delayed harvest of miscanthus—influences on biomass quantity and quality and environmental impacts of energy production," *European Journal of Agronomy*, vol. 19, pp. 45-63, 2003.
- [3] E. W. Becker, "Micro-algae as a source of protein," *Biotechnology Advances*, vol. 25, pp. 207-210, 2007.

- [4] A. Guccione, A. Biondi, G. Sampietro, L. Rodolfi, N. Bassi, and M. R. Tredici, "Chlorella for protein and biofuels: from strain selection to outdoor cultivation in a Green Wall Panel photobioreactor," *Biotechnol Biofuels*, vol. 7, p. 84, 2014.
- [5] Y. Chisti, "Biodiesel from microalgae," *Biotechnol Adv*, vol. 25, pp. 294-306, May-Jun 2007.
- [6] L. Gouveia and A. Oliveira, "Microalgae as a raw material for biofuels production," *Journal of Industrial Microbiology & Biotechnology*, vol. 36, pp. 269-274, 2009/02/01 2009.
- [7] C. Safi, B. Zebib, O. Merah, P.-Y. Pontalier, and C. Vaca-Garcia, "Morphology, composition, production, processing and applications of *Chlorella vulgaris*: A review," *Renewable and Sustainable Energy Reviews*, vol. 35, pp. 265-278, 2014.
- [8] P. J. I. B. Williams and L. M. L. Laurens, "Microalgae as biodiesel & biomass feedstocks: Review & analysis of the biochemistry, energetics & economics," *Energy & Environmental Science*, vol. 3, pp. 554-590, 2010.
- [9] E. Sierra, F. G. Acien, J. M. Fernandez, J. L. Garcia, C. Gonzalez, and E. Molina, "Characterization of a flat plate photobioreactor for the production of microalgae," *Chemical Engineering Journal*, vol. 138, pp. 136-147, May 1 2008.
- [10] R. Dillschneider, C. Steinweg, R. Rosello-Sastre, and C. Posten, "Biofuels from microalgae: Photoconversion efficiency during lipid accumulation," *Bioresource Technology*, vol. 142, pp. 647-654, 2013.
- [11] E. Günerken, E. D'Hondt, M. H. M. Eppink, L. Garcia-Gonzalez, K. Elst, and R. H. Wijffels, "Cell disruption for microalgae biorefineries," *Biotechnology Advances*, vol. 33, pp. 243-260, 2015.
- [12] P. R. Postma, T. L. Miron, G. Olivieri, M. J. Barbosa, R. H. Wijffels, and M. H. M. Eppink, "Mild disintegration of the green microalgae *Chlorella vulgaris* using bead milling," *Bioresource Technology*, vol. 184, pp. 297-304, 2015.
- [13] N.-H. Norsker, M. J. Barbosa, M. H. Vermuë, and R. H. Wijffels, "Microalgal production — A close look at the economics," *Biotechnology Advances*, vol. 29, pp. 24-27, 2011.
- [14] R. Rosello-Sastre, "Products from microalgae: An overview," in *Microalgal Biotechnology: Integration and Economy*, C. Posten and C. Walter, Eds., ed: de Gruyter, 2012, pp. 13-50.
- [15] M. Goettel, C. Eing, C. Gusbeth, R. Straessner, and W. Frey, "Pulsed electric field assisted extraction of intracellular valuables from microalgae," *Algal Research-Biomass Biofuels and Bioproducts*, vol. 2, pp. 401-408, Oct 2013.
- [16] W. Frey, C. Gusbeth, and T. Schwartz, "Inactivation of *Pseudomonas putida* by Pulsed Electric Field Treatment: A Study on the Correlation of Treatment Parameters and Inactivation Efficiency in the Short-Pulse Range," *The Journal of Membrane Biology*, vol. 246, pp. 769-781, 2013/10/01 2013.
- [17] C. Gusbeth, C. Eing, M. Goettel, R. Straessner, and W. Frey, "Fluorescence Diagnostics for Lipid Status Monitoring of Microalgae during Cultivation," *International Journal of Renewable Energy and Biofuels*, pp. accepted for publication, March 24, 2015, 2015.
- [18] C. Eing, M. Goettel, R. Straessner, C. Gusbeth, and W. Frey, "Pulsed Electric Field Treatment of Microalgae-Benefits for Microalgae Biomass Processing," *Ieee Transactions on Plasma Science*, vol. 41, pp. 2901-2907, Oct 2013.
- [19] A.-V. Ursu, A. Marcati, T. Sayd, V. Sante-Lhoutellier, G. Djelveh, and P. Michaud, "Extraction, fractionation and functional properties of proteins from the microalgae *Chlorella vulgaris*," *Bioresource Technology*, vol. 157, pp. 134-139, 2014.
- [20] C. Safi, A. V. Ursu, C. Laroche, B. Zebib, O. Merah, P.-Y. Pontalier, and C. Vaca-Garcia, "Aqueous extraction of proteins from microalgae: Effect of different cell disruption methods," *Algal Research*, vol. 3, pp. 61-65, 2014.
- [21] P. R. Postma, G. Pataro, M. Capitoli, M. J. Barbosa, R. H. Wijffels, M. H. M. Eppink, G. Olivieri, and G. Ferrari, "Selective extraction of intracellular components from the microalga *Chlorella vulgaris* by combined pulsed electric field-temperature treatment," *Bioresource Technology*, vol. 203, pp. 80-88, 2016.
- [22] M. Coustets, N. Al-Karablieh, C. Thomsen, and J. Teissie, "Flow Process for Electroextraction of Total Proteins from Microalgae," *Journal of Membrane Biology*, vol. 246, pp. 751-760, Oct 2013.
- [23] T. Kotnik, W. Frey, M. Sack, S. Haberl Meglič, M. Peterka, and D. Miklavčič, "Electroporation-based applications in biotechnology," *Trends in Biotechnology*, vol. 33, pp. 480-488, 2015.
- [24] A. Golberg, M. Sack, J. Teissie, G. Pataro, U. Pliquett, G. Saulis, T. Stefan, D. Miklavcic, E. Vorobiev, and W. Frey, "Energy-efficient biomass processing with pulsed electric fields for bioeconomy and sustainable development," *Biotechnology for Biofuels*, vol. 9, pp. 1-22, 2016.



Wolfgang Frey received the Diploma degree in high voltage engineering and plasma physics and the Ph.D. degree in laser triggering of rail gap switches from the University of Karlsruhe, Germany, in 1989 and 1996, respectively. He was an assistant professor with the High Voltage Institute, at the University of Karlsruhe, Germany, working on new pulse forming concepts, high voltage test engineering, and gas insulated spark gaps. In 1997, he joined the Pulsed Power Group of the former Research Center of Karlsruhe, Karlsruhe, Germany, now Campus North of Karlsruhe Institute of Technology (KIT). He started with surface coating by pulsed electron beam ablation, conducted research and engineering on electrodynamic fragmentation for material processing and switched to pulsed electric field effects on biological matter in 2001. He focused on application-oriented research on pulsed electric field treatment for bacterial decontamination, cell ingredient extraction from plant material and on basic diagnostics for ns-timescale membrane-voltage-dynamics measurement. Since 2006, he has been a team leader in Bioelectrics with the Institute for Pulsed Power and Microwave Technology, KIT, Campus North. Current research interest is pulsed electric field processing of microalgae for economic cell component extraction.

NOTES

Conductivity Tensor Imaging using MRI

Eung Je Woo

Department of Biomedical Engineering, College of Medicine, Kyung Hee University, Seoul, Korea

Abstract: The electrical conductivity of a biological tissue is a passive material property determining how much conduction current occurs for an applied voltage or injected current. Externally injected current into an electrically conducting object such as the human body produces distributions of current density, electric field and magnetic field, which are determined by the conductivity distribution as well as the boundary geometry and electrode configuration. At low frequency, some biological tissues such as the muscle and white matter exhibit relatively strong anisotropic properties stemmed from their structural directionality. *In vivo* imaging of anisotropic conductivity, current density and electric field distributions inside the human body is desirable in clinical applications such as tDCS, DBS and electroporation. This paper describes two recently developed techniques for high-resolution anisotropic conductivity tensor imaging using MRI. Both methods are based on diffusion MRI from which directions of the conductivity tensor are obtained. To determine magnitudes of the conductivity tensor, one method utilizes the MREIT technique where low-frequency currents are injected and the induced internal magnetic flux density distributions are measured. The other method uses the MREPT technique where high-frequency isotropic conductivity images are obtained from measured B1 maps. Briefly reviewing both methods, typical anisotropic conductivity tensor images from *in vivo* animal subjects are presented and future research directions are suggested.

ELECTRICAL CONDUCTIVITY AND ITS IMAGING AT LOW FREQUENCY

The electrical conductivity of a biological tissue is determined by concentrations and mobility of charge carriers such as ions and charged molecules. Unlike ion concentrations which are scalar quantities, their mobility at low frequency is influenced by the microscopic tissue structure such as directions and density of cells, extracellular matrix materials, viscosity of extracellular fluid, etc. Therefore, the low-frequency conductivity can be modelled as a tensor to express its anisotropic property.

Electrical impedance tomography (EIT) as a conductivity imaging modality has recently reached the stage of clinical applications especially for real-time functional imaging of lung ventilation. For high-resolution conductivity imaging at low frequencies, magnetic resonance electrical impedance tomography (MREIT) has been developed since 1990s. It succeeded the magnetic resonance current density imaging (MRCDI) technique where an MRI scanner is utilized as a tool to measure the magnetic flux density induced by an externally injected current. Measuring all three components of the magnetic flux density requires rotations of the imaging object inside the scanner since the scanner can measure only one component of the magnetic flux density parallel to its main magnetic field. Without rotating the imaging object, MREIT measures only one component of the magnetic flux density to reconstruct isotropic or equivalent isotropic conductivity images [1].

CONDUCTIVITY TENSOR IMAGING USING INJECTION CURRENTS

Diffusion tensor magnetic resonance electrical impedance tomography (DT-MREIT) combines DTI and MREIT to produce images of anisotropic conductivity tensor distributions [2]. It is based on the assumption that the electrical conductivity and water diffusion tensors share the same eigenvectors [3]. We speculate that this assumption is valid for most wet soft tissues since mobility of ions and water molecules in such a tissue are influenced by the same structural environment. Obtaining the eigenvectors from diffusion tensor images, we need to determine the pixel-dependent scale factor to determine the conductivity tensor. Recently, Kwon *et al.* developed a DT-MREIT method, which recovers the scale factor using the measured data of magnetic flux density (B_z) induced by externally injected currents.

We express a conductivity tensor $\mathbf{\Lambda}$ at a certain position as $\mathbf{\Lambda} = \eta \mathbf{D}$ where \mathbf{D} is a water diffusion tensor from DTI and η is a position-dependent scale factor. From Ohm's law, $\mathbf{J} = -\mathbf{\Lambda} \nabla u = -\eta \mathbf{D} \nabla u$ where \mathbf{J} and u are current density and voltage, respectively. Using the measured data of B_z , we first estimate the projected current density \mathbf{J}^P , which is a best approximation of the true current density \mathbf{J} . The DT-MREIT conductivity tensor image reconstruction algorithm iteratively finds the pixel-dependent scale factor η by using \mathbf{J}^P and the forward model of the imaging object. Once η is estimated from the measured data of magnetic flux density (B_z), we can produce the image of the anisotropic conductivity tensor.

To verify the proposed DT-MREIT technique, we performed *in vivo* canine brain imaging experiments by injecting imaging current of 2 mA through two pair of carbon-hydrogel electrodes ($30 \times 30\text{cm}^2$) attached on the surface of the head. We collected the B_z^i ($i = 1, 2$) data using the coherent steady state multi-gradient echo (CSS-MGRE) sequence. Imaging parameters were TR/TE = 300/2.3 msec, FOV = $160 \times 160 \text{mm}^2$, slice thickness = 5 mm, number of echoes = 13, NEX = 35, matrix size = 128×128 . We obtained DTI data with b -values of 800sec/mm^2 at the same slice position using the single-shot spin-echo EPI (SS-SE-EPI) sequence with TR/TE = 2000/67 msec. One reference MR data was also obtained without diffusion sensitized gradient to measure diffusion tensor. Imaging parameters were TR/TE = 8000/94 msec, FOV = $160 \times 160 \text{mm}^2$, matrix size = 112×112 , and total scan time to collect one set of diffusion tensor images was about 8.8 min.

Fig. 1(a) shows an MR magnitude image of the brain region. Fig. 1(b) and (c) plot the acquired B_z^1 and B_z^2 images subject to the horizontal and vertical, respectively, pairs of the surface electrodes. We computed the projected current density images $|\mathbf{J}_p^1|$ and $|\mathbf{J}_p^2|$ shown in Fig. 2(a) and (b) using the measured B_z^1 and B_z^2 data, respectively. Utilizing the acquired DTI images together with the current density images in Fig. 2(a) and (b), we estimated the pixel-dependent scale factor η shown in Fig. 2(c). The recovered scale factor η clearly shows position dependency, which indicates obvious heterogeneity of the conductivity distribution within the brain.

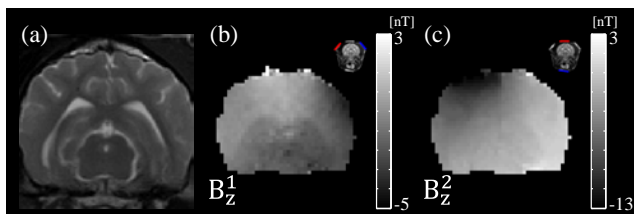


Figure 1: (a) MR magnitude image of a canine brain, (b) measured B_z^1 image subject to horizontal current injection and (c) measured B_z^2 image subject to vertical current injection.

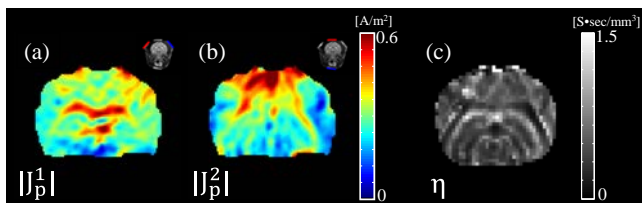


Figure 2: (a) projected current density $|\mathbf{J}_p^1|$ image computed by using B_z^1 data, (b) projected current density $|\mathbf{J}_p^2|$ image computed by using B_z^2 data and (c) image of the position-dependent scale factor η .

Using the estimated scale factor η , we reconstructed the anisotropic conductivity tensor image shown in Fig. 3. For comparison, we showed the tensor plots of the conductivity and water diffusion tensors in Fig. 4. Due to the position-dependent scale factor recovered by the proposed DT-MREIT method, the sizes of the reconstructed conductivity tensors are quite different from those of the water diffusion tensors.

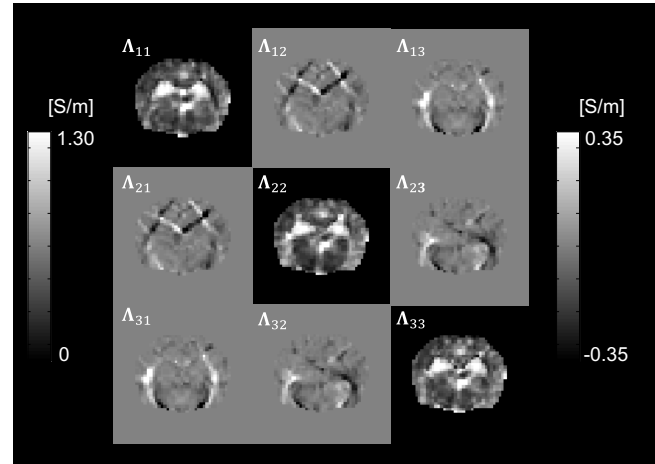


Figure 3: Reconstructed conductivity tensor image.

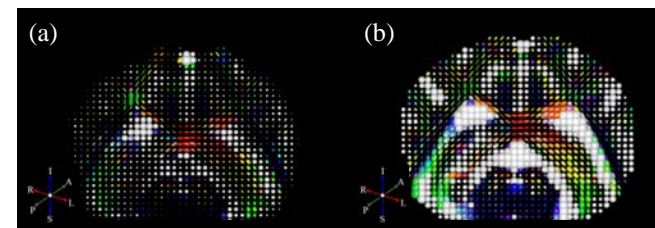


Figure 4: Tensor plots of (a) reconstructed conductivity tensor and (b) water diffusion tensor.

In diagnostic imaging applications of DT-MREIT and MREIT, the amount of injection current should be limited to a safe level below the threshold of perception preferably or the threshold of muscle contraction at least. Though there exists a safety standard such as the IEC 60601 for the auxiliary patient current of continuous sinusoidal waveform, there is no safety standard yet for pulse type imaging currents. For diagnostic DT-MREIT and MREIT imaging, there should be an established protocol to determine the amount of imaging current beforehand for each patient. For example, one may gradually increase the amount of imaging current to find the threshold of perception. Future studies should focus on how to improve the image quality when imaging currents are limited below 1 mA.

CONDUCTIVITY TENSOR IMAGING WITHOUT USING INJECTION CURRENTS

Though the DT-MREIT technique is applicable to such cases as tDCS, DBS and electroporation where currents are injected for the treatments anyway, it would be desirable to reconstruct anisotropic conductivity tensor images without injecting current for diagnostic imaging and also treatment planning. Lately, Kwon *et al.* developed a new method of conductivity tensor imaging (CTI) using the MREPT and multi-b diffusion MRI techniques [4]. Since both of them are implemented in a clinical MRI scanner without added hardware, its clinical applications are expected to be accelerated.

The CTI technique acquires high-frequency isotropic conductivity images using MREPT, which is based on the B1 mapping method. At 3 T, MREPT images are conductivity images at about 128 MHz where conductivity values of the extra-cellular and intra-cellular spaces are volume-averaged. If we inject current at low frequency, it cannot penetrate the insulating cellular membranes and flows through only the extra-cellular space. In CTI, we assume that the conductivity and water diffusion tensors share the same directional property since ions and water molecules exist in the same microscopic structural environment. Using the multi-b diffusion MRI technique, we remove the effects of the intra-cellular space from the acquired high-frequency conductivity images. Then, by incorporating the directional information of the water diffusion tensor into the conductivity tensor image reconstruction, we could produce *in vivo* conductivity tensor images of a canine brain as shown in Fig. 5.

DISCUSSION AND CONCLUSION

In vivo imaging of the anisotropic conductivity tensor distribution inside the canine brain with 128×128 image matrix and 1.25 mm pixel size has been experimentally demonstrated. The new imaging method called DT-MREIT successfully combined the directional water mobility information from DTI scans and the ion concentration information from MREIT scans to produce quantitative maps of the internal distribution of the anisotropic conductivity tensor. Current density and electric field imaging as well as conductivity tensor imaging using DT-MREIT may enable personalized treatment planning and monitoring of tDCS, DBS and electroporation.

CTI, on the other hand, is more for diagnostic imaging since it does not require current injection.

Conductivity tensor images are expected to provide diagnostic information related with the microscopic structural environment and also the average ion concentration in each voxel. Series of experimental DT-MREIT and CTI studies should follow for quantitative statistical analyses and interpretations of reconstructed anisotropic conductivity images. We suggest future studies of *in vivo* animal imaging experiments with numerous disease models and treatment methods to validate clinical significance of the DT-MREIT and CTI methods. Modeling and simulation studies of bioelectromagnetic phenomena can also benefit from the anisotropic conductivity tensor data from *in vivo* imaging experiments.

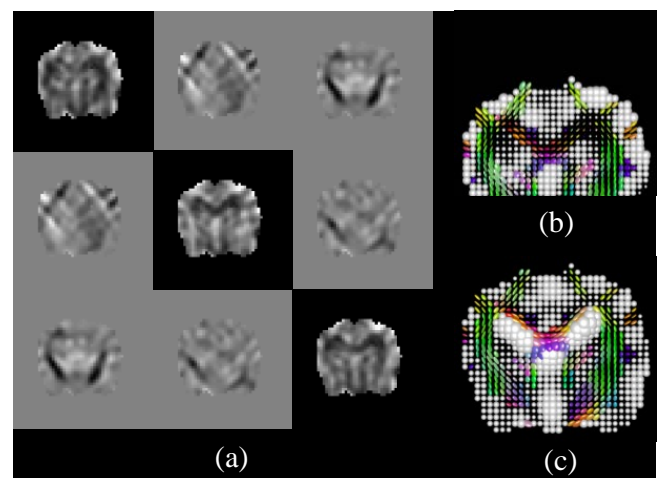


Figure 5: (a) Reconstructed conductivity tensor image of an *in vivo* canine head without using injection current. (b) and (c) Tensor plots of reconstructed conductivity and water diffusion tensors, respectively.

REFERENCES

- [1] J. K. Seo and E. J. Woo, J. K. Seo and E. J. Woo, "Electrical tissue property imaging at low frequency using MREIT," *IEEE Trans. Biomed. Eng.*, vol. 61, no. 5, pp.1390-1399, 2014.
- [2] D. S. Tuch, V. J. Wedeen *et al.*, "Conductivity tensor mapping of human brain using diffusion tensor MRI," *Proc. Nat. Acad. Sci.*, vol. 98, pp. 11697-11701, 2001.
- [3] O. I. Kwon, W. C. Jeong *et al.*, "Anisotropic conductivity tensor imaging in MREIT using directional diffusion rate of water molecules," *Phys. Med. Biol.*, vol. 59, pp. 2955-2974, 2014.
- [4] O. I. Kwon, E. J. Woo *et al.*, "Electrodeless conductivity tensor imaging," in preparation, 2016.

ACKNOWLEDGEMENT

This work was supported by the National Research Foundation (NRF) of Korea grant (2014R1A2A1A09006320).

NOTES

SHORT PRESENTATIONS

The influence of the self – learning mathematically control algorithm on the PEF modulator output characteristics

Mindaugas Visockis¹, Pranas Viškelis¹, Ramunė Bobinaitė¹, Justinas Barakauskas², Vytautas Markevičius², Saulius Šatkauskas³; ¹Lithuanian Research Centre for Agriculture and Forestry, Instituto all. 1, LT – 58344, Akademija town, LITHUANIA, ²Department of Electronics Engineering, University Kaunas of Technology, Studentu st. 48, LT- 51367 Kaunas, LITHUANIA, ³Vytautas Magnus University, Faculty of natural Sciences, Vileikos 8, LT – 44404 Kaunas, LITHUANIA;

INTRODUCTION

It has been reported that there are about 25 different parameters that can affect results of PEF processing in case that many of them are directly related to each other [1]. The most typical processing parameters that characterize PEF technology are electric field strength, pulse shape, pulse width, number of pulses, input energy and pulse repetition frequency [2]. But it is still less known about the influence of pulse shape on effectiveness of electroporation. The lack of knowledge exists despite the fact that thousands of papers have been published on PEF in the last decades.

Kotnik et. al. concluded that the pulse generators with sub – microsecond risetimes are not a necessity for successful electroporation [3] while Pliquett's results showed that when the slope of the stimulus is very steep, the voltage across the membrane rises faster than pores are created [4].

According to the latest results we suggest that pulse rise time should be considered as well as other output characteristics of PEF modulators.

METHODS

Our developed solid-state Marx modulator consists of 25 identical stages. Each stage is independently triggered by an optical fiber line. Stages are powered from controlled 0 – 1.2 kV power supply.

For power switching 4 IGBTs and 1 SiCFET per stage are used. Energy is stored in a battery of 30 μ F capacitance per stage.

The self-learning (self-tuning) algorithm is the innovation which provides with possibility to alter all pulse characteristics in real time. As mentioned before all stages are controlled independently and sum of all these stages' energy was delivered to the output. For better rise/fall times and high power, SiCFET and IGBT's combination are used for switching - in beginning of pulse forming all stage's transistors have been triggered at same time but than IGBT's conductance reaches max value, SiCFET are being turned off. Opposite sequence for turning current off – SiCFET switched on, IGBTs starts closing and when IGBT's conductivity is near 0, SiCFET turns off.

RESULTS

By using this switching technology, fast processing and measurement based on FPGA, independent stage control makes it possible to modulate almost any form of pulse or square pulse with changeable rise/fall times (Figure 1).

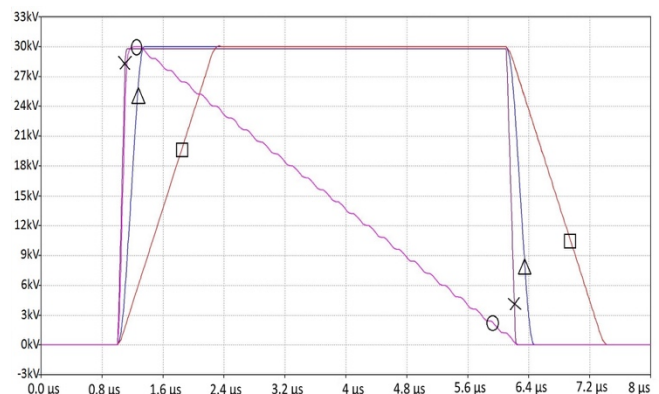


Figure 1: Example of changeable rise times and saw pulse shape.

Furthermore, there is a possibility to control stages by feedback signal – control unit measures difference between set and real pulses and increases current to reach needed voltage value. Therefore, when pulse is delivered to biological structure its shape and voltage amplitude is maintained practically the same as it was established on user control interface.

CONCLUSION

In order to increase the capacity of researches done, we developed a device, which provide possibility to use a wide range of pulse shapes and amplitudes.

REFERENCES

- [1] M. Kempkes et. al. Removing Barriers to Commercialization of PEF Systems and Processes. in *Proceedings of 3rd School on PEF processing of food*. 2016. pp. 171 – 176.
- [2] J. Raso. Microbial inactivation in foods by Pulsed Electric Fields. in *Proceedings of 3rd School on PEF processing of food*. Dublin, 2016. pp. 45– 53.
- [3] T. Kotnik et. al. Role of pulse shape in cell membrane electroporation. *Biophysica Acta*, vol. 16 (14), 2003. pp.193 – 200.
- [4] U. Pliquett. Electrical measurements for monitoring electroporation. in *Proceedings of IFMBE*, Portorož, vol. 53, 2015. pp. 79 – 82.

Creation of cell aggregates by dielectrophoresis for the in vitro study of electrochemotherapy

Jonathan Cottet^{1,2}, Marie Frénéa-Robin¹, François Buret¹, Philippe Renaud²; ¹ Univ Lyon, ECL, UCB Lyon 1, CNRS, AMPERE, F-69130, Ecully, FRANCE ² Laboratory of Microsystems 4, Ecole Polytechnique Fédérale de Lausanne (EPFL) Lausanne, SWITZERLAND

INTRODUCTION

Exposure of cells to short and intense electric pulses results in temporary permeabilization of the cell membrane. This increased membrane permeability is exploited in electrochemotherapy (ECT) where it enhances the delivery of drugs such as bleomycin directly in the cells. There are currently 150 cancer centers that already use ECT for treating skin tumors. However, the full development of this therapeutic approach requires a proper understanding of the electric field impact on biological tissues. Despite the useful information on how electric pulses induce cell membrane permeabilization provided by in vitro studies on isolated cells, more realistic 3D models are required to mimic the behavior of cells in a tumor or a tissue and optimise electroporation protocols.

METHODS

We present a microfluidic platform for cell aggregation in flow based on negative dielectrophoresis (nDEP). When specific experimental conditions are met (applied voltage and frequency, medium composition), cells are retained together in low field region and subsequently aggregate.

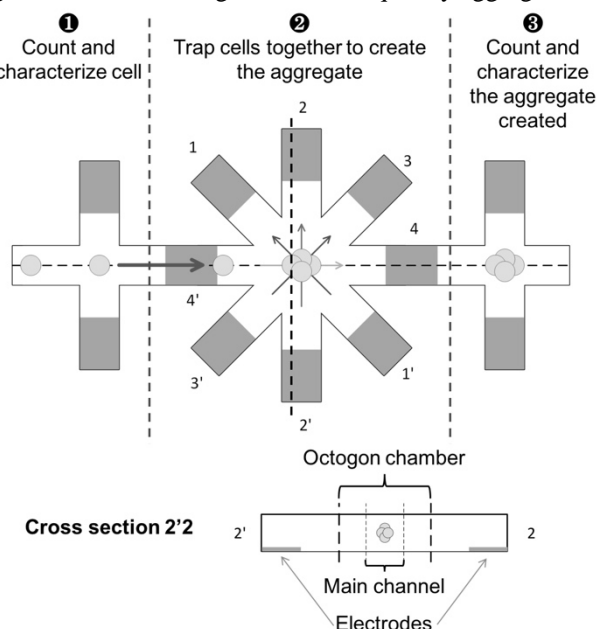


Figure 1: Concept of the chip developed to characterize cells and to create cell aggregates by dielectrophoresis.

The electrode configuration used for this device is based on a concept originally developed at EPFL known as “liquid electrodes” (Figure 1) [1]. This configuration exploits planar electrodes fabricated on the bottom of dead-end chambers placed on each side of a microfluidic channel and acting similarly to thick electrodes embedded in the channel walls.

The electrodes used for nDEP can also be used for cell aggregate electroporation or characterization.

RESULTS

2D Comsol simulations were performed to determine the spatial distribution of the DEP force which is proportional to ∇E^2 . By simulation we found a suited electrical potential arrangement that enables to trap cells in flow. The particle tracing mode was used to locate where the cells will be trapped in the chamber, position indicated with the gray point in the simulations (Figure 2).

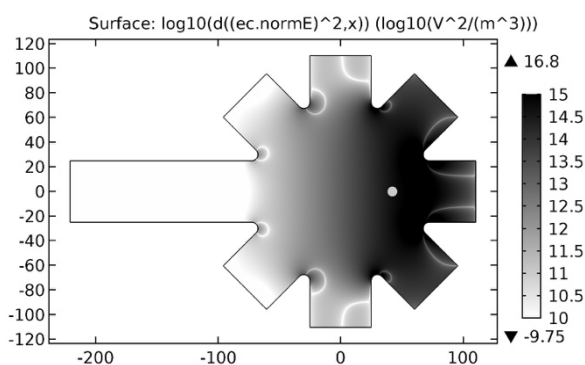


Figure 2: ∇E^2 along x axis. Axes scale is in μm and only the 3 electrodes located on the right are supplied with $10V_{\text{peak-to-peak}}$

CONCLUSION

The proposed microsystem will be used to create aggregates of cells (of different sizes and properties) which will be electroporated and characterized. The experimental data before and after electroporation will help to create an intermediary level to model electroporation from the cell to the tissue level.

REFERENCES

- [1] N. Demierre, T. Braschler, P. Linderholm, U. Seger, H. v. Lintel, and P. Renaud, " Characterization and optimization of liquid electrodes for lateral dielectrophoresis," *Lab on a Chip*, vol. 7, vol. 7, pp. 355-365, 2007

Pulsed Magnetic Field Assisted Electroporation of Yeast

Vitalij Novickij¹, Audrius Grainys¹, Eglė Lastauskienė², Rūta Kananavičiūtė², Dovilė Pamedydytė², Lilija Kalėdienė², Jurij Novickij¹, Damijan Miklavčič³; ¹ Institute of High Magnetic Fields, Vilnius Gediminas Technical University, Naugarduko 41, LT-03227 Vilnius, Lithuania; ² Department of Microbiology and Biotechnology, Vilnius University, Sauletekio 7, LT-03101 Vilnius, Lithuania; ³ Faculty of Electrical Engineering, University of Ljubljana, Trzaska 25, SI-1000 Ljubljana, SLOVENIA

INTRODUCTION

The biological effects of pulsed magnetic field (PMF) are poorly understood and the electroporation as the permeabilization mechanism during PMF treatment is hypothetical, while the PMF permeabilization methodology proved to be successful both *in vitro* and *in vivo* [1,2]. Therefore, we have conceived experiments in which we investigated the membrane electroporation in yeast using separate and simultaneous exposure of cells to pulsed magnetic and electric fields.

METHODS & RESULTS

For the pulsed magnetic field generation the 43 kJ pulse generator (see Fig. 1) was used [3]. The inductor (16 windings) with integrated 1 mm electrode gap electroporation cuvette was used as a load. The cuvette was connected to a square wave electroporator, which was synchronized with PMF system. The setup was capable of generating separate and simultaneous PEF (0–3 kV/cm, 100 ns – 1 ms) and PMF (0–9 T, 0.5 ms) pulses.

Candida lusitanae C18 strain was used in experiments. *C. lusitanae* cells were grown on the rich YPD medium (2% glucose, 2% peptone, 1% yeast extract and 1% agar).

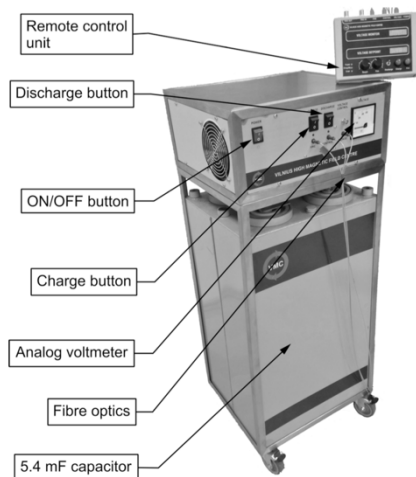


Figure 1: Photograph of 43 kJ PMF generator

After 48 h at 30 °C the cells were harvested and washed with 1 M sorbitol. For further experiments the 10¹⁰ cells/ml density suspension was prepared in 1 M sorbitol. The permeabilization was evaluated via the propidium iodide (PI) assay (50 μM). The single-pulse 8 kV/cm microsecond range (100–250 μs) protocol separately and in combination with PMF (3–9 T) was applied [4].

The results of *C. lusitanae* permeabilization in PMF and PEF are presented in Fig. 2. As expected, after the PEF pulse without the magnetic field component the number of PI fluorescent cells has increased up to 31±8% (8 kV/cm, 250 μs). The single 0.5 ms PMF pulse did not result in any permeabilization independently from the used amplitude. However, the simultaneous exposure of the cells to PMF and PEF resulted in a combinatorial effect, which was statistically significant (P<0.05) in the 6 and 9 T experiments in the whole range of applied PEF pulses.

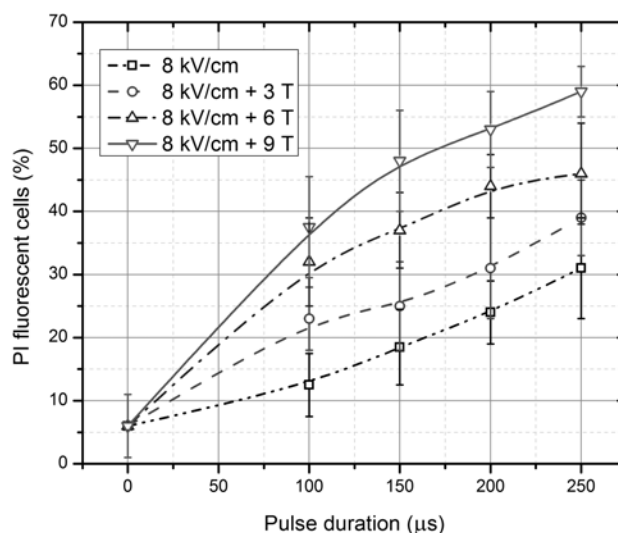


Figure 2: Permeabilization of *C. lusitanae* after pulsed electric and/or magnetic field treatment

REFERENCES

- [1] Kranjc, S. *et al.* “Electrochemotherapy by pulsed electromagnetic field treatment (PEMF) in mouse melanoma B16F10 *in vivo*”, *Radiol. Oncol.* vol. 50, pp. 39-48, 2016.
- [2] Towhidi, L. *et al.* “Lucifer Yellow uptake by CHO cells exposed to magnetic and electric pulses”, *Radiol. Oncol.* vol. 46, pp. 119-125, 2012.
- [3] Grainys, A. *et al.* “Single pulse calibration of magnetic field sensors using mobile 43 kJ facility”, *Measurement Science Review*, vol. 15, pp. 244-246, 2015.
- [4] Novickij, V. *et al.* “Pulsed Electromagnetic Field Assisted *in vitro* Electroporation: A Pilot Study”, *Scientific reports*, vol. 6, 33537, 2016.

Effect of time duration between HV and LV pulses on DNA electrotransfection efficiency *in vitro*

Milda Jakutavičiūtė¹, Sonam Chopra¹, Aurelija Kazlauskaitė¹, Paulius Ruzgys¹, Saulius Šatkauskas¹
¹*Vytautas Magnus University, Department of Biology, LT-3000 Kaunas, LITHUANIA*

INTRODUCTION

Gene electrotransfer is a promising and expanding technique for various clinical applications, such as DNA vaccination and gene therapy, which is becoming a suitable alternative to virus-based methods. The main focus of our study in this field was to improve gene electrotransfection efficiency by combining high voltage (HV) and low-voltage (LV) electric pulses [1,2]. We investigated the effect of time duration between high-voltage (HV) and low-voltage (LV) electric pulses on plasmid DNA electrotransfer efficiency to CHO cells *in vitro*. Green fluorescent protein (GFP) coding plasmid was used in the experiments. We evaluated electrotransfection efficiency for GFP coding plasmid using flow cytometry to determine the percentage of GFP positive cells and the fluorescence intensity in them. The best electrotransfection efficiency was obtained with minimum time duration between HV and LV pulses. However, cell viability at lowest time duration between HV and LV pulses was also significantly decreased.

MATERIALS AND METHODS

Chinese hamster ovary (CHO) cells were used in the experiments. For each experimental point, 45 μ l of cell suspension containing 9×10^5 cells were supplemented with 5 μ l of plasmid solution, reaching either 50 μ g/ml or 100 μ g/ml plasmid DNA concentration. The cells were then pulsed with one HV pulse that had pulse amplitude of 1200 V/cm and pulse duration of 100 μ s, and one LV pulse which had pulse amplitude of 100 V/cm and duration of 100 ms. The time durations between HV and LV pulses were set to be 1 μ s, 10 μ s, 100 μ s, 1 ms, 10 ms, 100 ms and 1 s. After electroporation, cells were incubated for 10 minutes at room temperature for the pores to reseal. For detection of GFP coding plasmid electrotransfer, cells were placed in 24-well plate and grown for 24 hours. Cell viability was determined, using clonogenic assay. After that, the percentage of GFP positive cells as well as average fluorescence intensity in them was detected with flow cytometer (BD Accuri C6, BD Biosciences, San Jose, USA). Results are represented as means from at least 6 experimental points + SEM.

RESULTS

In order to systematically determine the effect of microsecond to second length delay between HV and LV pulses on electrotransfection efficiency to cells *in vitro*, we transfected CHO cells with GFP coding plasmid. Flow cytometry based detection allowed us to estimate both the percentage of cells transfected with GFP coding plasmid and the fluorescence intensity in GFP positive cells that correlates with the amount of GFP coding plasmid transferred into the cells. Our results showed no significant difference between the number of GFP positive cells in

dependence of time duration between HV and LV. Unsurprisingly, 100 μ g/ml plasmid concentration yielded higher percentage of GFP positive cells than 50 μ g/ml plasmid concentration. The percentage of GFP positive cells was around 17 percent with lower plasmid concentration and around 23 percent with higher plasmid concentration and there were no statistically significant differences between points with different durations of delay between HV and LV. Also, higher plasmid concentration yielded higher overall fluorescence. For evaluation of the effect that delay between HV and LV pulses had on the fluorescence of GFP positive cells, a ratio between fluorescence with HV+LV protocol and single HV pulse was calculated (Figure 1). Delays up to 100 ms (for 50 μ g/ml plasmid concentration) or up to 10 ms (for 100 μ g/ml plasmid concentration) yielded statistically significant difference from 1 second delay. It should also be noted that 50 μ g/ml plasmid concentration shows more notable increase in efficiency of HV+LV protocol.

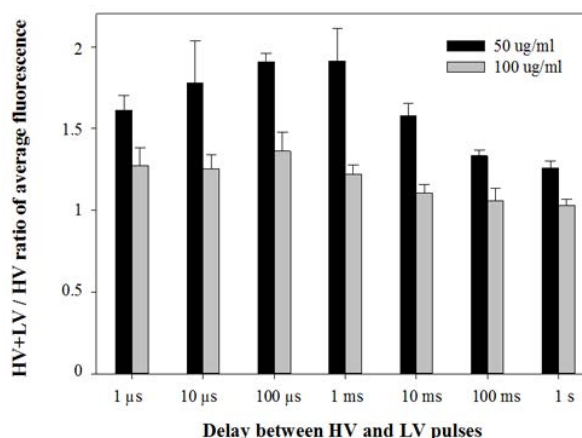


Figure 1: The increase in GFP positive cell fluorescence after HV+LV protocol in comparison to single HV protocol. Light grey bars: 50 μ g/ml plasmid concentration, black bars: 100 μ g/ml plasmid concentration.

REFERENCES

- [1] M. Kandušer, D. Miklavčič, and M. Pavlin, "Mechanisms involved in gene electrotransfer using high- and low-voltage pulses — an *in vitro* study," *Bioelectrochemistry*, vol. 74, pp. 265–271, Feb. 2009.
- [2] C. Rosazza, S. Meglic, A. Zumbusch, M.-P. Rols, and D. Miklavcic, "Gene Electrotransfer: A mechanistic perspective," *Current Gene Therapy*, vol. 16, pp. 98–129, Apr. 2016.

Effect of low-energy pulsed electron beams on bacterial spore DNA

Charlotte Da Silva¹, Camille Lamarche^{1,2}, Gauthier Demol², Marie-Pierre Rols¹, Flavien Pillet¹.

¹ CNRS UMR 5083, IPBS (Institut de Pharmacologie et de Biologie Structurale), 205 route de Narbonne BP64182, F-31077 Toulouse Cédex 04, FRANCE. ² ITHPP Alcen, Hameau de Drèle, F-46500 Thégra, FRANCE.

INTRODUCTION

High-energy continuous electron beam irradiation is commonly used in industrial sterilization processes for decontamination of pathogens. However, it is a large-size technology which requires complex shielding and high voltage not compatible with heat-sensitive products [1].

In this context, the International Technologies for High Pulsed Power (ITHPP) society has developed a compact low-energy pulsed electron beam (LEPEB) system with a high sterilization speed which delivers uniform nanosecond pulses without increasing the temperature.

However, the mechanism leading to bacterial death is not well understood. The main hypothesis is that LEPEBs deliver high dose rate that induces single and double strand breaks on DNA [1]. The purpose of this study is to investigate the effects of low-energy pulsed electron beam on spore DNA.

METHODS

Bacillus pumilus spores are spotted onto the surface of a Petri dish and air-dried at room temperature. Spots are irradiated and then recovered in water for DNA extraction, as described by Douki *et al.* [2] with adjustments. Briefly, after centrifugation, spores are decoated by suspending the pellets in a detergent solution for 90 min at 37°C. Genomic DNA is then extracted *in situ* in agarose by suspending the pellets in 2 mg/mL lysozyme and 0.2 mg/mL RNase A solution. After incubation for 2 h at 37°C, the suspension is mixed with an equal volume of 2% agarose, dispensed in a plug mold (Bio-Rad) and allowed to solidify at room temperature. Plug is transferred in 1 mg/mL proteinase K solution and incubated overnight at 50°C. The plug is digested overnight at 37°C with 30 U of *NotI*. DNA fragments are separated by pulsed-field gel electrophoresis (PFGE) using the CHEF-DR III system in 1% agarose gel and 0.5X TBE buffer for 20 h at 14°C and at 6 V/cm with pulse time increasing from 1 to 120 s at 120°. Gel is stained in 0.5 µg/mL ethidium bromide solution for 30 min and destained for 30 min in distilled water before visualization under UV-light transilluminator.

RESULTS

Critical steps were to extract the entire genomic DNA from spores which are very resistant structure and find the best PFGE parameters to obtain high-resoluted patterns (Figure 1).

The *NotI*-restriction profile obtained from non-irradiated *B. pumilus* spores reveals approximately 14 fragments between 24.5 kb and 776 kb.

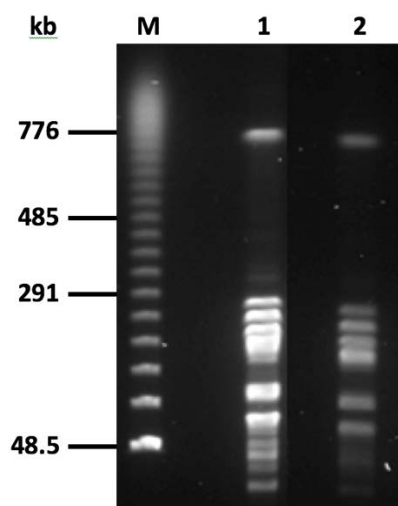


Figure 1: PFGE patterns of genomic DNA from non-irradiated *B. pumilus* spores after *NotI*-digestion. Lane M: lambda ladder (Bio-Rad), lane 1: DNA from suspension at $OD_{600\text{ nm}} = 5$, lane 2: DNA from suspension at $OD_{600\text{ nm}} = 2$.

CONCLUSION

We have successfully extracted DNA from *B. pumilus* spores and found the best electrical parameters for a high-quality PFGE analysis.

The next step will be to compare irradiated and non-irradiated DNA profiles. If LEPEB induces DNA damages, smears or new fragments should be observed for irradiated DNA.

ACKNOWLEDGEMENTS

This research is performed in the scope of the EBAM European Associated Laboratory (LEA). We are supported by the Centre National de la Recherche Scientifique (CNRS), the Direction Générale de l'Armement (DGA) and Direction Générale des Entreprises (DGE), DEEP Project.

REFERENCES

- [1] P. R. Chalise *et al.*, « Bacterial inactivation using low-energy pulsed-electron beam », *IEEE Trans. Plasma Sci.*, vol. 32, n° 4, p. 1532-1539, août 2004.
- [2] T. Douki, B. Setlow, et P. Setlow, « Effects of the binding of alpha/beta-type small, acid-soluble spore proteins on the photochemistry of DNA in spores of *Bacillus subtilis* and *in vitro* », *Photochem. Photobiol.*, vol. 81, n° 1, p. 163-169, févr. 2005.

High-frequency chips and oxidation induced chemiluminescence

Michal Cifra, Kateřina Červinková, Daniel Havelka, Ondrej Krivosudský, Michaela Poplová, Jiří Průša, Petra Vahalová. *Institute of Photonics and Electronics, The Czech Academy of Sciences, Chaberská 57, 18200, Prague, CZECHIA*

SUMMARY

Pulsed electric fields have already wide use and further great potential for novel applications in biomedicine and food industry. Although not fully explored, one mechanism of the electric pulses action in biological samples is through the electric field induced oxidation [1]. Our aim is to employ endogenous chemiluminescence for label-free interrogation of the oxidative effects [2] of us-ns electric pulses in biosamples [3] on chips. To this end, (i) to gain molecular understanding of complex permittivity which is required for accurate design and impedance matching of the future chips for the electric pulses exposition, we developed high-frequency chips to measure (Fig. 1) and employed molecular dynamics to predict (Fig. 2) the complex permittivity of simple biomolecular solutions and (ii) developed ultra-sensitive system for photon detection and demonstrated that the endogenous biological chemiluminescence is due to the oxidative reactions with biomolecules (Fig. 3).

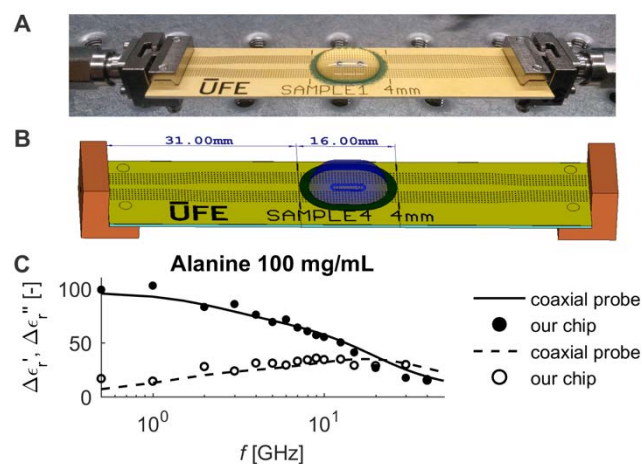


Figure 1: A The photo and B Computer Simulation technology (CST) Microwave Studio model of our chip and C complex permittivity (alanine 100 mg/mL) extracted from measurements with our chip (250 μ L sample) vs. reference measurement with bulk volume commercial method (5 mL sample).

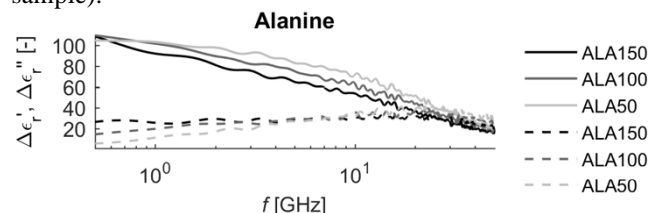


Figure 2: Real and imaginary parts of complex permittivity of alanine solutions extracted from molecular dynamics

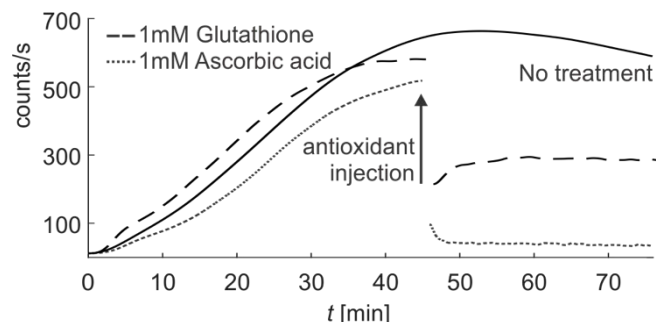


Figure 3: As a model system, all-trans retinoic acid differentiated HL-60 cells in RPMI-1640 medium (3 mL) are stimulated by phorbol 12-myristate 13-acetate to induce production of reactive oxygen species (ROS) which react with biomolecules in cells and cell medium to generate endogenous chemiluminescence (photon counts/s, smoothed signal). Antioxidants (1 mM glutathione or ascorbic acid) scavenge the ROS and decrease the chemiluminescence intensity, suggesting thus the oxidation based mechanism of chemiluminescence generation.

CONCLUSIONS

Our results provide the basis for new on-chip pulsed field/microwaves based generation and monitoring of the oxidative/radical processes in biosamples.

ACKNOWLEDGEMENTS

We acknowledge support by the Czech Science Foundation, project no. P102/15-17102S. Authors participate in COST Action BM1309 and bilateral exchange project between Czech and Slovak Academies of Sciences, no. SAV-15-22. Computational resources were provided by the CESNET LM2015042 and the CERIT Scientific Cloud LM2015085, provided under the programme "Projects of Large Research, Development, and Innovations Infrastructures"

REFERENCES

- [1] O.N. Pakhomova, et al. "Oxidative effects of nanosecond pulsed electric field exposure in cells and cell-free media." *Archives of biochemistry and biophysics*, vol. 527, pp. 55-64, 2012
- [2] M. Cifra and P. Pospíšil. "Ultra-weak photon emission from biological samples: definition, mechanisms, properties, detection and applications." *Journal of Photochemistry and Photobiology B: Biology* vol. 139, pp. 2-10, 2014
- [3] M. Maccarrone, et al. "Kinetics of ultraweak light emission from human erythroleukemia K562 cells upon electroporation." *Biochimica et Biophysica Acta (BBA)-Biomembranes*, vol. 1414, pp. 43-5, 1998.

The electroporation of guard cells improves the quality of dried Genovese basil (*Ocimum basilicum* L.) leaves

Stephen Kwao^a, Said Al-Hamimi^b, María Elena Vicente Damas^{ad}, Allan G. Rasmusson^c and Federico Gómez Galindo^a; ^a *Food Technology, Engineering and Nutrition, Lund University, PO Box 124, SE-221 00 Lund, SWEDEN.* ^b *Center for Analysis and Synthesis, Lund University, PO Box 124, SE-221 00 Lund, SWEDEN.* ^c *Department of Biology, Lund University, Sölvegatan 35B, SE-223 62 Lund, Sweden.* ^d *Optifreeze AB, Skiffervägen 12, SE-22478 Lund, SWEDEN*

INTRODUCTION

Aromatic herbs are very sensitive to drying due to a large loss of volatile aroma compounds in the process [1]. It often leads to products with drastically reduced quality [2], regarding flavour, appearance and rehydration properties [3]. In this study the effect of the application of pulsed electric fields (PEF) as pre-treatment before air drying of basil leaves at 50 °C was investigated.

MATERIALS AND METHODS

The parameters of the electric treatment were designed in such a way that they either (i) electroporated the tissue reversibly and without electroporating the guard cells in the stomata complex, (ii) electroporated the tissue reversibly causing the guard cells to open the stomata, or (iii) irreversibly electroporated the tissue leading to cell death.

The treated and untreated samples were dried in a convective air drier equipped with a balance that allowed for continuous monitoring of the process. Drying curves were produced, and the experimental data was fitted to the Newton Model for relative moisture ratio. Based on the experimental data, effective moisture diffusivities (D_{eff}) were calculated.

Treated and untreated basil leaves were dried to a final moisture content of 8%. Their colour, aroma compounds and rehydration capacity were analysed.

RESULTS

Dried samples with electroporated guard cells presented the smallest colour change, when compared to the rest of the treatments. The same PEF treatment also provided the best rehydration capacity (72.2 % of fresh basil leaf) and the chromatograms for the volatile compounds showed a greater retention of aroma. Irreversibly electroporated leaves presented the highest D_{eff} , followed by samples treated with irreversible electroporation of stomata (results shown in Table 1).

Table. 1: *Effective moisture diffusivities obtained for the different treatments*

Treatment	D_{eff} (m ² s ⁻¹)
Control	1.036*10 ⁻⁹
PEF-treated (non-electropotated stomata)	1.309*10 ⁻⁹
PEF-treated (electropotated stomata)	1.857*10 ⁻⁹
PEF-treated (irreversible)	2.586*10 ⁻⁹

CONCLUSIONS

Dehydration of basil leaves can be aided using PEF. If the applied conditions are such that stomata are irreversibly opened while the rest of the tissue remains viable, the drying process is faster and the product keeps a better colour, is richer in aroma compounds and has better rehydration capacity than the untreated control.

REFERENCES

- [1] Di Cesare, L.F., Forni, E., Viscardi, D., & Nani, R.C. (2003). Changes in the chemical composition of basil caused by different drying procedures. *Journal of Agricultural and Food Chemistry*, 51, 3575-3581.
- [2] Ratti, C. (2001). Hot air and freeze-drying of high-value foods: A review. *Journal of Food Engineering*, 49, 311-319.
- [3] Diaz-Maroto, M.C., Sánchez Palomo, E., Castro, L., González Viñas, M.A., & Pérez-Coello, M.S. (2004). Changes produced in the aroma compounds and structural integrity of basil (*Ocimum basilicum* L) during drying. *Journal of the Science of Food and Agriculture*, 84, 2070-2076.

Hydrogel / Carbon nanotubes Needle-free device for Electrostimulated Transdermal Delivery

Jean-François Guillet^{1,2,3}, Muriel Golzio^{1,2}, Emmanuel Flahaut^{1,3}; ¹Univ Paul Sabatier, Toulouse Cedex 9, France, ²IPBS-CNRS UMR5089, Toulouse, France, ³CIRIMAT-CNRS, Toulouse, FRANCE

INTRODUCTION

The permeability of skin allows passive diffusion across epidermis to reach blood vessel but this possible only for small molecule like nicotine. In order to make transdermal delivery of large molecules like insulin or DNA possible, permeability of skin and mainly the permeability of stratum corneum must be increased. More over alternative routes that avoid the use of needles will improve the quality of life of patients. A method named "electropermeabilisation" is shown to increase skin permeability. Here, we report the fabrication of an innovative biomedical device, made of nanocomposite material. This nanocomposite device aims at permeabilizing skin and delivering drug molecules at the same time. It includes a biocompatible polymer matrix (hydrogel) and double-walled-carbon-nanotubes (DWCNT) in order to improve both mechanical and electrical properties. Carbon nanotubes and especially DWNTs [3] are ideal candidates, combining high electrical conductivity with a very high specific surface area (ca. 1000 m²/g) together with a good biocompatibility when included in a material or deposited on a surface [4]. The preparation of the nanocomposite material as well as our first results of electrostimulated transdermal delivery using an ex vivo mouse skin model is presented.

MATERIAL AND METHODS

Preparation of solutions

Agarose (AG) solution was prepared by dissolving dry AG provide by Sigma-Aldrich in water (5% wt, 50 ml, 115-120°C) under stirring at 700-800 rpm for 20-30 min. Dispersion of DWCNT (extracted in HCL solution (37%) for 16 hours, rinse to reach neutral pH) was performed using first Ultraturax (20 min, 8000rpm), followed by probe sonication (1h in (50ml deionized water).

Preparation of the device

Hydrogel was prepared so that final concentration of AG was 2.5% wt. AG were solubilized and blend with sonicated DWCNT 0.5%, 1%, 2%, 3% wt. and treated with Ultraturax treatment (20 min, 80°C). The solutions were then poured into Petri dish and cooled under ambient conditions (20 – 25°C). To mimic penetration of molecule we used Fluorescein isothiocyanate –dextran (FD) (average mol wt 3,000-5,000 Da) from Sigma-Aldrich. The nanocomposite was incubated with 1 mM FD were dissolved in PBS for further use. We obtain a cylindrical gel with 0.7 mm of thickness and 10mm of diameter.

Electroporation of the Skin

The composite electrode device was disposed on skin mouse with copper electrode to insure the contact between the composite and the generator. Electrical parameters were set

at 300V/cm (between electrode) generators, period of 1 000 000 μs, with 10 repetitions are set (ELECTRO cell B10 HVLV), respectively with AGCTRL & AGDWCNT.

RESULTS AND FIGURES

We observe that the swelling ratio of AG and DWCNT AG is constant at pH (5 to 8). The influence of DWCNT on the swelling ratio of AG is shown in Figure 1. An decrease of 6 gr/gr is observed in the DWCNT AG samples.

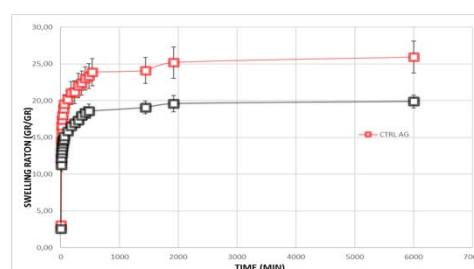


Figure 1: Swelling ratio in gr/gr in function of time of CTRL AG and DWCNT AG

The electroporation experiments were then performed. The lightest fluorescence microscopy images are observed for the samples containing DWCNT. This indicates that the DWCNT increase the release of FD in the skin. In the near future we are going to determine the penetration depth of FD molecules.

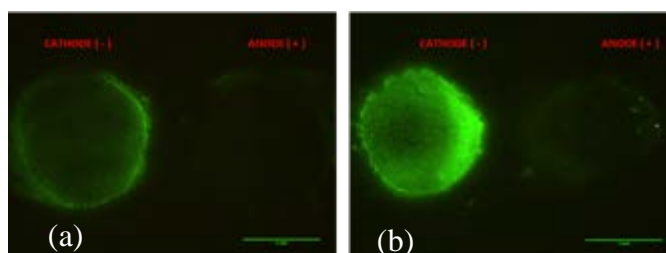


Figure 1: Fluorescence microscopy images of: (a)- CTRL AG and (b) – DWCNT AG

REFERENCES

- [1] E. Flahaut, R. Bacsa, A. Peigney, Ch. Laurent, "Gram-Scale CCVD Synthesis of Double-Walled Carbon Nanotubes", Chem. Commun., (2003), 1442-1443.
- [2] A. Bédouier, F. Seichepine, E. Flahaut, I. Loubinoux, L. Vaysse, Ch. Vieu, "Elucidation of the role of carbon nanotube patterns on the development of cultured neuronal cells", Langmuir, 28, (50), (2012), 17363 – 17371.

Improvement of flap necrosis in a rat random skin flap model by *in vivo* electroporation mediated HGF gene transfer

Morteza Jafari^{1,2,3}, Maziar Shafighi⁴, Helmut Beltraminelli¹, Thomas Geiser^{4,5}, Robert Hunger¹, Amiqa Gazdhar^{4,5}; ¹Department of Dermatology, Inselspital, Bern University Hospital, SWITZERLAND. ²Department of Dermatology, Inselspital, Bern University Hospital, Department of Clinical Research, University of Bern, SWITZERLAND. ³Graduate School for Cellular and Biomedical Sciences University of Bern, SWITZERLAND. ⁴Department of Clinical Research, University of Bern, SWITZERLAND. ⁵Department of Pulmonary Medicine, Bern University Hospital, SWITZERLAND.

INTRODUCTION

In spite of improved understanding in the mechanisms governing flap necrosis and recent advances in surgical techniques, tissue ischemia and skin flap necrosis remain crucial in clinical setting [1,2], This challenge provides an opportunity to explore novel methods to improve circulation, accelerate wound healing and increase flap survival [3]. In an attempt to enhance flap survival, a number of growth factors have been employed to promote angiogenesis and improve the local circulation [3-4]. Hepatocyte growth factor (HGF) is a pleotropic growth factor which regulates growth, motility and morphogenesis of various types of cells and has also demonstrated angiogenic effects[5,6], by administration via different routes [1]. However, the success of such procedures was limited due to the short life time of the growth factors *in vivo*. Hence, to resolve this problem, an efficient drug-transfer system like nonviral gene therapy offers a promising solution to enhance the efficiency of treatment [4]. In the current study, we investigated the feasibility and efficacy of electroporation mediated HGF gene delivery to random skin flap in a rat model with an aim to accelerate wound healing, facilitate vascularization and reduce flap necrosis.

METHODS

Fifteen male Wistar rats (290–320 g) were randomly divided in three groups. (a) control group (n=5), underwent the surgery and received no gene transfer, group (b) received electroporation mediated HGF gene delivery 24 hours after the surgery as a treatment, and group (c) received electroporation mediated HGF gene delivery 24 hours before the surgery as prophylaxis (n=5). Planimetry, Laser Doppler imaging and immunohistochemistry were used to assess the efficacy of HGF gene therapy among the groups.

RESULTS

Electroporation mediated HGF gene delivery significantly decreased flap necrosis percentage compared to the control group in prophylactic and treatment groups (p-value=0.0317, 0.0079, respectively) and increased significantly cutaneous perfusion compared to the control group (p-value=0.0317, 0.0159, respectively). Furthermore, significantly higher mean CD31+ vessel density was detected in treatment and prophylactic groups (p-value=0.0079, 0.0159, respectively). Additionally, quantitative image analysis revealed significantly higher HGF protein expression in groups b and c (p-value=0.0079 and 0.0079, respectively) (Figure 1).

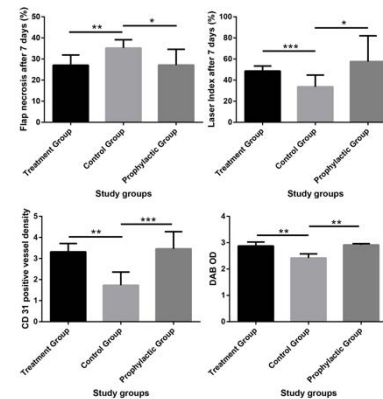


Figure 1: Comparison of important parameters among study groups

CONCLUSIONS

Our findings suggest *in vivo* electroporation mediated HGF gene delivery enhances viability and vascularity of the ischemic skin flap.

REFERENCES

- [1] Kryger, Z., et al., The effects of VEGF on survival of a random flap in the rat: examination of various routes of administration. *Br J Plast Surg*, 2000. 53(3): p. 234-239.
- [2] Basu, G., et al., Prevention of distal flap necrosis in a rat random skin flap model by gene electro transfer delivering VEGF(165) plasmid. *J Gene Med*, 2014. 16(3-4): p. 55-65.
- [3] Yang, L.W., et al., Vascular endothelial growth factor gene therapy with intramuscular injections of plasmid DNA enhances the survival of random pattern flaps in a rat model. *Br J Plast Surg*, 2005. 58(3): p. 339-347.
- [4] Fujihara, Y., et al., Gene transfer of bFGF to recipient bed improves survival of ischemic skin flap. *Br J Plast Surg*, 2005. 58(4): p. 511-517.
- [5] Nakagawa, A., et al., Improvement of survival of skin flaps by combined gene transfer of hepatocyte growth factor and prostacyclin synthase. *J Gene Med*, 2007. 9(12): p. 1087-1094.
- [6] Nakagami, H., et al., Hepatocyte growth factor as potential cardiovascular therapy. *Expert Rev Cardiovasc Ther*, 2005. 3(3): p. 513-519.

Electroporation-induced blood-brain barrier disruption for the treatment of glioblastoma multiforme

Yael Bresler^{1,2,3}, Shirley Sharabi^{1,3}, Nizan Cauzmer^{1,3}, Yael Mardor^{1,3}, Itzik Cooper²; ¹ The Advanced Technology Center, Sheba Medical Center, Tel-Hashomer, 52621, ISRAEL ² Sagol Neuroscience Center, BBB-Group, Sheba Medical Center, Tel-Hashomer, 52621, ISRAEL ³ Sackler Faculty of Medicine, Tel-Aviv University, Tel-Aviv, ISRAEL

INTRODUCTION

Despite aggressive therapy, existing treatments offer poor prognosis for glioblastoma multiforme (GBM) patients. Reasons for the poor outcome include tumor infiltration into the surrounding brain parenchyma as well as poor penetration of most drugs across the blood brain barrier (BBB). In addition, GBM cells are also highly resistant to therapeutic apoptotic stimuli, although they exhibit a paradoxical propensity for extensive cellular necrosis [1,2]. On top of these challenges, malignant brain gliomas are able to evade and suppress the immune system [3]. Therefore, when treating the tumor mass the infiltrating zone surrounding the tumor should be efficiently treated as well. We have recently developed [4] a strategy to apply both irreversible and reversible EP in the same treatment while disrupting BBB in large volume by employing a single intracranial needle electrode placed in the brain tissue and an external surface electrode pressed against the skin. The electric field produced by this electrode configuration is highest at the intracranial electrode tissue interface and then decays in an exponential fashion. Therefore, the electric fields surrounding the needle electrode induce irreversible effects that gradually taper down to reversible EP effects. A major consideration when planning EP protocols for the treatment of brain tumors is the effect of EP on endothelial integrity and viability. Studies conducted in our lab [5,6] showed that EP in the brain has also the ability to disrupt the BBB in a controlled manner. The results suggest that when treating brain tumors with EP it should be possible to take advantage of the fact that reversible EP breaches the BBB in volumes extending beyond the irreversibly affected volumes. Our current research project is focused on studying the effects of combined reversible/irreversible EP as well as the unclear mechanism of BBB disruption induced by EP in vitro. For this purpose we are applying a well-established BBB in-vitro system composed of primary brain endothelial cells co-cultured with primary astrocytes cells, allowing us to investigate the cellular mechanisms involved in EP-induced BBB disruption. We will also investigate the effects of reversible EP on the in-vitro model including tumor cells, targeting towards breaching the BBB and allowing internalization of cytotoxic agents for targeted cell death.

METHODS

Barrier integrity - is studied using trans-endothelial electrical resistance (TEER) measurements. *Endothelial viability* - is studied using MTT assays. *BBB Permeability* - of small/large (methotrexate, Herceptin, albumin) molecules

across the in-vitro BBB system will be assessed following EP treatments with various parameters. *Mechanisms of action* - A set of immunocytological stainings will be conducted after EP for main tight junction (TJ) proteins (occludin, claudin-5 and ZO-1) as well as F-actin (to assess the possible remodelling of the cytoskeleton). *Possible changes in expression/function of trans cellular related efflux pump*: such as P-glycoprotein (P-gp) will be evaluated using the vinblastine exclusion assay and immunocytochemistry for Pgp after EP. *Contribution of astrocytes to BBB disruption* - will be evaluated for different protocols- using the BBB in-vitro system with/without the addition of astrocytes. *In vitro efficacy study* - will be conducted using a brain-cancer-related 3 components experimental system. The 3 components are: the glioma cells, plated at the abluminal (brain-like) side; MTX, added at the luminal (blood-like) side; and EP, which enables the penetration of MTX at desirable rates and at sufficient concentrations required to destruct the glioma cells, located at the brain side.

REFERENCES

- [1] Brat DJ, Van Meir EG. Vaso-occlusive and prothrombotic mechanisms associated with tumor hypoxia, necrosis and accelerated growth in glioblastoma. *Laboratory investigation; a journal of technical methods and pathology*, 84(4):397-405, 2004.
- [2] Raza SM, Lang FF, Aggarwal BB, Fuller GN, Wildrick DM, Sawaya R. Necrosis and glioblastoma: a friend or a foe? A review and a hypothesis. *Neurosurgery*, 51(1):2-13, 2002.
- [3] Li F, Cheng Y, Lu J, Hu R, Wan Q, Feng H. Photodynamic therapy boosts anti-glioma immunity in mice: a dependence on the activities of T cells and complements C3. *Journal of cellular biochemistry*, 112(10):3035-3043, 2011.
- [4] Sharabi S, Last D, Guez D, Daniels D, Hjouj MI, Salomon S, Maor E, Mardor Y. Dynamic effects of point source electroporation on the rat brain tissue. *Bioelectrochemistry*, 99:30-39, 2014.
- [5] Sharabi S, Last D, Guez D, Daniels D, Hjouj MI, Salomon S, Maor E, Mardor Y: Dynamic effects of point source electroporation on the rat brain tissue. *Bioelectrochemistry*, 99:30-39, 2014.
- [6] Hjouj M, Last D, Guez D, Daniels D, Sharabi S, Lavee J, Rubinsky B, Mardor Y: MRI study on reversible and irreversible electroporation induced blood brain barrier disruption. *PloS one*, 7(8):e42817, 2012.

Permeabilizing Phospholipid Bilayers with Non-Normal Electric Fields

F. Castellani^{1,2}, P. T. Vernier¹

¹Frank Reidy Research Center for Bioelectrics, Old Dominion University, Norfolk, VA 23508, USA

²Biomedical Engineering Institute, Frank Batten College of Engineering and Technology, Old Dominion University, Norfolk, VA 23529, USA

INTRODUCTION

Molecular simulations of lipid bilayers show that the application of a transverse electric field induces the formation of conductive pores [1–4]. Increasing the electric field magnitude decreases the pore initiation time [5]. When an electric field is applied to an entire cell, however, the field is normal to the membrane only at the poles of the cell along the axis in the direction of the field. The electric field vector at points on the membrane away from the poles can be resolved into perpendicular and parallel components, relative to the plane of the membrane. We report here the contributions of the perpendicular and parallel components of the electric field to pore initiation time.

MATERIALS AND METHODS

Molecular dynamics (MD) simulations were performed using the GROMACS set of programs, version 4.6.6. [6], on the Old Dominion University High Performance Computing (HPC) Turing cluster <http://www.odu.edu/hpc>.

Systems contain 128 POPC (1-palmitoyl-2-oleoyl-*sn*-glycero-3-phosphatidylcholine), 22 K⁺, 22 Cl⁻, and approximately 9,000 water molecules, for a KCl concentration of about 80 mM. The initial simulation volume is approximately 6 nm x 6 nm x 12 nm. Systems are equilibrated for 200 ns before electric field application to allow ion-lipid interactions to stabilize. The field is applied as in [1], but with five different magnitudes in one of three directions relative to the plane of the bilayer: parallel (along the x-axis), perpendicular (along the z-axis), and at various oblique angles (Table 1). Five simulations were run for each condition.

RESULTS AND CONCLUSIONS

Pores formed in each of the five simulations where the field was applied normal to the bilayer plane. No pores are formed within 25 ns when the field is applied only parallel to the bilayer. Pore formation when the field is applied at an angle between 0° and 90° (oblique) depends on the magnitude of the field component normal to the plane of the bilayer. Figure 1 shows that the pore initiation time decreases linearly with increasing values for the z component of the electric field. Simulations showing the effect of in-plane components of the field are in progress.

Angle	E _{oblique} (MV/m)	E _z (MV/m)	E _x (MV/m)	Trials
θ = 0°	0	400	0	5
θ = 45°	200	141	141	5
θ = 45°	300	212	212	5
θ = 45°	400	283	283	5
θ = 90°	0	0	400	2
θ = 69°	400*2 ^{1/2}	200	529	5
θ = 58°	400*2 ^{1/2}	300	480	5
θ = 45°	400*2 ^{1/2}	400	400	5
θ = 28°	400*2 ^{1/2}	500	265	5
θ = 8°	400*2 ^{1/2}	560	77	5

Table 1: Simulation conditions.

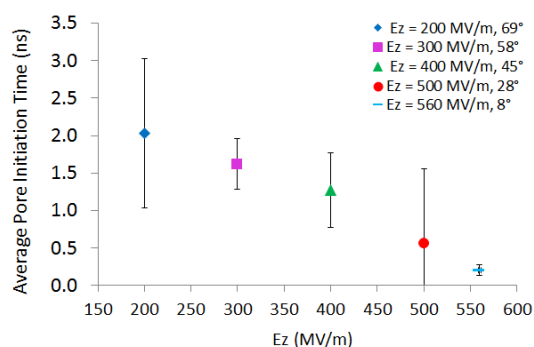


Figure 1: Pore initiation time decreases with increasing values for the magnitude of the component of the electric field vector normal to the plane of the bilayer.

REFERENCES

- [1] Tieleman DP, “The molecular basis of electroporation”, *BMC Biochem* 5:10, 2004.
- [2] Tarek M, “Membrane electroporation: a molecular dynamics simulation”, *Biophys J* 88:4045-4053, 2005.
- [3] Ziegler MJ, Vernier PT, “Interface water dynamics and porating electric fields for phospholipid bilayers”, *J Phys Chem B* 112:13588–13596, 2008.
- [4] Gurtovenko AA, Vattulainen I, “Pore Formation Coupled to Ion Transport through Lipid Membranes as Induced by Transmembrane Ionic Charge Imbalance: Atomistic Molecular Dynamics Study”, *J Am Chem Soc* 127:17570-17571, 2005.
- [5] Zachary AL, Vernier PT, “Life Cycle of An Electropore: Field-Dependent and Field-Independent Steps in Pore Creation and Annihilation”, *J Membr Biol* 236:27-36, 2010.
- [6] Van der Spoel D, Lindahl E, Hess B, and the GROMACS development team GROMACS, *User Manual version 4.6.6*, www.gromacs.org, 2014.

The Role of Temperature in the Inactivation of Microorganisms by Pulsed Electric Fields

Felix Schottroff, Henry Jaeger; *Institute of Food Technology, University of Natural Resources and Life Sciences (BOKU), Muthgasse 18, A-1190 Vienna, AUSTRIA*

INTRODUCTION

Apart from the variety of different applications of pulsed electric fields (PEF) in biotechnology and medicine, such as gene transfer and drug delivery, this process can be deployed as a powerful tool for the inactivation of microorganisms at temperatures lower than the ones used in conventional pasteurization. Thus, adequate log reductions of bacterial counts can be achieved, while the negative impact on valuable compounds, such as vitamins, proteins, or enzymes, is significantly decreased, compared to thermal processes. This makes the technology ideal for applications in the food industry, where mild pasteurization, which leaves valuable compounds intact, while achieving high levels of food safety, is a great advantage.

However, besides the electrical parameters, such as the electric field strength (E) or the specific energy intake (W_{specific}), several other process parameters have to be taken into account, especially when a continuous treatment is desired. One of the most crucial parameters is temperature, since it may influence the result of the inactivation in both a negative and positive manner, depending on the individual design of the process [1].

OBJECTIVES

The objective of this presentation is to emphasize the importance of the process variable temperature in the inactivation of microorganisms by PEF.

In this context, several effects of temperature have to be taken into consideration, i.e. growth temperature, which may affect the membrane composition, as well as treatment temperature, and the temperature increase during the exposure of the product to the electric field. In this respect, the individual effects of the electric field and heat have to be distinguished.

MATERIALS AND METHODS

Selected results from different studies will be compiled, with parameters ranging from field strengths of 10 – 40 kV cm⁻¹, frequencies of 10 – 250 Hz, and a corresponding energy intake of 50 – 200 kJ kg⁻¹, as well as process temperatures in the range of 4 – 140 °C. The inactivation of model microorganisms will be observed, e.g. *P. aeruginosa*, *E. coli*, and *B. subtilis*.

Inactivation was determined by plate counts on appropriate agars and subsequent incubation. Furthermore, viability was investigated by using flow cytometry and fluorescent dyes, such as propidium iodide (PI) or carboxyfluorescein diacetate (CFDA).

RESULTS AND DISCUSSION

Considering the impact of growth temperature on the inactivation, a 0.7 log reduction of *E. coli* was observed at an energy intake of 74 kJ kg⁻¹ in whole milk, when cells were

grown at 7 °C, in comparison to 2.8 log at a growth temperature of 40 °C. Thus, the effect of the PEF treatment significantly increased when the strain was grown at a higher temperature [2].

At a field strength of 28 kV cm⁻¹ and a total treatment time of 34 μs at inlet temperatures of 4 – 55 °C, inactivation of *P. aeruginosa* in whole milk progressively increased from 0.09 log at 4 °C to 0.87, 0.83, 2.94, and > 6 at 30, 40, 45, and 50 °C, respectively [3].

As temperature increases during the PEF treatment, depending on W_{specific} , additional inactivation effects may arise. Thus, it is important to be able to distinguish the effects caused by the electric field and temperature. This phenomenon is also dependent on the individual configuration of the treatment chamber, as distinct temperature peaks arise at the wall of the electrodes [4].

Bacterial endospores are not affected by the electric field alone. However, it could be shown that a combination of PEF and preheating temperatures in the range of 70 – 90 °C, resulting in maximum process temperatures of 105 – 140 °C, were able to inactivate spores (*B. subtilis*, *G. stearothermophilus*) more efficiently than heat only [5].

REFERENCES

- [1] F.J. Barba, O. Parniakov, S.A. Pereira, A. Wiktor, N. Grimi, N. Boussetta, J.A. Saraiva, J. Raso, O. Martin-Belloso, D. Witrowa-Rajchert, N. Lebovka, E. Vorobiev, “Current applications and new opportunities for the use of pulsed electric fields in food science and industry”, *Food Res. Int.*, vol. 77, pp. 773-798, 2015.
- [2] O. Rodriguez-Gonzalez, M. Walkling-Ribeiro, S. Jayaram, M.W. Griffiths, “Cross-protective effects of temperature, pH, and osmotic and starvation stresses in *Escherichia coli* O157:H7 subjected to pulsed electric fields in milk”. *Int. Dairy J.*, vol. 21, pp. 953-962, 2011.
- [3] P. Sharma, I. Oey, P. Bremer, D.W. Everett, “Reduction of bacterial counts and inactivation of enzymes in bovine whole milk using pulsed electric fields”. *Int. Dairy J.*, vol. 39, pp. 146-156, 2014.
- [4] H. Jaeger, N. Meneses, J. Moritz, D. Knorr, “Model for the differentiation of temperature and electric field effects during thermal assisted PEF processing”, *J. Food Eng.*, vol. 100, pp. 109-118, 2010.
- [5] K. Reineke, F. Schottroff, N. Meneses, D. Knorr, “Sterilization of liquid foods by pulsed electric fields - an innovative ultra-high temperature process”. *Front. Microbiol.*, vol. 6: 400, 2015.

Extraction of lipids from micro-algae, combining the use of electrical field solicitations and mechanical stress within a microfluidic device

S. Bensalem^{1,2}, F. Lopes², D. Pareau², O. Français¹, B. Le Pioufle¹; ¹ SATIE, UMR CNRS 8029, ENS Cachan, 61 av du Pdt Wilson 94230 Cachan, FRANCE ² LGPM, EA 4038, Ecole CentraleSupélec, Grande Voie des Vignes, 92295 Chatenay-Malabry, FRANCE

INTRODUCTION

For the past few years, feedstock from microalgae has revealed its inherent potential as a biofuel resource. Microalgae are photosynthetic microorganisms that produce, along with lipids for biofuel production, other compounds of interest such as pigments, omega-3 and 6.

However, despite the high potential of microalgae, several scientific, technological and economical bottlenecks must be overcome before large-scale production of biodiesel from microalgae takes place. It is now clearly recognized that harvesting/dewatering and lipids extraction steps are highly energy intensive. In the particular case of extraction (40-60% of the product cost), significant breakthroughs are needed to improve the oil recovery, the sustainability and ultimately the cost efficiency of the overall bioprocess [1, 2].

In this work, lipid extraction from microalgae is therefore investigated. We propose to develop a new methodology combining a pulse electric field treatment and mechanical stresses for the extraction of lipid compounds produced by microalgae; its performances will then be optimized in terms of efficiency, extraction yield and energy demand.

METHODS

In order to reduce the need for solvent in the extraction process, the cells, after accumulating lipids under stress conditions (for example by depleting nutrients such as nitrogen), are subject to an intense electric field pulse which leads to the creation of transient and reversible pores on the cell membrane [3, 4]. Subsequently, a mechanical stress is applied by forcing their passage into micro-fluidic channels where pressure on the cell walls is generated.

Figure 1: Microfluidic setup including electroporation chambers under microscopic observation.



We intend to characterize biophysical phenomena induced by the electrical and mechanical stresses in real time on a dedicated micro-fluidic chip with a resolution of a single cell.

Microscopic observation permits to examine the effect of these treatments on the morphology of the cell and on its intracellular organisation. Different probes are used depending on the target: lipids (Bodipy), membrane permeability (Sytox Green), enzymatic activity (FDA)...

Figure 2: Microscopic observation of the microalgae *Chlamydomonas Reinhardtii* after 7 days of stress conditions and after different pre-treatment. Lipids are visualized by BODIPY 505/515 staining (green) and cell wall by Concanavalin A staining (orange); chloroplasts show red autofluorescence. (a) cell without pre-treatment; (b) cell after electroporation; (c) cell after sequential electroporation and mechanical treatment

RESULTS AND PERSPECTIVES

Our first microscopic observations of cells pre-treated by mechanical stress showed lipid droplets in the medium (Figure 3). Nevertheless, more experiments are required to confirm and explain these observations.

Figure 3: Microscopic observation of the microalgae *Chlamydomonas Reinhardtii* under bright field, after mechanical treatment.



As shown on Figure 2, preliminary microscopic observations suggest that physical effects of the pre-treatments on the cell occur. Complementary experiments are therefore in progress.

The effect of sequential combination of these two pre-treatment methods will also be investigated in terms of lipid extraction efficiency.

REFERENCES

- [1] M. Vanthoor-Koopmans, R.H. Wijffels, M.J. Barbosa, M.H.M. Eppink, "Biorefinery of microalgae for food and fuel," *Bioresour. Technol.* 135 (2013) 142–9.
- [2] G.S. Araujo, L.J.B.L. Matos, J.O. Fernandes, S.J.M. Cartaxo, L.R.B. Gonçalves, F.A.N. Fernandes and W.R.L. Farias, "Extraction of lipids from microalgae by ultrasound application: Prospection of the optimal extraction method," *Ultrasonics Sonochemistry*, vol. 20, pp. 95-98, 2013.
- [3] C. Joannes, C. S. Sipaut, J. Dayou, S. M. Yasir, and R. F. Mansa, "The Potential of Using Pulsed Electric Field (PEF) Technology as the Cell Disruption Method to Extract Lipid from Microalgae for Biodiesel Production," *International Journal of Renewable Energy Research*, vol. 5, pp. 598-621, 2015.
- [4] P. Bodénès, F. Lopes, D. Pareau, B. Le Pioufle, O. Français, "Microdevice for studying the in situ permeabilization and characterization of *Chlamydomonas reinhardtii* in lipid accumulation phase," *Algal Research*, Elsevier, 2016, 1.

Antitumor effectiveness of cisplatin and oxaliplatin based electrochemotherapy on B16F10 melanoma cells *in vitro* and murine B16F10 tumor *in vivo*

Katja Uršič¹, Špela Kos¹, Urška Kamenšek¹, Maja Čemažar^{1,2}, Gregor Serša¹;

¹Department of Experimental Oncology, Institute of Oncology Ljubljana, Ljubljana, SLOVENIA

²Faculty of Health Sciences, University of Primorska, Izola, SLOVENIA

INTRODUCTION

Electrochemotherapy (ECT; a combination of chemotherapeutic drug and electric pulses) potentiates the antitumor effect of chemotherapy (CT) by increasing the internalization of drug into the cell. While ECT with cisplatin (CDDP) is already a well-established treatment for variety of different tumors, ECT with oxaliplatin (OXA) still awaits evaluation [1].

Besides binding to DNA, CDDP and OXA also trigger cancer cell death via non-DNA interactions. Their use has been renovated particularly because of the newly described beneficial effects on the immune system. In contrast to OXP, CDDP fails to induce immunogenic cell death (ICD), which is defined as a release of at least three danger-associated molecular pattern molecules (ATP, high mobility group box 1 protein, and calreticulin (CRT)). Namely, CDDP fails to induce CRT redistribution from endoplasmic reticulum (ER) to the plasma membrane [2]. However, combining CDDP CT with CRT inducers leads to ICD *in vitro*. Furthermore, ICD could also be achieved by combining CDDP with ER stress inducers [3].

Efficiency of ECT with CDDP or OXA has not been compared neither *in vitro* nor *in vivo*. It is also not known whether combining CDDP with electroporation pulses (EP stressors) causes ICD. To answer these questions, we studied the effects of ECT with CDDP or OXA on melanoma B16F10 cancer cells *in vitro* and on murine melanoma B16F10 tumors *in vivo*.

METHODS

After trypsinization and washing with ice cold electroporation (EP) buffer, we prepared cell suspension of B16F10 cells in EP buffer. CDDP or OXA in 6 final molar concentrations (5, 10, 15, 20, 50 and 100 μM) or cell growth medium (control) was added to the cell suspension ($1 \times 10^6/100\mu\text{l}$), half of the suspension was used as a control (CT alone), and the other half for ECT (parallel plate electrodes with 2 mm gap, 260 V, duration 100 μs , pulse repetition frequency 1 Hz, 8 pulses). 5 minutes after the ECT cells were resuspended in 2 ml of medium. For clonogenic assay, cells were plated in 6 cm Petri dish in 4 ml of medium. After 6 days, formed colonies were stained with crystal violet solution and counted. The results are presented as surviving fraction, which is calculated from the plating efficiency as described before [4].

RESULTS

According to the clonogenic assay, effectiveness of CT with CDDP and OXA is comparable. Application of electric pulses potentiates the effect of both cisplatin based chemotherapeutics (Figure 1). ECT with CDDP resulted in comparable ICD₅₀ as OXA, however survival of B16F10

treated with ECT with CDDP is lower in comparison to ECT with OXA at 100 μM .

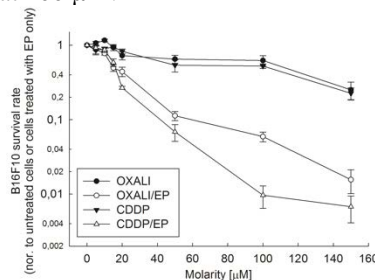


Figure 1: Clonogenic assay, comparing the sensitivity of B16F10 melanoma cell line to CDDP and OXA ECT (with standard errors).

CONCLUSIONS

Our preliminary results indicate that application of electric pulses potentiates the effectiveness of both chemotherapeutic drugs, CDDP and OXA. However, further research is needed to answer other questions, predominantly to prove the speculated occurrence of ICD after ECT with CDDP.

ACKNOWLEDGEMENTS

This research was conducted in the scope of LEA EBAM and ARRS.

REFERENCES

- [1] M. L. Yarmush, A. Golberg, G. Serša, T. Kotnik, and D. Miklavčič, "Electroporation-Based Technologies for Medicine: Principles, Applications, and Challenges.," *Annu. Rev. Biomed. Eng.*, vol. 16, pp. 295–320, 2014.
- [2] S. V. Hato, A. Khong, I. J. M. De Vries, and W. J. Lesterhuis, "Molecular pathways: The immunogenic effects of platinum-based chemotherapeutics.," *Clin. Cancer Res.*, vol. 20, no. 11, pp. 2831–2837, 2014.
- [3] I. Martins, O. Kepp, F. Schlemmer, S. Adjemian, M. Tailler, S. Shen, M. Michaud, L. Menger, a Gdoura, N. Tajeddine, a Tesniere, L. Zitvogel, and G. Kroemer, "Restoration of the immunogenicity of cisplatin-induced cancer cell death by endoplasmic reticulum stress.," *Oncogene*, vol. 30, no. 10, pp. 1147–1158, 2011.
- [4] A. Munshi, M. Hobbs, and R. E. Meyn, "Clonogenic cell survival assay.," *Methods Mol. Med.*, vol. 110, pp. 21–28, 2005.

The sensitivity of radio-resistant human squamous cell carcinoma cell line to electrochemotherapy with cisplatin and bleomycin

Martina Niksic Zakelj, Vesna Todorovic, Ajda Prevc, Andreja Brozic, Gregor Sersa, Primoz Strojjan;
Institute of Oncology Ljubljana, Zaloska 2, SI-1000 Ljubljana, SLOVENIA

INTRODUCTION

Electrochemotherapy is already an established method for treatment of cutaneous and subcutaneous tumours of different histologies, with high objective response rates (70 – 80%) [1]. Recent studies indicate that the effectiveness of the electrochemotherapy depends not only on tumour histology and size, but also on eventual previous treatment(s). The pre-treatment (radio- or chemotherapy) in fact significantly reduces the response rate of the treated tumours [2]. The reduced responsiveness of the pre-treated tumours might be, among other, due to the intrinsic resistance of the tumour cells to the chemotherapeutic agents. Therefore, our aim was to compare the sensitivity of radio-resistant human squamous cell carcinoma cell line (FaDu IR-4x) and its parental cell line (FaDu) to bleomycin and cisplatin after continuous exposure and to electrochemotherapy with these two chemotherapeutics *in vitro*.

METHODS

By fractionated irradiation of the FaDu cell line (a total dose of 120 Gy), we have established a radio-resistant cell line FaDu IR-4x. These two cell lines were exposed to different concentrations of bleomycin or cisplatin, both continuously and in combination with electroporation. For electroporation, we used parallel plate electrodes with 2 mm gap and applied eight square wave pulses of amplitude 260 V (amplitude over distance ratio (electric field intensity) was 1300 V/cm), pulse duration 100 μ s, and frequency 1 Hz. To determine and compare the effect of increasing amplitude of electric field to the level of cell membrane permeabilization (electropermeabilization), we measured the uptake of propidium iodide after electroporation using FACSCanto II flow cytometer (BD Biosciences). The clonogenic assay was used to determine the cell survival.

RESULTS

Radio-resistant cell line FaDu IR-4x was more sensitive to treatment with bleomycin and less sensitive to treatment with cisplatin, compared to FaDu cells (Figure 1). Furthermore, the same pattern was observed after electrochemotherapy with these two chemotherapeutics - indicating altered electrochemosensitivity of the radio-resistant cells. The measured uptake of propidium iodide showed no difference in cell electropermeabilization between the two cell lines. The underlying molecular mechanisms are under investigation.

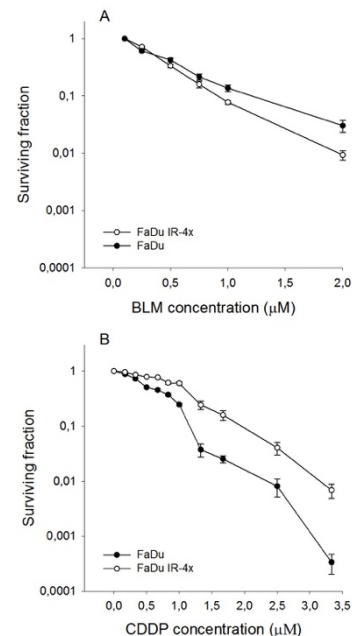


Figure 1: Survival of FaDu and FaDu IR-4x cells after continuous exposure to bleomycin (A) and cisplatin (B).

CONCLUSION

Our *in vitro* data indicate a better anti-tumour effect of electrochemotherapy with bleomycin in radio-resistant cell line FaDu IR-4x, compared to cisplatin, which may have clinical implication. These results suggest the presence of altered intrinsic sensitivity to different chemotherapeutic drugs in radio-resistant cells. They also indicate that the observed pattern is not due to different level of cell electropermeabilization, but must be due to different mechanisms of action of bleomycin and cisplatin, which should be further explored.

ACKNOWLEDGEMENTS

This research was conducted in the scope of LEA EBAM and financially supported by the ARRS.

REFERENCES

- [1] B. Mali, T. Jarm, M. Snoj, G. Sersa and D. Miklavcic, "Antitumor effectiveness of electrochemotherapy: a systematic review and meta-analysis," *EJSO*, vol. 39, pp. 4–16, 2013.
- [2] L.G. Campana, B. Mali, G. Sersa, S. Valpione, C.A. Giorgi, P. Strojjan, D. Miklavcic and C.R. Rossi, "Electrochemotherapy in non-melanoma head and neck cancers: a retrospective analysis of the treated cases," *Br J Oral Maxillofac Surg*, vol. 52, pp. 957-64, 2014.

Electric Field Distribution Generated by Two Needle Electrodes in an Anatomical Model of a Deep-Seated Breast Carcinoma

Adriana L. Vera Tizatl¹, Carlos A. Ramírez Martínez¹, Arturo Vera Hernández¹, Lorenzo Leija Salas¹, Pablo R. Hernández Rodríguez¹, Sergio Rodríguez Cuevas²; ¹ *Department of Electrical Engineering, Bioelectronics, CINVESTAV, Av. Instituto Politécnico Nacional 2508, MX-07360 Mexico City, MEXICO* ² *Institute of Breast Diseases, FUCAM, Av. Bordo 100, MX-04980 Mexico City, MEXICO*

INTRODUCTION

In Mexico, breast cancer is reported to be the first cause of death in women and current treatments include highly invasive techniques. Outcomes obtained with electrochemotherapy (ECT) encourage the development of minimally invasive treatment techniques. The design of an electroporation system to be used in a deep-seated breast carcinoma, corresponding to a real clinical case, is presented in this work [1, 2].

METHODOLOGY

In order to build a high voltage source, three regulated high voltage DC to DC programmable converters with an output voltage ranging from 0 V to 500 V are used. The connection in series of these modules allows to generate 1500 V. The control of these converters was carried out by using isolated Inter-Integrated Circuit (I²C) communication. The control of each module has a resolution of 12 bits. The generation of pulses is made by a PWM and a power switching MOSFET.

Based on the anatomical model presented in [3], the reconstruction of the surrounding breast healthy tissue was added to the model as shown in Fig. 1. The finite element method (FEM) (COMSOL Multiphysics®) was used to determine electric field distribution caused by the application of the electric potential generated by the electroporation system designed.

RESULTS

Based on the outcomes previously reported in [3], the application of maximum electric voltage of 500 V was used. Electric conductivity of 0.05 s/m and 0.5 S/m for healthy breast tissue and tumoral tissue respectively, were simulated. The resultant electric field magnitudes for each tissues are shown in Table 1. The electric field distribution can be observed in Fig 2.

Table 1: Electric field magnitude generated in the model.

Electric Field [V/cm]	Healthy breast tissue	Breast Carcinoma
Average	2.37	651.26
Minimum	0	9.35
Maximum	43.17	900.42

CONCLUSION

The anatomical model presented in this work represents an approach to a patient-specific treatment planning. It can be seen that an average electric field magnitude of 651.26 V/cm (651.26 V/cm) is achieved when applying 500 V through just

two needle electrodes. Assuming that an electric field of 400 V/cm is necessary for the ECT treatment of tumors and based on results showed in Table 1, an electric voltage lower than 500 V is suggested for this specific model.

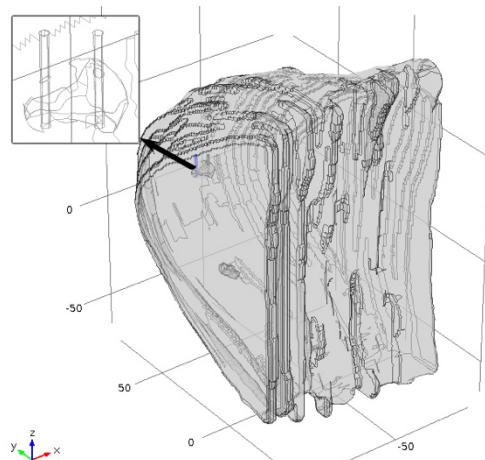


Figure 1: Model of a left breast and two needle electrodes.

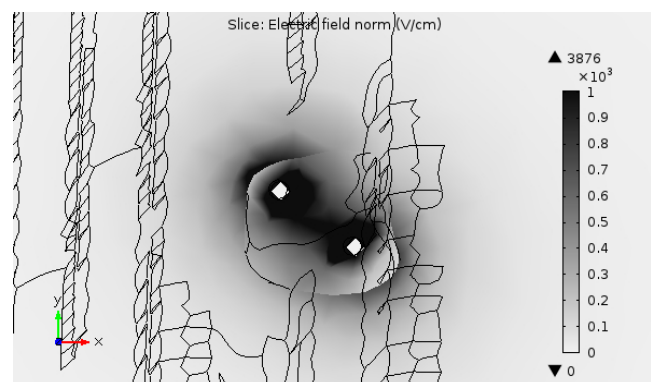


Figure 2: Electric field distribution in the complete model.

REFERENCES

- [1] A. L. Vera-Tizatl, S. A. Rodríguez-Cuevas, L. Leija Salas and A. Vera-Hernández, "Review of electrochemotherapy-based Treatment of Cutaneous, Subcutaneous and Deep-seated Tumors towards Specific Treatment Planning", GMEPE/PAHCE, Madrid, Spain, April 4-9, 2016.
- [2] D. Pavliha, B. Kos, A. Zupanic, M. Marcan, G. Sersa and D. Miklavcic, "Patient-specific Treatment Planning of Electrochemotherapy: Procedure Design and possible pitfalls", *Bioelectrochemistry*. vol. 87, pp. 265–273, Jan. 2012.
- [1] [3] A. L. Vera Tizatl et. Al, "Electric Field Distribution in an Anatomical Model with the Finite Element Method based on the 3D Reconstruction of a Breast Carcinoma", 13th. International Conference on Electrical Engineering, Computing Science and Automatic Control (CCE), Mexico City. Sept. 26-30, 2016.

Electrochemotherapy in a Cutan Recurrence of Postirradiation Angiosarcoma of the Breast after Mastectomy

Bottyán Krisztina¹, Németh István¹, Varga Erika¹, Korom Irma¹, Kahán Zsuzsanna³, Baltás Eszter¹, Lázár György², Oláh Judit¹, Kemény Lajos¹, Kis Erika¹; ¹*Department of Dermatology and Allergology, University of Szeged, Korányi fasor 5., 6720 Szeged, HUNGARY* ²*Department of Surgery, University of Szeged, Semmelweis u.8., 6720 Szeged, HUNGARY* ³*Department of Oncology, University of Szeged, Korányi fasor 12., 6720 Szeged, HUNGARY*

CASE REPORT

Invasive ductal adenocarcinoma (GrIIIpT2) of the breast was diagnosed in a 66 years old female at the Department of Oncology of Szeged in 2008. Surgical excision and Sentinel lymphnode biopsy were performed, and adenocarcinoma metastases were confirmed in the removed lymphnodes. Regarding the patients's request, and the negative results of the staging examinations, the oncoteam opted for a combination of radiotherapy and adjuvant Letrozole therapy. 6 years later, an elevated, erythematous lesion arised in the previously irradiated area.

The histological verification of an excisional biopsy proved the diagnosis of postirradiation angiosarcoma. Right-sided mastectomy was performed with a 3 cm safety zone. The defect was covered with a split-thickness mesh graft.

Two month later, at the upper margin of the skin graft, we observed recurrence of the angiosarcoma, which was confirmed histologically.

Our oncoteam decided electrochemotherapy as the spectrum of the therapeutic possibilities in postirradiation angiosarcoma is quite tight [1], and according to the results of a published metaanalysis [2] it is a highly effective therapeutic modality in sarcomas.

The patient fulfilled the requirements for electrochemotherapy.

ECT was performed under general anesthesia, with intravenously administered 15000IU/m² Bleomycin. Electric pulses were delivered between 8-28 minutes following the administration of Bleomycin. The treatment was carried out with hexagonal needle electrode, the average current was 1,5-3 A. Around the lesions 3 cm safety zone was also treated laterally.

The treatment was well tolerated by the patient.

After six weeks we observed complete response on the smaller (0,5-1 cm) lesions, and partial response on the lesion >3 cm, and mild hyperpigmentation on the treated area.

Outside the treated area new skin nodules showed progression of the disease, therefore we performed a second session of ECT, and a Thalidomide therapy was planned combined with ECT, but the patient interrupted the treatment.

For local tumour control electrochemotherapy could be an effective alternative therapy for very invasive tumours that are not suitable for surgery [1,2].

[breast cancer: high recurrence rate and poor survival despite surgical treatment with R0 resection](#)", *Annals of Surgical Oncology*, vol. 19, pp. 2700-2706, 2012.

- [2] B. Mali, T. [Jarm](#), M. [Snoj](#), G. [Sersa](#) and D. [Miklavcic](#), "Antitumor effectiveness of electrochemotherapy: a systematic review and meta-analysis", *European Journal of Surgical Oncology*, vol. 39, pp. 4-16, 2013.

REFERENCES

- [1] J.M. Seinen, E. Styring, V. Verstappen, F. Vult von Steyern, A. Rydholm, A.J. Suurmeijer and H.J. Hoekstra, "[Radiation-associated angiosarcoma after](#)

Faculty members



Damijan Miklavčič
University of Ljubljana, Faculty of Electrical Engineering, Tržaška 25, SI-1000 Ljubljana, Slovenia
E-mail: damijan.miklavcic@fe.uni-lj.si



Lluís M. Mir
UMR 8532 CNRS-Institut Gustave-Roussy, 39 rue Camille Desmoulins, F-94805 Villejuif Cédex, France
E-mail: Luis.MIR@gustaveroussy.fr



Marie-Pierre Rols
IPBS UMR 5089 CNRS, 205 route de Narbonne, F-31077 Toulouse, France
E-mail: marie-pierre.rols@ipbs.fr



Gregor Serša
Institute of Oncology, Zaloška 2, SI-1000 Ljubljana, Slovenia
E-mail: gserša@onko-i.si



Mounir Tarek
UMR CNRS 7565 Nancy – Université, BP 239 54506 Vandœuvre-lès-Nancy Cedex, France
E-mail: mounir.tarek@univ-lorraine.fr



Justin Teissié
IPBS UMR 5089 CNRS, 205 route de Narbonne, F-31077 Toulouse, France
E-mail: justin.teissie@ipbs.fr



P. Thomas Vernier
Old Dominion University, Frank Reidy Center for Bioelectronics, 442 Research Park II, Norfolk, VA 23529, USA
E-mail: pvernier@odu.edu



Julie Gehl
Herlev Hospital, Herlev Ringvej 75, 2730 Herlev, Denmark
E-mail: julie.gehl@regionh.dk

